

SPATIO-TEMPORAL ASSESSMENT OF GROUNDWATER USING GEOSPATIAL TOOLS

Ph.D. THESIS

by

RAJAT AGARWAL



**DEPARTMENT OF CIVIL ENGINEERING
INDIAN INSTITUTE OF TECHNOLOGY ROORKEE
ROORKEE – 247667 (INDIA)
DECEMBER, 2014**

SPATIO-TEMPORAL ASSESSMENT OF GROUNDWATER USING GEOSPATIAL TOOLS

A THESIS

*Submitted in partial fulfilment of the
requirements for the award of the degree*

of

DOCTOR OF PHILOSOPHY

in

CIVIL ENGINEERING

by

RAJAT AGARWAL



**DEPARTMENT OF CIVIL ENGINEERING
INDIAN INSTITUTE OF TECHNOLOGY ROORKEE
ROORKEE – 247667 (INDIA)
DECEMBER, 2014**

**©INDIAN INSTITUTE OF TECHNOLOGY ROORKEE, ROORKEE-2014
ALL RIGHT RESERVED**



INDIAN INSTITUTE OF TECHNOLOGY ROORKEE ROORKEE

CANDIDATE'S DECLARATION

I hereby certify that the work which is being presented in the thesis entitled **SPATIO-TEMPORAL ASSESSMENT OF GROUNDWATER USING GEOSPATIAL TOOLS** in partial fulfilment of the requirements for the award of the degree of Doctor of Philosophy and submitted in the Department of Civil Engineering of the Indian Institute of Technology Roorkee is an authentic record of my own work carried out during a period from Jan, 2010 to Dec, 2014 under the supervision of Dr. P. K. Garg, Professor, Geomatics Engineering Group, Civil Engineering Department, Indian Institute of Technology Roorkee, Roorkee.

The matter presented in the thesis has not been submitted by me for the award of any other degree of this or any other Institute.

(RAJAT AGARWAL)

This is to certify that the above statement made by the candidate is correct to the best of our knowledge.

(P. K. Garg)
Supervisor

Date:

*Dedicated
to
My Beloved Parents*

ABSTRACT

Groundwater is an important source of water supply throughout the World, but it becomes contaminated and its level is likely being declined day by day due to mismanagement of this resources. The decreasing water table and groundwater contaminations found to be are critical problems in a Loni and Morahi watersheds of UP State, India. To overcome this problem spatio-temporal analysis has been carried out with the help of Remote Sensing (RS) and Geographical Information System (GIS). Groundwater flow modeling was carried out and finally, a web enabled geoportal using open source GIS technology was created.

The spatial and non-spatial (attribute data) database was created and designed in GIS environment using ArcGIS 9.3 and ERDAS Imagine 9.3 software. Spatial database contained different thematic maps that were represented in a vector format; RS images, field data and Global Positioning System (GPS) measurements were represented in ArcGIS compatible format. For physical implementation of the spatial database, a layer based approach was used. For its physical implementation, a relational structure was used and different relational tables were created within ArcGIS domain. To demonstrate the reliability of the developed database for a spatial decision-making as well as to extract some information to be needed for further studies, geographical data processing, in particular construction of DEM from the topographic maps entered into the GIS. The generated database was efficiently used for derivation of results and their analysis.

In this study, groundwater potential zones map is delineated using RS, GIS and Multi Criteria Decision Making Technique (MCDM) techniques. Groundwater potential map is categorized into five zones, viz., 'very poor', 'poor', 'good', 'very good' and 'excellent'. The area falling in excellent category is about 150.93 km² (7.06% of the total study area), that lies along Ganga river. However, the area having very poor category is about 372.03 km² (17.42% of the total study area) which lies along Loni river, rest of the area falling poor, good and very good category is about 815.39, 594, 202.94 km², respectively. Results have been validated using yield data of wells and found to be satisfactory. The developed groundwater potential zones map will be helpful to the decision makers in identifying suitable locations for drilling production wells and/or monitoring wells as well as in protecting the vital groundwater resources.

The study also reveals that remotely sensed data and GIS based approach is more appropriate and effective than the conventional methods for evaluation of drainage

morphometric parameters and their influence on landforms, soils and eroded land characteristics at sub-watershed level. Interpretation of multi-spectral satellite sensor data was of great help in analysis of drainage parameters and morphometric characteristics which could be used for accurate delineation of distinct geological and landform units. The results of morphometric analysis show that sub-watershed LSW6 is prone to relatively high erosion and soil loss. Hence, suitable control measures are urgently required in this sub-watershed to preserve the land from further degradation.

Rainfall-runoff modeling was carried out in GIS environment where major inputs were derived from topographic maps, satellite images and field data. Fairly accurate classification of Land Use/Land Cover (LULC) types from satellite images helped in computing the Curve Number (CN) values distributed over the sub-watershed required for Soil Conservation Service curve number (SCS-CN) model.

In this study, 22 suitable locations for artificial recharge sites were identified. During field visit, 4 sites were verified that match with the identified location using remote sensing and GIS technique. RS and GIS was found to be an effective tool for integrating hydrological, LULC and morphometric parameters as per user defined criteria to identify suitable artificial recharge sites. The study assesses the necessity of having a suitable type of water harvesting structure in each sub-watershed. It not only indicates the suitability of the structures, but also helps whether a particular sub-watershed requires treatment or not, in terms of water harvesting structures.

On the basis of groundwater recharge modeling using GEC guidelines (MOWR, 2011); it was found that Sikandarpur Karan and Sareni blocks fall in critical category while the offer blocks have significantly decline in groundwater level.

On the basis of Mann Kendall's trend test and linear regression analysis, it was found that most of the wells have declining trend in pre- and post-monsoon season, and As per the results in pre-monsoon season, 58% wells showed falling trends which can be due to high pumpage of water and less recharge, while about 5% wells showed rising trends, most of which are located near pond and canal. In post-monsoon season, 63% wells showed falling trends and about 7% wells showed rising trends. However, 61% wells showed falling trends and 6% showed rising trend in both the pre- and post-monsoon seasons. These results provide useful information for groundwater analyses required to ensure sustainable groundwater development. For protecting groundwater from further depletion, the groundwater development needs to be taken up in a planned manner in order to prevent adverse impact on groundwater. The artificial recharge can be implemented to avoid the declining trend in groundwater levels. Water-logging

and soil salinity problems, resulting from gradual rise of groundwater levels, are observed in study area. This is due to the surface water irrigation without environmental considerations. So, there is also a need to adopt conjunctive water use strategy in the areas experiencing water logging problem.

The steady state calibration of the model shows a close agreement between the simulated and observed heads with the residual mean of -0.32 m, variance 1.27 m and correlation coefficient 0.975. In transient state calibration, the model shows a close agreement between simulated and observed heads with the residual mean of 0.01 m, variance 2.36 m and correlation coefficient 0.953. The calibrated and validated statistics for different time steps of RMS error has been found in the range of 1.24 m to 1.63 m throughout the calibration period, which is in acceptable range. Residual mean has been found to lie within -0.49 m and 0.49 m, absolute residual mean within a range of 0.9 m to 1.25 m throughout the calibration period.

On the basis of calibration and validation of the model by observing the calibrated aquifer parameters, hydraulic conductivity was found to lie between 15.4 and 93.1 m/day in the area, and specific yield is in the range of 0.002 to 0.12 in different zones of area. Hydraulic conductivity, storage parameters (specific yield) and recharge were selected as the most uncertain parameters. On the basis of sensitivity analysis, it was found that recharge and hydraulic conductivity are most sensitive parameter as compared to specific yield, as indicated by the relative mobility in the mean errors between the mean error corresponding to calibrated values and errors. The RMS error has increased by 1.6 times with a decrease in hydraulic conductivity by 80%, whereas it has increased by 1.1 times with an increase in hydraulic conductivity by 80%. For recharge, the model is more sensitive as compared to hydraulic conductivity. RMS error has increased by 4.1 times with a decrease in recharge by 80%, whereas it has increased by 3.7 times with an increase in recharge by 80%. In case of specific yield, small change is observed as compared to recharge and hydraulic conductivity.

The modified DRASTIC model DRASIC-LU has been used to investigate the groundwater vulnerable zones in study area. It uses six DRASTIC parameters and land use as an extra parameter in a GIS environment. The normalized DRASTIC index varied between 0.21 and 0.96, which was divided on the basis of histogram into four classes; low, moderate, high and very high, considering as the higher the index, the greater the relative pollution potential. It indicates that 13.44% area is categorized as very high vulnerable zone, while 32.56% and 19.95% of the areas are categorized as moderate and high vulnerable, respectively. Similarly, 34.05% of the total area is classified as low vulnerable zone. The result is validated using measured nitrate and fluoride data of 40 different locations collected from UP Jal Nigam,

Unnao. All the tested samples were overlaid on the groundwater vulnerability map using GIS in order to study the number of wells with high concentration of nitrate and fluoride is found within different vulnerable zones. Nevertheless, it was found that majority of sampled sources which violated BIS, 2011 limit value of nitrate and fluoride are located in high to very high vulnerable zones. A relationship between nitrate and groundwater depth was established, and found that concentration of nitrate was higher in shallow water table as compared to deeper water table. This confirms that model results are satisfactory.

Groundwater quality index has been categorized into five classes namely; excellent, very good, good, poor and unfit for drinking. It was found that the area falling in excellent groundwater quality is about 240.6 km² (11.2% of the total study area), which covers central portion of Bighapur block and Eastern south part of study area, that lies in Sumerpur and Khiron block. However the area unfit for drinking is about 117 km² (5.46% of the total study area), which falls in western part of Sikandarpur block, and it is nearby the Unnao city and industrial area of Unnao district.

Groundwater quality map for irrigation purpose has been categorized into four classes namely: excellent, good, permissible and doubtful. It was found that most of the area (about 99%) is suitable for irrigation except few area (about 1%) in Bichhiya block are in doubtful range.

The web GIS based application using open source technology has been developed and demonstrated the groundwater resources. This tool provides a complete GIS solution in web browser environment. The advantage of web technology has also been derived i.e. through internet it can be used simultaneously by a large number of users as the knowledge of basic software is not necessary to handle web GIS based module. The software to develop Web GIS module are also available free of cost which is a great advantage in a developing country, like India.

ACKNOWLEDGEMENT

First of all I would like to thank GOD for giving me the opportunity to be part of this prestigious institute and guiding me and helping me to complete this work.

It is a privilege to express my sincere and profound gratitude to Dr. P. K. Garg, Professor, Geomatics Engineering Group, Department of Civil Engineering, IIT Roorkee, Roorkee for their guidance, encouragement and suggestions at every stage of this study, in spite of their busy schedule, without which it would have been very difficult to complete this work in time.

I would also like to express my sincere gratitude to Dr. R.D. Garg, Associate Professor, Geomatics Engineering Group, Department of Civil Engineering, IIT Roorkee, Roorkee and the Chairman of my SRC committee for their valuable suggestion and financial support by own DST funded project.

I am thankful to my SRC (Student Research Committee) members: Prof. Deepak Khare, Head, Department of Water Resources Engineering, IIT Roorkee, Roorkee and Dr. S. K. Ghosh, Professor, Geomatics Engineering Group, Department of Civil Engineering, IIT Roorkee, Roorkee, for their valuable comments and suggestions towards the improvement of my Ph.D. work right from the beginning. Their critical comments have always been for the betterment of my own work.

My heartfelt thank to all my friends and colleagues: Dr. Sandeep Gupta, Mrs. Shipra, Amit Verma, Amita, Kuldeep, Urvashi, Gaurav, Mr. Deepak Singh, Vijendra, Amit Sharma, Anuj, Vishal, Vikas who have helped by sparing their valuable time by sharing their thoughts with me and also providing some light moments amidst the stress of the project.

A very special thanks goes to my dear friends Dr. Rashmi Kandwal, Mrs. Etishree Gupta, Mrs. Susheela Dahiya, Mr. D.C. Bala, Dr. Rakesh K. Dwivedi, Dr. Priyadarshi Upadhyaya and Mrs. Vandita whom I found standing by my side whenever I needed them. Special mention for Mr. D.C. Bala sir, he helps me very much in my critical phase of life during Ph.D., with our positive attitude.

I wish to express my heartiest thanks to research scholars and M.Tech. Students, who directly or indirectly helped me for successful completion of this project work.

I feel greatly invigorated and privileged to express my highest degree of regards and deep sense of gratitude to my parents, my wife Pooja, my lovely son Ainesh, my sister Mrs. Shalini Gupta and my brother Mr. Vivek Agarwal and Mr. Abhishek Agarwal. I express my sincere regards to my brother-in-law, sister-in-laws and relatives for their constant support and love. Last but not the least; I want to extend my sincere gratitude to my father and mother for their support and prayer.

As a number of teachers, staff members and my colleagues have helped in completing my Ph.D., it is my duty to put on record my sincere thanks to all of them

And above all, I am thankful to the almighty whose divine grace gave me the required courage, strength and perseverance to overcome various obstacles that stood in my way.

(Rajat Agarwal)

CONTENTS

	Pg. No.
Candidate's Declaration	i
Abstract	ii-v
Acknowledgements	vi-vii
Contents	viii-xv
List of Figures	xvi-xxi
List of Tables	xxii-xxiii
List of Abbreviations used	xxiv-xxvi
CHAPTER 1 INTRODUCTION	1-9
1.1 PROLOGUE	1
1.2 ROLE OF SPATIO-TEMPORAL ANALYSIS	3
1.3 REMOTE SENSING, GIS & GROUNDWATER MODELING	4
1.4 PROBLEM IDENTIFICATION AND SCOPE OF STUDY	6
1.5 OBJECTIVES OF THE STUDY	7
1.6 ORGANISATION OF THESIS	7
CHAPTER 2 LITERATURE REVIEW	10-32
2.1 PROLOGUE	10
2.2 APPLICATION OF REMOTE SENSING AND GIS IN GROUNDWATER STUDIES	10
2.2.1 Groundwater Potential	10
2.2.2 Groundwater Recharge Zones	15
2.2.3 Groundwater Vulnerability	18
2.2.4 Groundwater Quality Index	21
2.3 GROUNDWATER MODELING	23
2.4 OPEN SOURCE WEB GIS	29

2.5	CONCLUDING REMARK	32
CHAPTER 3 THE STUDY AREA, DATA AND SOFTWARE USED		33-40
3.1	THE STUDY AREA	33
3.1.1	Location and Accessibility	33
3.1.2	Climate	34
3.1.3	Water Resources and Irrigation Practices	35
3.1.4	Geomorphology	35
3.1.5	Soil	36
3.1.6	Hydrogeology	36
3.2	DATA USED	37
3.3	SOFTWARE, TOOL, SCRIPT AND TECHNOLOGY USED	39
CHAPTER 4 CREATION OF SPATIAL & NON- SPATIAL DATABASE		41-58
4.1	PROLOGUE	41
4.2	DATA COLLECTION AND VERIFICATION	41
4.3	GEOGRAPHIC DATABASE CREATION IN GIS	42
4.3.1	Spatial Frame Work for Geographic Database	42
4.3.2	Spatial Data Normalization	43
4.3.3	Spatial Database Creation in GIS	43
4.3.4	Digitization of Features	43
4.3.4.1	Point feature class	44
4.3.4.2	Polyine feature class	44
4.3.4.3	Polygon feature class	44
4.4	METHODOLOGY OF WATERSHED DELINEATION	45
4.4.1	Fill DEM	45
4.4.2	Flow Direction Grid	45
4.4.3	Flow Accumulation Grid	45
4.4.4	Snap Pour Point	45
4.4.5	Watershed	46
4.5	CREATION OF GIS LAYERS	47
4.5.1	Drainage Layer	47
4.5.2	Drainage Density Layer	47
4.5.3	Digital Elevation Model (DEM) Layer	48

4.5.4	Slope Layer	48
4.5.5	Geomorphology Layer	50
4.5.6	Geology Layer	50
4.5.7	Soil Layer	52
4.5.8	Land Use/Land Cover Layer	53
4.5.9	Rainfall Layer	54
4.5.10	Pre-monsoon Groundwater Depth Layer	55
4.5.11	Post-monsoon Groundwater Depth Layer	55
4.5.12	Water Level Fluctuation Layer	57
4.5.13	Village Layer of Watersheds	57

CHAPTER 5 GROUNDWATER MANAGEMENT USING REMOTE

	SENSING AND GIS	59-92
5.1	PROLOGUE	59
5.2	GROUNDWATER POTENTIAL ZONES MAPPING	59
5.2.1	Weight Assignment and GIS-based Modeling	62
5.2.2	Verification of Groundwater Potential Zones Map	62
5.3	RAINFALL RUNOFF MODELING USING SCS-CN METHOD	64
5.3.1	SCS-CN Method	64
5.4	MORPHOMETRIC ANALYSIS	65
5.5	ARTIFICIAL RECHARGE STRUCTURES	67
5.6	RESULTS AND DISCUSSIONS	69
5.6.1	Groundwater Potential Zones Mapping	69
5.6.1.1	Geomorphology map	69
5.6.1.2	Geology map	69
5.6.1.3	Soil map	69
5.6.1.4	Land use/ land cover map	69
5.6.1.5	Slope map	70
5.6.1.6	Drainage density map	70
5.6.1.7	Water table fluctuation map	70
5.6.1.8	Rainfall map	71
5.6.1.9	Groundwater potential zones map	71
5.6.1.10	Verifying groundwater potential zones map	71
5.6.2	Rainfall Runoff Modeling	72

5.6.2.1	Curve number layer	72
5.6.2.2	Runoff coefficient	73
5.6.3	Morphometric Analysis	74
5.6.3.1	Linear aspects	74
5.6.3.2	Relief parameters	79
5.6.3.3	Aerial aspects	79
5.6.3.4	Prioritization of sub-watersheds	81
5.6.4	Artificial Recharge Structures	82
5.6.4.1	Buffer map of drainage junctions	83
5.6.4.2	Buffer map of habitated area	84
5.6.4.3	Buffer map of canals	85
5.6.4.4	Groundwater depth map	85
5.6.4.5	Runoff map	86
5.6.4.6	Site suitability map	86
5.6.4.7	Morphological parameters	87
5.7	CONCLUDING REMARK	90

CHAPTER 6 ANALYSIS OF GROUNDWATER CONDITION AND ESTIMATION OF DYNAMIC GROUNDWATER RESOURCES

93-122

6.1	PROLOGUE	93
6.2	GROUNDWATER SUBSURFACE CONDITION	94
6.3	METHODOLOGY OF GROUNDWATER ASSESSMENT USING GEC	99
6.3.1	Groundwater Draft Estimation	99
6.3.2	Estimation of Annual Groundwater Recharge	99
6.3.2.1	Recharge from other sources	100
6.3.2.1.1	<i>Recharge due to canal seepage</i>	100
6.3.2.1.2	<i>Recharge from surface water & groundwater irrigation</i>	100
6.3.2.1.3	<i>Recharge from ponds and tanks</i>	100
6.3.2.2	Water Table Fluctuation (WTF) method	103
6.3.2.3	Rainfall Infiltration Factor (RIF) method	103
6.3.3	Net Annual Groundwater Availability	107
6.3.4	Categorisation of Areas for Groundwater Development	108

6.3.4.1	Stage of groundwater development	108
6.3.4.2	Long term groundwater level trend	110
6.3.5	Categorization of Areas for Groundwater Development	115
6.3.5.1	Safe areas with potential for development	115
6.3.5.2	Semi-critical areas for cautious groundwater development	116
6.3.5.3	Critical areas	116
6.3.5.4	Over-exploited areas	116
6.3.6	Well Wise Trend Analysis	117
6.3.7	Analysis of Salt Affected Area	121
6.4	CONCLUDING REMARK	121

CHAPTER 7	GROUNDWATER FLOW MODELING	123-156
7.1	PROLOGUE	123
7.2	GROUNDWATER MODELING	123
7.2.1	General Equation of Groundwater Flow	125
7.2.2	Flow in a Confined Aquifer	126
7.2.3	Flow in an Unconfined Aquifer	127
7.3	GROUNDWATER FLOW MODEL DESIGN	128
7.4	CONCEPTUALIZATION OF GROUNDWATER SYSTEM	128
7.4.1	Grid Designing	130
7.4.2	Time Discretisation	132
7.4.3	Model Parameterisation	132
7.4.3.1	Hydraulic parameters	132
7.4.3.2	Groundwater levels	133
7.4.3.3	Groundwater recharge & withdrawal	134
7.4.3.4	Boundary conditions	134
7.4.3.5	Time step	135
7.4.3.6	Tolerance criteria	135
7.5	DIRECT AND INVERSE PROBLEM	135
7.6	CALIBRATION OF GROUNDWATER FLOW MODEL	137
7.6.1	Parameter Optimization using PEST	138
7.6.2	Calibration Parameters	139
7.6.3	Control Parameters of PEST	139

7.6.4	Statistical Approach for Error Criteria	140
7.6.5	Steady State Simulation	141
7.6.6	Transient State Simulation	142
7.7	VALIDATION OF GROUNDWATER FLOW MODEL	145
7.8	RESULTS AND DISCUSSIONS	150
7.8.1	Calibrated Aquifer Parameter & Recharge	150
7.8.2	Sensitivity Analysis	150
7.8.3	Zone Budget	154
7.9	CONCLUDING REMARKS	156
 CHAPTER 8 GROUNDWATER VULNERABILITY MAPPING		157-167
8.1	PROLOGUE	157
8.2	METHODOLOGY	157
8.3	RESULTS AND DISCUSSIONS	159
8.3.1	Depth to Water Layer	159
8.3.2	Net Recharge Layer	160
8.3.3	Aquifer Media Layer	161
8.3.4	Soil Layer	162
8.3.5	Impact of Vadose Zone Layer	162
8.3.6	Hydraulic Conductivity of the Aquifer (C)	163
8.3.7	LULC Layer	164
8.3.8	Groundwater Vulnerability Map	164
8.3.9	Validation of Groundwater Vulnerability Map	165
8.4	CONCLUDING REMARK	167
 CHAPTER 9 GROUNDWATER QUALITY MODELING		168-188
9.1	PROLOGUE	168
9.2	METHODOLOGY	168
9.3	RESULT AND DISCUSSION	168
9.3.1	Spatial Variation of Groundwater Quality	168
9.3.1.1	pH layer	170
9.3.1.2	Total Dissolved Solids (TDS) layer	170
9.3.1.3	Calcium layer	172
9.3.1.4	Magnesium layer	173

9.3.1.5	Chloride layer	174
9.3.1.6	Nitrate layer	175
9.3.1.7	Fluoride layer	176
9.3.1.8	Sulfate layer	176
9.3.1.9	Bicarbonate layer	177
9.3.2	Statistical Correlation among various Quality Parameters	179
9.3.3	Hydrogeochemical Facies	179
9.3.4	Evaluation of Groundwater Quality Index (GWQI)	181
9.3.5	Groundwater Quality Analysis for Irrigation	182
9.3.5.1	Salinity	183
9.3.5.2	Chlorinity	184
9.3.5.3	Sodium Absorption Ratio (SAR) layer	184
9.3.5.4	Sodium percent (Na %) layer	186
9.3.5.5	Groundwater quality index for irrigation	187
9.4	CONCLUDING REMARK	188

CHAPTER 10 OPEN SOURCE WEB GIS TOOL FOR GROUNDWATER

	RESOURCE MANAGEMENT	189-204
10.1	PROLOGUE	189
10.2	GEOPORTAL	189
10.3	METADATA	190
10.4	METHODOLOGY USED	191
10.5	RESULTS AND DISCUSSIONS	193
10.6	CONCLUDING REMARK	204

CHAPTER 11 CONCLUSIONS AND RECOMMENDATIONS

11.1	CONCLUSIONS	205
11.2	RESEARCH CONTRIBUTION	206
11.3	FUTURE RECOMMENDATIONS	207

	REFERENCES	208-230
--	-------------------	---------

APPENDIXES

APPENDIX-I	Exploratory Boreholes Data	I
APPENDIX-II	Field Photographs	III
APPENDIX-III	Publications from the Study	VI

LIST OF FIGURES

Figures	Title of figures	Pg.
Fig. 1.1	World fresh water scenario	1
Fig. 1.2	Annual groundwater recharge	2
Fig. 1.3	Groundwater level fluctuation (1999-2008) for post-monsoon and pre-monsoon	3
Fig. 3.1	The study area	33
Fig. 3.2	Transportation network	34
Fig. 3.3	Rainfall pattern	35
Fig. 3.4	Topographical map sheets (scale 1:50,000) covering the study area	38
Fig. 4.1	Flowchart depicting study of data collection	42
Fig. 4.2	Methodology for geo-referencing	43
Fig. 4.3	Methodology for GIS database creation	44
Fig. 4.4	Methodology for watershed delineation	45
Fig. 4.5	Watersheds delineation through DEM	46
Fig. 4.6	Drainage layer	47
Fig. 4.7	Drainage density layer	48
Fig. 4.8	DEM layer	49
Fig. 4.9	Slope layer	50
Fig. 4.10	Geomorphology layer	51
Fig. 4.11	Geology layer	51
Fig. 4.12	Soil layer	52
Fig. 4.13	Hydrological soil group layer	53
Fig. 4.14	Landuse/landcover layer	54
Fig. 4.15	Rainfall layer	55
Fig. 4.16	Pre-monsoon groundwater depth layer	56
Fig. 4.17	Post-monsoon groundwater depth layer	56
Fig. 4.18	Water Level Fluctuation Layer (2006)	58
Fig. 4.19	Village map	58

Fig. 5.1	Flowchart of groundwater potential zones mapping	60
Fig. 5.2	Methodology of rainfall runoff modeling	66
Fig. 5.3	Methodology for delineation of suitable sites & artificial recharge structures	68
Fig. 5.4	Groundwater potential zones map	72
Fig. 5.5	Curve number layer	73
Fig. 5.6	Runoff map	74
Fig. 5.7	Drainage order map	76
Fig. 5.8	Prioritization map for water conservation	83
Fig. 5.9	Buffer map of drainage junctions	84
Fig. 5.10	Buffer map of habitated area	85
Fig. 5.11	Buffer map of canal layer	86
Fig. 5.12	Site suitability map for artificial recharge structures	87
Fig. 5.13	Location of proposed and already existing artificial recharge structures	90
Fig. 6.1	Location wells and raingauge stations	95
Fig. 6.2	Hydrogeological cross section along line AA'	96
Fig. 6.3	Hydrogeological cross section along line BB'	97
Fig. 6.4	Hydrogeological cross section along line CC'	98
Fig. 6.5	Methodology of groundwater assessment using GEC (1997, 2011) guidelines	101
Fig. 6.6 (a)	Groundwater draft in monsoon season (2004)	102
Fig. 6.6 (b)	Groundwater draft in non-monsoon season (2004)	102
Fig. 6.7 (a)	Groundwater recharge in monsoon season (2004)	104
Fig. 6.7 (b)	Groundwater recharge in non-monsoon season (2004)	107
Fig. 6.8	Net annual groundwater availability (2004)	109
Fig. 6.9	Stage of groundwater development (2004)	109
Fig. 6.10 (a)	Groundwater level trend in Bichhiya block	113
Fig. 6.10 (b)	Groundwater level trend in Bighapur block	113
Fig. 6.10 (c)	Groundwater level trend in Khiron block	113
Fig. 6.10 (d)	Groundwater level trend in Lalganj block	114
Fig. 6.10 (e)	Groundwater level trend in Purwa block	114

Fig. 6.10 (f)	Groundwater level trend in Sareni block	114
Fig. 6.10 (g)	Groundwater level trend in Sikandarpur Karan block	114
Fig. 6.10 (h)	Groundwater level trend in Sikandarpur Sarausi block	115
Fig. 6.10 (i)	Groundwater level trend in Sumerpur block	115
Fig. 6.11	Categorization of areas for groundwater development (2004)	117
Fig. 6.12	Spatial variation GWL trend in pre-monsoon season	120
Fig. 6.13	Spatial variation GWL trend in post-monsoon season	120
Fig. 6.14	Landsar TM image and salt-affected area for year 1989	122
Fig. 6.15	Landsar TM image and salt-affected area for year 2010	122
Fig. 7.1	Steps of groundwater flow modeling	129
Fig. 7.2	Conceptual model of study area	130
Fig. 7.3	Grid design of groundwater flow model	131
Fig. 7.4	Spatial distribution of hydraulic conductivity of study area alluvial aquifer	133
Fig. 7.5 (a)	Direct problem in groundwater hydrology	136
Fig. 7.5 (b)	Inverse problem in groundwater hydrology	136
Fig. 7.6	Steps in automatic calibration	138
Fig. 7.7	Equipotential map of simulated and observed hydraulic heads	142
Fig. 7.8	Scattergram between observed and calculated heads, steady state simulation	144
Fig. 7.9	Scattergram between observed and calculated heads, transient state simulation	144
Fig. 7.10	Errors (seasonal) during the calibration period (0-2920) and Validation period (2920 – 4015 days)	145
Fig. 7.11 (a)	Groundwater level elevations for Ajabkhera well after calibration and validation	146
Fig. 7.11 (b)	Groundwater level elevations for Asgarganj well after calibration and validation	146
Fig. 7.11 (c)	Groundwater level elevations for Babu Khera well after calibration and validation	146
Fig. 7.11 (d)	Groundwater level elevations for Baksar well after calibration and validation	147
Fig. 7.11 (e)	Groundwater level elevations for Bara well after calibration and validation	147

Fig. 7.11 (f)	Groundwater level elevations for Bhagwant Nagar well after calibration and validation	147
Fig. 7.11 (g)	Groundwater level elevations for Bichhiya well after calibration and validation	147
Fig. 7.11 (h)	Groundwater level elevations for Chanda well after calibration and validation	148
Fig. 7.11 (i)	Groundwater level elevations for Gangaghat well after calibration and validation	148
Fig. 7.11 (j)	Groundwater level elevations for Lalganj Piezo well after calibration and validation	148
Fig. 7.11 (k)	Groundwater level elevations for Lalganj-2 (OW) after calibration and validation	148
Fig. 7.11 (l)	Groundwater level elevations for Paliyaveer Singhpur well after calibration and validation	149
Fig. 7.11 (m)	Groundwater level elevations for Pariyar well after calibration and validation	149
Fig. 7.11 (n)	Groundwater level elevations for Purwa well after calibration and validation	149
Fig. 7.11 (o)	Groundwater level elevations for Ralpur well after calibration and validation	149
Fig. 7.11 (p)	Groundwater level elevations for Saraiya well after calibration and validation	150
Fig. 7.11 (q)	Groundwater level elevations for Sumerpur well after calibration and validation	150
Fig. 7.12	Calibrated hydraulic conductivity of study area	151
Fig. 7.13	Calibrated specific yield of study area	151
Fig. 7.14	Sensitivity analysis of hydraulic conductivity	152
Fig. 7.15	Sensitivity analysis of specific yield	153
Fig. 7.16	Sensitivity analysis of recharge	153
Fig. 8.1	Methodology for DRASIC-LU model	158
Fig. 8.2	Average depth to water layer from (1985-2007)	160
Fig. 8.3	Net Recharge layer (1997-2004)	161
Fig. 8.4	Aquifer Media layer	162
Fig. 8.5	Impact of Vadose Zone layer	163
Fig. 8.6	Hydraulic conductivity layer	164

Fig. 8.7	Groundwater vulnerability map overlaid with nitrate data	165
Fig. 8.8	Groundwater vulnerability map overlaid with fluoride data	166
Fig. 8.9	Relationship between groundwater depth and nitrate in shallow aquifer	167
Fig. 9.1	Flowchart used for preparing GWQI	169
Fig. 9.2	pH layer	171
Fig. 9.3	TDS layer	171
Fig. 9.4	Calcium layer	172
Fig. 9.5	Magnesium layer	173
Fig. 9.6	Chloride layer	174
Fig. 9.7	Nitrate layer	175
Fig. 9.8	Fluoride layer	177
Fig. 9.9	Sulfate layer	178
Fig. 9.10	Bicarbonate layer	178
Fig. 9.11	Piper trilinear diagram	180
Fig. 9.12	Groundwater quality index map	182
Fig. 9.13	Salinity index for the groundwater samples of the study region	183
Fig. 9.14	Electrical conductivity layer	184
Fig. 9.15	Chlorinity index for the groundwater samples of the study region	185
Fig. 9.16	Sodium Adsorption Ratio layer	186
Fig. 9.17	Sodium percent layer	187
Fig. 9.18	Groundwater quality index map for irrigation purpose	188
Fig. 10.1	The architecture of MapGuide open source (MapGuide, 2010)	190
Fig. 10.2	Methodology used	192
Fig. 10.3	Website Main Page	194
Fig. 10.4	Geoportal main page	195
Fig. 10.5	Feature information using identify tool	196
Fig. 10.6	Coverage analysis using buffer tool	197
Fig. 10.7	Thematic map of block layer	198
Fig. 10.8	Thematic map of soil layer	198
Fig. 10.9	Thematic map of geomorphology layer	199
Fig. 10.10 (a)	Metadata of soil map (feature view)	200

Fig. 10.10 (b)	Metadata of soil map (data view)	200
Fig. 10.11	Mashup application using web services (Sub-watershed overlay on Google Earth image)	201
Fig. 10.12	Mashup application using web services (Road is overlay on Google map)	201
Fig. 10.13 (a)	Spatial query	202
Fig. 10.13 (b)	Result of spatial query	203
Fig. 10.14	Groundwater quality of Loni sub-watershed 1	203

LIST OF TABLE

Tables	Title of Tables	Pg. No.
Table 2.1	Decision rules for selecting favorable artificial recharge sites	16
Table 3.1	Data collection and their sources	37
Table 3.2	Sensor specifications	38
Table 4.1	Categories used for classification of slope layer	49
Table 4.2	Hydrological soil group and major soil types	53
Table 4.3	Blocks and villages in study area	57
Table 5.1	Saaty's scale	61
Table 5.2	Weightage of different parameters for groundwater potential zones mapping	63
Table 5.3	Formulae used for computation of morphometric parameters	67
Table 5.4	Criteria used for site selection for artificial recharge structures	68
Table 5.5	Groundwater potential zones and pumping well yield data	71
Table 5.6 (a)	Morphometric parameters of sub-watersheds	77
Table 5.6 (b)	Morphometric parameters of sub-watersheds	77
Table 5.6 (c)	Morphometric parameters of sub-watersheds	78
Table 5.7	Prioritization of sub-watersheds	82
Table 5.8	Area statistics of buffer map of drainage junctions	83
Table 5.9	Area statistics of buffer map of habitated area	84
Table 5.10	Area statistics of buffer map of canals	85
Table 5.11	Area statistics for site suitability map of artificial recharge structures	87
Table 5.12	Morphometric parameters and proposed structures of sub-watersheds	89
Table 6.1	Sub-surface geology	94
Table 6.2	Gross groundwater draft	99
Table 6.3	Total recharge from the other sources	105
Table 6.4	Rainfall recharge by water table fluctuation method	106
Table 6.5	Rainfall recharge by Rainfall Infiltration Factor (RIF) method	106
Table 6.6	Rainfall recharge during monsoon season	107
Table 6.7	Net annual groundwater availability	108
Table 6.8	Categorization of groundwater assessment unit	116

Table 6.9	Analysis of groundwater level trends in pre-monsoon season using the Mann-Kendall test for wells of period 1985-2009	118
Table 6.10	Analysis of groundwater level trends in post-monsoon season using the Mann-Kendall test for wells of period 1985-2009	119
Table 7.1	Time discretisation adopted for different parameters	132
Table 7.2	Convergence threshold adopted in solver (WHS)	136
Table 7.3	Range of initial values of hydraulic parameters used in the calibration process	139
Table 7.4	Initial setting is used in Parameter Estimation (PEST) calibration	141
Table 7.5	Average errors of calibration and validation time periods	145
Table 7.6	Changes in error during sensitivity analysis of hydraulic conductivity	152
Table 7.7	Changes in error during sensitivity analysis of specific yield	153
Table 7.8	Changes in error during sensitivity analysis of recharge	154
Table 7.9	Water budget of the whole model for each stress period	155
Table 8.1	DRASIC-LU parameters normalized weights	159
Table 9.1	Statistical analysis of physical and chemical groundwater quality parameters	169
Table 9.2	Area statistics of pH layer	170
Table 9.3	Area statistics of TDS layer	170
Table 9.4	Area statistics of calcium layer	172
Table 9.5	Area statistics of magnesium layer	173
Table 9.6	Area statistics of chloride layer	174
Table 9.7	Area statistics of nitrate layer	175
Table 9.8	Area statistics of fluoride layer	176
Table 9.9	Area statistics of sulfate layer	177
Table 9.10	Area statistics of bicarbonate layer	177
Table 9.11	Correlation matrix for groundwater quality variables	179
Table 9.12	Suitability of groundwater for irrigation based on electrical conductivity	184
Table 9.13	Suitability of groundwater for irrigation based on sodium adsorption ratio	186
Table 9.14	Suitability of groundwater for irrigation based on sodium percent	187

ABBREVIATIONS USED

AHP	Analytical Hierarchical Process
AJAX	Asynchronous JavaScript and XML
AMC	Antecedent Moisture Condition
AMSL	Above Mean Sea Level
ARS	Artificial Recharge Structures
ASTER	Advance Space Borne Thermal Emission and Reflection Radiometer
BGL	Below Ground Level
CGWB	Central Ground Water Board
Cl	Chloride
CN	Curve Number
CPCB	Central Pollution Control Board
CSW	Catalogue Service for the Web
DEM	Digital Elevation Model
EC	Electrical Conductivity
ERDAS	Earth Resources Data Analysis System
ESRI	Environmental System Research Institute
ETM+	Enhanced Thematic Mapper
F	Fluoride
FAO	Food and Agriculture Organization
GCP	Ground Control Points
GEC	Groundwater Estimation Committee
GIS	Geographical Information System
GLCF	Global Land Cover Facility
GSI	Geological Survey of India
GPS	Global Positioning System
GWFM	Groundwater Flow Model
GWPI	Groundwater Potential Index
GWQI	Groundwater Quality Index
GWPZ	Groundwater Potential Zones
HSG	Hydrological Soil Groups
IIS	Internet Information Services

IMD	Indian Meteorological Department
IMSD	Integrated Mission for Sustainable Development
INCOH	Indian National Committee on Hydrology
IRS	Indian Remote Sensing
K	Hydraulic conductivity
Km	Kilo meter
Km ²	Square Kilo meter
LISS	Linear Imaging Self Scanning
LPM	Litre Per Minute
LULC	Land Use/Land Cover
m	meter
m ²	Square meter
m ³	Cubic meter
MAE	Mean Absolute Error
MCDM	Multi-Criteria Decision Making
MCM	Million Cubic Meter
ME	Mean Error
MySQL	My Structured Query Language
Na	Sodium
NBSS&LUP	National Bureau of Soil Survey & Landuse Planning
NRSC	National Remote Sensing Center
PAN	Panchromatic
PHP	Hypertext Preprocessor
PMWIN	Processing Modflow for Windows
RMS	Root Mean Square
RS	Remote Sensing
SAR	Sodium Absorption Ratio
SESS	Spatial Expert Support System
SGWB	State Groundwater Board
SRTM	Shuttle Radar Topographic Mission
S _s	Specific Storage
SCS	Soil Conservation Service
SOI	Survey of India
S _y	Specific yield

TDS	Total Dissolved Solids
TIN	Triangulated Irregular Network
TM	Thematic Mapper
UPPCB	Uttar Pradesh Pollution Control Board
USGS	United State Geological Survey
VES	Vertical Electrical Surroundings
WFS	Web Feature service
WMS	Web Map Service

1.1 PROLOGUE

Groundwater is a precious natural resource of water that is held in aquifer. It is an important source of water supply throughout the world (Singh *et al.*, 2013). The management of groundwater resources is the pre-requisite for whole world due to increasing demand of water, as these resources remain constant. The total volume of water on Earth is about 1.4 billion km³, out of these 35 million km³ or about 2.5% of the total volume is freshwater (UNEP, 2008) as shown in Figure 1. The 70% or 24 million km³ volume of the total freshwater resources are in the form of ice and permanently snow covered in mountainous regions, the Antarctic & Arctic regions. About 30% of the world's freshwater resources are available in the form of groundwater (Figure 1.1). The total usable freshwater supply for all living beings is about 200000 km³ of water; which will be less than 1% of all freshwater resources (Gleick, 1993; Shiklomanov, 1999).

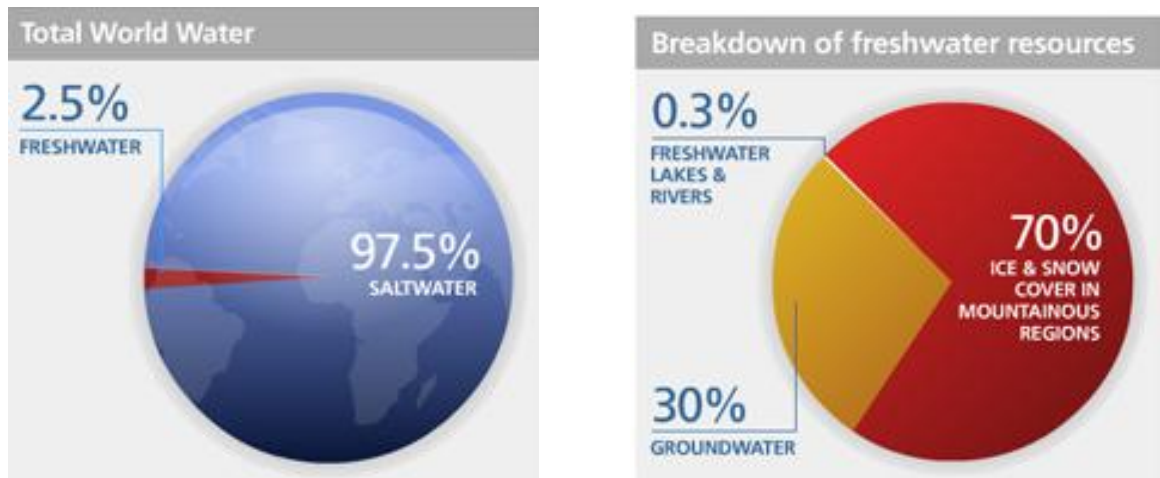


Fig. 1.1: World fresh water scenario

Population-wise, India is one of the biggest countries in the world, and area-wise it has only 1/50th part of the world's land, and the water resources are 1/25th part of total available water resources (Water Management Forum, 2003). The groundwater is a dynamic resource which is replenished every year. The main sources of groundwater recharge are rainfall, return flow from irrigation, seepage from canal & water bodies and recharge due to artificial water conservation structures (CGWB, 2006). Out of these, rainfall is major contributor in groundwater recharge as shown in Figure 1.2. The annual replenish able groundwater resource

for the whole country is 433 billion cubic meters (BCM) out of these 231 BCM are draft for irrigation, domestic & industrial uses. Keeps 34 BCM in account of natural discharge, and only 168 BCM of groundwater are left for future utilization.

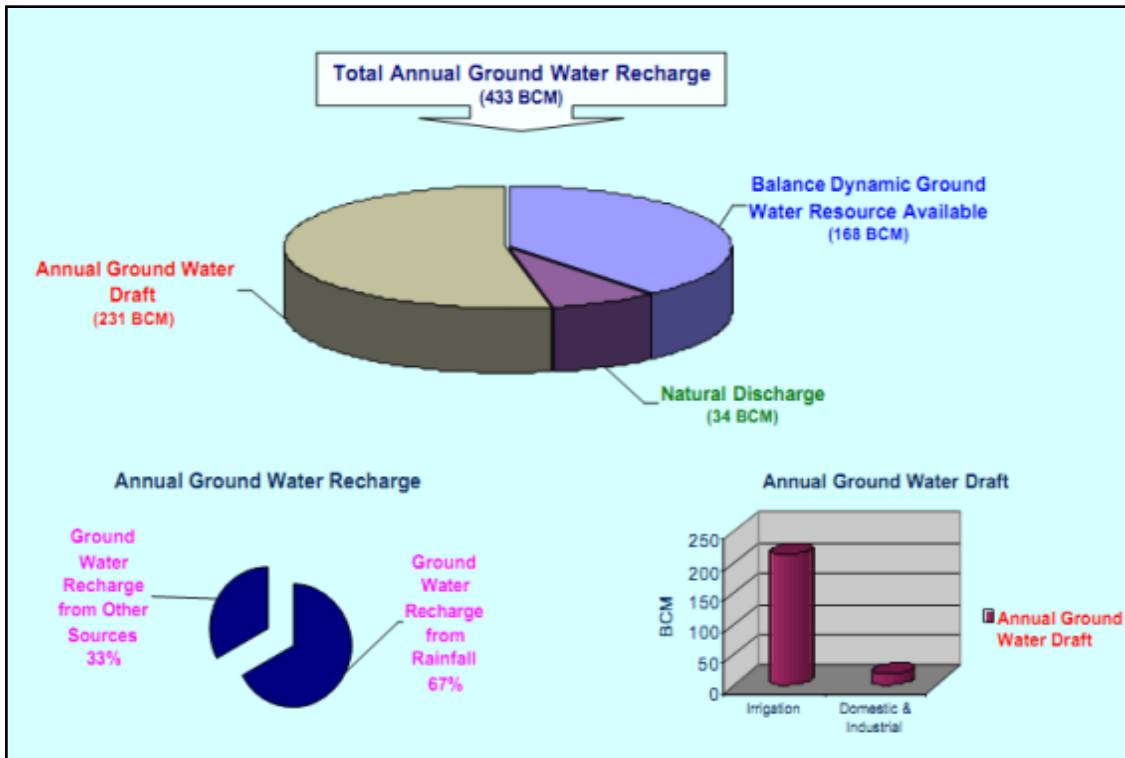


Fig. 1.2: Annual groundwater recharge (Source: National Informatics Centre, 2007)

In India, 30% urban and more than 90% of the rural population depend upon groundwater for their basic needs (Reddy *et al.*, 1996). Unfortunately, shortage of surface water resources and high usage of groundwater resources without appropriate management plans are common in several parts of India (Rodell *et al.*, 2009; Tiwari *et al.*, 2009; Jha *et al.*, 2010). Due to increasing water scarcity and the climate change affect on water resources, it is essential that groundwater must be used efficiently and in a cost-effectively manner both for present and future generations. Safe drinking water is a basic need for human being to sustain a healthy life.

A comparative map on depth of water level during pre-monsoon (May 2009) and post-monsoon (November 2009) with decadal mean (1999-2008) shown in Figure 1.3. It is disclosed that in pre-monsoon period water level is declined in entire country except some states; Andhra Pradesh, Gujarat, Karnataka and Tamil Nadu, where most of the wells shows rising trend as well as in post-monsoon period water level is declined only in rainfall deficient states (CGWB, 2010).

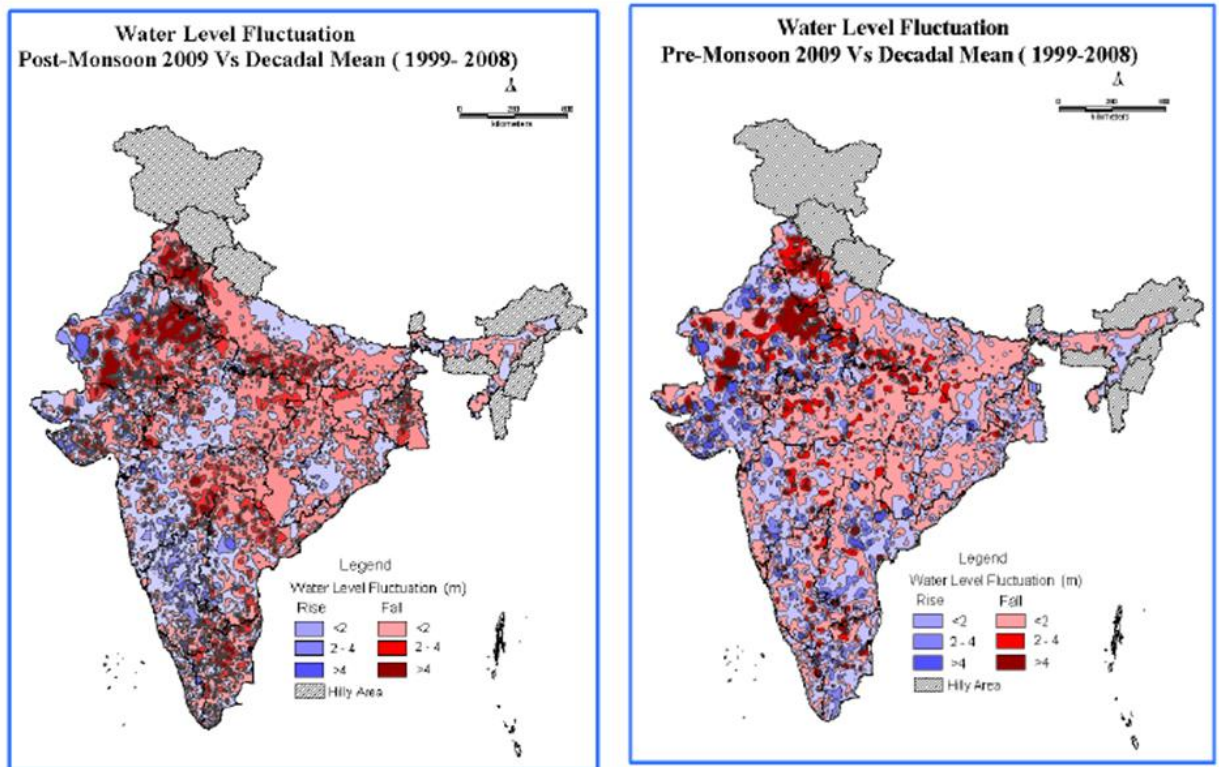


Fig.1.3: Groundwater level fluctuation (1999-2008) for post-monsoon and pre-monsoon (Source: CGWB, 2010)

In India, not only fall the groundwater table, groundwater quality also degraded due to rapid unplanned urbanization, high growth of population, modern agricultural practices (such as, extensive use of fertilizers and pesticides in agriculture), poor sewage system and not proper disposable sites for waste water of household and industrial activities (Rao and Gupta, 2000; Barker *et al.*, 2001; Ghosh, 2002; Saxena *et al.*, 2004; Mondal *et al.*, 2005; Tariq *et al.*, 2005; Venugopal *et al.*, 2008; Mondal *et al.*, 2009; Pathak & Hiratsuka 2009). Once groundwater is contaminated, it is very expensive to make it uncontaminated as its takes long time to recover. Additionally, spatial inconsistency and data limitations preclude monitoring of all waters and make remediation activities expensive and often impractical (Babiker *et al.*, 2005; Qinghai *et al.*, 2007; Yang, 2010). Groundwater contamination not only affects the water quality but also menaces to human health, economic development, and social wealth (Sadat-Noori *et al.*, 2014).

1.2 ROLE OF SPATIO-TEMPORAL ANALYSIS

In the past, both spatial and temporal analyses have not been used frequently. Spatial analysis has been focused on sustaining the modeling and querying of geometries associated with objects in a database (Guting, 1994). While, temporal analysis has been focused on

broaden the knowledge kept in a database of current and past of the real world (Erwig *et al.*, 1999). But, many people think that spatial and temporal analysis are closely related to each other because they both deal with some kind of “dimensions” or “spaces”, and their integration is very significant for many applications. In other words, spatio-temporal analysis means dealing with the geometries of real world that change with respect to time. It has been widely used in many real world studies, such as groundwater trend analysis, climate change, traffic monitoring, crop inventory etc (Brahmabhatt *et al.*, 2000; Ray *et al.*, 2002; McBride *et al.*, 2003; Raghunath *et al.*, 2005; Ahmadi & Sedghamiz, 2007; Zhang *et al.*, 2009; Machiwal *et al.*, 2012; Shen *et al.*, 2014).

1.3 REMOTE SENSING, GIS & GROUNDWATER MODELING

Groundwater can't be seen directly from the surface of earth, but variety of techniques that provides the information about its potential occurrence, directly or indirectly. Remote Sensing (RS) is one of the advanced technologies that have been used for understanding sub-surface water condition (Todd, 1980) with an advantage of spectral, spatial and temporal availability of data that covers huge inaccessible areas within a short span of time; it has become a very handy tool for accessing, preserving and monitoring the groundwater resources (Gupta *et al.*, 2010). For decades, RS images have been successfully used for the mapping and extraction of surface structures, like geomorphology, geology, slope, soil type, landuse, fractures, recharge & discharge areas salinity, crop and lineament etc (Srivastava *et al.*, 1997; Ray and Dadhwal, 2001; Shaban and Dikshit, 2002; Ramasamy *et al.*, 2006; Mukherjee *et al.*, 2007; Dar *et al.*, 2010). Integration of these layers with the help of hydro-geological investigation provides rapid and profitable delineation of groundwater potential zones. Although, it has been possible to integrate these layers visually to delineate the groundwater potential zones but it is difficult, time consuming and erroneous (Pothiraj and Rajagopalan, 2012).

Contour maps that can be developed or created using Geographical Information System (GIS) software can be exported directly to the others formats and taking as it is in groundwater modeling. On the other hand, all data including RS images can be organized and stored in GIS system. Groundwater related parameters, such as water table contour maps, aquifer bottom, aquifer thicknesses, hydraulic parameters (permeability, porosity, transmissivity, storativity and others), and other type of information can be analyzed effectively using GIS (Howari, 2007).

In the recent years, GIS has been adopted rapidly in groundwater management studies. GIS is now widely used to create digital geographic database and it has also helpful for creation of input data for various models and to display the results of model outputs. GIS, combing all data in a logical structure that link to a computing environment, provides a powerful tool for hydro-geological studies. A hydro-geological GIS database offers facilities for hydro-geological modeling. These functions allow primarily overlay or index operations, but newly available GIS functions support the requirement of process based approaches (Gogu *et al.*, 2001; Thach *et al.*, 2012).

GIS is not only effectively works on potential recharge studies but also it plays a major role in groundwater pollution studies (Praharaj *et al.*, 2002; Babikar *et al.*, 2004 & 2007; Asadi *et al.*, 2007). In contrast with surface water contamination, groundwater contamination is difficult to detect, and is even more difficult to control, which may persist for years, decades, or even centuries (Todd, 1980; Rahman *et al.*, 2008). Groundwater vulnerability is defined as the possibility of groundwater contaminants through percolation and diffusion from the ground surface (Vrba & Zoporozec, 1994; Babiker *et al.*, 2005; Jamrah *et al.*, 2007). Therefore, the vulnerability studies can provide valuable information for stakeholders working on preventing further deterioration of the environment (Mendoza and Barmen 2006). Additionally, aquifer vulnerability studies are useful in the evaluation of economic impacts of waste disposal in highly vulnerable areas. Moreover, they provide preliminary information and criteria for decision-making in such areas as designation of land-use controls, delineation of monitoring networks, and management of water resources in the context of regional planning as related to protection of groundwater quality (Bachmat and Collin, 1990; Kim *et al.*, 2009).

The International Association of Hydrologists (1994) proposed the definition of vulnerability as "an intrinsic property of a groundwater system which depends on the sensitivity of that system to human and/or natural impacts. The ultimate goal of a vulnerability map is a subdivision of an area into several units that show the differential potential for a specified purpose and use. Results of a vulnerability assessment are portrayed on a map that shows various homogeneous areas, each of which has unique levels of vulnerability, and do not represent absolute values".

According to Robins (1998), "the management of both groundwater resources and of individual groundwater sources cannot sensibly be undertaken without some knowledge of

recharge: its quantity, its seasonality and above all, the different routes through the sub-soil and the unsaturated zone by which it can occur". Recharge plays a major role in the assessment of groundwater vulnerability to contamination.

According to Foster (1998) "since the transport of most groundwater contaminants, with the exception of density driven contaminants, such as DNAPLs (Dense Nonaqueous Phase Liquids), to saturated aquifers occurs in the aqueous phase as part of the recharge process, assessing aquifer pollution vulnerability, is inextricably linked with understanding groundwater recharge mechanisms". Groundwater vulnerability maps are very useful for municipal planners and developers regarding landuse allocation, well locations and pumping regulations. This is especially important in areas where the underlying aquifers are exploited extensively.

Groundwater models can be used to simulate historical conditions and predicting future aquifer conditions. For future, predictions model should be capable of reproducing the field observations. Before predicting the future scenario, it is necessary to assess the uncertainty of the model calibrated parameters. Groundwater modeling in spatial variables is a data intensive task for which GIS techniques have become a popular tool because of their capacity to handle both spatial and non-spatial data (Hendricks *et al.*, 2006).

Integrated RS and GIS can be used as a platform to analyze diverse data sets. Numerical groundwater modeling techniques can be used to simulate the groundwater system. Combining satellite measurements with a physically based model supported by GIS may be the only practical approach for understanding the role of groundwater in the global water cycle (Becker, 2006).

1.4 PROBLEM IDENTIFICATION AND SCOPE OF STUDY

Throughout the world regions, sustainable groundwater balance is shrinking due to over abstraction, water logging and salinization. As well as groundwater is contaminated due to agricultural, industrial and other human activities. The decreasing water table and groundwater contamination are critical problems in effective groundwater management of Loni and Morahi watershed, the sub-watershed of Ganga basin in UP State, India. In this study, spatio-temporal analysis has been carried out with the help of RS, GIS and groundwater flow modeling to manage groundwater resources of the watersheds in an effective way.

Although surface water is the main source of water for agriculture, the region depends on groundwater for domestic purposes and small scale irrigation and water supply schemes. Over the last decade, groundwater usage through tube wells has increased sharply in the area but groundwater is not properly managed as an additional source. Sustainable aquifer exploitation occurs when the rate of groundwater extraction is equal or less than the natural rate of groundwater replenishment for any level of aquifer storage. Thus to be able to exploit aquifer in a sustainable manner with minimal impact on the environment, there is a need to demarcate and evaluate the aquifer potential. Already it has been reported that in similar regions of Asia, the groundwater table is falling at an alarming rate (Seckler *et al.*, 2001).

Since the groundwater of the area is not adequately investigated, lack of information and knowledge may be a problem for the development and management of the aquifer in the area. In order to ensure a judicious management of groundwater, proper evaluation is required. In addition, its present status should be studied and prediction for the future status attempted. It is therefore necessary to allocate areas with high groundwater potential and better to improve control of abstraction rates to ensure proper groundwater management. Due to the lack of reliable data on the particular basin, the proposed work will serve for the future hydro-geological study in this area. Moreover, this work can be extended to the entire catchment as more detail information is collected and added to the database. In addition to above, the scope of this work is to develop a web interface, and online decision making tool that supports GIS to facilitate sustainable development of groundwater resources.

1.5 OBJECTIVE OF THE STUDY

- Collection of relevant data and creation of a GIS database for Loni & Morahi watersheds with the help of RS images and ancillary data.
- Mapping of quality and quantity of groundwater.
- Groundwater flow modeling using PMWIN.
- Identification of artificial recharge structures using RS and GIS technique.
- Groundwater management in affected areas.
- Development of a web-enabled tool to study ground water resources.

1.6 ORGANISATION OF THESIS

The complete thesis has been divided into 11 chapters. The arrangement of the chapters is as given below:

Chapter 2 Literature review

This chapter focuses on the literature review of groundwater potential, recharge, quality, flow modeling studies to manage the groundwater resources in an efficient manner. It also links some literature related to development of web-enabled tool.

Chapter 3 The study area, data and software used

In this chapter, details of study area, software and data used to map and manage the groundwater resources and develop the web enabled tool, have been described.

Chapter 4 Creation of spatial and non-spatial database

This chapter provides the basics steps for creation of spatial and non spatial databases.

Chapter 5 Groundwater management using RS and GIS techniques

This chapter describes the details methodology of estimation of groundwater potential map, rainfall runoff modeling, morphometric analysis to find out the suitable location of artificial recharge structures using RS and GIS.

Chapter 6 Analysis of groundwater condition to estimation of dynamic groundwater resource and trend analysis

This chapter explains the overall approach as well as stepwise procedure for analysis of groundwater condition, estimation of groundwater resources using Groundwater Estimation Committee (GEC) guidelines (MOWR, 2011) to find out the trend of groundwater level.

Chapter 7 Groundwater flow modeling

This chapter contains the overall approach as well as detailed methodology for the application of a groundwater flow model using PMWIN package.

Chapter 8 Groundwater vulnerability mapping using GIS

This chapter covers the overall approach as well as detailed methodology for the development of groundwater vulnerable zones map using GIS, and subsequently verification of output map with nitrate and fluoride concentration.

Chapter 9 Analysis of suitability of groundwater quality for irrigation and drinking purposes

This chapter describes the overall approach as well as detailed methodology for the development of a groundwater suitability index map for drinking and irrigation purposes.

Chapter 10 Development of web enabled tool for groundwater resource management

This chapter outlines the development of a web-enabled tool for groundwater resource assessment.

Chapter 11 Conclusions and recommendations

This chapter concludes the major outcomes of this work, and provides the recommendations for future to carry out groundwater management studies using RS and GIS technology.

2.1 PROLOGUE

Several studies have been carried out related to various aspects of groundwater management & modeling at national and international level by scientific, technical and research community. However, it is found that the approaches adopted are site specific, and the definition of problem, methods proposed and solution achieved are unique in nature for the area. In this chapter, few case studies carried out in the past to manage the groundwater resources using advanced techniques like RS, GIS and groundwater modeling based studies has been discussed. It is also described as to how these methods are effective in groundwater related problems. In addition, some studies related to development of open source web based GIS tool are also listed.

2.2 APPLICATION OF RS AND GIS IN GROUNDWATER STUDIES

2.2.1 Groundwater Potential

Groundwater potential is defined as the total available amount of groundwater in respective area but from groundwater investigation view, it can be defined as the possibility of groundwater happening in an area. Appropriate information of groundwater potential will be very helpful for decision and policy makers to identify the suitable locations for drilling production and/or monitoring wells. It is also helpful to protect vital groundwater resources from contamination (Jha *et al.*, 2010). In the past, several researchers from India and abroad (Krishnamurthy and Srinivas, 1995; Kamaraju *et al.*, 1996; Krishnamurthy *et al.*, 1996; Murthy, 2000; Shahid *et al.*, 2000; Jaiswal *et al.*, 2003; Rao and Jugran, 2003; Sikdar *et al.*, 2004; Sener *et al.*, 2005; Pirasteh *et al.*, 2006; Solomon and Quiel, 2006; Ganapurama *et al.*, 2008; Chenini *et al.*, 2010; Rashid *et al.*, 2011; Magesh *et al.*, 2012; Suganthi *et al.*, 2013; Elmahdy *et al.*, 2014) have successfully used RS and GIS techniques for the assessment of groundwater potential. Thematic layers used for delineating groundwater potential zones using RS and GIS techniques are significantly vary from one study to other, and their selection is random. The assignment of weights to different thematic layers and their classes are solely based on their personal decisions. Some of these discussed below:

Krishnamurthy and Srinivas (1995) choose three different sites in Karnataka state of India to estimate various groundwater occurrence factors. They outlined the usefulness of Indian Remote Sensing (IRS) satellite sensor data in groundwater studies. The comparative study shows that all the three drainage basins have similar types of hydro-geomorphic landforms, but they vary in terms of their characteristic, behaviour and spatial distribution. The result demonstrates that IRS sensor data are very useful for to delineating groundwater occurrence factors (such as lithology, structures and landforms) in hard rock areas.

Kamaraju *et al.*, (1996) delineates the groundwater prospect map using GIS in west Godavari district, Andhra Pradesh, India. They analyzed various factors viz., lithology, geomorphology, structure, and recharge condition to determine the occurrence and distribution of groundwater in the study area. They firstly converted conventional data, such as existing map of different scales and records into meaning full GIS database to delineate the groundwater prospect map. The study has revealed that the GIS techniques are cost-effective and can be employed successfully in the planning stages of a groundwater exploration programme. In addition, the GIS data generated for the study of groundwater prospects can be updated and used for the planning and management of groundwater resources of the district.

Krishnamurthy *et al.*, (1996) delineated groundwater potential map of Marudaiyar basin, TamilNadu, India using RS and GIS techniques. Thematic maps of lithology, landforms, lineaments, surface water bodies are extracted from satellite image and drainage density and slope map has been prepared using SOI (Survey of India) toposheets. All the thematic maps were integrated with the set of logical conditions in a GIS environment to delineate groundwater potential zone map. Finally, the groundwater potential zone map was verified with the help of field data, which exhibits a good correlation.

Murthy (2000) investigated the groundwater potential in huge geographical area with orientation to watershed planning in Varaha River basin, A.P., India. All thematic maps viz., Land Use/Land Cover (LULC), soils and hydro-geomorphology, are interpreted from RS images of Landsat TM (Thematic Mapper) and IRS satellite images. Slope and other layers are extracted from topographic maps. Groundwater potential map was delineated to assign subjective weight to individual thematic and topographic layer according to its infiltration capacities using overlay operation. The final map is categorized into seven classes; very good to very poor according to their relative importance. Finally, the groundwater potential map is

verified using geophysical survey. About 47 Vertical Electrical Surroundings (VES) were conducted to randomly selected locations in various groundwater potential zones identified by GIS, and geophysical survey shows positive result.

Shahid *et al.*, (2000) delineated the groundwater potential zones using GIS tool in the soft rock area of Midnapur district, West Bengal, India. They used seven hydrogeological themes viz. geomorphology, lithology, soil, drainage density, surface water bodies, slope and net recharge. All the themes are delineated or derived from IRS-1B LISS-II (Linear Imaging Self Scanning-II) RS data, except slope and net recharge. Slope is calculated using topographic map, and net recharge is calculated using groundwater fluctuation data. All the thematic layers and their individual classes are assigned weights according to its relative importance towards demarcation of groundwater potential zones. The developed GIS based model was verified with boreholes and pumping test data, and a good correlation was found.

Singh *et al.*, (2002) demarcated groundwater potential maps of Sonbhadra, Mirzapur & Chaundali districts of U.P., India using RS, GIS and geoelectrical techniques. In this study, hydro-geomorphological and lineament maps are prepared using IRS-1B LISS-II data and other maps, such as slope, aquifer thickness, lineament and clay thickness are prepared from topographical maps and field data. All the thematic maps are integrated in ArcInfo grid environment to develop a groundwater potential map. It is then verified using the yield data and a good correlation was achieved.

Jaiswal *et al.*, (2003) developed a village-wise groundwater prospects zones map to identify the suitable locations for the potable water for rural population using RS and GIS in Gorna sub-basin, a part of the Son watershed, Madhya Pradesh, India. In this study, LISS III and Panchromatic images of IRS are used to prepare the maps of lithology, landforms, LULC, lineaments, surface water bodies and soils, village, drainage density and slope. To demarcate the groundwater prospects zones, all the thematic layers are assigned suitable weight according to their importance in groundwater studies and then these are integrated in GIS environment using weighted overlay analysis of ArcInfo software.

Sikdar *et al.*, (2004) used RS and GIS technique to identify the major change occurs in LULC of Raniganj area from 1972 to 1998 and to find out the groundwater potential zones for future groundwater development. The study indicates that settlement and vegetation areas has

been decreased in the expense of mining activity due to this overload dump, barren land, waste land and abandoned quarry filled with water area increases. To develop a groundwater potential zones map, thematic layers, such as drainage texture, geomorphology, lithology, current landuse and steepness of slope and frequency of lineaments are integrated using overlay and multi-criteria technique in GIS environment. They also suggested groundwater structures that are feasible in various potential zones.

Sener *et al.*, (2005) used RS and GIS technique for investigation of new water resource in Burdur city and its surrounding villages. To demarcate the new water resource, they delineated groundwater potential zones. All the thematic maps, such as geology, lineament density, LULC, annual rainfall, topography, slope and drainage density are prepared from Landsat TM image and topographic maps. Groundwater potential zone map was prepared using a model developed based on GIS techniques. It proved to be a suitable method for estimation of groundwater potential.

Sreedevi *et al.*, (2005) delineated groundwater potential zones in the Pageru River basin of Cuddapah district, A.P., India using RS and geophysical techniques. They delineated various geo-morphological units based on their characteristics, such as textures, tones, vegetative cover, lineaments and relief linearity using IRS-1B, LISS-II data. The hydro-geomorphological data were supported from evidence of the pre and post monsoon water table fluctuation data. They also conducted VES at 112 locations using Schlumberger electrode configuration to verify the hydro-geomorphological map. To delineate groundwater potential map all the thematic layers viz. hydrogeology, geomorphology and interpolated resistivity map were integrated in GIS environment, and classified to in three classes and proved that it is an efficient technique to delineate the groundwater potential zones with greater accuracy

Solomon and Quiel (2006) delineated groundwater potential zones in Eritrea using the combination of RS, Digital Elevation Models (DEM), GIS and field work techniques. Geomorphology, lithology, slope and lineament maps are prepared using RS data and DEM. Field data are used to verify the derived maps. The overall study reveals that RS and GIS are potentially powerful tools for groundwater resource assessment and designing an appropriate investigation plans.

In the recent past, many researchers have used Multi Criteria Decision Making (MCDM) technique for finding the weights, which provides a cost-effective tool for groundwater potential modeling and groundwater management. Saaty's Analytical Hierarchical Process (AHP) is a widely used MCDM technique in the field of water resources engineering (Pawattana and Tripathi, 2008). The method was developed by Professor Thomas L. Saaty in the 1977s. Since then, the method has received numerous applications in natural resources and environmental planning and management (Saaty, 1980). AHP has been accepted by the international researcher community as a very efficient tool for dealing with complex decision problems. So many users employ MCDM technique to carry out the groundwater potential modeling (Srivastava and Bhattacharya, 2006; Chowdhury *et al.*, 2009; Murthy *et al.*, 2009; Jha *et al.*, 2010; Fashae *et al.*, 2013; Bhunia *et al.*, 2014; Mallick *et al.* 2014; Shekhar *et al.*, 2014). Some of these are discussed below:

Srivastava and Bhattacharya (2006) demarcated the groundwater potential index in hard rock terrain of Bargarh district, Orissa, India. They extracted thematic layers from RS images and collateral data collected from field studies and re-sampled at same resolution. Each thematic layer and its features have been assigned weight according to its potency of contributing towards groundwater assessment. To normalize the weights for better results AHP procedure developed by Saaty is used after applying the concept of fuzzy logic for integration of various thematic maps to develop groundwater potential index. The result is verified with the field data collected from VES survey and pumping test data. They found a good correlation.

Murthy *et al.* (2009) used various geologic, physiographic and hydrologic factors, such as geomorphology, lithology, structure, landcover, slope, and drainage to identifying the groundwater potential zones in the Moyale-Teltele sub-basin of the Genale Dawa River basin in South Ethiopia using RS and GIS. They used weighted overlay analysis and MCDM technique to delineate the groundwater potential zone map. The result was verified using groundwater yield data of bore-wells and springs, collected from the field studies and previous reports. The study indicates that integration of RS, GIS, and MCDM is very important in assessment of groundwater, especially in large, unattainable, and hard rock areas.

Chowdhury *et al.*, (2009) delineated the groundwater potential zones of West Medinipur district, West Bengal, India using RS, GIS and GPS techniques. The various thematic layers viz. lithology, drainage density, landform, recharge, soil, slope and surface

water body used in the study were prepared using the IRS-1D imagery and conventional data. All the thematic layers and their individual classes are assigned weights according to their relative importance in the occurrence of groundwater. All the weights were normalized on the basis of Saaty's AHP. Finally, to develop a groundwater potential zone map, all the thematic layers were integrated in GIS environment and classified into three zones, namely 'good', 'moderate' and 'poor'. Additionally, the usable average annual groundwater kept in the good zone was expected to be 0.29 MCM (Million Cubic Meter)/km², whereas 0.25 MCM/km² in moderate and 0.13 MCM/km² in poor zones. Results justified that RS, GIS and GPS techniques are very competent & valuable for identifying the groundwater potential zones.

Jha *et al.*, (2010) developed a groundwater potential map using RS, GIS, geo-electrical and multi-criteria decision analysis techniques in Salboni block, West Bengal (India). They divided the available hydrologic and hydrogeologic data into two groups, exogenous (hydrologic) and endogenous (subsurface). They used exogenous (such as geomorphology, soil, recharge, drainage density, slope and proximity to surface water bodies) and endogenous (such as geology, aquifer thickness, resistivity and depth of post-monsoon groundwater level) thematic layers separately to delineate groundwater potential map, and found that integrated studies are more useful for long term groundwater assessment as compared to individual estimation of groundwater potential.

2.2.2 Groundwater Recharge Zones

RS and GIS applications are not only limited to delineate groundwater potential zones, but they are effectively used for delineation of recharge zones and to find the suitable locations of artificial recharge. Several researchers have worked in this field. Some related studies are given below:

Saraf and Choudhury (1998) extracted the information on the hydro-geomorphic features and the suitable sites for groundwater recharge in a hard rock terrain of the Sironj area in Vidisha district of Madhya Pradesh, India using GIS technique by utilizing the IRS LISS-II data along with the other datasets, such as DEM, drainage and groundwater data. The criterion for GIS analysis and weightage assignment is based on the groundwater conditions and according to relative importance to occurrence of groundwater in the study area. This integrated study is very helpful for designing a suitable groundwater management plan in a hard rock terrain.

Rao and Bhaumik (2003) identified the suitable sites for water harvesting structures in Song watershed, Uttarakhand, India using Spatial Expert Support System (SESS). They used RS and GIS technique to monthly estimate the of water balance to augment the proposed water harvesting structures. They also used technical guidelines of Indian National Committee on Hydrology (INCOH) and Integrated Mission for Sustainable Development (IMSD) for making the decision rules in the knowledge base shell of the developed SESS model. This knowledge based model is modifiable on the basis of requirement and expert knowledge.

Ravishankar and Mohan (2006) identified the favorable groundwater recharge zones, and also found the suitable artificial recharge technique on the basis of specific site with the help of GIS based hydro-geomorphic approach in Bhatsa and Kalu river basins of Thane district, western Deccan Volcanic Province of India. They firstly delineated the groundwater potential zones map using several thematic maps corresponding to hydro-geomorphic parameters in GIS environment and re-classified the groundwater potential zones map into four classes i.e., high, medium, low and very low groundwater potential zones. On the basis of decision rules that are derived from using the hydro-geomorphic parameters, only medium-to-low category groundwater-potential zones are adopted while other categories are excluded. Table 2.1 show that the decision rules, which are used to identifying the suitable locations for artificial recharge zones.

Table 2.1: Decision rules for selecting favorable artificial recharge sites

Set	Parameter	Value
Groundwater level data	Water level fluctuation	> 4 m
Geological data	Lineament density	> 1.5 Km/Km ²
	Depth of bedrock	> 8 m
	Soil cover	> 0.75 m
Geomorphological data	Drainage density	< 2Km/Km ²
	Landform	Plain
	Landuse/landcover	Barren land, Cultivated land
	Slope	< 5°

Jasrotia *et al.*, (2007) delineated the groundwater recharge sites using RS and GIS. They delineated lithology, geomorphology and LULC from fused satellite image of LISS-III & PAN sensors. Other layers, such as slope, drainage and soil are prepared using topographic and soil

map. Thematic layers of aquifer parameters (i.e. pre & post-monsoon, groundwater depth, transmissivity, storativity, specific capacity, permeability and infiltration) are prepared using pumping test data of dug-wells. All the thematic layers are integrated in GIS environment to develop artificial recharge zone map. It is verified with the field data for correctness, and was found to have a good agreement with the field conditions. A drainage network map was overlaid on artificial recharge zone map, to identifying the suitable sites for groundwater recharge.

Chowdary *et al.*, (2009) used RS & GIS techniques followed the IMSD guidelines to develop a watershed management plan of Mayurakshi watershed, Jharkhand state, India. They delineated lithology, fracture, LULC, soil, slope, well inventory, and hydro-geomorphology layers using IRS-1C LISS-III satellite data along with other field & collateral data, that are essential for water resources development. All the layers are combined in GIS environment with logical conditions for preparing a water resource development map of each watershed, and also identifying the suitable areas for recharge sites and developmental structures, such as farm pond, underground barrier, check dam and percolation tanks on the basis of terrain condition. They also applied Boolean logic for selection of artificial recharge sites. Thus, they showed that integration of these techniques is appropriate for analysis of large volume of multi-disciplinary data as well as for decision making regarding development of an integrated water resource development plan.

Ramakrishnan *et al.*, (2009) identified the suitable sites for creation of runoff harvesting structures like percolation pond, farm pond, check dam and subsurface dyke in Kali watershed the sub-watershed of Mahi river basin in Gujarat, India. The suitable sites are identified on the basis of runoff potential, slope, and fracture pattern at micro-watershed level. They followed the IMSD and FAO (Food and Agriculture Organization) guidelines for selection of water harvesting/recharging structures. The derived sites were verified on the basis of field investigation and they achieved high level accuracy at implementation level.

Pandey *et al.*, (2010) used RS and GIS to identifying the suitable sites for soil and water conservation structures. They used drainage, soil, slope and LULC maps as input in GIS environment, and integrated them for development of soil and water conservation plan. Coupling with morphometric parameters, these are further useful for decision making for watershed development and management plan as well as for prioritization.

Sargaonkar *et al.*, (2011) have identified the potential sites for locating the groundwater recharge structures on sub-watershed of Kanhan River, Nagpur, Maharashtra, India using GIS technique. To find the suitable site, firstly GIS based rainfall runoff modeling is carried out to evaluate the monthly runoff from June to October in gridded form, and then total monsoon runoff is calculated. In GIS, flow accumulation analysis is carried out with total runoff as input grid to determine the location of pour points (pour points is defined as where maximum runoff accumulates) in the watershed. They determined five potential pour points location P1, P2, P3, P4 & P5. Geological and geomorphological factors are also considered because these are important for identifying groundwater recharge potential. An AHP with expert judgment is used to determine the ranking of sites. On the basis of expert ranking to all the input features, pour point P5 was highly suitable site for artificial recharge for groundwater in the study area.

Many researchers around the world (Brema and Arulraj, 2012; Nasiri *et al.*, 2013; Kaliraj *et al.*, 2013; Singh *et al.*, 2013; Mahmoud, 2014; Russo *et al.*, 2014) also used RS and GIS techniques to delineate the groundwater recharge zones as well as proposed suitable sites for artificial recharge.

2.2.3 Groundwater Vulnerability

The notion of vulnerability of groundwater contamination was firstly introduced by Margat in 1968. Traditionally groundwater vulnerability to pollution is calculated on the basis of three methods.

- i) **Process Based:** In this method, numerical model is developed; it is useful for local level modeling not for regional level.
- ii) **Statistical:** In this method, correlation is found out between the measured water quality parameters to the spatial variables and it required large site specific dataset.
- iii) **Overlay and Indexed:** In this method, multiple parameter maps are integrated that affect the transport of contaminants from the surface to groundwater, and then assigned an index value to both the parameters, the results are a spatially vulnerability index.

Overlay and indexed methods are more suitable for larger areas. These methods are further categorized into several indices for aquifer vulnerability assessment mapping such as DRASTIC (Aller *et al.*, 1987), GOD (Foster 1987), AVI (Van Stempvoort *et al.*, 1992), and SINTACS (Civita 1994) etc. Conventional methods (i.e. DRASTIC, AVI, GOD, SINTACS) are able to distinguish degrees of vulnerability at regional scales where different lithologies

exist (Vias *et al.*, 2005). The DRASTIC method has been widely used to identify the areas where groundwater supply is most vulnerable to contamination. It is developed by U.S. Environmental Protection Agency (Shahid, 2000). DRASTIC method is based on numerical ranking composite description of all the major geological and hydrological factors that affect and control groundwater movement into, through, and out across the vertical profiles of an area (Yang, 2010).

The DRASTIC method coupling with GIS techniques has been widely used in aquifer vulnerability mapping by various researchers in North America (Hearne *et al.*, 1992; Atkinson and Thomlinson, 1994; Kalinski *et al.*, 1994; Navulur and Engel, 1998; Fritch *et al.*, 2000; Shukla *et al.*, 2000) and around the world, including India, China, Italy, Portugal, South Africa, and Algeria (Lynch *et al.*, 1994; Napolitano and Fabbri, 1996; Chandra Sekhar *et al.*, 2000; Shahid, 2000; Dai *et al.*, 2001; Hrkal, 2001; Menani, 2001; Rupert, 2001; Lake *et al.*, 2003; Lobo-Ferreira and Oliveira, 2003; Panagopoulos *et al.*, 2006; Jamrah *et al.*, 2007; Rahman, 2008; Jin *et al.*, 2011; Shiraji *et al.*, 2012; Yin *et al.*, 2013; Kumar *et al.*, 2014). Thirumalaivasan *et al.* (2003) developed a software package AHP-DRASTIC to derive ratings and weights of modified DRASTIC model parameters. Some of the researchers modified the DRASTIC method and added different parameters, such as lineaments, land use index, aquifer thickness, and impact of contaminants (Secunda *et al.* 1998; Lee, 2003; Mendoza and Barmen, 2006; Wang *et al.*, 2007; Lima *et al.*, 2011).

Secunda *et al.*, (1998) used DRASTIC model and GIS technology to find the potential pollution sites in the Sharon region coastal aquifer of Israel. They used long-term agricultural landuse data over an aquifer media as an additional parameter in DRASTIC model to develop Composite DRASTIC Index (CDI) to evaluate the potential level of groundwater vulnerability to pollution. In this study, DRASTIC Index (DI) and the CDI are validated by comparing the index values of both the models and also validates with groundwater quality data. The results show convinced correspondence between the DI, CDI and high nitrate concentration level, such that this model is feasible for applying world-wide to delineate high pollution risk areas.

Lee (2003) used DRASTIC model and GIS to depict the groundwater pollution vulnerability of the Young Kwang County in Korea. He modified the DRASTIC model by adding the new parameter lineament density map to take into account that contaminants can be

preferential migrated through lineaments. This model is successfully used to screen the location of waste disposal sites to protect the groundwater resources.

Mendoza and Barmen (2006) used DRASTIC and GOD models to find relative pollution potential in Rio Artiguas basin in central Nicaragua. They modify the DRASTIC model with inclusion of geological structure lineament, to find the influence of lineament on the vulnerability.

Wang *et al.*, (2007) developed a new modified model DRAMIC in place of DRASTIC model for vulnerability mapping of contamination in groundwater in Wuhan city, China. This model is developed for densely populated cities because the DRASTIC model has some limitation in urban areas, such as hydraulic conductivity is closely related to aquifer media, topography is ignored in most of urban areas because of flat terrain topography and lastly the densely populated cities most of the area is built up so it is not feasible to obtain the comparable values of soil media. In DRAMIC model, factors D, R, A and I are same as DRASTIC parameters but topography factor is ignored due to some places have almost flat terrain. The factor soil media and hydraulic conductivity is replaced by aquifer thickness (M) and impact of contamination (C). Authors collected 32 samples from quaternary aquifer of Wuhan and tested in laboratory, and found that mostly contaminated samples fall in densely populated areas. Out of all the organic contaminants, Benzene, Toluene, Ethylene and Xylene (BTEX) contamination of shallow groundwater is serious and widespread at Wuhan. They found a good correlation between vulnerability maps developed using DRAMIC model and the organic contamination investigation results; hence it is proved that DRAMIC model worked well in urban areas vulnerability mapping studies.

Lima *et al.*, (2011) modified a DRASTIC-P model by adding additional parameter landuse to assess the actual and forecast future vulnerability scenario in Dulce Creek basin, Buenos Aires Province. The main aim of the study, to show that the expansion of agricultural activities, increases level of groundwater pollution. The result will be analyzed using Landuse map simulated in Dyna-CLUE model for the year 2020, and shows that very high aquifer vulnerability in the area where increment in crop and pasture. This landuse change model will be very helpful to identify the critical location for future environmental changes.

Several researchers (Huan *et al.*, 2012; Wang *et al.*, 2012; Nishat *et al.*, 2013; Alam *et al.*, 2014) also modified the DRASTIC model to demarcate groundwater vulnerability zones.

2.2.4 Groundwater Quality Index

The definition of water quality is not primary objective, but it depends on the desired use of water. Different uses require different water quality index (Babiker *et al.* 2007). To develop a ground water quality index (GWQI) and making the decision based on it, is a crucial issue because it depends upon several number of quality parameters. Traditionally, groundwater researchers compare the drinking water quality status by individual quality parameter with standard values as per guideline. Due to inherent complexity and variability in water quality, it is essential that all the information is presented in a meaningful way that's make easy to taking decision for policy makers, and ultimately to the general public. The GWQI is the single composite information of water quality parameters (Terrado *et al.*, 2010). In other words, GWQI is a mathematical calculation that transforms large quantities of water quality data into a single number which represents the water quality level (Chatterjee *et al.*, 2009; Ramakrishnaiah *et al.*, 2009; Saidi *et al.*, 2009; Saeedi *et al.*, 2010).

The overall quality of groundwater for drinking purposes can be assessed using the water quality index (WQI). Babiker *et al.*, 2007; Simoes *et al.*, 2008; Khodapanah *et al.*, 2009; Ramakrishnaiah *et al.*, 2009; Adhikary *et al.*, 2010; Saeedi *et al.*, 2010; Shankar *et al.*, 2010; Adhikary *et al.*, 2012; El Fadel *et al.*, 2014; Sadat-Noori *et al.*, 2014 used the WQI in different ways and for different purposes and used several water quality parameters.

Babiker *et al.* (2007) developed a GIS-based GWQI that focus on potential risk of drinking water on human health using seven water quality parameters. Out of seven parameters, six (Chloride (Cl⁻), Sodium (Na⁺), Calcium (Ca²⁺), Magnesium (Mg²⁺), Sulphate (SO₄²⁻), and Total Dissolved Solids (TDS)) fall under the category of chemically derived contaminants and Nitrate (NO₃⁻) fell under the category of chemicals that may be a cause of potential health risk. To check the reliability of index, map removal sensitivity analysis is used which also measures the impacts of removing any quality parameter from the computation of the GWQI.

Simoes *et al.*, (2008) developed a WQI to Medio Paranapanema Watershed in Sao Paulo State, Brazil to subsidize management actions for a simple pollution indicator in aquaculture activity. The index is based on three computable environmental factors: dissolved

oxygen, total phosphorus and turbidity. The concentration of all the parameters is normalized at a scale ranging from 0 to 100 and after that quality index is categorized into five classes (excellent, good, regular, fair and poor). The results indirectly determine that aquaculture activity is degraded the quality in watershed, which is more promising than the any other routinely used methods of determining water quality.

Khodapanah *et al.*, (2009) investigated and evaluated the chemical characteristics of groundwater in Eshtehard district. To analyze the water quality parameters, such as pH, electrical conductivity (EC), TDS, Na^+ , Potassium (K^+), Ca^{2+} , Mg^{2+} , Bi-carbonate (HCO_3^-), Cl^- , and SO_4^{2-} collects the groundwater samples from tube-wells, dug-wells and qanats. He also calculates chemical indices like Sodium Percent (Na%), Sodium Adsorption Ratio (SAR), Salinity diagram and Wilcox diagram on the basis of analytical results, and found that most of the water samples are not suitable for domestic & irrigation purposes.

Ramakrishnaiah *et al.*, (2009) evaluated the WQI for the groundwater of Tumkur taluk using 12 quality parameters viz. pH, Total Hardness (TH), Ca^{2+} , Mg^{2+} , HCO_3^- , Cl^- , NO_3^- , SO_4^{2-} , TDS, Iron (Fe), Manganese (Mn) and Fluoride (F). The analysis discloses that the groundwater can be consumed after some purification, and it also needs to protect the groundwater from menaces of contamination.

Adhikary *et al.*, (2010) analyze the groundwater samples of wells to assess the risk of groundwater pollution in Najafgarh, NCT of Delhi. They used geo-statistical methods (Ordinary and Indicator kriging) to generate the thematic maps of groundwater quality parameters. On the basis of kriging method, found that experimental semi-variogram values of water quality parameters, such as bicarbonate, chloride, electrical conductivity, magnesium, sodium and sulphate are fitted in spherical model and calcium & nitrate in exponential model. The thematic maps of groundwater quality parameters show that groundwater pollution is increasing from northern and western part of the study area towards the southern and eastern part.

Saeedi *et al.*, (2010) evaluated the groundwater quality index, and analyzed the effect of landuse change on groundwater quality parameters using methodology based on multivariate analysis in the Qazvin province, west central of Iran. The main aim was to identify the places of best drinking water quality.

Shankar *et al.*, (2010) the study area Paravanar basin lies in the Cuddalore District of Tamil Nadu. The groundwater samples are collected from the villages' lies in Paravanar sub-basin after that interpolate them using Arcview software. Major elements thematic maps of Ca^{2+} , Mg^{2+} , Na, K, HCO_3^- , Cl^- and SO_4^{2-} are prepared from the hydrochemistry data. Different classes in thematic maps were categorized as good, moderate and poor. All the quality parameters are above the prescribed limit, except SO_4^{2-} for drinking purpose.

2.3 GROUNDWATER MODELING

The effective groundwater management has the ability to predict recharge. In mid 1960s, the deterministic, distributed-parameter, computer simulation model is developed for analyzing flow and recharge in groundwater systems. A model is defined as a representation of a real system or process. A conceptual model is a hypothesis for how a system or process operates. This hypothesis can be expressed quantitatively as a mathematical modeling. Mathematical models are abstractions that represent processes as equations, physical properties as constants or coefficients in the equations and measures of state or potential in the system as variables (Delleur, 1999). Most groundwater models in use today are mathematical models (Thach *et. al.*, 2007). Mathematical groundwater models are based on conservation of mass, momentum & energy that describe cause and effect relations. A mathematical model can be used as a design tool to determine the necessity of artificial recharge. Many researchers around the world have attempted to carry out groundwater modeling using RS and GIS tools.

Bekesia and McConchie (1999) used Monte Carlo technique to develop a groundwater recharge model for Manawatu region of New Zealand. It is often used to calculate regional groundwater recharge. Recharge was calculated for a 28 years period and 300 simulations for each station were found adequate to estimate mean annual recharge to within 10 mm. They found a good relationship between the observed and predicted Groundwater Levels (GWL). The output (recharge and uncertainty) are incorporated in the form of color-coded maps, which are easily used by resource planners. This methodology has great significance to calculate groundwater recharge in non-arid regions.

Gnanasundar and Elango (2000) developed a groundwater flow model in coastal aquifer near Chennai, India using MODFLOW. The model was calibrated for steady and transient state conditions. The spatial distribution of groundwater head and well hydrograph was compared with the historic data. They concluded that rapid urbanization would lead to further lowering of

water table at few locations along the Northern coast of the aquifer system. They found that model is sensitive even for 5% reduction in recharge.

Gogu *et al.*, (2001) created a GIS-based hydro-geological database to carry out groundwater vulnerability study as well as groundwater modeling of Walloon region, Belgium. They have included the database of five River basins, with contrasting hydro-geological characteristics. To integrate GIS technology and groundwater simulation model, a “loose-coupling” tool was created between the spatial-database & the groundwater modeling interface GMS (Groundwater Modeling System). The hydro-geological data stored in the database can be efficiently used for time and spatial queries within different groundwater numerical models.

Arora and Goyal (2003) highlighted the importance of GIS in development of conceptual groundwater flow model of Hanumangarh and Sriganaganagar districts, Rajasthan. All the layers such as canal network, geology, Digital Terrain Model (DTM), recharge zones etc used in model are developed using GIS software and then transferred to finite difference grid for developing mathematical groundwater flow model of the area.

Pliakas *et al.*, (2005) modeled the groundwater recharge by re-activating an old stream bed of Kosynthos River in Bedin Xanthi plain, Thance, Greece. MODFLOW package is used to simulates the aquifer system of the study area, which involves both the model calibration and prediction of the aquifer system response. The model is validated for 9 years (1995-2003) period out of these first 7 years (1995-2001) period are predicted successful, while the respective the last 2 years (2002-2003) result are not within acceptable limits.

Fayez and Tamer (2006) carried out groundwater flow modeling of Mujib aquifer, Jordan. They simulate the groundwater flow model under different stress periods using MODFLOW code of PMWIN package. The model was calibrated for steady and transient state using well data of 11 years (1985-1996) and validated for 7 years (1996-2002), and found a good agreement between measured and simulated contours in steady state conditions as well as good relationship between observed and calculated GWLs in transient state condition. Different scenarios are analyzed to predict the response of aquifer in different conditions and found that model is highly sensitive to hydraulic conductivity as compared to recharge and also sensitive to specific yield.

Shammas and Jacks (2007) used the codes of MODFLOW and MT3DMS to examine the groundwater quality and identifying the movement of fresh water into saltwater of Salalah plain aquifer in Oman. A 3D flow and solute transport model was constructed and calibrated by history matching under steady state flow and saltwater conditions against the observed hydraulic heads of collected from Department of Water Resources of year 1992. The underflow recharge was derived from the calibrated steady-state flow model at 50 Mm³. The model is calibrated for 13 years (1993-2005) under transient flow and solute transport state to predict the future condition. The method of artificial recharge of the treated wastewater is very beneficial it is acts as a hydrostatic barrier to prevent saline water intrusion from the sea, as well as to stabilize groundwater levels in aquifer in agricultural and residential strips. In addition, in terms of resource conservation, this water will be useful as a source of water for irrigation in the future, particularly in the traditional farms. They concluded that new water source and additional conservation measures should be taken into account to ensure the preservation of fresh water resources for coming generations and found good correlation. This scheme can also be applied to other regions with similar conditions.

Elango (2008) developed a 3D numerical model to assess the behavior of the system with respect to changes occur in hydrological stresses of the coastal aquifer, which located nearby southern part of Chennai city, India. To simulate the groundwater flow the finite difference code of MODFLOW with GMS has been used and found that aquifer system is stable under the present pumping scenario. On the basis of sensitivity analysis revealed that the model is very sensitive to recharge as compared to hydraulic conductivity and specific yield. It is also revealed that, if pumping rates increase by 10% the groundwater head is declined by 0.5 to 1.5 m that causes seawater to encroach in aquifer system of coastal regions. To prevent this situation groundwater abstraction is restricted upto 4.25 million gal/day.

Rejani *et al.*, (2008) have developed a 2D groundwater flow and transport model for Balasore Coastal Basin, Orissa, India using Visual MODFLOW package to overcome the problem of sea water intrusion and over exploitation of groundwater resources. To manage the groundwater resources efficiently, the model simulates for analyzing the aquifer response at different strategies. The model calibrates and validates successfully, and found a good correlation between measured and observed. Using the validated model, groundwater response to five pumping scenarios under existing cropping conditions was simulated. The results of the sensitivity analysis indicated that the Balasore aquifer system is more susceptible to the river

seepage, recharge from rainfall and interflow than to horizontal and vertical hydraulic conductivities and specific storage. Based on the five pumping scenarios best outcome to manage the Balasore basin was to reduce the 50% pumpage from downstream regions of second aquifer and increase pumpage upto 150% from first and second aquifer at potential sites.

Zume and Tarhule (2008) simulated the impact of groundwater pumping on stream-flow aquifer in semiarid region of Beaver North Canadian River (BNCR) in northwestern Oklahoma, USA using visual MODFLOW. MODFLOW's stream flow routing package, pumping induced changes in base flow and stream leakage were analyzed to estimate stream flow depletion in the BNCR system. The result of simulation indicate that groundwater pumping has been reduced the base flow to streams upto 29% and increase of stream leakage into the aquifer upto 18% for a net stream flow loss of 47%.

Goyal *et al.*, (2009) used finite element groundwater flow model, HYDRUS 2D for simulating the groundwater recharge of shallow water table condition of Haryana, India. The main objective of the study was to measure the applicability of simulating draw-up and drawdown on pressure heads during recharge and recovery cycles at different buffer storage volumes (BSVs) and storage time in a cavity-type Aquifer Storage Recovery (ASR) well. The HYDRUS 2D model is executed efficiently for simulating rise & fall with Root Mean Square Error (RMSE) values ranging from 0.26 m to 1.29 m and modeling efficiency lies between 94.57 to 99.9%. Radial influencing zone increases with BSV with a mean value of 122 m during recharge. Which indicates that the next tube-well should be installed at least 122 m away from the existing ASR well.

Jaworska-Szulc (2009) developed a three dimensional numerical model of Gdansk hydro-geological system of Poland to evaluate the groundwater resources. The model predicts that the system is mainly recharge by precipitation (about 19.8 % of total annual precipitation). Finally, the model has been determining the groundwater resources of entire aquifer system and individual geomorphological units. This model also helps to determine the exploited areas, especially in coastal zones to avoid the intrusion of salt water from the Bay of Gdansk. The verification of the sustainable yield according to the Bredehoeft equation (2002) showed that the present pumping rate is close to the amount needed for sustainable development.

Szucs *et al.*, (2009) used MODFLOW-2000 & MT3DMS simulation module of Processing Modflow for windows (PMWIN Pro) modeling package to remediation of over-produced and contaminated aquifers in Debrecen, Hungary. Over-production and contamination creates many problems, such as ground compaction and land subsidence due to over production. Contamination causes the quality of groundwater is degraded not suitable for drinking. To overcome this problem, aquifers are simulated to recharge artificially, from surface water sources. The adopted methodology, based on the complex hydro-geological study and groundwater simulation approach for selecting and designing of the most favourable remediation technology for over-produced and contaminated aquifers have been elaborated successfully.

Tamer and Fayej (2010) developed a mathematical groundwater flow model by using computer code of MODFLOW for Mujib aquifer, Jordan. They calibrated and validated the different scenarios of future abstractions and artificial recharge with reasonable accuracy. This paper is a continuity of the work presented in Abdulla and Al-Assa'd (2006) study on developing a groundwater flow model for Mujib aquifer. In Mujib aquifer artificial recharge occurs mainly through injecting water directly to aquifer or recharge from reservoir. To study the modelling response, three different scenarios are performed, out of these best scenarios that provide a good recovery of groundwater table reduces the current abstraction upto 20% and implements the artificial recharge rates 26 Mm³/year. This model is very helpful for researcher and decision makers for optimum management strategies in arid and semi-arid regions.

Chenini *et al.*, (2010) carried out the groundwater resources development in arid regions, mainly to delineate the suitable locations of artificial recharge using coupling of GIS and numerical modeling techniques in Maknassy basin, Central Tunisia. The thematic layers are integrated using ArcView software, to demarcate artificial recharge zone map. Groundwater model was used to evaluate the impact of recharge on the piezometric behavior of the hydrological system. Groundwater flow modeling of the study area specified that twenty four percent of rainfall recharge occurred annually. Artificial recharge zone map was used to simulate the piezometric behavior up to 3rd level of aquifer. In modeling two scenarios were considered; the first one consisting of the management of a unique hill in the outlet of each basin and the second scenario considered serial hills managed in the principal watercourse of the watershed. In both scenarios, the groundwater extraction is assumed to be constant. MODFLOW software was used to simulate the impact of the potential recharge in each

scenario. The present methodology is appropriate, especially in arid regions, where the occurrence of groundwater is limited.

Martinez-Santos *et al.*, (2010) modeled the impact of low permeability aquifer of Madrid, Spain on urban water supply, which are based on groundwater. Groundwater model is calibrated on monthly basis using groundwater level data of piezometer for last 32 years. The calibrated model revealed that the flow of stream is partially depends on groundwater levels. It is simulated that nonstop pumping over the last decades had significantly declines the water table at the native scale, varying aquifer discharge into surface water bodies. The groundwater management scenario are planned and modeled together with a representative of the Tagus River Basin authority. Model results also revealed that long term groundwater extractions would not prompt significant changes in stream flows.

Kallioras *et al.*, (2010) simulated the groundwater flow in a sedimentary aquifer system located in Northern Greece. The groundwater flow model was divided into two stress periods; each contains two different time steps. The aquifer is simulated using the MODFLOW code, and found satisfactory results. The model is also used for prediction of future hydro-geological conditions of aquifers, on the basis of two scenarios. In first scenario hydrologic and hydro-geologic conditions are same for a decade (2003-2013) and in second scenario groundwater abstraction rate is increased by 5%. On the basis of first and second scenario it was identified that the water losses are $26.989 \times 10^6 \text{ m}^3$ and $43.89 \times 10^6 \text{ m}^3$.

SenthilKumar and Elango (2011) assessed the impact of a subsurface barrier/dam on groundwater flow in the lower Palar River basin, Tamil Nadu, India. A sub-surface barrier/dam was proposed across Palar River to meet increasing demand of groundwater for nuclear power station. Groundwater model predicted that groundwater levels would be rise 0.1 to 0.3 m widen out a distance of about 1.5 to 2 km from the upstream side of the barrier, while on the downstream side, the groundwater head would be fall upto 0.1 to 0.2 m. The model had also predicted that with the sub-surface barrier in place, an additional $13,600 \text{ m}^3/\text{day}$ groundwater requirement is met, with minimum decline in regional groundwater head.

Taheri and Zare (2011) carried out groundwater recharge modeling of Kangavar Basin, a semi-arid region in the western part of Iran. MODFLOW was selected to simulate the aquifer. Calibration was attempted for water levels in existing piezometers during the year 2003.

Groundwater fluctuations from the year 2004 to 2008 were predicated to verify the model. In the study, observed water level data were adjusted to achieve a reasonable fit with calculated data. Artificial recharge impacts were assessed in different positions. Groundwater level mound of 3 m with recharged water volume of 3.42 MCM at two sites, and upconing of 6 m in 3 sites with recharged water volume of 7 MCM were obtained. The maximum radial effect of these artificial recharge sites was found to be 1.5 km.

Gaaloul (2014) developed a groundwater model for El Hicha aquifer in arid region of southeast Tunisia using GIS based package of MODFLOW software for sustainable agriculture production using saline water. In the study, observed water level data were adjusted to achieve a reasonable fit with calculated data. The model reliability is tested on the basis of long term historical groundwater monitoring data and the model is used to predict the future groundwater scenario until 2020 and 2050. On the basis of model, he found that groundwater level has significantly declined which may lead to the intrusion of sea water in El hicha aquifer. To protect the aquifer, it is necessary to reduce the groundwater exploitation in that area.

Groundwater modeling is widely used as a management tool to understand the behavior of aquifer systems under different hydrological stresses, whether induced naturally or by human activities. From the various literatures, it is clearly known that management policy can be framed for the future protection/ management of aquifer with the help of ground water models and with various prediction scenarios.

2.4 OPEN SOURCE WEB GIS

The beginning of internet and introduction of HTML 2.0 specifications with support for form and table tags, there was a serious interest in developing Decision Support System (DSS) on web-based platforms (Power, 2007). In more recent years, with the advent of web 2.0 and its capability to explicitly represent and visualise information (Chavarriaga & Macias, 2009), the internet has become an attractive platform to develop applications with rich user interfaces. Compared to desktop application interfaces, the web platform also provides a similar look and feel. There exists the capability to add menus, toolbars, pop up windows and context menus into today's web applications.

With the increase in internet bandwidth and technologies such as AJAX (Asynchronous JavaScript and XML), the responsiveness of the web applications are not second to their desktop counterparts. Growing trend of the adoption of open source technologies for WEBGIS is largely due to the fact that many successful open source software projects have proven under many circumstances to perform at acceptable and sometimes exceptional levels compared to proprietary products (Cuylenburg *et al.*, 2005). Given the similarity between web-based and desktop platforms for application development, a web-based Spatial Decision Support System (SDSS) has a number of advantages over a desktop-based system (Gupta *et al.*, 2004; Wu *et al.*, 2008).

Web-based SDSS provide faster update of information. Information can be updated by multiple groups of people spread across multiple locations. This is vital for real-time systems that depend on data as it becomes available. As the web-based system uses a client-server model, it provides a wider access to many users at the same time. This significantly increases the dissemination of the system. Also since multiple users have access to the same system, the maintenance and update of the system can be achieved much more easily.

Web-based systems only require a browser to use. With today's widespread availability of internet access, it can be argued that majority of the non-technical users are familiar with using a web-browser and have used at least some kind of web based application such as facebook, MySpace, YouTube or Webmail. However, one key limitation of a web-based system is the heavy load on the server which can result in low bandwidth and time outs. Spreading the system across multiple servers could alleviate this with some compromise regarding the maintenance and update capability. Taking all these factors into consideration, a web-based implementation of a SDSS will allow more effective and productive use of the system in the hands of non-technical users. Many researchers develop web enabled open source SDSS, some of the studies related to these are described below:

Caldeweyher *et al.* (2006) developed an open source GIS based community information system with its purpose “empowers grassroots through GIS technology”. This web-based system is built with open source software, and as a result of this, it is meant to be affordable and readily available to the general population. The system in its final stage has the capability to display a map and add layers to it, such as population data and index of education and occupation. It also consists of a “classification wizard” which can help the user to associate

different styles, patterns and symbols with the layers. The system has the capability to generate charts to display time series data. Limitations of the system are that it does not consist of a fully automated layer addition and classification feature and also the map generation parameters are hard coded which limit the way users can visualize data and may not necessarily be in accordance with the user's requirements. Also, if the developer had implemented a time series slider function to the system, which the user can move to "travel" through different time periods and simultaneously receive updates of relevant data on the map, it would have improved the interactivity and the usability of the system. To some extent, the lack of interactive capability in this system can be attributed to under utilization of proper web 2.0 techniques, such as AJAX technology. However improper and over utilization of AJAX could also reduce the responsiveness of the tasks due to complex calculation and connection speed limitations.

Debebe and Amer (2008) developed a centralized GIS based web enabled information system "Qatar wide groundwater Resource Information System (QaGWRIS)" which has the capability to store and manage large amount of information related to groundwater resources and environments. The main goal of these system is to understand about the resources and ultimately for exploration, exploitation, monitoring, and protection of these resources.

Wang and Cheng (2008) developed a web-based SDSS for the purpose of flood forecasting and flood risk mapping. An interesting feature of this proposed SDSS is that it combines together various databases from different organizations to obtain real-time data and aims to provide the users with comprehensive support for distributed information retrieval, analysis and modeling.

Through the existing literature, it is possible and promising to extract and get an idea of the basic components of a web-based SDSS. Usually this type of system consists of a database tier, server tier and client tier. The database tier is the place where all the information necessary for the system is located. In a SDSS, there are two types of data, spatial and attribute (Wu *et al.*, 2008). Spatial data consists of raster and vector-based geographic data such as layers and maps (Malczewski, 2006) which need to be stored and handled differently to attribute data such as population and health data. The server tier is responsible for the main logic of the system. This is where the calculating models of the system fit in. Muracevic and Orucevic (2008) describe a high level platform called MapGuide open source that helps to develop interactive web-based

GIS. This software provides a repository and a map server that has the capability to handle and serve spatial data and also it provides customizable and extendable client-side viewers that can be used to display spatial and attribute data and obtain user input interactively. Compared to online mapping tools such as Google and Bing Maps, MapGuide open source provides a higher level of interactivity. On top of this it provides a well structured architecture to build web based applications. It is possible to create simple static map based web site using Google Maps, for example. However, this could be too limiting when providing advanced decision making capability.

2.5 CONCLUDING REMARK

Many studies have been done nationally and internationally using RS, GIS and conventional modeling to tackle the problems related to groundwater. Out of these only few studies integrated used RS, GIS and conventional modeling to assess the groundwater related problem as well as design and developed open source web enabled tool.

3.1 THE STUDY AREA

3.1.1 Location and Accessibility

The Loni and Morahi watersheds, covering an area of about 2145 km² in the Unnao and Rae Bareli districts of Uttar Pradesh state, lying between latitude 26°01'0.5" to 26°40'13.24" N and longitude 80°16'28" to 81°01'50" E (Figure 3.1), respectively, have been selected as the study area. These watersheds cover falls in nine administrative blocks of Unnao and Rae Bareli districts. The major cities in the area are Unnao, Gangaghat, Bighapur, Bhagwant Nagar and Lalganj, with Unnao as the district headquarter.

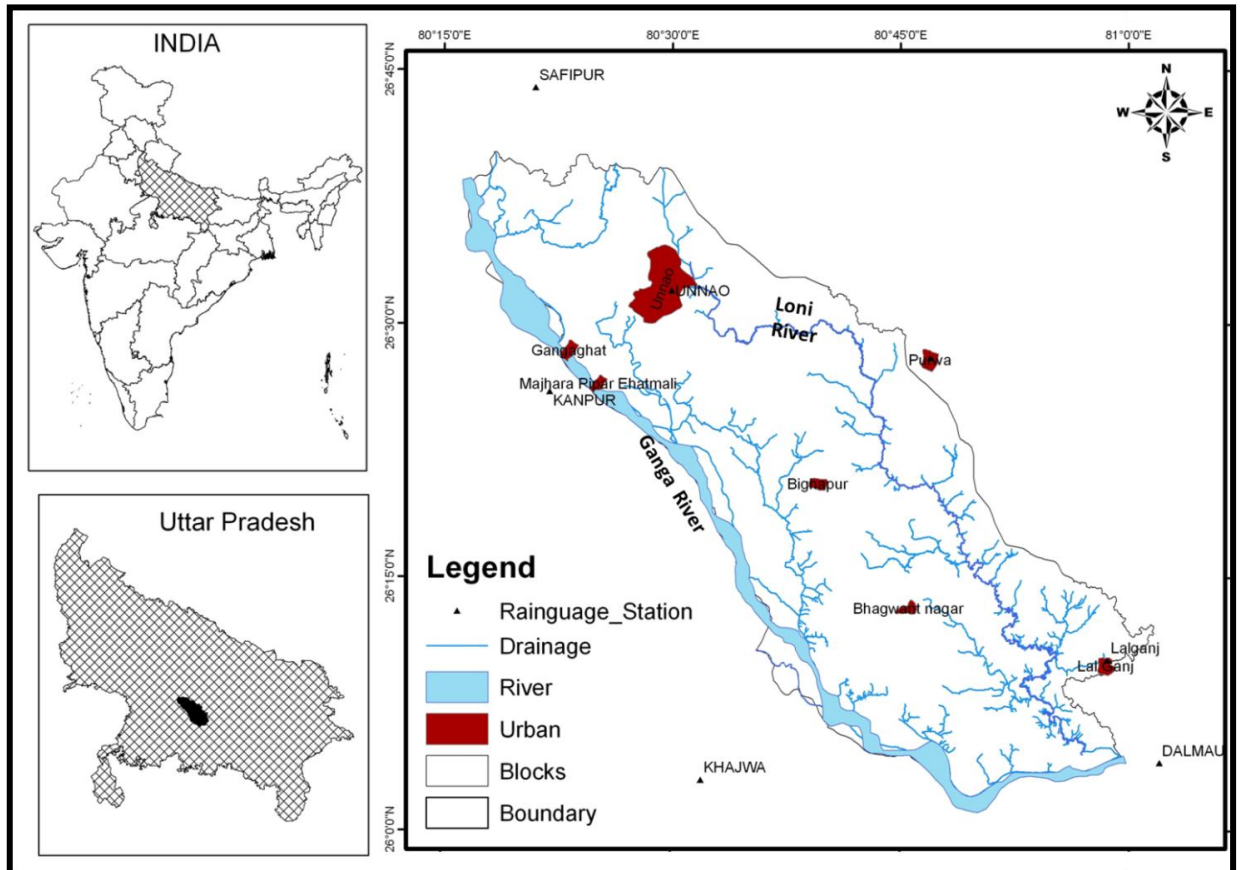


Fig. 3.1: The study area

The area is well connected with adjoining major cities by rail and roads. The National Highway 25 (NH-25) passes through the area that connects the Unnao city with major neighboring cities, like Lucknow and Kanpur. The two state highways SH-13 and SH-38 also

pass through the area connecting all the cities within area as well as all nearby cities. Almost all the villages of the area are approachable by motorable roads, as shown in Figure 3.2.

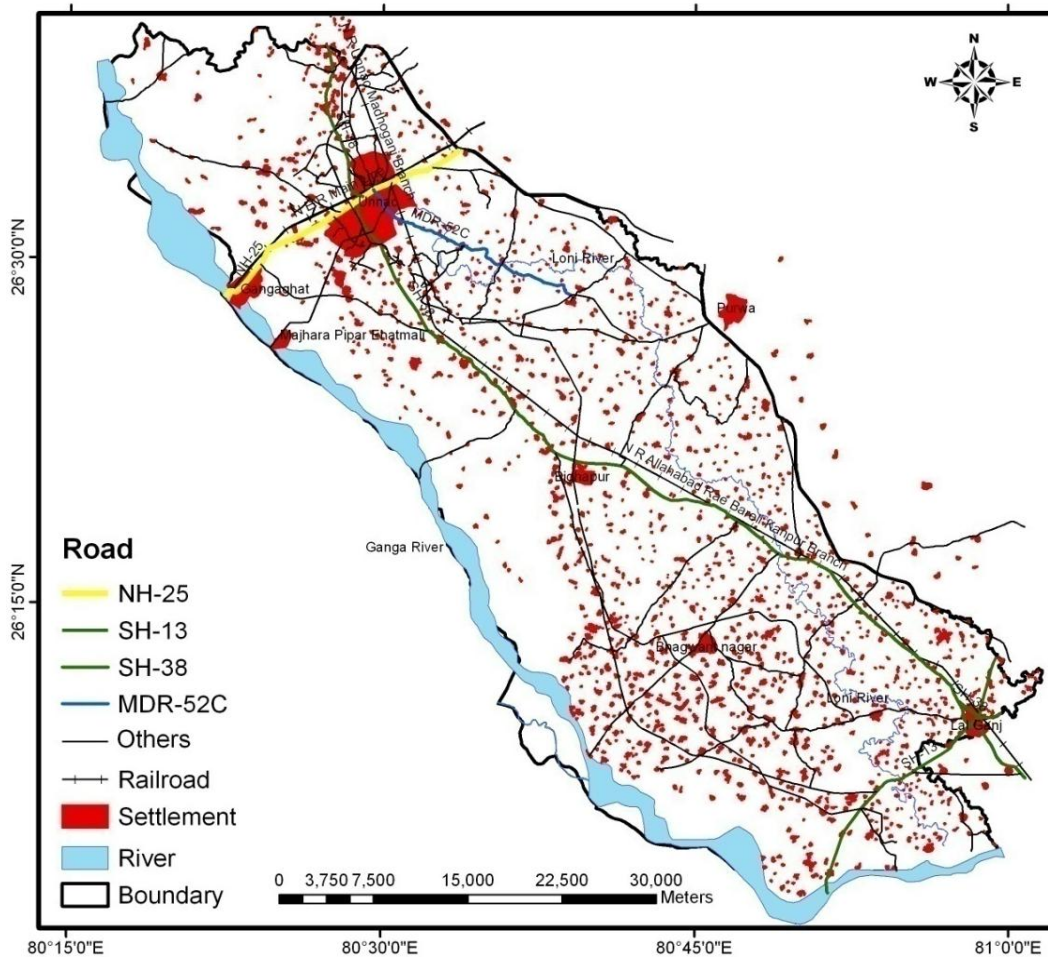


Fig. 3.2: Transportation network

3.1.2 Climate

The climatic condition of an area can be classified as sub-tropical, and it is characterized by general aridness apart from the concise span of monsoon season. It has a hot summer and a cold winter. The complete year is divided into three seasons; hot cold and rainy season. The period from the mid of November to ends of February is the cold season. The hot season which follows, continues up to the end of June. The rainy season spans over the period of mid June to September. In the study area, more than 85% rainfall occurs during monsoon season (June to September), with an average annual rainfall of 800 mm to 900 mm. The annual 12 year (1993-2004) rainfall is shown in Figure 3.3. The post-monsoon or the pre-winter extending from mid-September to mid-November follows this. The minimum and maximum monthly temperature lies in the range of 3° to 45°C (Anonymous, 2013).

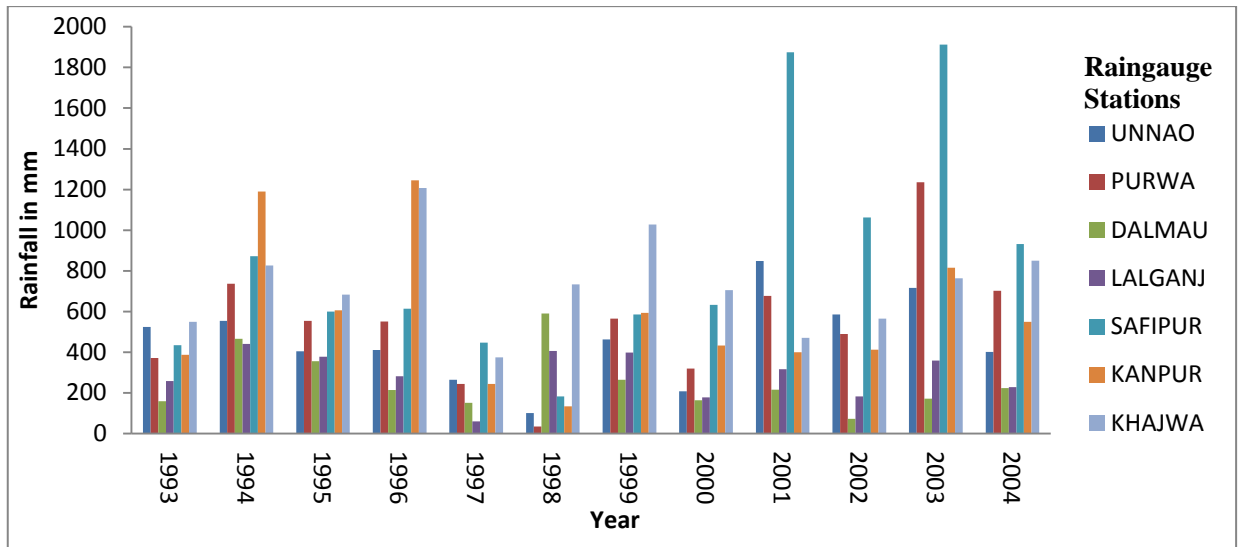


Fig. 3.3: Rainfall pattern (1993-2004)

3.1.3 Water Resources and Irrigation Practices

The Loni and Morahi rivers are the major tributaries in the study area. They run parallel to Ganga River and join it later. In the northern India, alluvium region of the Gangetic plain is well known for agricultural and industrial activities due to existing of natural basic infra-structural resources, such as the most fertile soils and suitable climatic conditions throughout the year. High fluoride contents are found in the soil of the region. In this region, various complex industrial activities with different operating industrial units exist, such as tanneries, steel rolling, distillery and chemical processing (CGWB, 1999). Domestic sewage, treated effluents from the common effluent treatment plant and untreated effluents from other industries in the region are carried by Loni River. The rivers, tributaries and ponds are major surface water sources in the region, while the dug well, bore well, tube well, and hand-pump constitutes the groundwater sources.

3.1.4 Geomorphology

Geologically, it is part of the vast Indo-Gangetic alluvial plain. The area is overwhelmed with alluvium of Quaternary age consisting of older alluvium of middle to upper Pleistocene and newer alluvium of Holocene (Gowd *et al.*, 2009). The alluvium formation of the area comprises of sand, silt and clay with occasional gravel. The older alluvium called bhangar, forms slightly elevated terraces usually above the flood levels. Geomorphologically, the plain shows a south to southeasterly sloping planar surface in the northern part, formed due to reduction and development of alluvial fans in response to the climatic changes during the Quaternary (Ghosh and Singh, 1988). There is a regional plateau or upland surface (T2) sloping

towards east and south-east. Another regional surface (T1) is developed within the major river valleys. These surfaces have developed in response to sea-level and climatic changes during Quaternary period (Singh, 1987). It is observed that in rivers flowing NW-SE, the southern bank shows prominent cliffs, while in the north, broad flood plains are developed (Singh and Rastogi, 1973).

Through time, the Gangetic plain has expanded southwards in response to thrust-fold loading in the Himalaya. The sub-surface data in the alluvium of the southern marginal plain shows that above the basement, there is a succession of sediment derived from the Peninsular region, dominated by pink-colored arkoses sands. This zone is capped by a sequence of sediments from Himalayan source, which are essentially grey coloured, micaceous sub-greywacke type (Singh and Bajpai, 1989).

Geomorphology and drainage type combined with sedimentation processes play a substantial role on dispersion and transport patterns of metals bound to sediments and soils. It has been divided into five independent geochemical domains on the basis of sediment-geomorphic, hydrological and geochemical characters. The monsoon hydrography and physico-chemical parameters (pH, conductivity) of the river and urban drain waters play a prominent role in regulating the concentrations and behavior of the metals in the aquatic system of the plain.

3.1.5 Soil

Soil found in watersheds show evidences of wide inconsistency in composition and appearance. The major portion of an area consists of common soils known locally as Bhur or sand on the ridges, Matiar or clay in the topographic lows and Dumat or loam on the plains. Clay is dominant in the areas where "Reh" or Usar prevails. Alluvial soils of river valleys notable the "Kachhar" of the Ganga formed by repeated deposition of silt brought down by the existing river system during floods (Singh *et al.*, 2013).

3.1.6 Hydrogeology

The area is a part of the Central Ganga alluvial plain mainly constituted of the clay, silt, sand, gravel and kankar sediments of quaternary age. These alluvial deposits of the area may be broadly classified into newer and older litho-units on the basis of sedimentary constitution, depositional and developmental geological history (Singh *et al.*, 2013).

3.2 DATA USED

For the present study, data have been collected from various Government agencies and Organizations, like National Remote Sensing Centre (NRSC), Survey of India (SOI), Geological Survey of India (GSI), State Ground Water Board (SGWB), Central Ground Water Board (CGWB), National Bureau of Soil Survey & Landuse Planning (NBSS&LUP), Uttar Pradesh Pollution Control Board (UPPCB), Jal Nigam, Indian Meteorological Department (IMD) and Census of India, Topographical maps, satellite images, soil and geological maps, GWL data, groundwater quality data, socio-economic data. Some technical reports are also collected from UP Jal Nigam, Lucknow. Details regarding conventional and RS data used are given in Table 3.1, and the specifications of sensors are given in Table 3.2.

Table 3.1 Data collection and their sources

Thematic Maps (Hard Copy)				
S. No.	Data	Data Source	Scale	
1	Toposheets 63 B/ 6, 7, 10, 11, 12, 15 & 16	SOI, Dehradun	1:50,000	
2	District Planning Map	SOI, Dehradun	1:250,000	
3	District Resource Map	GSI, Lucknow	1:250,000	
4	Soil Map	NBSS&LUP, Nagpur	1:10,00,000	
5	Village Map	Census of India, Lucknow	1:50,000	
6	District Census Hand Book	Census of India, Lucknow		
Remote Sensing Digital Data				
	Sensor		Path	Row
7	IRS P6 LISS III	NRSC Hyderabad	100	53
8	Landsat TM	GLCF & USGS website	144	42
9	SRTM (Elevation data)	GLCF website	144	42
10	ASTER (Elevation data)	USGS website	-	-
Hydrological, Geological and Meteorological data				
	Data	Format	Organisation/Source	Year
11	Water Table Data	Hard and soft Copy	SGWB, Lucknow	1984-2009
12	Litholog Data	Hard Copy	CGWB, Lucknow	
13	Rainfall Data	Soft Copy	IMD, Pune	1993-2007
14	Groundwater Quality Data	Hard Copy	Jal Nigam Unnao &U.P., UPPCB, SGWB, Lucknow	

Table 3.2 Sensor Specifications

Specification	IRS P6 LISS III	LANDSAT TM	SRTM	ASTER
Spectral Bands	1-4	1-7	C-band & X-band	4-9
Spatial Resolution	23.5 m	30 m	90 m	30 m
Swath Width	141	185×185 Km	185×185 Km	120×150 Km
Radiometric Resolution (bits)	7	8	1 Arc-Second	1 Arc-Second

Topographical maps are very important source of information to carry out the geospatial studies as these maps give the basic terrain information. All the maps and satellite images are geo-referenced with the help of topographic maps. Figure 3.4 shows the mosaic of topographical maps covering the study area.

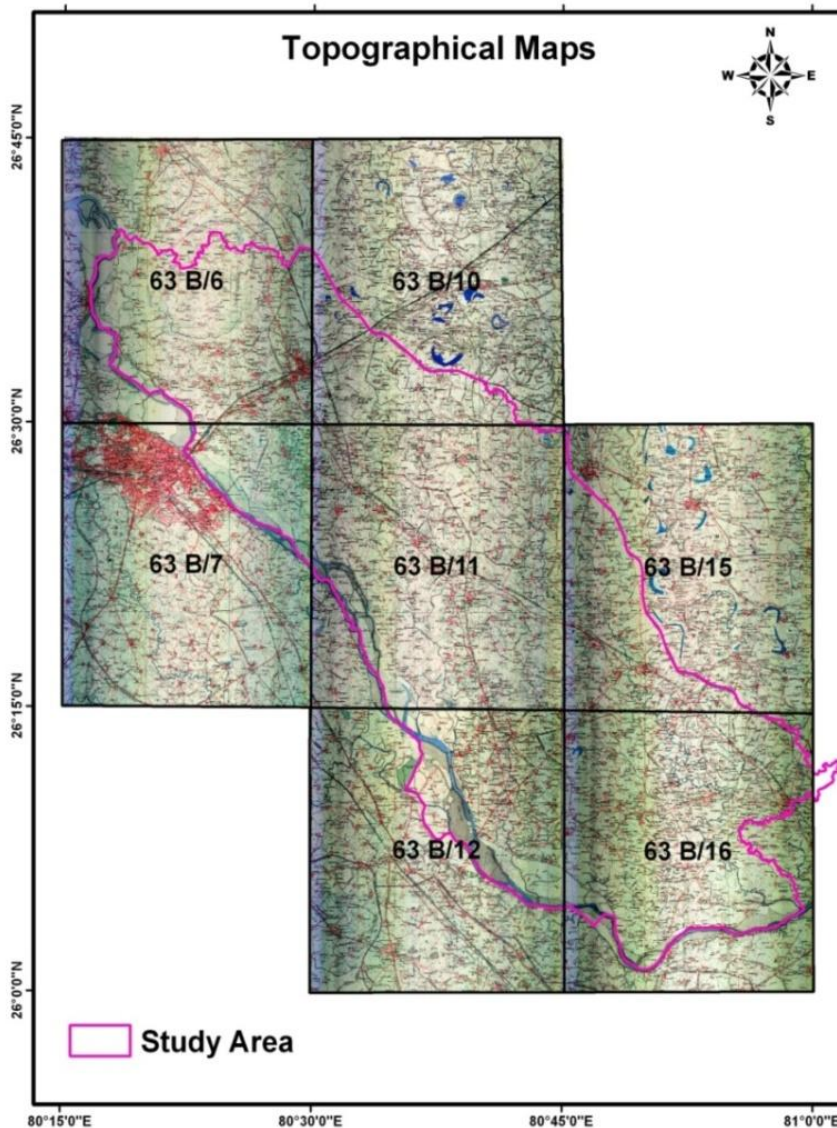


Fig. 3.4: Topographical map sheets (scale 1:50,000) covering the study area

3.3 SOFTWARE, TOOL, SCRIPT AND TECHNOLOGY USED

The details are given below:

1.	ERDAS IMAGINE	It is one of the best world's leading image processing software that is developed by Leica geosystems that work on geospatial data. It is used to perform advanced RS analysis and spatial modeling to create new information. In addition, it is used to visualize the results in 2D, 3D, movies, and on cartographic quality map compositions. Optional add-on modules providing specialized functionalities are also available to enhance your productivity and capabilities. IMAGINE Virtual GIS is a powerful yet easy-to-use visual analysis tool that offers GIS functions and capabilities in a 3D environment.
2.	ArcGIS	ArcGIS Desktop is GIS software that is developed by ESRI. It is a group of modules that are used for different-2 purposes (a) ArcMap: it is used to editing, mapping, geo-processing and visualization. (b) ArcCatalog: it is used to create geodatabase and shapefiles as well as for data management. (c) 3D visualization with ArcGlobe and ArcScene, (d) ArcSDE: It is used for creating online geo-database. (e) ArcServer and ArcIMS: It is used to publish GIS layers on web.
3.	PMWIN	It is graphical user-interface for windows, which is used to create and simulate models. The modeling tools also include the presentation tool (a) Result Extractor: It is used to extract the simulation results and the results are also being save in ASCII or SURFER compatible files. (b) Field Interpolator: it is used to interpolate the measured data. (c) Field Generator: It is based on Mejía's (1974) algorithm. "It generates fields with heterogeneously distributed transmissivity or hydraulic conductivity values. It allows the user to statistically simulate effects and influences of unknown small-scale heterogeneities. (d) Water Budget Calculator: It is used to calculate the water budget of user specified zones and calculates the exchange of flows between such zones. This facility is very useful in many practical cases. It

		allows the user to determine the flow through a particular boundary. (e) Graph Viewer: it is used to display the simulation results in the form of graphs.
4.	XAMPP 1.7.3	It is an freely available open source web server solution that consists of mainly of the following: a) Apache Hypertext Transfer Protocol (HTTP) Server b) MySQL database c) Interpreters for scripts.
5.	PHP	It is a scripting language that is used to create dynamic web pages.
6.	MySQL	MySQL is a Relational database Management System (RDBMS) that runs as a server and database can be access by multi-users at a time.
7.	JavaScript	JavaScript very quickly gained widespread success as a client-side scripting language for web pages. JavaScript is a scripting language. It is used for client side validation. It is supported by all major browsers like Chrome, Internet Explorer, and Mozilla Firefox etc.
8.	AJAX	Ajax, shorthand for “Asynchronous JavaScript and XML”, is used for partial page refreshment so that the entire web page does not have to be reloaded each time the user requests a change.
9.	PostgreSQL	Database Server
10.	POSTGIS	Spatial Database gateway
11.	Geoserver	GIS server for publishing OGC web services
12.	OpenLayer	Development of GeoWeb 2.0 application
13.	GeoExt	Rich web GIS GUI
14.	Apache Tomcat	Web server

CHAPTER 4

CREATION OF SPATIAL AND NON -SPATIAL DATABASE

4.1 PROLOGUE

To manage the groundwater resources, a large volume of spatial and non-spatial data is required. These data have been organized and analyzed in a proper manner to achieve the defined objectives. In the present days, geospatial techniques or models are one of the best techniques to analyze and manage the huge data in more affordable manner (Kumar and Sharma, 2006).

To assess the groundwater problems in watershed area, temporal data is required to assess the spatial changes with time. RS data overcomes this problem because numerous sensors with different spatial, temporal and radiometric resolutions are available to capture the data regarding earth surface all over the world, including IRS mission of India (Chitale *et al.*, 2000; Chowdhury *et al.*, 2003; Jha *et al.*, 2007). GIS is one of the best tools that analyze and manage RS and other data in very efficient manner. Presently, GIS and RS are the basic tools along with conventional modeling to assess the natural resources as well as planning and management. This chapter outlines the detailed methodology of creation of a GIS database required for groundwater modeling studies.

4.2 DATA COLLECTION AND VERIFICATION

It is one of the most important steps after the problem identification. For any application based study in which result depends on spatial and thematic data, authentic and reliable data is required. Sometimes, primary data is not available for the study undertaken, so in such cases information can be extracted on the basis of interview and questionnaire of respondents. Collected data may be spatial and non-spatial in nature and available in any form, such as documents, drawing, digital data and spread sheets at different scale and levels. After the data has been collected from different sources, it may have to be collated and managed so that it can be easily understood and interpreted. This process is called data collation, and will usually require summarizing and tabulating the information.

After collecting the data, it is examined and checked properly for error. Especially, conventional method of collection and management of large volume of hydrological and meteorological data are cumbersome. In India, the data obtained from different organizations

regarding rainfall, water level and quality data etc. are generally available in hand written document so there may be chances of errors while entering the records. Types of data collected and steps before GIS database creation has been explained in Figure 4.1.

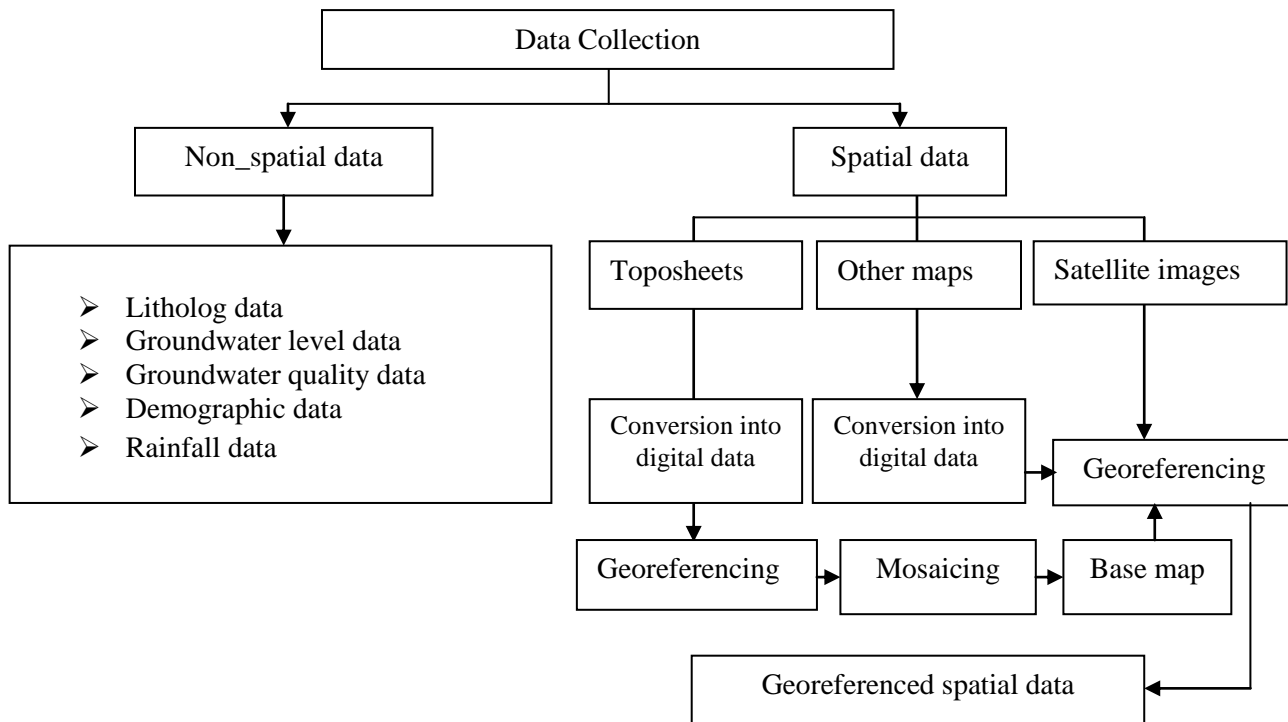


Fig. 4.1: Flowchart depicting study of data collection

4.3 GEOGRAPHIC DATABASE CREATION IN GIS

There are two types of geographical data; spatial and non spatial. The geographical database is designed properly depending on the application for which it is developed. In the present study, geographic database for Loni and Morahi watersheds has been created at scales 1:50,000 and 1:250,000. Watershed boundary has been used as basic spatial unit. Most of the thematic layers have been generated at a scale of 1:50,000 to 1:250,000, except soil map which is prepared at 1: 10, 00,000 scale.

4.3.1 Spatial Frame Work for Geographic Database

This defines the actual geographic area for which database is to be created. Loni and Morahi watersheds are covered by seven toposheets numbered as 63 B/ 6, 7, 10, 11, 12, 15 & 16 at 1:50,000 scale. Each toposheet is georeferenced at UTM WGS 84 projection system. A standard georeferencing procedure has been adopted for the entire geographic database as shown in Figure 4.2. After georeferencing, a mosaic was created using mosaicking tool in ERDAS software.

4.3.2 Spatial Data Normalization

This process is used to avoid repetition of common information available in different thematic maps, and thus reduces the redundancy in data. It also ensures that common features in different maps are coincident, thereby limiting sliver problem in overlaying. Boundaries of sub-watersheds have been taken as first order normalization and a reference layer (shapefile, .shp format) containing sub-watersheds. Reference shapefile (sub-watershed boundary layer) has been digitized once, and is used as a base layer for the preparation of all vector and raster layers.

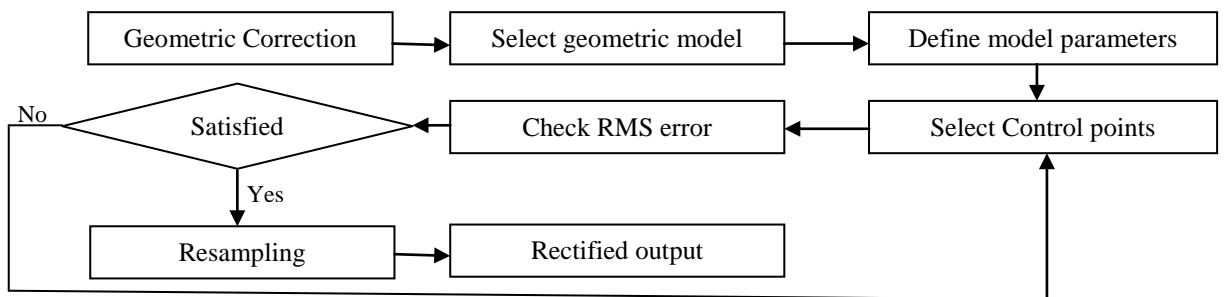


Fig. 4.2: Methodology for geo-referencing

4.3.3 Spatial Database Creation in GIS

Various thematic information for the study area (i.e., shapefile and coverage) are created using ArcGIS package. ArcGIS has capability to create, manage, integrate and analyze the geographical data in an efficient manner (Sharholly *et al.*, 2007). Methodology of database creation has been shown in Figure 4.3.

4.3.4 Digitization of Features

The data are collected in many phases as per availability from different sources. All the data collected from different sources are firstly geo-referenced with the help of toposheet mosaic. All the features are digitized in the form of point, polyline and polygon feature classes to develop various thematic maps.

4.3.4.1 Point feature class

A point has been used to represent the feature that is too small in a map for example, observation well. In the present study, spot heights have been digitized in point feature class to generate a DEM. Other point feature classes, such as raingauge stations, observation wells, pumping wells, lithologs have been created directly from database file which have XYZ

coordinates. Litholog map, rain gauge stations, observation wells, pumping wells feature classes have been created from the tabular data obtained from Central Ground Water Board (CGWB) reports.

4.3.4.2 Polyline feature Classes

A polyline has been used to represent features that are linear in nature, for example, road network, rail line, canal, contour and drainage network etc. In the present study all the linear features are firstly digitized from topographical map and then updated with the help of high resolution satellite images.

4.3.4.3 Polygon feature Class

Polygons are represented by a closed set of lines and are used to define feature, such as administrative boundaries. In general, polygon feature classes are not digitized directly for avoiding sliver error. Firstly, it is digitized as polyline feature class then it is converted into polygon feature class using construct topology command available in ArcGIS software. In the present study, district boundary map has been prepared from topographical map of Survey of India.

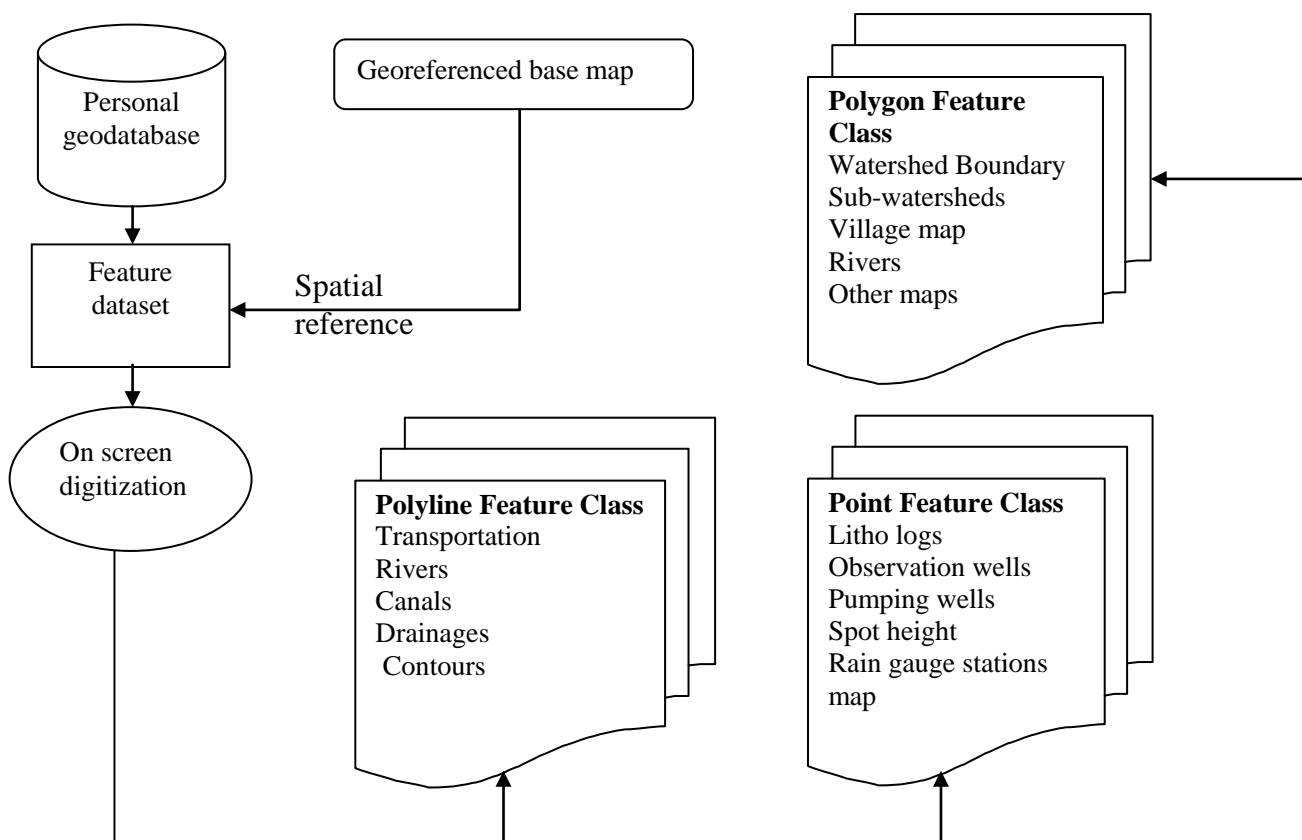


Fig. 4.3: Methodology for GIS database creation

4.4 METHODOLOGY OF WATERSHED DELINEATION

The overall watershed delineation process is shown in Figure 4.4.

4.4.1 DEM

The DEM is prepared using Advance Space Borne Thermal Emission and Reflection Radiometer (ASTER) satellite data.

4.4.2 Fill DEM

The function of fill DEM is to remove the imperfections from the DEM as shown in Figure 4.5.

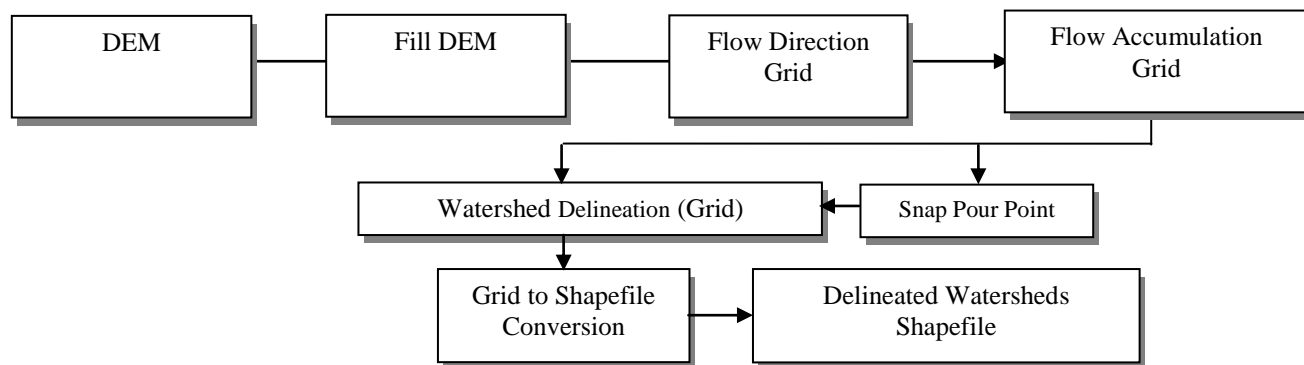


Fig. 4.4 Methodology for watershed delineation

4.4.3 Flow Direction

It determines the direction of flow in a grid on the basis of eight nearest neighbours. The ultimate aim was determining the direction of the steepest descent from that cell. The flow direction map is shown in Figure 4.5.

4.4.4 Flow Accumulation Grid

Flow accumulation of cell is determined as the sum of flow accumulation values of the neighbouring cells which flow into it. It is an iterative process. All iteration has a forward and backward pass and its run until the flow accumulation value calculated by two successive iterations are identical. The calculated flow accumulation grid is shown in Figure 4.5.

4.4.5 Snap Pour Point

Snap Pour Point is used to ensure the selection of points of high accumulated flow for delineating watershed. It has been created as point shapefile and the point will be added at the center of highest flow accumulation cell in a grid.

4.4.6 Watershed

The watershed has been delineated on the basis of pour point, flow direction grid and flow accumulation grid, as shown in Figure 4.5 and delineated watersheds are converted into vector format using raster to vector conversion tool of ArcGIS package.

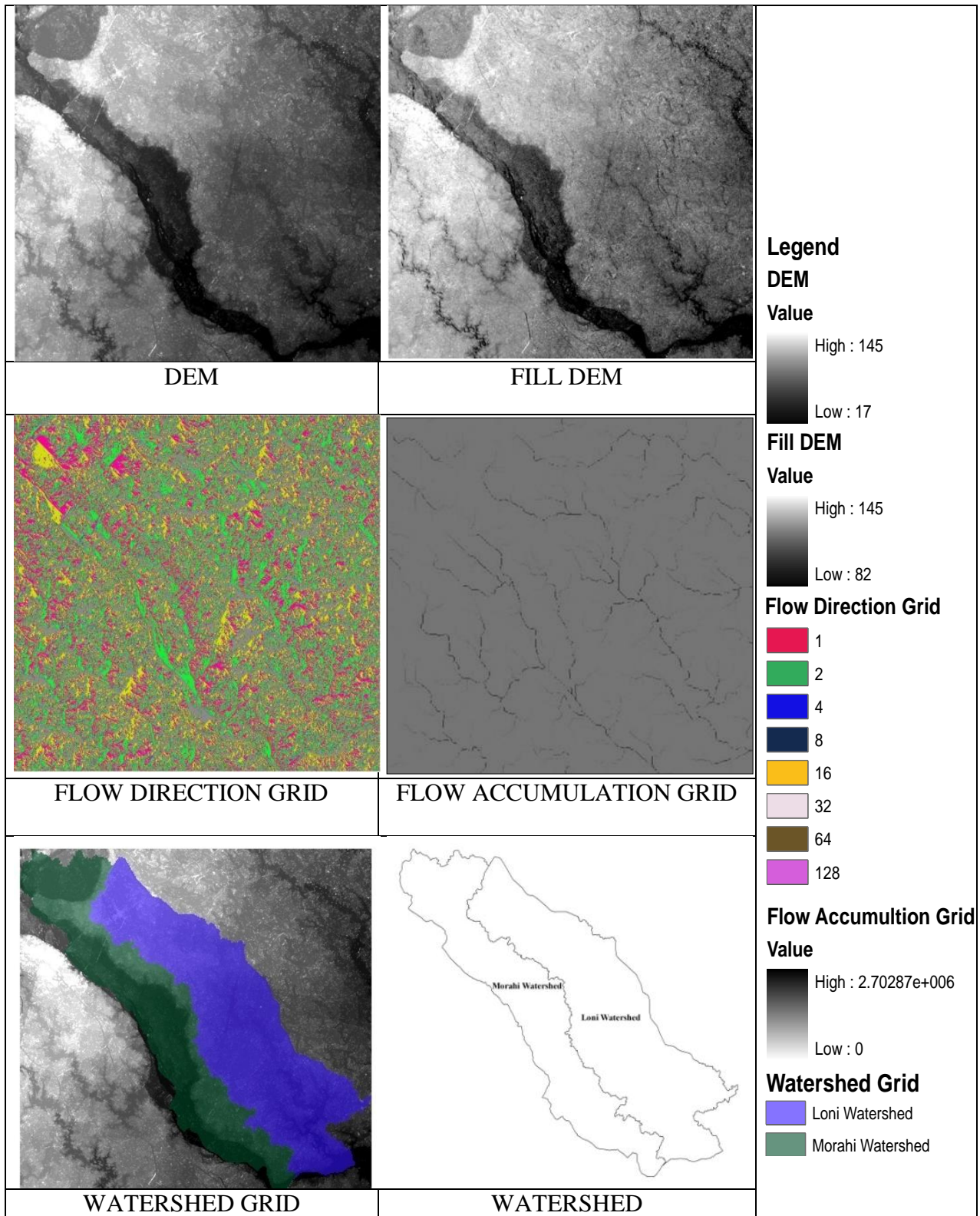


Fig. 4.5 Watersheds delineation through DEM

4.5 CREATION OF GIS LAYERS

4.5.1 Drainage Layer

Drainage network is an important feature, as it decides the hydrological and geomorphological characteristics of the watershed. It has been generated using SOI toposheets at 1:50,000 scale. Subsequently, it is updated with the satellite image (Landsat Enhanced Thematic Mapper plus (ETM+) & Advanced Spaceborne Thermal Emission and Reflection Radiometer (ASTER)). It has been used in this study for morphometric analysis and delineation of groundwater potential zones. It is shown in Figure 4.6.

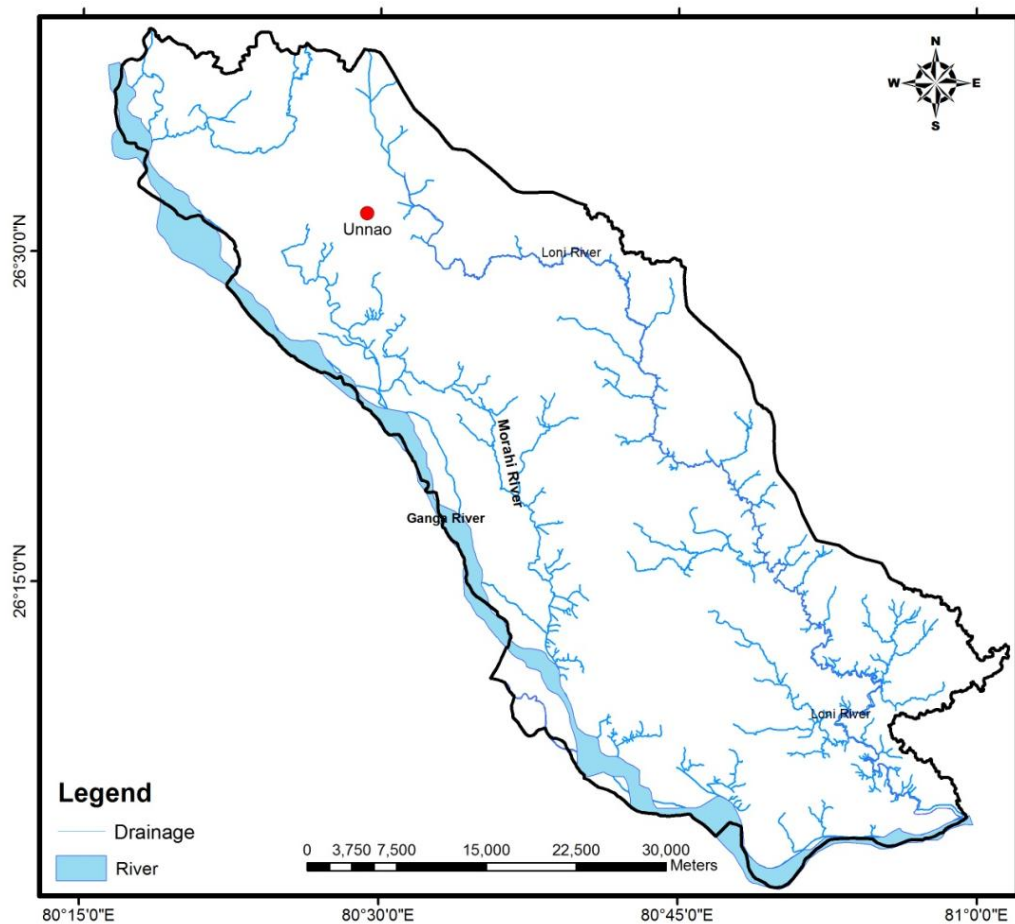


Fig. 4.6 Drainage layer

4.5.2 Drainage Density Layer

Drainage density is defined as the closeness of spacing of stream channels. In other words, it is a measure of total length of the streams channels per unit area. It is an inverse function of permeability. The less permeable a rock is, the less rate of rainfall infiltration, which conversely tends to be concentrated in surface runoff. Drainage density of the study area

is calculated using line density analysis tool in ArcGIS 9.3 software. The drainage density lies between 0.12 to 1.3 km/km². It is further classified into five classes, as shown in Figure 4.7.

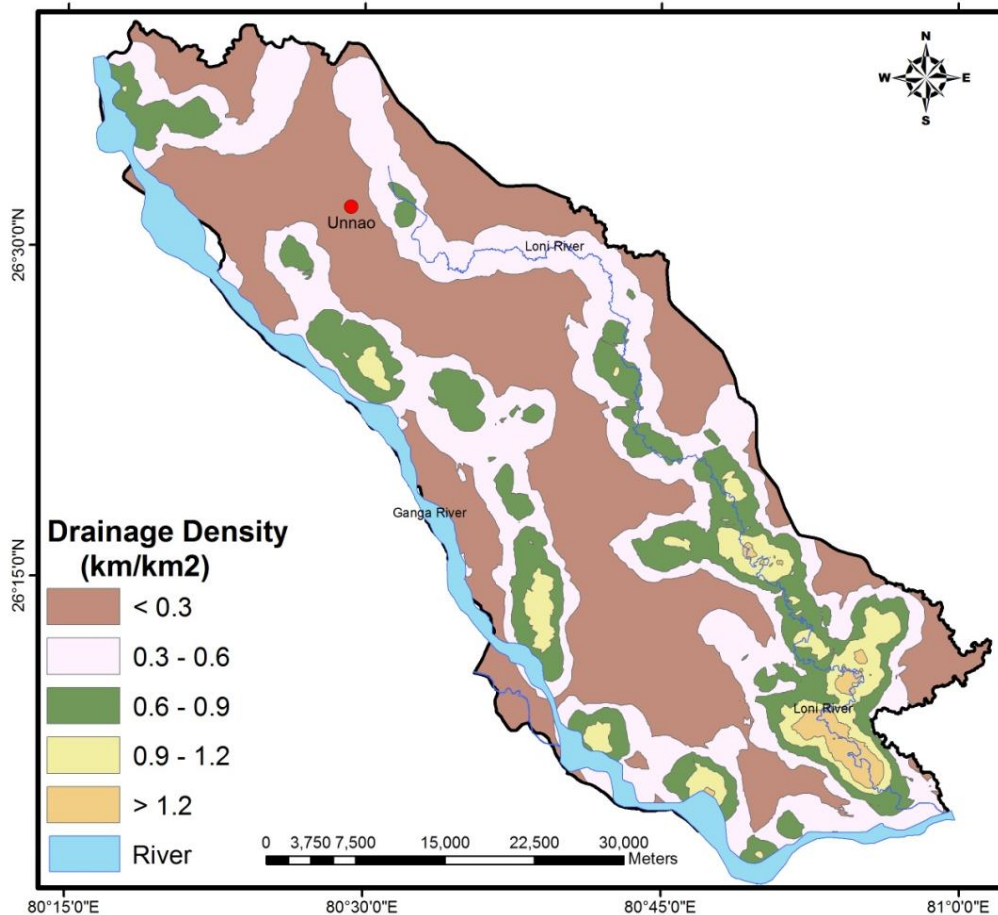


Fig. 4.7 Drainage density layer

4.5.3 Digital Elevation Model (DEM) Layer

The DEM is prepared using ASTER satellite data as shown in Figure 4.8. The area has almost flat topography with small variation in elevations. For comparative study it is categorized into five classes. The highest elevations value is about 138 m from MSL which exists in the northeastern portions of the area. This area persuades highest runoff and hence less possibility of rainfall recharge as compared to other areas. The elevation is usually low in the southwest and south portions of the area so in these areas high possibility of recharge and low runoff.

4.5.4 Slope Layer

Topographical elevation map and DEM were prepared from the ASTER data (USGS 2011) by filling sinks to remove local depressions and applying two directional gradient filters

(one in x-direction and another in y-direction). The filtering was done by using in-built linear filters available in the software. The resultant maps were used to compute a slope map.

The slope map of the study area is shown in Figure 4.9. It is classified into five classes as shown in Table 4.1, which are: (1) 0–1%, (2) 1-3%, (3) 3-5%, (4) 5-10%, (5) >10%. The slope of the study area mainly lies between 0-5 %, and this region is assigned higher rank due to almost flat terrain while the class having highest value is categorized as lower rank due to relatively high run-off and low recharge.

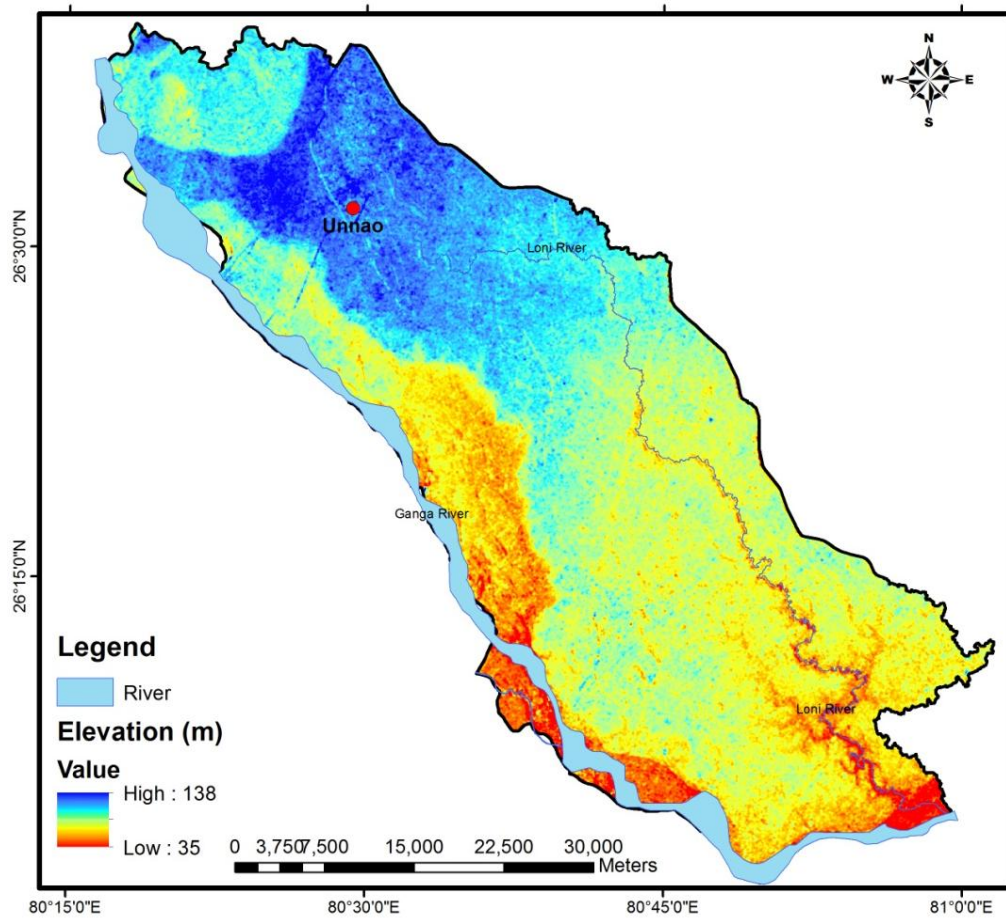


Fig. 4.8 DEM layer

Table 4.1 Categories used for classification of slope layer

S. No.	Slope Category	Slope (%)
1.	Nearly level	0 - 1
2.	Very gently sloping	1 – 3
3.	Gently sloping	3 – 5
4.	Moderately sloping	5 - 10
5.	Strongly sloping	> 10

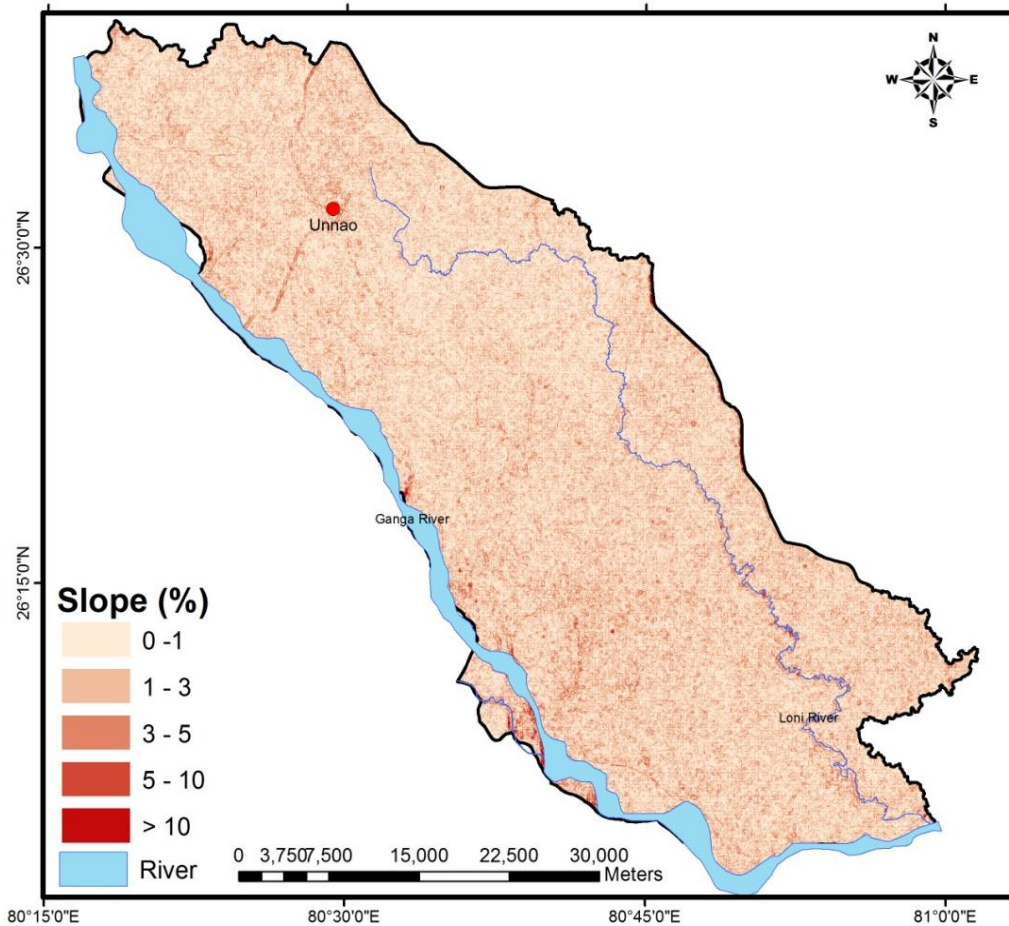


Fig. 4.9 Slope layer

4.5.5 Geomorphology Layer

It was prepared on the basis of the specific tone, size, texture, shape and association characteristics seen on Landsat TM image. Geomorphologically, the study area consists of active floodplain, older flood plain, alluvial plain, lacustrine plain deposit and their landforms Meander scars and paleo channels are shown in Figure 4.10. Active flood plain has higher water level surface, hence it is best landform for occurrence of high groundwater.

4.5.6 Geology Layer

Geology map is prepared using visual interpretation of satellite image with the aid of Geological Survey of India (GSI) map. In the present study area, four types of geology namely; Channel Alluvium, Terrace Alluvium, Lacustrine Deposits and Older Alluvium are present, as shown in Figure 4.11.

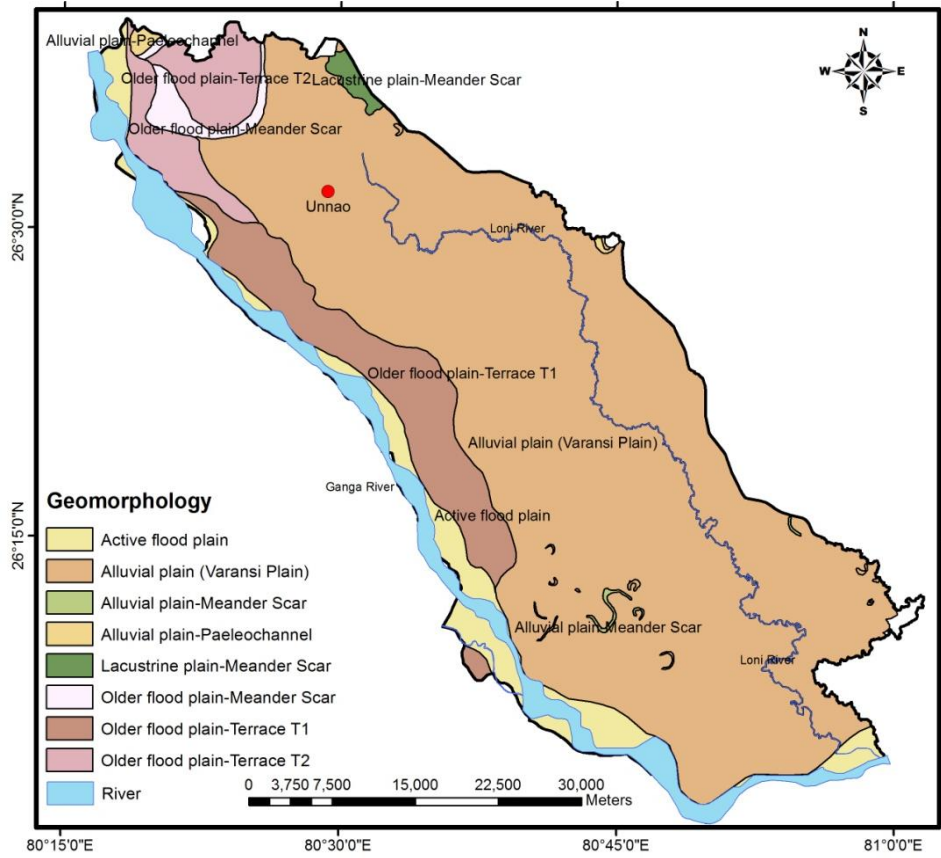


Fig. 4.10 Geomorphology layer

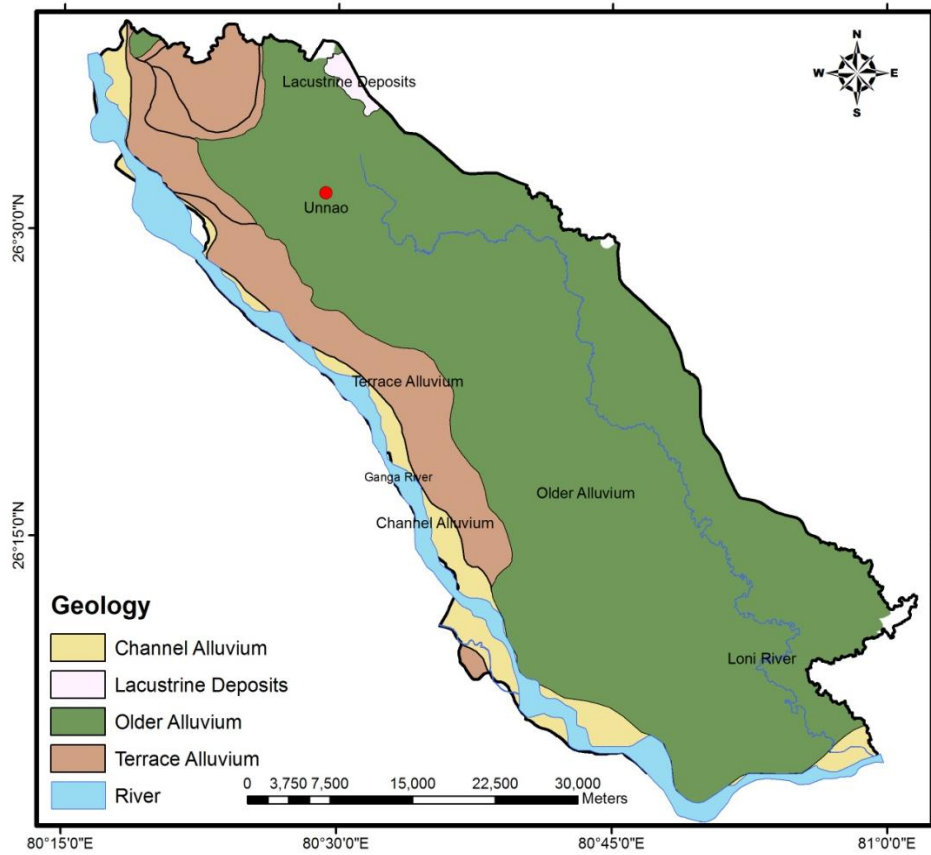


Fig. 4.11 Geology layer

4.5.7 Soil Layer

It is prepared using the soil map obtained from the NBSS & LUP, Nagpur at 1:5,000,000 scales. It has further updated with the help of geomorphology layer and satellite image of Landsat TM. The soils for the study area reveal five main soil categories, namely; sand, sandy loam, silt loam, silt loam & loam and silty clay loam & clay loam. In the Loni and Morahi watersheds, all soils having high salt content, locally these soils are termed as reh, rehala or namkeen. The common outwardly feature of this type of soil is the presence of extensive white, grayish-white or ash colored fluffy deposits of salts on the surface of the land, either in patches scattered. Inwardly, the soil possesses an open structure. The texture of the soil varies from loamy sand to loam; but the soil and subsoil are not compact and dense or inherently impervious to water (Singh *et al.*, 2013). Figure 4.12 shows wheat grown in these types of soils. Ranking of soil has been assigned on the basis of their infiltration rate. Sandy soil has high infiltration rate, hence it is given higher priority. While the clayey soil has least infiltration rates, hence it is given low priority.

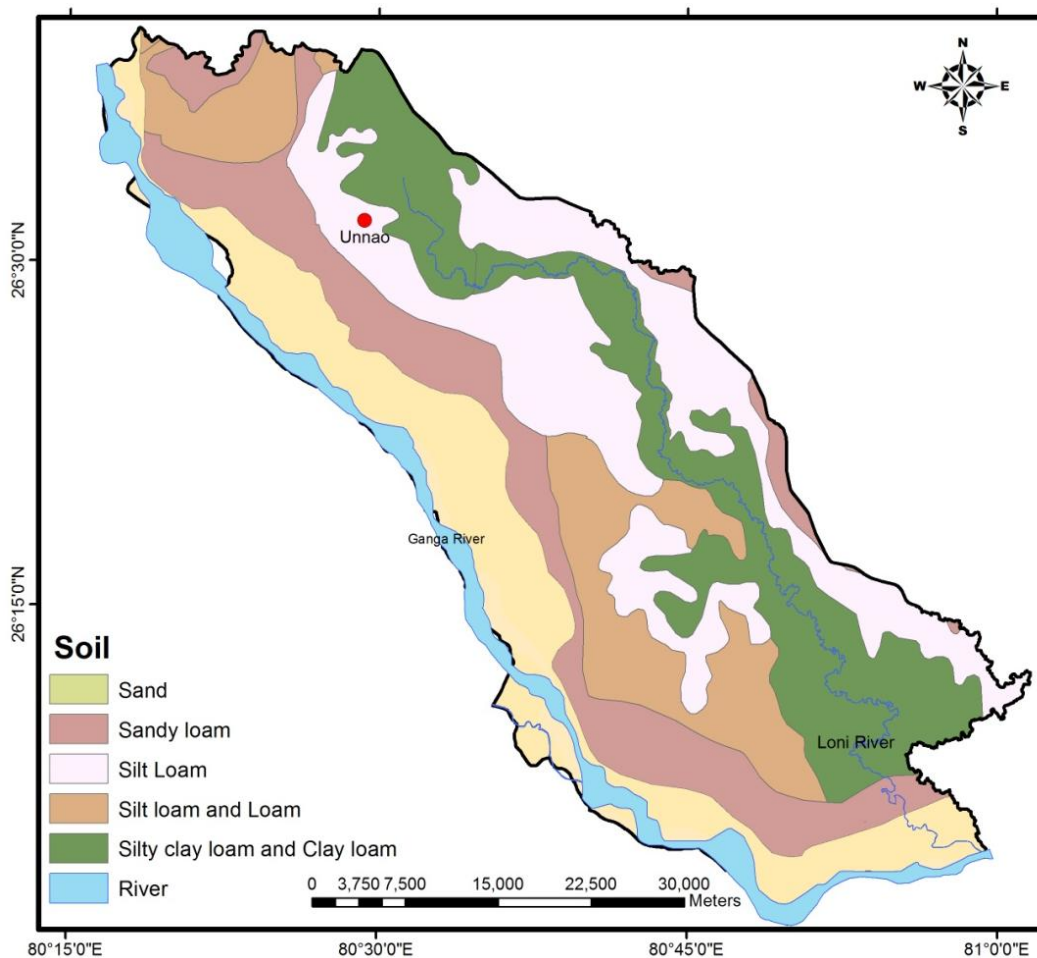


Fig.4.12: Soil layer

Further soil map has been classified into Hydrological Soil Groups (HSG) A, B, C and D on the basis of soil properties, as shown in Table 4.2. The classified HSG layer is shown in Figure 4.13, and it is evident that the region predominantly comprises of HSG B (38.26%) and D (20.84%). While, HSG C is absent, HSG A (40.9%) is restricted to bazada, flood plains and natural levees, which suggest high surface runoff tendency of the watershed.

Table 4.2: Hydrological soil group and major soil types

HSG	Description	Soil Taxanomy	Infiltration (Inch/hr)	Distribution (%)
A	Deep, Well Drained, Fine Loamy Soil with Loamy Surface and Slight Erosion	Sand, loamy sand, or sandy loam.	> 0.30	40.90
B	Deep, Imperfectly Drained, Coarse Loamy, Calcareous Soil with Loamy Surface, Moderately Saline and Sodic	Silt loam or loam	0.15 – 0.30	38.26
D	Deep, Well Drained, Fine Loamy, Calcareous Soil with Loamy Surface, Slightly Erosion, Slightly Saline and Sodic	Clay loam, silty clay loam, sandy clay, silty clay, or clay.	0.00 - 0.05	20.84

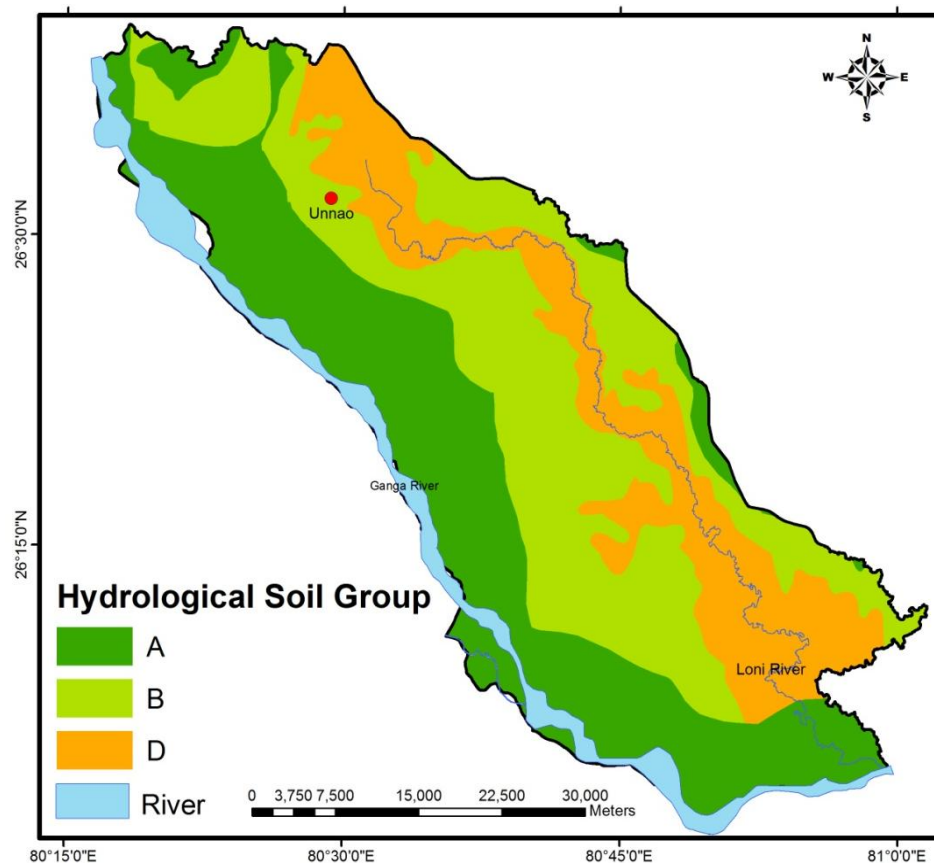


Fig. 4.13: Hydrological soil group layer

4.5.8 Land Use/Land Cover Layer

It was generated using Landsat TM imagery at 30 m spatial resolution pertaining to 11 Oct 2006 in seven spectral bands. For generation of LULC map, supervised classification

method has adopted using Bayesian Maximum Likelihood Classifier (MLC). MLC is a parametric decision rule and well developed method from statistical decision theory that has been widely applied to classify TM image. Accuracy assessment of the LULC map was determined by correlating ground truth information and achieved 89% accuracy and value of kappa coefficient (κ) is 0.8325.

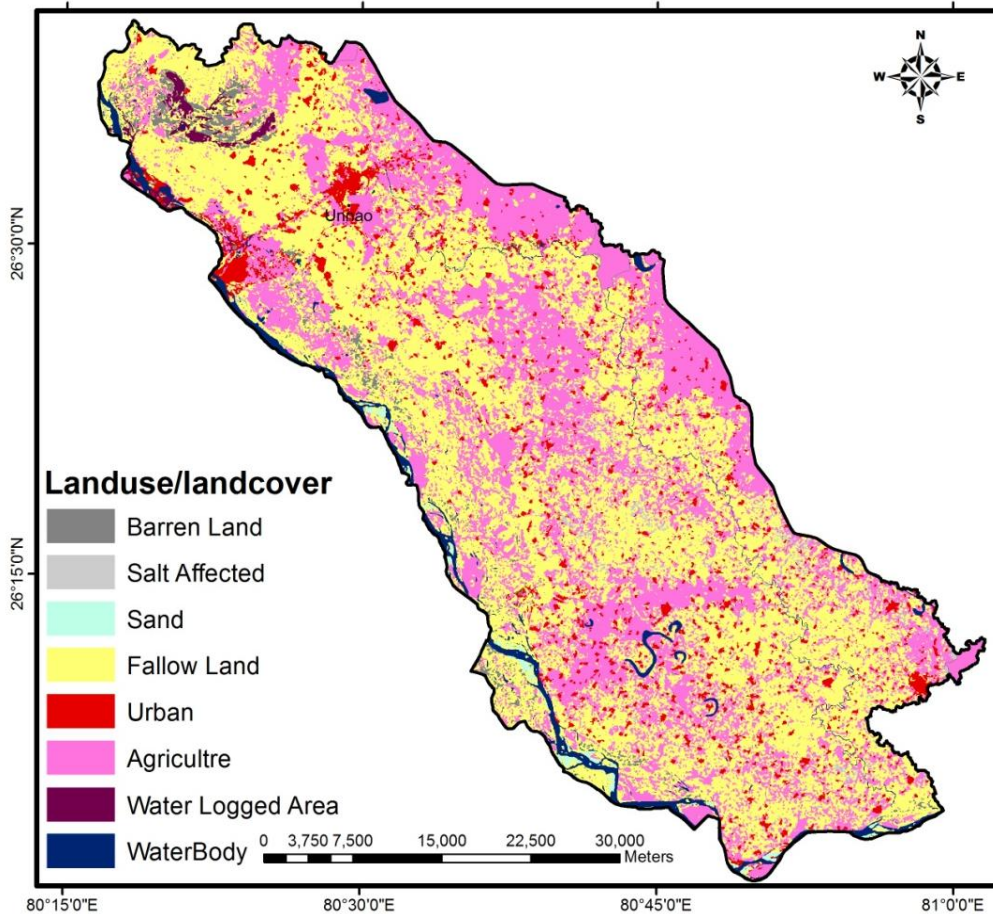


Fig. 4.14: Landuse/landcover layer

4.5.9 Rainfall Layer

Daily rainfall data of 7 raingauge stations lying in and near the study area have been acquired from IMD, Pune. The mean annual rainfall based on 13 years (1993–2005) data at 7 rainfall stations were used to create a point rainfall map for the study area. This point map was converted into a polygon layer by Thiessen Polygon method.

Rainfall has the major contribution to recharge the ground sources. It determines the amount of water that would be available to infiltrate into the groundwater system. Monthly rainfall data of the study area for period of 15 years (i.e. 1993–2007) and the location of

rain gauge station were obtained from the IMD, Pune. The data has been interpolated using Thiessen Polygon method to produce the rainfall map of the area (Figure 4.15). The resulting map was categorized into four classes namely < 600; 600–700; 700–800 and >800 mm/year. It is observed that northern and west southern part of the area receives the largest amount of rainfall, while the southern part receives the lowest amount of rainfall.

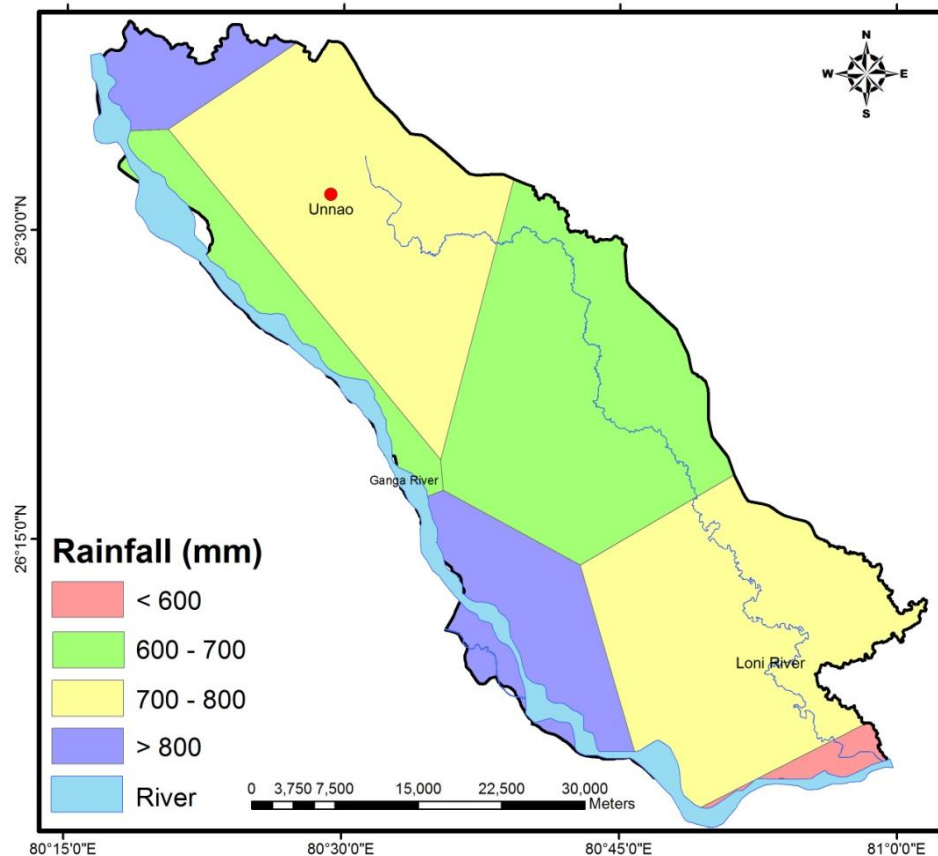


Fig. 4.15: Rainfall layer

4.5.10 Pre-monsoon Groundwater Depth Layer

Contour maps of pre-monsoon and post-monsoon season have been prepared from groundwater level data, collected from CGWB, Lucknow. In pre-monsoon season (Figure 4.16), groundwater depth generally ranges from 2.66 to 20.55 m, with a major portion of the area having 4 to 12 m depth. In the northwestern and southern part of the area, groundwater depth is 12 to 20.55 m.

4.5.11 Post-monsoon Groundwater Depth Layer

On the other hand, the post-monsoon season (Figure 4.17), groundwater depth ranges from 1.85 to 18 m, with a majority of the study area having 4 to 12 m depth. Thus, there is a

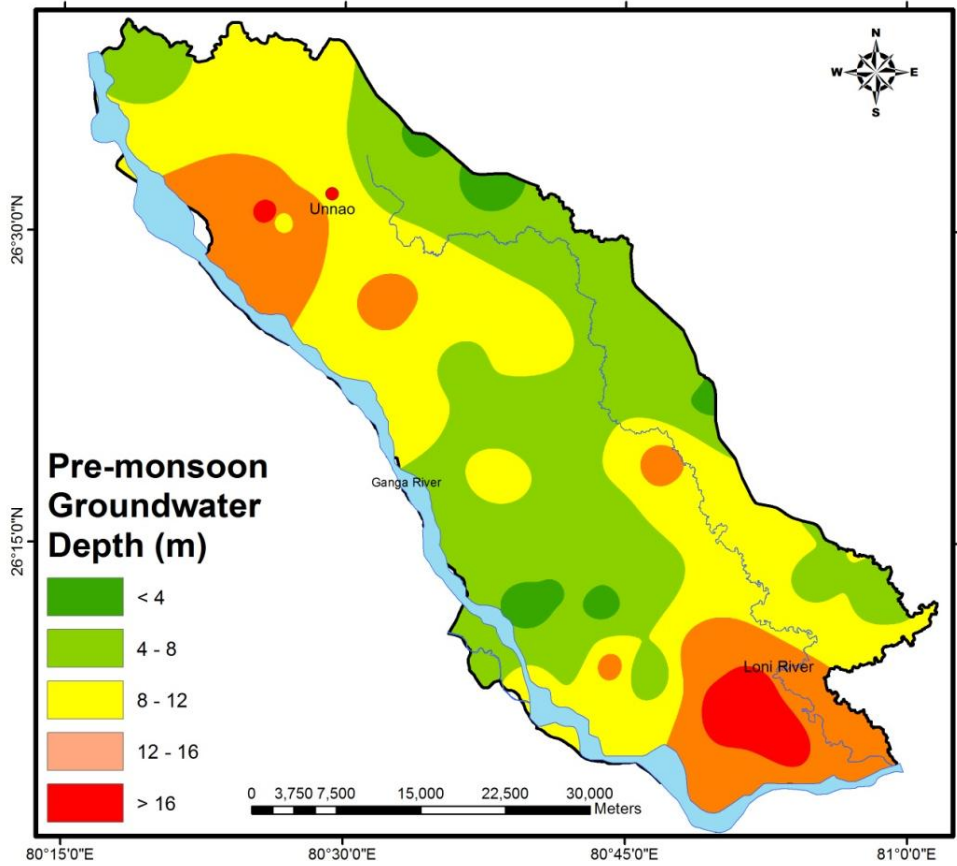


Fig. 4.16: Pre-monsoon groundwater depth layer (2006)

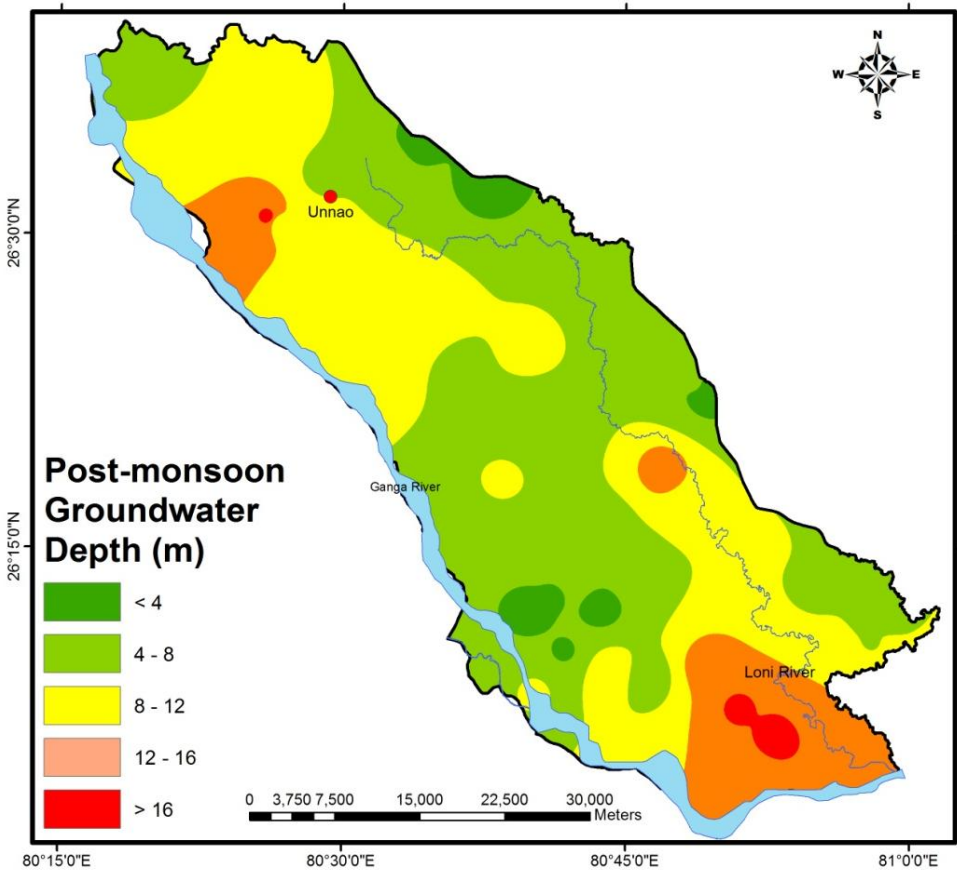


Fig. 4.17: Post-monsoon groundwater depth layer (2006)

considerable seasonal fluctuation of groundwater levels over the study area, which is mainly attributed to southwest monsoon rains. On the basis of the groundwater depth maps, it was found that the depth to water table was very deep in the southern part of the study area.

4.5.12 Water Level Fluctuation Layer

The measurement of water level fluctuations in observation wells is an important facet of groundwater studies (Freeze and Cherry, 1979). The difference between successive rise and fall in the water level in observation wells during a year is called fluctuation, where rise is due to the recharge and fall because of the discharge. Positive fluctuations are those which show rise in water level during post-monsoon. Negative fluctuation shows further decline in post-monsoon season. Positive and negative groundwater fluctuations would pertain to the conditions where groundwater recharge components exceeds the groundwater discharge and vice versa.

The water level fluctuations are represented by differences in pre-monsoon and post-monsoon groundwater levels. A map of water level fluctuation is shown in Figure 4.18, which has been divided into four classes' viz. (i) 0-1 (ii) 1-2 (iii) 2-3 and (iv) 3-4 m.

4.5.13 Village Boundary Layer of Watersheds

Block and village boundary layer is prepared using Census data administrative boundaries. Figure 4.19, shows the block and village boundary map of the area. The blocks and villages are shown in Table 4.3.

Table 4.3 Blocks and villages in study area

S. No.	Blocks	Villages
1.	Bichhiya	69
2.	Bighapur	124
3.	Khiron	47
4.	Lalganj	82
5.	Purwa	83
6.	Sareni	156
7.	Sikandarpur Karan	119
8.	Sikandarpur Sarausi	99
9.	Sumerpur	190

Thematic maps regarding observation wells and pumping wells have been given in next chapters. Other maps have been shown in previous section while describing the study area.

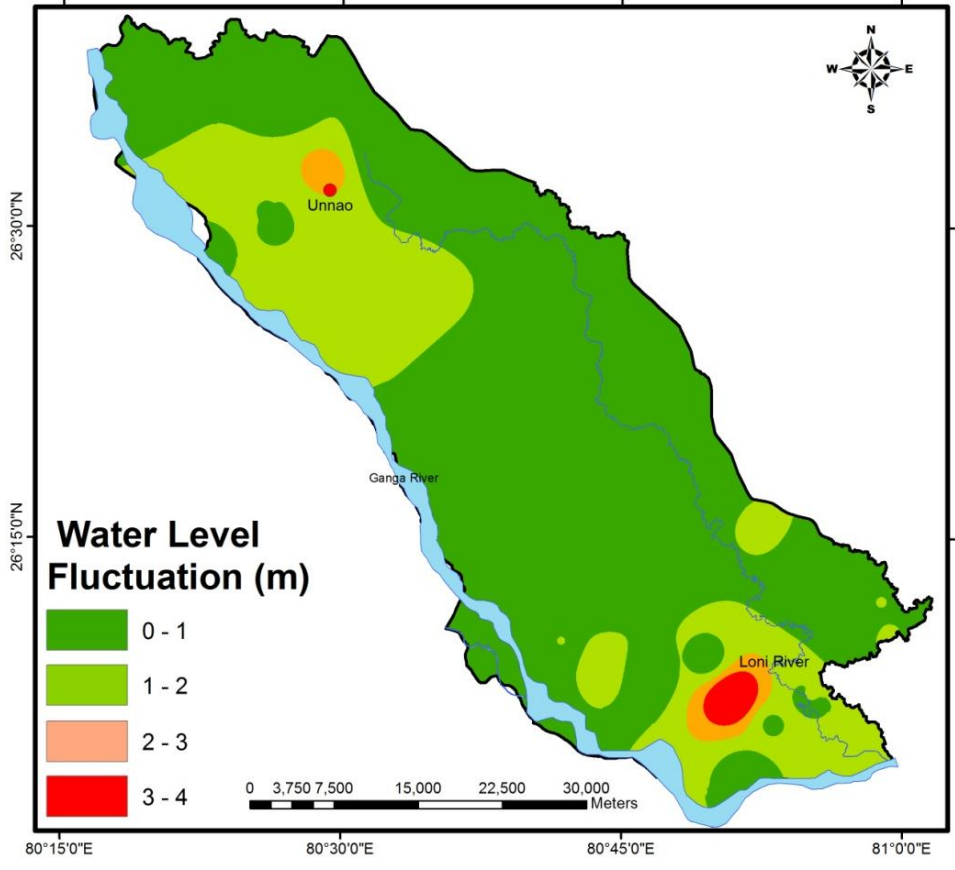


Fig. 4.18: Water level fluctuation (pre- and post-monsoon 2006)

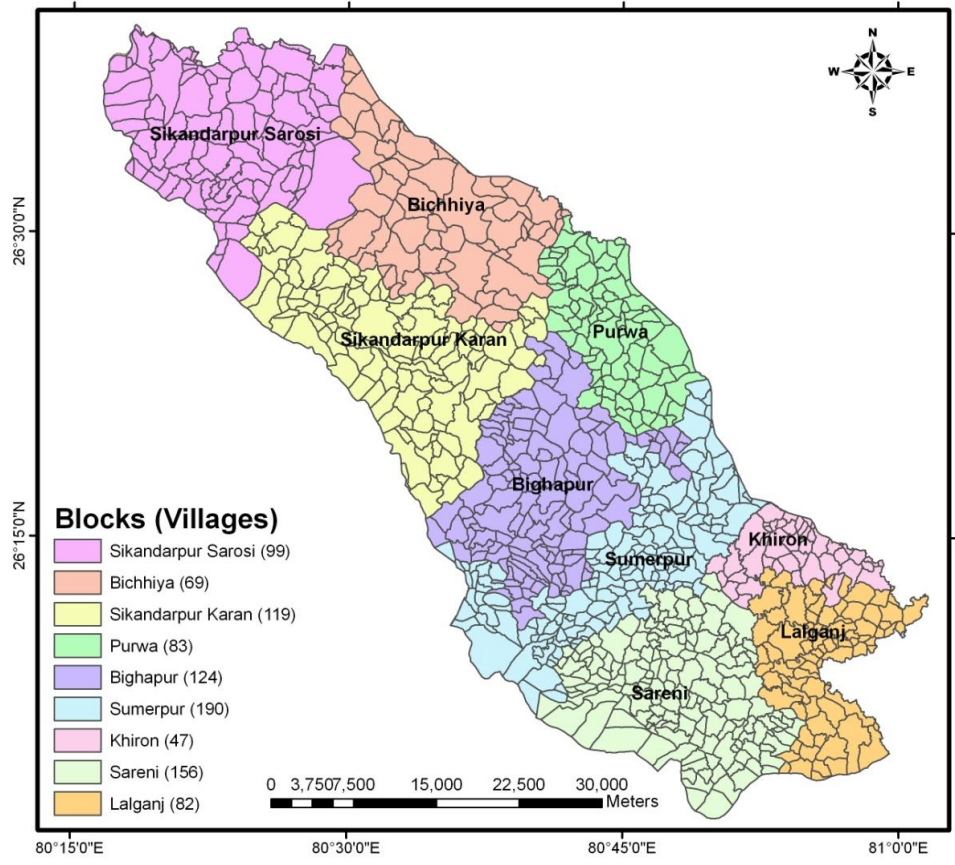


Fig. 4.19 Village boundary layer

5.1 PROLOGUE

Groundwater is a precious natural resource having limited extent and volume. With increasing use of groundwater for agricultural, municipal and industrial needs, the annual extraction of groundwater happens to be generally far in excess of its net average natural recharge. Additionally, interventions in hydrological regime and climatic change have significant impact on natural recharge. Consequences of over-exploitation of groundwater all over the world include decrease in water table, resulting in lower agricultural productivity, sea water intrusion in coastal aquifer, land subsidence, groundwater quality degradation, droughts etc. (Samadder *et al.*, 2011). To manage and protect this precious resource from overuse and contamination, it is necessary to identify the groundwater potential zones, recharge zones, groundwater quality status and artificial recharge structures, such as farm ponds, check dams, percolation tanks and nala bunds, etc.

In this chapter, the capabilities of RS and GIS techniques have been demonstrated to map and manage the groundwater resources.

5.2 GROUNDWATER POTENTIAL ZONES MAPPING

The term groundwater potential indicated the amount of groundwater availability in a particular area. However, from groundwater exploration view, this term can be defined as the possibility of groundwater occurrence in an area. Appropriate information and knowledge of groundwater potential will be very helpful for decision makers to identifying the suitable locations for drilling production wells and/or monitoring wells as well as to protect the vital groundwater resources from contamination. The overall methodology to identify and delineate groundwater potential zones using RS, GIS alongwith MCDM techniques is illustrated in Figure 5.1.

In this study, eight hydrologic themes, namely; geology, geomorphology, LULC, soil, slope, drainage density, Water Table Fluctuation (WTF) and rainfall were created in raster format and integrated in a GIS environment. Individual theme and class was assigned a weight on the basis of Saaty's scale (Table 5.1), considering two themes and classes at a time on the basis of their relative importance to determine the groundwater potential. Thereafter, pair-wise comparison

matrices of assigned weights to different thematic maps and their individual features were constructed using Saaty's AHP (Saaty, 1980) and then weights were normalized by eigenvector approach.

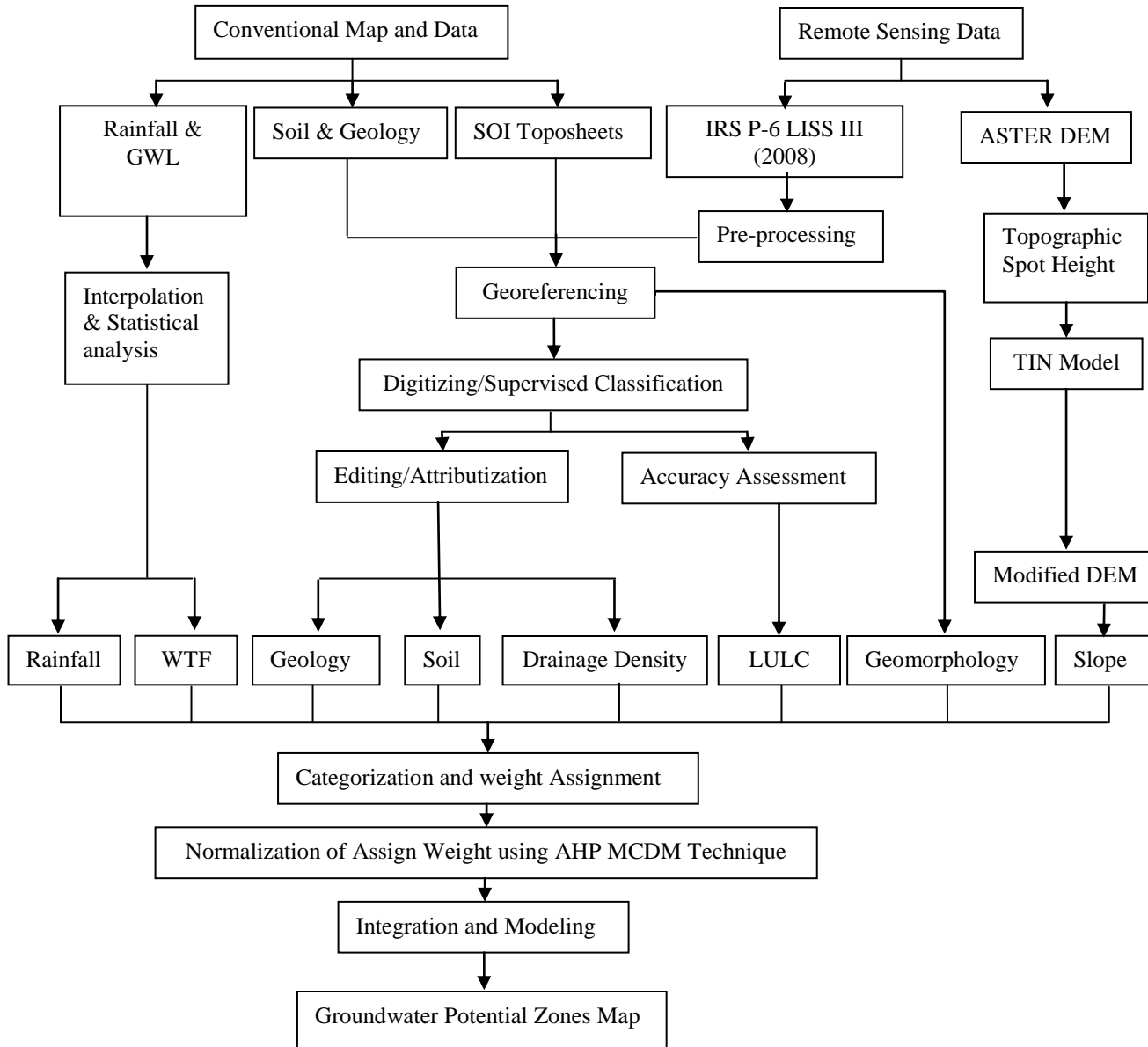


Fig. 5.1: Flowchart of groundwater potential mapping

The normalized weights of the themes and their features, thus obtained, were examined for consistency by computing a Consistency Ratio (CR), as recommended by Saaty (1980). The CR values indicate the probability that the matrix ratings are randomly generated.

Table 5.1 Saaty's scale

Less Important				Equally Important	More Important			
Extremely	Very Strongly	Strongly	Moderately		Moderately	Strongly	Very Strongly	Extremely
1/9	1/7	1/5	1/3	1	3	5	7	9

The following steps were followed to compute the CR for the themes and their classes (Saaty, 2005):

- (1) The normalized pair-wise comparison matrix A_1 is built as:

$$A_1 = \begin{bmatrix} a_{11}' & a_{12}' & \dots & a_{1n}' \\ a_{21}' & a_{22}' & \dots & a_{2n}' \\ \vdots & \vdots & \ddots & \vdots \\ a_{n1}' & a_{n2}' & \dots & a_{nn}' \end{bmatrix}, a_{ij}' = \frac{a_{ij}}{\sum_1^n a_{ij}} \text{ for } i, j = 1, 2, \dots, n \quad (5.1)$$

- (2) The eigenvalue and the eigenvector are calculated as:

$$W = \begin{bmatrix} w_1 \\ w_2 \\ \vdots \\ w_n \end{bmatrix} \text{ and } w_i = \frac{\sum_1^n a_{ij}'}{n} \text{ for } i = 1, 2, \dots, n \text{ \& } W' = AW = \begin{bmatrix} w_1' \\ w_2' \\ \vdots \\ w_n' \end{bmatrix},$$

$$\& \lambda_{max} = \frac{1}{n} \left(\frac{w_1'}{w_1} + \frac{w_2'}{w_2} + \dots + \frac{w_n'}{w_n} \right) \quad (5.2)$$

Where W is the eigenvector, w_i is the eigenvalue of criterion i , and λ_{max} is the average eigenvalue of the pair wise comparison matrix.

- (3) To judge the uncertainty Saaty's measure of consistency is given, called Consistency Index (CI), as deviation or degree of consistency using the following equation:

$$CI = \frac{\lambda_{max} - n}{n - 1} \quad (5.3)$$

Where n is the number of classes or features.

(4) Consistency Ratio (CR) is a measure of consistency of pairwise comparison matrix, and is given by equation:

$$CR = \frac{CI}{RI} \quad (5.4)$$

Where RI is the Ratio Index. The value of RI is taken from standard table given by Saaty (1980). The CR is acceptable if CR value is smaller or equal to 0.1, otherwise to avoid inconsistency, the corresponding weights should be re-evaluated.

5.2.1 Weight Assignment and GIS-based Modeling

All the thematic maps and their individual features have been assigned suitable weights according to their hydrological importance for occurrence of groundwater in the study area. The normalization of weights of individual thematic map and its different features on the basis of AHP is shown in Table 5.2. After deriving the normalized weights of all the thematic maps, these were integrated in the GIS environment using the equation 5.5, as given by Malczewski (1999):

$$GWPZ = \sum_{w=1}^m \sum_{i=1}^n (w_j \times x_i) \quad (5.5)$$

Where, GWP = Ground Water Potential Zones, x_i = normalized weight of the i^{th} class/feature of theme and w_j = normalized weight of the j^{th} theme, m = total number of themes, and n = total number of classes in a theme.

The output map is classified into five equal classes on the basis of low to high sum, i.e. 'very poor', 'poor', 'moderate' 'good', and 'very good', in order to delineate the groundwater potential zones.

5.2.2 Verification of Groundwater Potential Zones Map

The delineated groundwater potential zone map was verified using the available yield data of 40 pumping wells. Mean discharge of all the pumping wells was computed and compared with individual groundwater potential category.

Table 5.2: Weightage of different parameters for groundwater potential zones mapping

Parameters	Weights	Detailed classes	Weights
GEOLOGY	0.19	Channel Alluvium	0.52
		Terrace Alluvium	0.24
		Varanasi Alluvium	0.17
		Lacustrine deposits	0.07
GEOMORPHOLOGY	0.23	Active flood plain	0.23
		Alluvial plain (Varansi plain)	0.09
		Alluvial plain-Meander Scar	0.10
		Alluvial plain-Paeleochannel	0.15
		Lacustrine plain-Meander scar	0.06
		Older flood plain-Meander scar	0.11
		Older flood plain-Terrace T1	0.13
		Older flood plain-Terrace T2	0.13
LULC	0.05	Barren land	0.06
		Salt Affected	0.05
		Sand	0.07
		Fallow Land	0.09
		Urban	0.05
		Agriculture Land	0.27
		Water logged Area	0.11
		Water bodies	0.30
DRAINAGE DENSITY (Km/Km ²)	0.09	< 0.3	0.50
		0.3 – 0.6	0.26
		0.6 – 0.9	0.13
		0.9 – 0.12	0.07
		> 0.12	0.04
WATER TABLE FLUCTUATION (m)	0.19	< 1	0.47
		1- 2	0.28
		2 - 3	0.17
		3 - 4	0.08
SLOPE (%)	0.05	0 – 1%	0.44
		1 – 3%	0.26
		3 – 5%	0.16
		5 - 10%	0.09
		>10%	0.05
SOIL	0.09	Sand	0.51
		Sandy loam	0.26
		Silt loam & Loam	0.13
		Silt loam	0.07
		Silty clay loam & Clay loam	0.03
RAINFALL (mm)	0.11	<600	0.10
		600-700	0.16
		700-800	0.28
		>800	0.46

5.3 RAINFALL RUNOFF MODELING USING SCS-CN METHOD

In earlier decades, the runoff was estimated as a percentage of storm rainfall, where the percentage of runoff increases with the increase in rainfall (Linsley *et al.*, 1958). The Soil Conservation Service (SCS) has developed a widely used runoff curve number procedure for estimating the runoff, in which the effects of LULC, various soil cover and Antecedent Moisture Condition (AMC) condition were considered. If more than one landuse or soil cover occurs in a watershed, the composite Curve Number (CN) method was adopted (Anon 1973). The basic assumption of the SCS-CN is that, for a single storm event, potential maximum soil retention is equal to the ratio of direct runoff to available rainfall. This relationship, after algebraic manipulation and inclusion of simplifying assumptions, results in the following equations (USDA-SCS 1985), where, curve number represents the potential maximum soil retention (Ponce and Hawkins 1996). The work flow of adopted methodology to carry rainfall runoff modeling is given in Figure 5.2.

In this study, four hydrologic thematic maps, namely; LULC, HSG, slope and rainfall were created in vector format and intersect to each other to derive CN map and on the basis of CN map runoff map has been generated using SCS-CN method.

5.3.1 SCS-CN Method

The SCS-CN method provides an empirical relationship estimating initial abstraction and runoff as a function of soil type and LULC. The water balance equation is expressed by:

$$P = I_a + F + Q \quad (5.6)$$

$$\frac{Q}{P-I_a} = \frac{F}{S} \quad (5.7)$$

$$I_a = \lambda S \quad (5.8)$$

where P is the total precipitation (mm); I_a the initial abstraction (mm); F the cumulative infiltration (mm); Q the direct runoff (mm); S the potential maximum retention (mm) and λ the initial abstraction coefficient (0.2).

The SCS-CN equation, as expressed below, is derived from the combination of the first two equations:

$$Q = \frac{(P - I_a)^2}{P - I_a + S} \quad (5.9)$$

which is valid for $P \geq I_a$. Otherwise, $Q = 0$. For a constant value of I_a (0.2S), S can be determined from the P-Q data. In practice, S is derived from a mapping equation expressed in terms of the CN:

$$S = \frac{25400}{CN} - 254 \quad (5.10)$$

The CN (dimensionless number ranging from 0 to 100) is determined from a table, which based on LULC, HSG, and AMC (USDA-SCS, 1985, 1993). HSG is expressed in four groups (A, B, C and D), according to the soil's infiltration rate, which is obtained for a bare soil after prolonged wetting. AMC is expressed at three levels (I, II and III), according to rainfall limits for dormant and growing seasons (Geetha *et al.*, 2007).

Although SCS method is originally designed for small watersheds having area upto 15 km², it has been modified for larger watersheds by weighing curve numbers (CN_w) with respect to watershed area using the following equation:

$$CN_w = \frac{\sum(CN_i * A_i)}{A} \quad (5.11)$$

Where, CN_w is weighted curve number, CN_i is the curve number from 1 to N sub-watershed, A_i is the area with curve number CN_i & A is the total area of watershed.

5.4 MORPHOMETRIC ANALYSIS

In morphometric analysis, drainage order, elevation and sub-watershed layers were used as input. Morphometric analysis provides a quantitative description of the watershed geometry to understand initial slope or inequalities in the rock hardness, structural controls, recent diastrophism, geological and geomorphic history of watershed (Strahler, 1964). It is also defined by Clarke (1966) as the measurement and mathematical analysis of the configuration of the earth surface, shape and dimensions of its landforms. Morphometric analysis is a significant tool for

prioritization of sub-watersheds even without considering the soil map (Biswas *et al.*, 1999). It involves the measurement of linear, areal and relief aspects of the watershed and slope contribution (Nag and Chakraborty, 2003; Pandey *et al.*, 2004; Narendra and Rao, 2006).

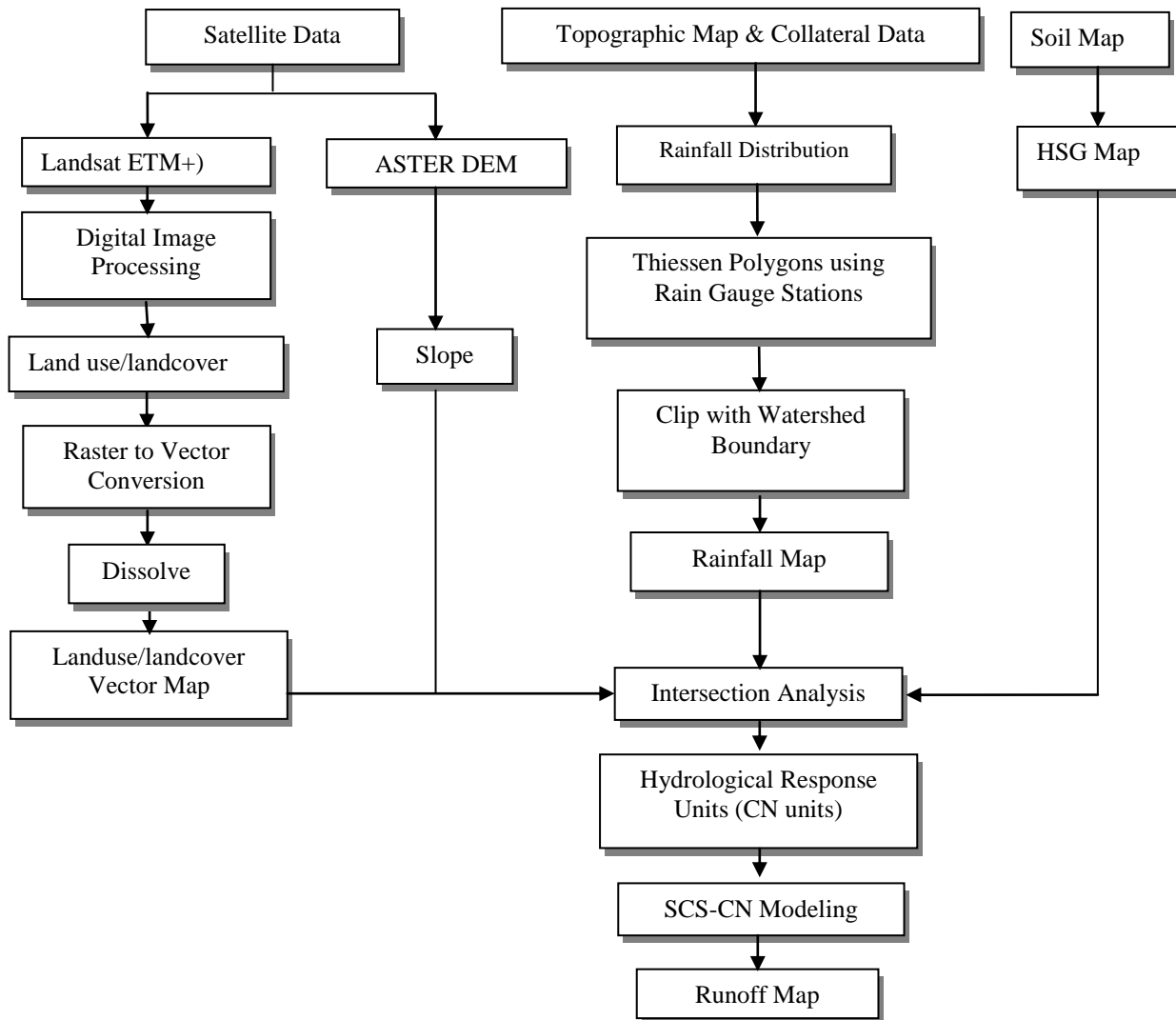


Fig. 5.2: Methodology for rainfall runoff modeling

In the present study, morphometric analysis and prioritization of sub-watersheds in Loni and Morahi watersheds are based on the integrated use of RS and GIS techniques. Various morphometric parameters, such as linear aspects of the drainage network: stream order (N_u), stream length (L_u), mean stream length (L_{sm}) stream length ratio (R_L) and bifurcation ratio (R_b), and areal aspects of the drainage basin: drainage density (D_d), stream frequency (F_s), drainage texture (R_t), elongation ratio (R_e), ruggedness number (R_N), circularity ratio (R_c), form factor ratio

(R_f), length of overland flow (L_g) of the basin, were computed using the well-known relationships, as presented in Table 5.3.

Table 5.3: Formulae used for computation of morphometric parameters

SI. No.	Morphometric Parameters	Formula	Reference
1.	Stream Order	Hierarchical rank	Strahler (1964)
2.	Stream Length (L_u)	Length of the Stream	Horton (1945)
3.	Mean Stream Length (L_{sm})	$L_{sm} = L_u/N_u$	Strahler (1964)
4.	Stream Length Ratio (R_L)	$R_L = L_u/L_{u-1}$	Horton (1945)
5.	Bifurcation Ratio (R_b)	$R_b = N_u/N_{u+1}$	Schumm (1956)
6.	Mean Bifurcation Ratio (R_{bm})	$R_{bm} = \text{Average of bifurcation ratio of all orders}$	Strahler (1957)
7.	Total Relief (H)	$H = h_{max} - h_{min}$	
8.	Relief Ratio (R_h)	$R_h = H / L_b$	Schumm (1956)
9.	Drainage Density (D_d)	$D_d = L_u/A$	Horton (1932)
10.	Stream Frequency (F_s)	$F_s = N_u/A$	Horton (1932)
11.	Drainage Texture (R_t)	$R_t = N_u/P$	Horton (1945)
12.	Elongation Ratio (R_e)	$R_e = 2 \sqrt{(A / \pi)} / L_b$	Schumm (1956)
13.	Circularity Ratio (R_c)	$R_c = 4 * \pi * A / P^2$	Miller (1953)
14.	Form Factor (R_f)	$R_f = A / L_b^2$	Horton (1932)
15.	Length of Overland Flow (L_g)	$L_g = 1/D_d * 2$	Horton (1945)
16.	Ruggedness number (R_N)	$R_N = H * D_d$	
17.	Compactness Coefficient (C_c)	$C_c = 0.2821 * P / (A)^{0.5}$	Horton (1945)
18.	Constant of Channel Maintenance	$C = 1/D_d$	Schumm (1956)

L_u = Total stream length of order 'u', L_{u-1} = The total stream length of its next lower order, N_u = Total no. of stream segments of order 'u', N_{u+1} = Number of segments of the next higher order, L_b = Basin length, A = Area of the Basin (km^2), P = Perimeter (km) & $\pi = 3.14$.

5.5 ARTIFICIAL RECHARGE STRUCTURES

In this study, various artificial recharge structures have been proposed, such as percolation tank, nala bund and check dam. The work flow of methodology is given in Figure 5.3 which involves the preparation of several thematic maps or layers viz., drainage junction buffer, urban area buffer, canal buffer, groundwater fluctuation map, slope and runoff maps, using RS data and conventional sources in GIS environment. For identification of suitable sites, these thematic layers were overlaid in GIS using a set of logical conditions, and following the guidelines adopted from IMSD (1995), Chowdhary *et al.*, (2009), Pandey *et al.*, (2010) and Indian National Committee on Hydrology (INCOH) (Verma and Tiwari, 1995), as presented in Table 5.4.

To propose suitable structures for artificial recharge, morphometric analysis was carried out because watershed morphometry played an important role in hydro-geological investigations for selecting sites to plan construction of artificial recharge structures. Quantitative morphometric analysis was carried out in all the sub-watersheds for determining their linear, areal and relief aspects. The morphometric analysis of these sub-watersheds was done quickly through GIS, as analysis of these parameters by conventional method is laborious and cumbersome.

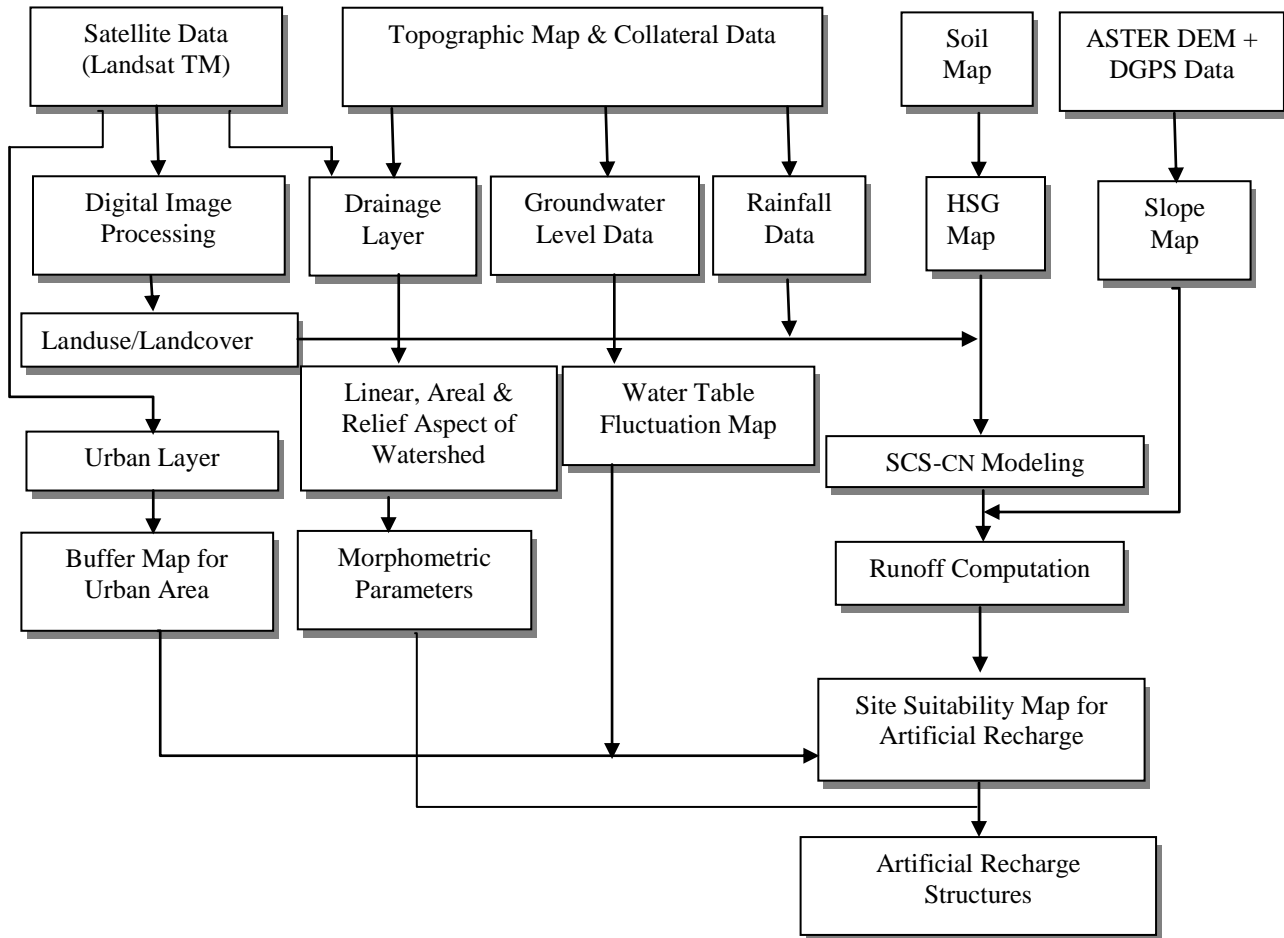


Fig. 5.3: Methodology for delineation of suitable sites & artificial recharge structures

Table 5.4: Criteria used for site selection for artificial recharge structures

Name of structure	Slope type (%)	Landuse type	Soil type	Drainage order	Watershed area (Km ²)
Percolation tank	Nearly level to very gentle (upto 3)	Open land/waste land	Clay loam	2 nd or 3 rd	> 0.05
Nala bund	Nearly level to gentle slope (upto 5)	Open land/waste land	Clay loam	1 st or 2 nd	> 0.20
Check dam	Nearly level to gentle slope (upto 5)	River stream (Near agriculture land)	Clay loam	3 rd or 4 th	Up to 0.25

5.6 RESULTS AND DISCUSSIONS

5.6.1 Groundwater Potential Zones Mapping

5.6.1.1 Geomorphology map

Geomorphologically, the study area consists of active floodplain, older flood plain, alluvial plain, lacustrine plain deposit and their landforms Meander scars and paleo channels as shown in Figure 4.10. Active flood plain has higher water level surface, hence it is best landform for high groundwater occurrence.

5.6.1.2 Geology map

The four types of geology are found in the study area namely, Channel Alluvium, Terrace Alluvium, Lacustrine Deposits and Older Alluvium as shown in Figure 4.11. Most of the area is covered by older alluvium. Channel Alluvium is given higher preference in determining the groundwater occurrence. Because it is the confined within the bank of Ganga River as point and channel bars and is composed of unoxidised grey micaceous sand and silt clay, it has better productivity due to presence of water in sand and gravel beds.

5.6.1.3 Soil map

The soils of the study area reveal five main soil categories namely; sand, sandy loam, silt loam, silt loam & loam and silty clay loam & clay loam, as shown in Figure 4.12. Sandy soil is present along Ganga river plain and clay loam is present in Loni river plain. Ranking of soil has been assigned on the basis of their infiltration rate. Sandy soil has high infiltration rate, hence it is given higher priority, and while the clayey soil has least infiltration rate, hence it is given low priority.

5.6.1.4 Land use/land cover map

LULC map was classified into eight classes, such as agriculture (39.68%), fallow land (51.58%), urban area (1.97%), river sand (0.32%), water body (2.1%), salt affected (2.1%), barren land (1.55%) and water logged (0.7%), as shown in Figure 4.14. The classification accuracy of LULC map was evaluated by constructing an error matrix, and found as 85% and 88% for the producer and user estimate, respectively. Almost 90% of the total area is covered by agricultural

and fallow land. LULC affects the surface runoff, evapotranspiration and groundwater recharge. Water body, agriculture land and waterlogged area are excellent sources of groundwater recharge, while urban and salt affected area are considered to be less significant. Therefore, highest weightage is given to water body, and lowest for urban area and salt affected for groundwater occurrence.

5.6.1.5 Slope map

The slope map was classified into five slope classes: (1) 0–1%, (2) 1-3%, (3) 3-5%, (4) 5-10%, (5) >10%, as shown in Figure 4.9. The slope map indicates that, slope of the study area mainly lies between 0-5 percent, which is assigned higher rank while the maximum slope is given as lower rank due to relatively high runoff.

5.6.1.6 Drainage density map

Drainage density has been classified into five classes namely; < 0.3, 0.3–0.6, 0.6-0.9, 0.9-1.2 and > 1.2, as shown in Figure 4.7. High drainage density (1.3 km/km^2) is recorded in southern parts of the study area. High drainage density values are favorable for runoff, and hence indicate low groundwater potential. High ranks are assigned to low drainage density areas and vice versa.

5.6.1.7 Water table fluctuation map

DEMs of pre-monsoon and post-monsoon seasons have been prepared from groundwater level data, collected from CGWB Lucknow. In pre-monsoon season (Figure 4.16), groundwater depth generally ranges from 2.66 to 20.55 m, with a major portion of the area having 4 to 12 m depth. In the northwestern and southern part of area, groundwater depth is 12 to 20.55 m. On the other hand, the post-monsoon season (Figure 4.17), groundwater depth ranges from 1.85 to 18 m, with a majority of the study area having 4 to 12 m depth. Thus, there is a considerable seasonal fluctuation of groundwater levels over the study area, which is mainly attributed to southwest monsoon rains. On the basis of the groundwater depth maps, it was found that the depth to water table varies deep in the southern part of the study area. Groundwater fluctuation map is prepared by subtracting the post-monsoon water table image from the pre-monsoon water table image. It is an important indicator or directly related to groundwater recharge. The central part of the image shows low fluctuation, and gradually increases towards northern west and southern corners, and reaches up to 4 m, as shown in Figure 4.18.

5.6.1.8 Rainfall map

The rainfall was categorized into four classes, namely < 600; 600–700; 700–800 and >800 mm/year, as shown in Figure 4.15. It is observed that northern and west southern part of the areas receive largest amount of rainfall, while the southern part receives the lowest amount of rainfall. High rainfall is more favorable as compared to low rainfall area so it has been given high ranking for groundwater occurrence.

5.6.1.9 Groundwater potential zones map

The groundwater potential zones map of the study area (Figure 5.4) reveals five distinct zones representing 'very poor', 'poor', 'good', 'very good' and 'excellent' groundwater potential. It is found that the area falling in excellent groundwater potential is about 150.93 km² (7.06% of the total study area), which covers a major portion of Ganga river area. It discriminates the areas where the terrain is most suitable for groundwater storage, and also indicates the availability of water below the ground. However, the area having very poor groundwater potential is about 372.03 km² (17.42% of the total study area), and covers the Loni river southeastern portion and some area in northeastern side. The area having poor, good and very good groundwater potential is about 815.39, 594, 202.94 km², respectively.

5.6.1.10 Verifying groundwater potential zones map

The delineated groundwater potential zones map was verified using the available yield data of 40 pumping wells that were acquired from CGWB. The wells falling in 'excellent' zone have higher average yield than the wells falling in 'very good' zone. Similarly, the average yield of the wells lying in the 'very good' zone is higher than the wells falling in the 'good' zone and so on as shown in Table 5.5.

Table 5.5: Groundwater potential zones and pumping well yield data

Groundwater potential zones	No. of wells	Observed yield (m ³ /h)	Observed average yield (m ³ /h)
V. Poor	15	45 - 90	75.05
Poor	7	80 - 110	105.18
Good	9	100 - 130	120.86
V. Good	5	120 - 145	133.32
Excellent	4	130 -160	146.32

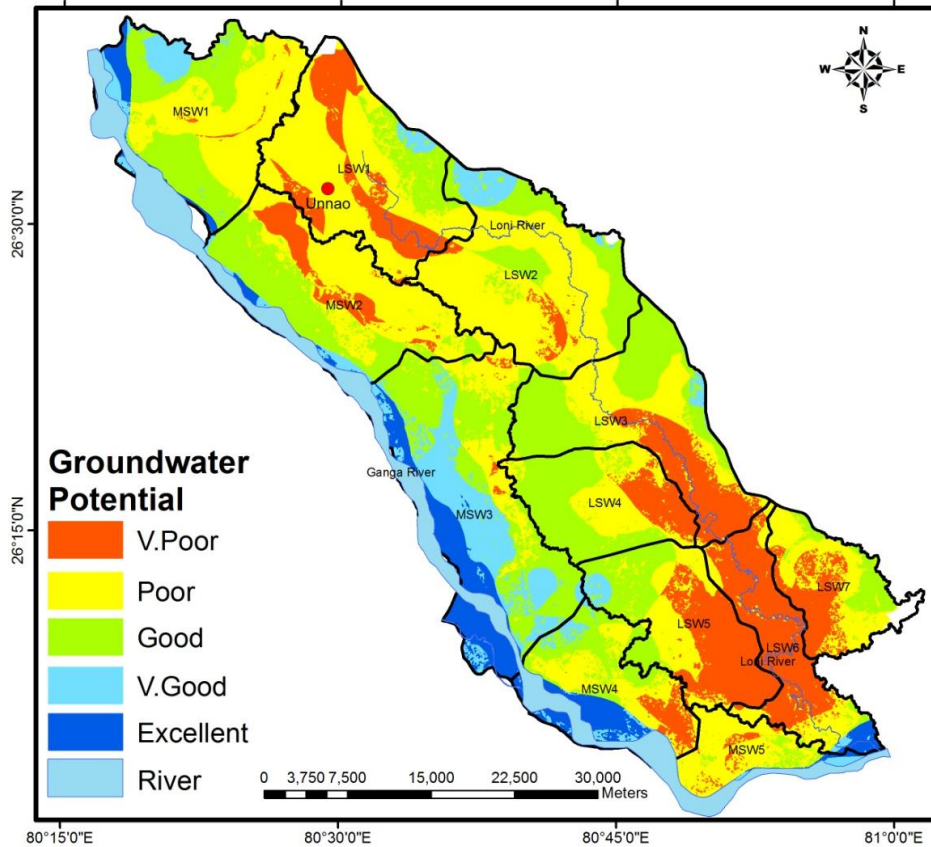


Fig. 5.4: Groundwater potential zones map

On the basis of above discussion, it is observed that the delineated groundwater potential zones map using RS, GIS and MCDM techniques are trustworthy. The developed groundwater potential zones map will be helpful to the decision makers in identifying the possible locations for drilling production wells and/or monitoring wells as well as in taking the appropriate measures for protecting the vital groundwater resources in the area.

5.6.2 Rainfall Runoff Modeling

5.6.2.1 Curve number layer

As the SCS-CN method is very sensitive to CN values. Accurate determination of this parameter is very important. CN is a function of HSG, land use, slope and AMC. The AMC is determined by the total rainfall in the 5-day spell preceding a storm. As the soil moisture increases due to rainfall in the early spell, the runoff during storm event increases. In the present case, depending on the total rainfall in 5-day period, the AMC condition is classified as AMC I

(<35mm), AMC II (35–53mm) and AMC III (>53mm) (Geetha *et. al.*, 2007). To determine the CN value, all input layers are intersected with each other in GIS, standard CN values assigned. It has been classified into five classes, as shown Figure 5.5. It is found that low CN values lies near Ganga River and high CN values near Loni River.

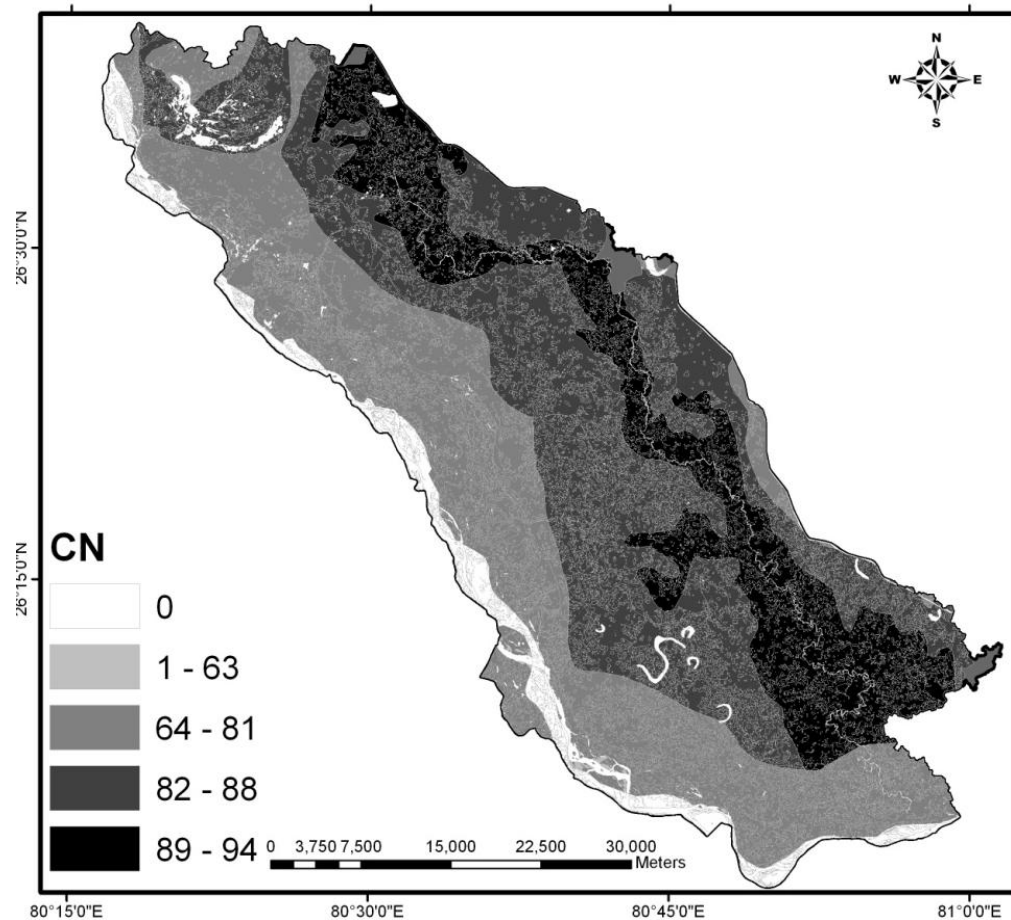


Fig. 5.5: Curve number layer

5.6.2.2 Runoff coefficient

Runoff is estimated on the basis of SCS-CN equation 5.9. For the given mean intensity and total precipitation, the values of maximum potential retention (S) are obtained from the weighted CN_w . For 40 mm/day storm event, runoff depth estimates range between 23.87 mm/day and 4.4 mm/day. Accordingly, the runoff coefficient of each HSG landuse combination (expressed as a percentage of total precipitation) is computed in GIS and a runoff potential map generated. It is evident from Figure 5.6 that 19 % of the study area falls under 1.71 to 2.02 mm/day (high) runoff potential class.

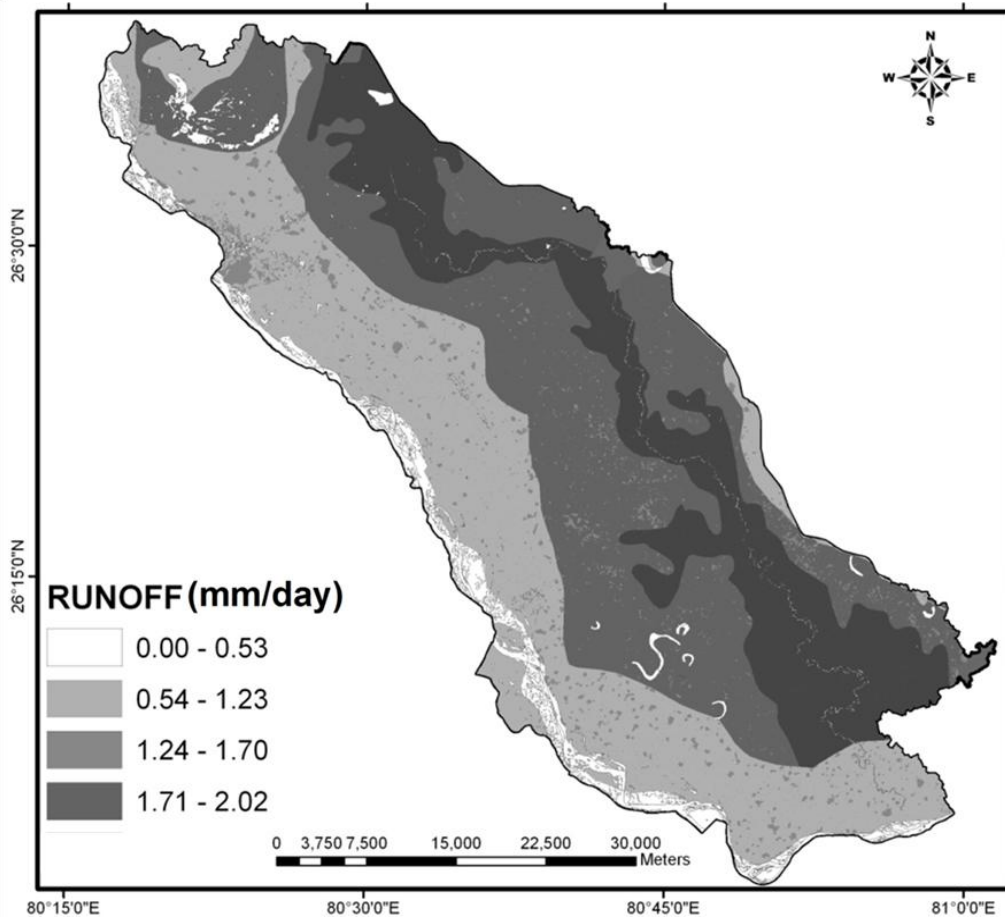


Fig. 5.6: Runoff map

5.6.3 Morphometric Analysis

The measurement of various morphometric parameters, namely stream order (N_u), stream length (L_u), mean stream length (L_{sm}), stream length ratio (R_L), bifurcation ratio (R_b), total relief (H), relief ratio (R_h), drainage density (D_d), stream frequency (F_s), drainage texture (R_t), elongation ratio (R_e), ruggedness number (R_N), circularity ratio (R_c), form factor ratio (R_f), length of overland flow (L_g), compactness constant (C_c) and constant of channel maintenance (C) of the watershed has been carried out, and the results are presented in Table 5.6.

5.6.3.1 Linear aspects

The linear aspects include the stream order, stream length, mean stream length, stream length ratio and bifurcation ratio, which were determined, and results have been presented in Table 5.6.

Stream order (N_u): The stream order is the first step in the drainage basin analysis. In the present study, ranking of streams has been done according to Strahler's stream ordering system (1964). According to Strahler (1964), the smallest fingertip tributaries are designated as order 1. Where two first order streams join, a channel segment of order 2 is formed; Where two of orders 2 join, a segment of order 3 is formed and so forth as shown in Figure 5.7. The trunk stream through which all discharge of water and sediment passes is therefore the stream segment of highest order. The study area has maximum 5th order stream. The stream orders of all the sub-watershed are presented in Table 5.6. Among all the sub-watersheds, the LSW6 is of 5th order stream, whereas LSW3, LSW5 & MSW3 are upto 4th order stream, and remaining sub-watersheds are of 3rd order stream, except MSW5. Drainage patterns of stream network from the watershed have been observed as mainly sub-dendritic type which indicates the homogeneity in texture and lack of structural control. This pattern is characterized by a tree like or fernlike pattern with branches that intersect primarily at acute angles.

Stream length (L_u): Stream length is measured from mouth of a river to drainage divide with the help of ArcGIS 9.3 software. This has been computed based on Horton (1945). Usually, the total length of stream segments in first order streams are maximum and it decreases as the stream order increases, but in the present case little variation has been found from the general observation, as shown in Table 5.6.

Mean stream length (L_{sm}): Mean stream length is a characteristic property related to the drainage network components and its associated basin surfaces (Strahler, 1964). This has been calculated by dividing the total stream length of order (u) by the number of streams of the same order. The results of mean stream length are presented in Table 5.6.

Stream length ratio (R_L): Stream length ratio is the ratio of the mean length of the one order to the next lower order of the stream segments. The R_L values are presented in Table 5.6. The stream length ratio between the streams of different orders of the study area shows a change in each sub-watershed. This change might be attributed to variation in slope and topography, indicating the late youth stage of geomorphic development in streams of the study area (Vittala *et al.*, 2004).

Bifurcation ratio (R_b): Bifurcation ratio is also considered as an index of relief and dissections (Horton, 1945). According to Schumn (1956), it may be defined as the ratio of the number of the stream segments of given order to the number of segments of the next higher orders. Strahler (1957) demonstrated that R_b shows only a small variation for different regions with different environments except where powerful geological control dominates. Lower R_b values are the characteristics of structurally less disturbed watersheds without any distortion in drainage pattern. Low R_b value indicates the less structural disturbance whereas high R_b value indicates high structural complexity and low permeability of the terrain. The R_b values in sub-watersheds of the study area range from 1.65 to 2.61 indicating that the sub-watersheds fall under normal basin category (Strahler, 1957).

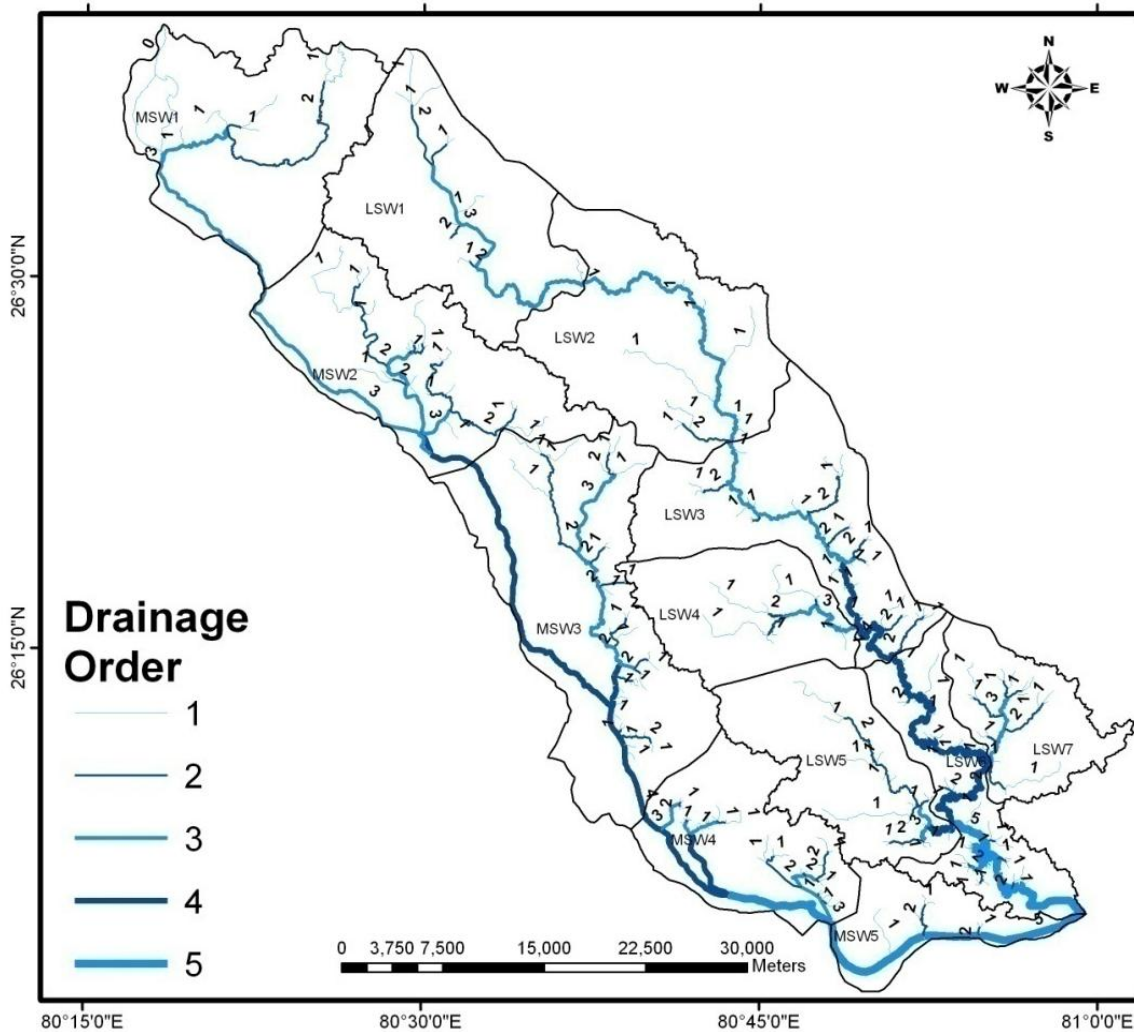


Fig. 5.7: Drainage order map

Table 5.6 (a): Morphometric parameters of sub-watersheds

SWSD No.	SWSD Name	Stream Order	Basin Area (Km ²)	Stream Order (N _u)					Stream Length in Km (L _u)					Perimeter (P) (Km)	Basin Length (Km)
				I	II	III	IV	V	I	II	III	IV	V		
1	LSW1	III	222.73	12	6	4	-	-	18.54	9.25	24.68	-	-	79.32	22.20
2	LSW2	III	235.67	10	2	9	-	-	23.97	4.28	28.65	-	-	82.82	23.40
3	LSW3	IV	204.08	38	13	17	11	-	29.60	20.90	20.42	15.1	-	82.40	23.60
4	LSW4	III	128.18	10	4	5	-	-	7.36	5.04	10.06	-	-	53.20	19.34
5	LSW5	IV	152.22	20	11	4	4	-	27.14	16.48	3.78	3.74	-	72.51	20.74
6	LSW6	V	121.50	51	19	4	18	17	36.20	7.00	2.05	34.74	19.46	87.07	23.68
7	LSW7	III	101.86	18	10	6	-	-	22.97	13.95	7.28	-	-	58.25	15.74
8	MSW1	III	230.38	6	3	2	-	-	18.55	18.78	41.82	-	-	79.32	20.60
9	MSW2	III	222.00	26	16	8	-	-	40.38	27.27	12.90	-	-	85.53	27.40
10	MSW3	IV	304.54	42	23	6	5	-	41.95	25.83	21.44	3.48	-	101.2	30.92
11	MSW4	III	145.4	38	16	17	-	-	24.37	9.8	12.62	-	-	65.23	16.40
12	MSW5	II	76.51	6	3	-	-	-	9.12	3.7	-	-	-	58.83	16.20

Table 5.6 (b): Morphometric parameters of sub-watersheds

SWSD No.	SWSD Name	Mean Stream Length in Km (L _{sm})					Stream Length Ratio (R _L)				Total Relief (H) in meter	Relief Ratio (R _h)	Drainage Density (D _d) (Km/Km ²)	Stream Frequency (F _s)	Texture Ratio (R _t)
		I	II	III	IV	V	II/I	III/II	IV/III	V/IV					
1	LSW1	1.54	1.54	6.17	-	-	0.50	2.67	-	-	30	.00135	0.23	0.098	0.28
2	LSW2	2.39	2.14	3.18	-	-	0.18	6.69	-	-	42	.00179	0.24	0.089	0.25
3	LSW3	0.78	1.60	1.20	1.37	-	0.71	0.98	0.74	-	48	.00203	0.42	0.387	0.96
4	LSW4	0.73	1.26	2.01	-	-	0.68	2.00	-	-	26	.00278	0.17	0.148	0.36
5	LSW5	1.37	1.5	0.94	0.93	-	0.61	0.23	0.99	-	34	.00164	0.34	0.256	0.54
6	LSW6	0.71	0.37	0.51	1.93	1.08	0.19	0.29	16.95	0.56	53	.00223	0.82	0.897	1.25
7	LSW7	1.27	1.39	1.20	-	-	0.61	0.52	-	-	28	.00178	0.43	0.334	0.57
8	MSW1	3.09	6.26	20.91	-	-	1.01	2.23	-	-	68	.0033	0.34	0.048	0.14
9	MSW2	1.55	1.70	1.61	-	-	0.68	0.47	-	-	84	.00306	0.36	0.225	0.58
10	MSW3	1.00	1.12	3.57	0.70	-	0.62	0.83	0.16	-	93	.0030	0.30	0.250	0.75
11	MSW4	0.64	0.61	0.74	-	-	0.40	1.29	-	-	38	.00231	0.32	0.490	1.09
12	MSW5	1.52	1.23	-	-	-	0.41	-	-	-	44	.00271	0.17	0.118	0.15

Table 5.6 (c): Morphometric Parameters of sub-watersheds

SWSD No.	SWSD Name	Bifurcation Ratio R_b				Mean Bifurcation Ratio (R_{bm})	Elongation Ratio (R_e)	Circularity Ratio (R_c)	Form Factor (R_f)	Ruggedness Number (R_N)	Length of Overland Flow Ratio (L_g)	Compactness Coefficient (C_c)	Constant of Channel Maintenance (C) (Km^2/Km)
		I/II	II/III	III/IV	IV/V								
1	LSW1	2.00	1.50	-	-	1.75	0.76	0.44	0.45	.0070	2.17	1.50	4.35
2	LSW2	5.00	0.22	-	-	2.61	0.74	0.43	0.43	.0011	2.08	1.52	4.17
3	LSW3	2.92	0.76	1.54	-	1.74	0.68	0.38	0.37	.0200	1.19	1.63	2.38
4	LSW4	2.50	0.80	-	-	1.65	0.66	0.57	0.34	.0047	2.94	1.32	5.56
5	LSW5	1.80	2.75	1.00	-	1.85	0.67	0.36	0.35	.0120	1.51	1.66	2.94
6	LSW6	2.68	4.75	0.22	1.06	2.17	0.53	0.20	0.22	.0430	0.61	2.23	1.22
7	LSW7	1.80	1.67	-	-	1.73	0.72	0.38	0.41	.0012	1.16	1.63	2.33
8	MSW1	2.00	1.50	-	-	1.75	0.83	0.46	0.54	.0230	1.47	1.47	2.94
9	MSW2	1.63	2.00	-	-	1.82	0.61	0.38	0.30	.0300	1.38	1.62	2.77
10	MSW3	1.83	3.83	1.20	-	2.29	0.64	0.37	0.32	.0280	1.67	1.64	3.33
11	MSW4	2.38	0.94	-	-	1.66	0.83	0.43	0.54	.0122	1.56	1.53	3.12
12	MSW5	2.00	-	-	-	2.00	0.61	0.28	0.29	.0070	2.94	1.90	5.88

* I, II, III, IV and V are represents drainage order

5.6.3.2 Relief parameters

Total relief (H): Total relief aspects of the sub watershed play an important role in drainage development, surface and sub-surface water flow, permeability, landforms development and erosion properties of the terrain. The analysis reveals that all the sub-watershed has relief less than 93 m (Table 5.6). The low value of H indicates the gravity of water flow, high infiltration and low runoff conditions.

Relief ratio (R_h): Relief ratio is defined as the ratio of total relief and the basin length; the basin length being the longest distance in the sub-watershed. It measures the overall steepness of a drainage basin, and is an indicator of the intensity of erosion processes operating on the slopes of the basin. In the present study, values vary from 0.00135 to 0.0033, as shown in Table 5.6. Relief ratio of the watersheds plays an important role in drainage development, surface and sub-surface water flow, permeability, and landform development and associated features of the terrain.

Ruggedness number (R_N): It indicates the structural complexity of the terrain. The value of R_N ranges from 0.001 to 0.043. The sub-watershed having greater value of R_N is considered to be highly susceptible to erosion (Table 5.6).

5.6.3.3 Aerial aspects

The aerial aspects, like drainage density, texture ratio, stream frequency, form factor, circularity ratio, and elongation ratio, length of overland flow, compactness coefficient and constant channel maintenance are given in Table 5.6.

Drainage density (D_d): Drainage density is defined as the total length of streams of all orders per drainage area (Table 5.3). It indicates the closeness of spacing of channels. It provides a numerical measurement of landscape dissection and runoff potential. They range between 0.17 to 0.82 km/km² indicating low drainage density. The low drainage density indicates that the watershed is highly permeable sub-soil and thick vegetation cover.

Stream frequency (F_s): Stream frequency is defined as the total number of stream segments of all orders per unit area (Table 5.3). Stream frequencies for all sub-watersheds are given in Table 5.6. It is indicative of low relief and high infiltration capacity of bedrock. In the

present study, F_s exhibits positive correlation with the drainage density values of the sub-watersheds, which indicates increase in stream population with respect to increase in drainage density.

Drainage texture (R_t): Drainage texture is the total number of stream segments of all orders per perimeter of that area (Horton, 1945) (Table 5.3). R_t is an important factor in the drainage morphometric analysis which depends on the underlying lithology, infiltration capacity and relief aspect of the terrain. Smith (1950) has classified drainage density into five different textures. The drainage density less than 2 indicates very coarse, between 2 and 4 is related to coarse, between 4 and 6 is moderate, between 6 and 8 is fine and greater than 8 is very fine drainage texture. In present study, drainage density is of very coarse to coarse drainage texture, as shown in Table 5.6.

Elongation ratio (R_e): Schumm (1956) used an elongation ratio which is defined as the ratio of diameter of a circle of the drainage basin to the maximum basin length. It is a very significant index in the analysis of basin shape which helps to give an idea about the hydrological character of a drainage basin. Values near to 1.0 are typical of regions of very low relief (Strahler, 1964). The value R_e of the study area ranges 0.53 to 0.83 which indicates that the low relief of the terrain and elongated in shape.

Circularity ratio (R_c): Miller (1953) defined a dimensionless circularity ratio as the ratio of sub-watershed area to the area of circle having same perimeter as the sub-watershed (Table 5.3). All the sub-watersheds (except SW4) have the circularity ratios less than 0.5, indicating their elongated shape.

Form factor ratio (R_f): The form factor values range between 0.22 to 0.54, indicating lower values of form factor, thus representing the elongated shape. The elongated basin with low form factor indicates that the watershed will have a flatter peak of flow for longer duration. Flood flows of such elongated basins are easier to manage than that of the circular basin.

Length of overland flow (L_g): Horton (1945) defined L_g as the length of water over the ground before it gets concentrated into definite stream channels. It relates inversely to the average slope of the channel. The length of overland flow approximately equals to half of the

reciprocal of drainage density. In the present study, computed values of L_g for all sub-watersheds vary from 0.61 to 2.94.

Compactness coefficient (C_c): Horton (1945) defined that the compactness coefficient is the ratio of watershed perimeter to perimeter of circle of watershed area. The ranges of C_c are 1.32 - 2.23, as shown in Table 5.6.

Constant channel maintenance (C): Schumn (1956) has used the inverse of drainage density as a property termed constant channel maintenance. It indicates the area of watershed surface that required sustaining one unit of channel length. The constant channel maintenance was computed for all the sub-watersheds (Table 5.6). This factor depends upon not only the rock type and permeability but also on duration of erosion and climatic history. In general, this constant will be extremely low in areas of close dissection.

5.6.3.4 Prioritization of sub-watersheds

The morphometric parameters i.e., bifurcation ratio (R_b), compactness coefficient (C_c), drainage density (D_d), stream frequency (F_s), drainage texture (R_t), length of overland flow (L_g), form factor (R_f), circularity ratio (R_c), constant of channel maintenance (C) and elongation ratio (R_e) also termed as erosion risk assessment parameters, have been used for prioritizing the sub-watersheds. The linear parameters, such as drainage density, stream frequency, bifurcation ratio, drainage texture, length of overland flow have a direct relationship with erodibility, higher the value, more is the erodibility. Hence for prioritization of sub-watersheds, the highest value of linear parameters was rated as rank 1, second highest value was rated as rank 2 and so on, and the least value was rated last in rank. Average of all the linear parameters was then taken.

Shape parameters, such as elongation ratio, compactness coefficient, circularity ratio, constant of channel maintenance and form factor have an inverse relationship with erodibility, lower the value, more is the erodibility. Thus, the lowest value of shape parameters was rated as rank 1, next lower value was rated as rank 2 and so on and the highest value was rated last in rank. Average of all the shape parameters was taken.

Compound parameter (C_p) was computed to taking the average value of linear as well as shape parameters. On the basis of compound parameters, assigned the high priority to the

lowest score and low priority to the highest score was assigned as shown in Table 5.7. The sub-watersheds were then categorized into five classes on the basis of priority, as shown in Figure 5.8. The result of morphometric analysis shows that sub-watershed LSW6 falls under highest priority, and therefore it is prone to relatively high erosion and soil loss. Hence, suitable control measures are urgently required in this sub-watershed to preserve the land from further erosion.

Table 5.7: Prioritization of sub-watersheds

Sub-watersheds	Morphometric parameters												Compound Parameter	Final Priority
	Linear parameters						Shape parameters							
	D _d	F _s	L _g	R _b	R _t	C _p Values	R _c	R _e	R _f	C _c	C	C _p Values		
LSW1	0.23 (10)	0.098 (10)	2.17 (2)	1.75 (7)	0.28 (9)	7.7	0.44 (7)	0.76 (9)	0.45 (10)	1.5 (3)	4.3 (10)	7.8	7.75	5
LSW2	0.24 (9)	0.089 (11)	2.08 (3)	2.61 (1)	0.25 (10)	6.8	0.43 (6)	0.74 (8)	0.43 (9)	1.52 (4)	4.16 (9)	7.2	7.0	5
LSW3	0.42 (3)	0.387 (3)	1.19 (9)	1.74 (8)	0.96 (3)	5.2	0.38 (5)	0.68 (6)	0.37 (7)	1.63 (7)	2.38 (3)	5.6	5.4	3
LSW4	0.17 (11)	0.148 (8)	2.94 (1)	1.65 (11)	0.36 (8)	7.8	0.57 (9)	0.66 (4)	0.34 (5)	1.32 (1)	5.88 (11)	6.0	6.9	4
LSW5	0.33 (6)	0.256 (5)	1.51 (6)	1.85 (5)	0.54 (7)	5.8	0.36 (3)	0.67 (5)	0.35 (6)	1.66 (9)	3.03 (6)	5.8	5.8	3
LSW6	0.82 (1)	0.897 (1)	0.61 (11)	2.17 (3)	1.25 (1)	3.4	0.20 (1)	0.53 (1)	0.22 (1)	2.23 (11)	1.22 (1)	3.0	3.2	1
LSW7	0.43 (2)	0.334 (4)	1.16 (10)	1.73 (9)	0.57 (6)	6.2	0.38 (5)	0.72 (7)	0.41 (8)	1.63 (7)	2.33 (2)	5.8	6.0	3
MSW1	0.34 (5)	0.048 (12)	1.47 (7)	1.75 (7)	0.14 (12)	8.6	0.46 (8)	0.83 (10)	0.54 (11)	1.47 (2)	2.94 (5)	7.2	7.9	5
MSW2	0.36 (4)	0.225 (7)	1.38 (8)	1.82 (6)	0.58 (5)	6.0	0.38 (5)	0.61 (2)	0.30 (3)	1.62 (6)	2.77 (4)	4.0	5.0	2
MSW3	0.30 (8)	0.250 (6)	1.67 (4)	2.29 (2)	0.75 (4)	4.8	0.37 (4)	0.64 (3)	0.32 (4)	1.64 (8)	3.33 (8)	5.4	5.1	2
MSW4	0.32 (7)	0.490 (2)	1.56 (5)	1.66 (10)	1.09 (2)	5.2	0.43 (6)	0.83 (10)	0.54 (11)	1.53 (5)	3.12 (7)	7.8	6.5	4
MSW5	0.17 (11)	0.118 (9)	2.94 (1)	2.00 (4)	0.15 (11)	7.2	0.28 (2)	0.61 (2)	0.29 (2)	1.90 (10)	5.88 (11)	5.4	6.3	4

5.6.4 Artificial Recharge Structures

Spatial information on runoff coefficient, lithology, slope, drainage, morphological parameters, and groundwater depth layer play a crucial role in site selection for runoff harvesting/recharging structures. Different thematic layers viz., drainage junction buffer, urban area buffer, canal buffer, groundwater depth map of pre and post-monsoon and runoff maps (LULC, soil (HSG layer), rainfall and slope layers have already been used in runoff map computation, so these layer are not used further) are used to identify the suitable location for artificial recharge sites, and proposing a suitable structure in GIS environment using a set of logical conditions.

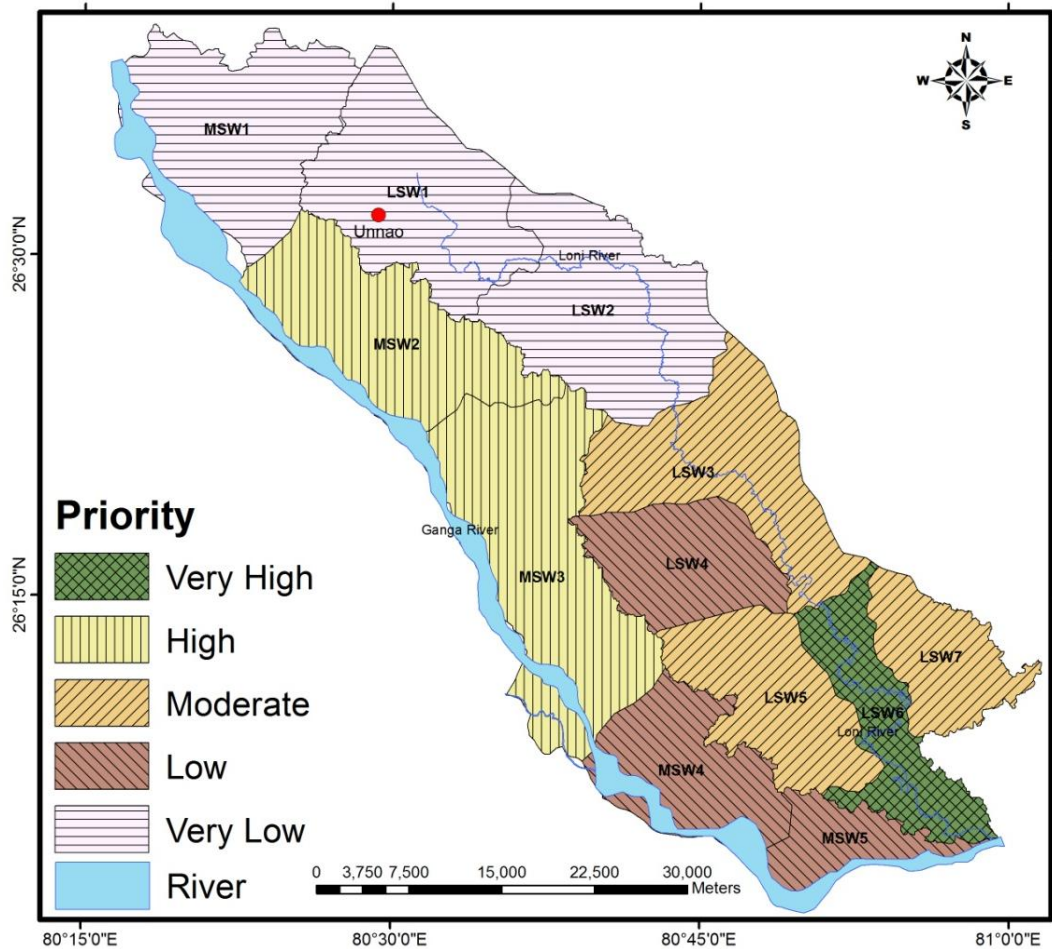


Fig. 5.8: Prioritization map for water conservation

5.6.4.1 Buffer map of drainage junctions

Drainage junction is the location where two or more drainages are met to each other. A buffer map is created along the junction within a distance of 1000 m to 15000 m, and categorized into five classes, as shown in Figure 5.9. All the classes are assigned ranks namely; very poor, poor, moderate, good and very good on the basis of their relative importance in identification of suitable sites for artificial recharge structures, as shown in Table 5.8.

Table 5.8: Area statistics of buffer map of drainage junctions

S. No.	Buffer distance (m)	Category	Area (Km ²)	Area (%)
1	1000	Very Good	417.54	19.46
2	2000	Good	547.40	25.52
3	3000	Moderate	443.98	20.70
4	4000	Poor	323.90	15.10
5	>4000	Very poor	412.31	19.22

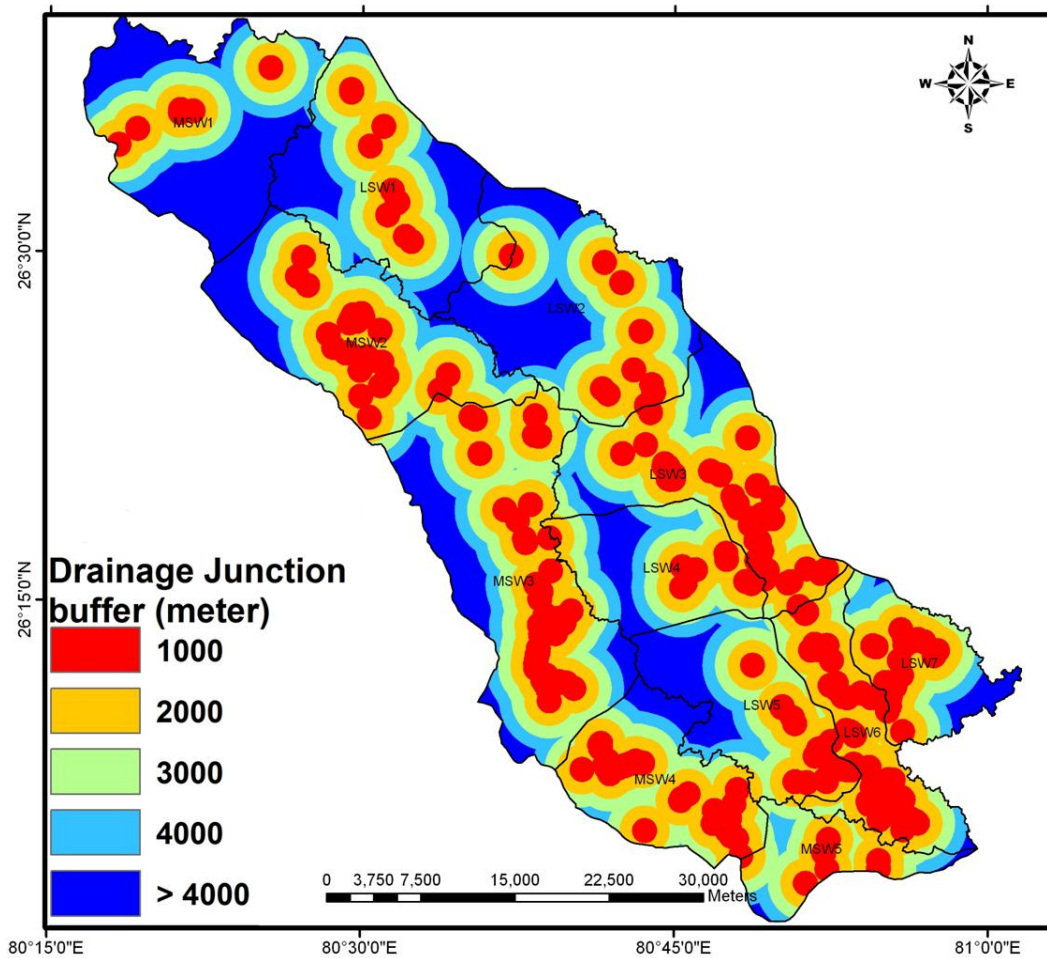


Fig. 5.9: Buffer map of drainage junctions

5.6.4.2 Buffer map of habitated area

A buffer map of 500 to 7000 m is created along the habitated areas for GIS based analysis, as shown in Figure 5.10. After creation of buffer map, erase analysis technique has been applied to eliminate the habitated area from analysis, because recharge sites should not be falls on built-up area. All the classes are assigned ranks namely; very poor, poor, moderate, good and very good on the basis of their relative importance in identification of suitable sites for artificial recharge structures, as shown in Table 5.9.

Table 5.9: Area statistics of buffer map of habitated area

S. No.	Buffer Distance (m)	Category	Area (Km ²)	Area (%)
1	500	Very Good	1127.13	52.53
2	1000	Good	540.41	25.18
3	1500	Moderate	168.00	7.83
4	2000	Poor	90.56	4.22
5	>2000	Very poor	219.77	10.24

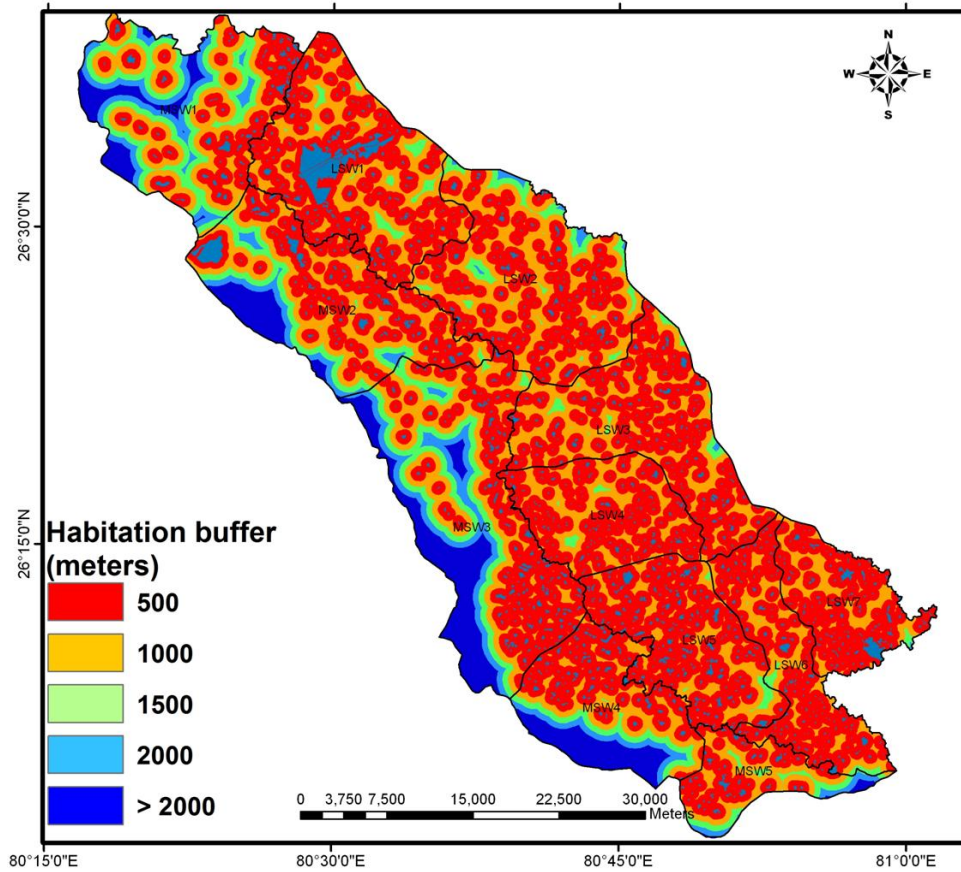


Fig. 5.10: Buffer map of habitated area

5.6.4.3 Buffer map of canals

A buffer map of distance 500 to 10000 m is created along the canals for GIS based analysis, as shown in Figure 5.11. The canal buffer is used to eliminate the area that falls near canals because the area falls adjacent to canals are highly salt affected mainly due to high water table. All the classes are assigned ranks namely; very poor, poor, good and very good on the basis of their relative importance in identification of suitable sites for artificial recharge structures, as shown in Table 5.10.

Table 5.10: Area statistics of buffer map of canals

S. No.	Buffer Distance (m)	Category	Area (Km ²)	Area (%)
1	500	Very poor	191.86	8.94
2	1000	Poor	501.18	23.36
3	1500	Good	691.65	32.23
4	> 1500	Very good	761.14	35.47

5.6.4.4 Groundwater depth map

The preparation of groundwater depth map of pre and post-monsoon season has been explained in previous section 4.5.10 and 4.5.11. It is shown in Figure 4.16 and 4.17.

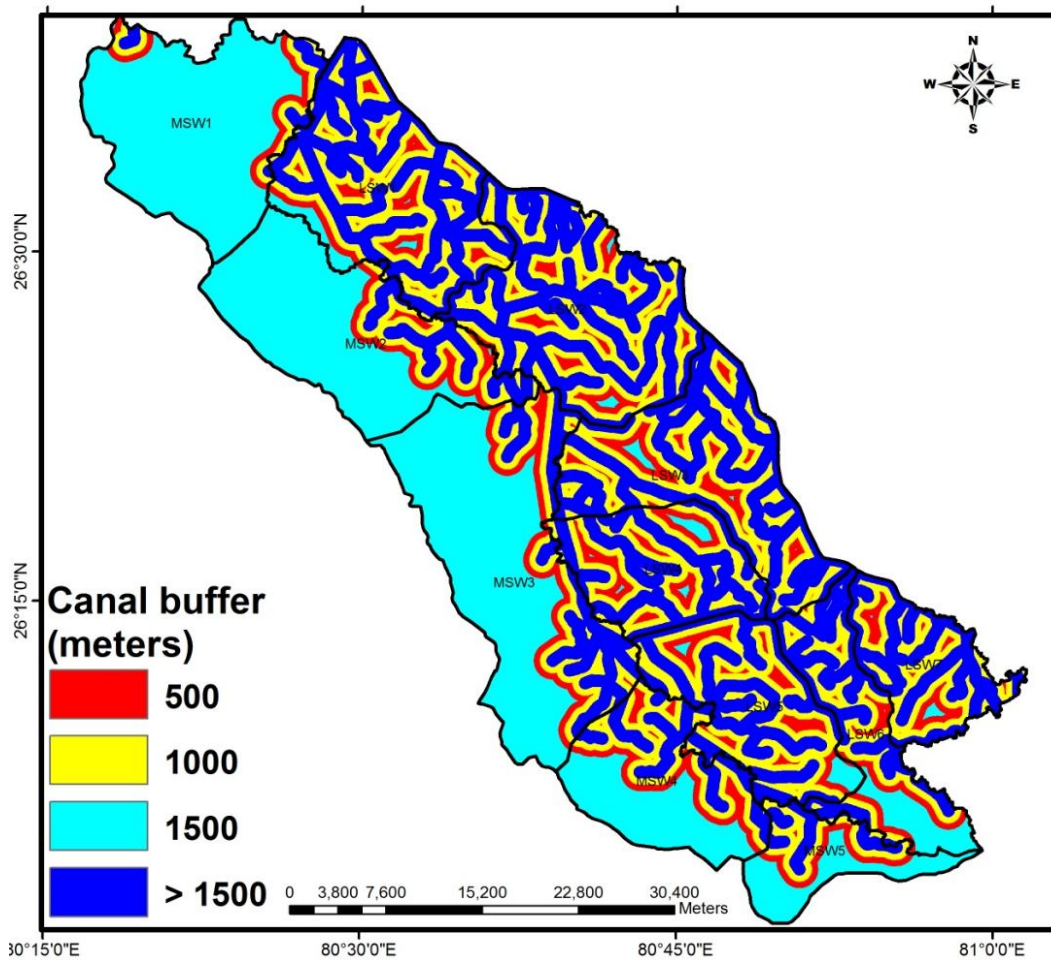


Fig. 5.11: Buffer map of canal layer

5.6.4.5 Runoff map

The procedure to generate runoff map is described earlier (section 5.3) and the output layer is shown in Figure 5.6. It is an important layer which has been used to identify the suitable sites of artificial recharge. High runoff area is more suitable for recharge so it gives high ranking as compared to low runoff areas. Mostly high runoff area falls along Loni River due to the presence of surface clay.

5.6.4.6 Site suitability map

To delineate the site suitability map, all thematic layers viz., drainage junction buffer, urban area buffer, canal buffer, groundwater depth map of pre and post-monsoon and runoff maps are integrated using weighted overlay analysis in ArcGIS 9.3. The output map is classified into five classes, namely 'very high', 'high', 'moderate', 'low' and 'very low', as shown in Figure 5.12. The area statistics is shown in Table 5.11. This map has been considered for planning the artificial recharge structures.

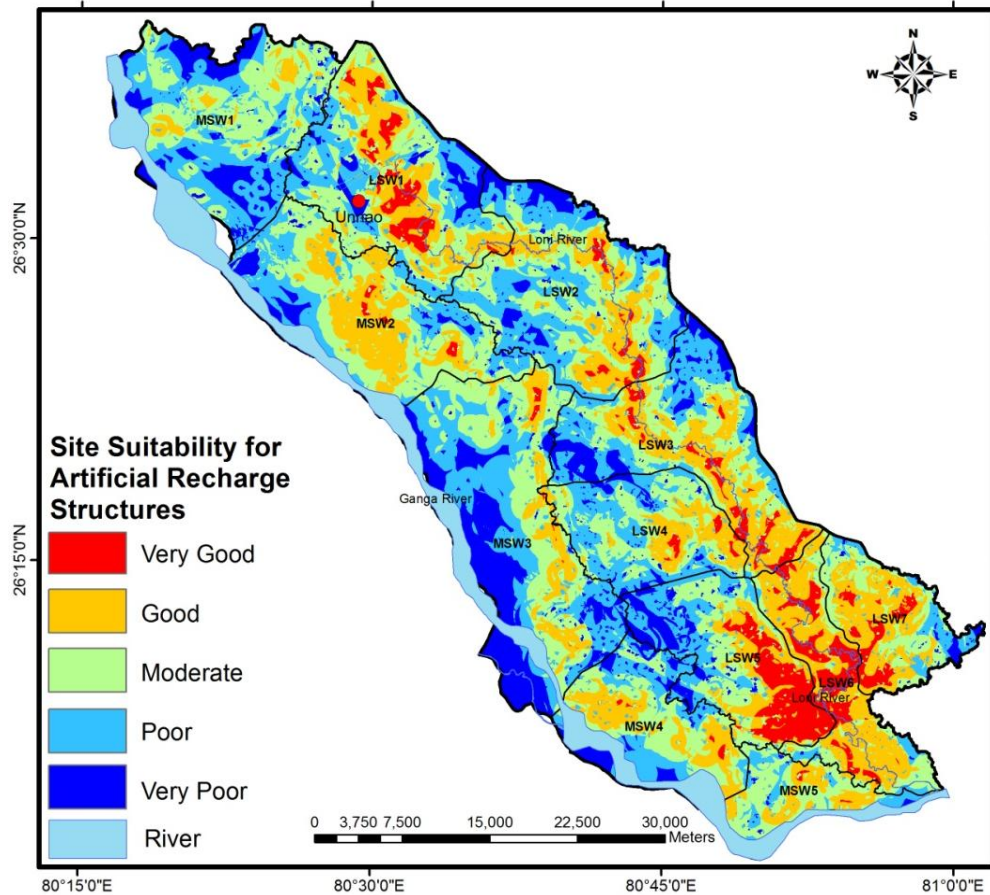


Fig. 5.12: Site suitability map for artificial recharge structures

Table 5.11: Area statistics for site suitability map of artificial recharge structures

S. No.	Category	Area (Km ²)	Area (%)
1	Very High	120.20	5.61
2	High	473.67	22.10
3	Moderate	657.98	30.70
4	Low	597.24	27.86
5	Very Low	294.45	13.74

5.6.4.7 Morphological parameters

Morphological parameters were calculated for all the sub-watersheds of Loni and Morahi watershed, and are presented in Table 5.12. Morphological parameters, namely the bifurcation ratio, elongation ratio, drainage density, ruggedness number, relief ratio, and circulatory ratio were considered as guiding tools for identifying the necessity of selecting a particular type of soil and water conservation structure in sub-watersheds.

(a) Bifurcation ratio (R_b)

The bifurcation Ratio (R_b) is computed earlier in section 5.6.3.1. The mean bifurcation ratio (R_{bm}) may be defined as the average of bifurcation ratios of all orders (Strahler, 1957)

shown in Table 5.12. Higher values of R_{bm} for a sub-watershed indicate high runoff, low recharge, and mature topography. For example, the high value of bifurcation ratio R_{bm} (2.61) for LSW2 clearly indicates that either check dam or nala bund may be planned instead of percolation tank due to low soil permeability and high erosion rate from the sub-watershed.

(b) Drainage density (D_d)

Drainage density (D_d) is computed earlier in section 5.6.3.3. The lowest and the highest values of D_d are observed in LSW4 and LSW6, respectively as shown in Table 5.12. In general, low value of D_d is more likely to occur in regions of highly permeable subsoil material under dense vegetative cover, and in situations where relief is low. In contrast, high value of D_d is developed in regions of weak or impermeable subsurface materials, sparse vegetation, and mountainous relief (Nag and Chakraborty, 2003). Low D_d value for LSW4 indicates that it has highly permeable subsoil material with dense vegetative cover and low relief. Hence, small water harvesting structures, such as percolation tanks may be constructed to improve the ground water recharge. Soil in the LSW4 is mostly silty clay loam and silt loam type. Creation of a percolation tank will also provide irrigation facility to the adjoining agricultural fields.

(c) Circularity ratio (R_c)

It is also computed earlier in section 5.6.3.3. Circularity ratio (R_c) values range from 0.2 to 0.57 for different sub-watersheds of study area (Table 5.12). Sub-watershed having circular to oval shape allows quick disposal of runoff and results in a high peaked and narrow hydrograph, while elongated shape of sub watershed allows slow disposal of water, and results in a broad and low peaked hydrograph (Singh and Singh, 1997). The circular shape of the LSW6 suggests that the quick and high peaked runoff will promote soil erosion. Therefore, reduction of runoff velocity is achieved by providing water-harvesting structures, like a check dam in LSW6.

(d) Elongation ratio (R_e)

It is also computed earlier in section 5.6.3.3. The R_e values can be grouped into three categories, namely circular (>0.9), oval (0.8–0.9), less elongated (<0.7) (Chopra *et al.*, 2005). A circular basin is more efficient in runoff discharge than an elongated watershed (Singh and Singh, 1997). Elongation ratio (R_e) for various sub-watersheds in the study area ranged from 0.53 to 0.83. High values of elongation ratio (R_e) indicate high infiltration capacity and low

runoff therefore, high elongation ratio (0.83) for MSW1 and MSW4 suggests for a percolation tank and low elongation ratio of LSW6 suggests for a check dam.

(e) *Ruggedness number (R_N)*

It is also computed earlier in section 5.6.3.2. The value of R_N ranges from .0011 to .043, as shown in Table 5.12. The lowest and the highest values of R_N were found to be in LSW2 and LSW6, respectively. The sub-watershed having greater value of R_N is highly susceptible to erosion. High ruggedness value (0.043) for the LSW6 suggests provision of a nala bund and a check dam structures to reduce the runoff velocity and arrest soil erosion of sub-watersheds.

(f) *Relief ratio (R_h)*

It is computed earlier in section 5.6.3.2. The lowest and highest value of total relief (H) ranged from 26 to 93 m, lowest relief in LSW4 and highest relief in MSW3, respectively. It measures the overall steepness of a watershed, and is an indicator of erosion processes operating on the slope of watershed. The R_h normally increases with decreasing watershed area and its size. It is noticed that the high value of R_h indicates steep slope and high relief, while the lower values indicate the presence of basement rocks that are exposed in the form of small ridges and mounds with lower degree of some of the suggested measures include nala bund, and percolation tanks along with suitable vegetative measures.

Table 5.12: Morphometric parameters and proposed structures of sub-watersheds

SWSD No.	SWSD Name	Basin Area (Km ²)	Perimeter (P) (Km)	Relief Ratio (R_h)	Drainage Density (D_d) (Km/Km ²)	Mean Bifurcation Ratio (R_{bm})	Elongation Ratio (R_e)	Circularity Ratio (R_c)	Ruggedness Number (R_N)	Proposed Structure
1	LSW1	222.73	79.32	.00135	0.23	1.75	0.76	0.44	.0070	Percolation tank
2	LSW2	235.67	82.82	.00179	0.24	2.61	0.74	0.43	.0011	Check dam & Nala bund
3	LSW3	204.08	82.40	.00203	0.42	1.74	0.68	0.38	.0200	Percolation tank, Check dam & Nala bund
4	LSW4	128.18	53.20	.00278	0.17	1.65	0.66	0.57	.0047	Check dam, Percolation tank
5	LSW5	152.22	72.51	.00164	0.34	1.85	0.67	0.36	.0120	Percolation tank, Check dam & Nala bund
6	LSW6	121.50	87.07	.00223	0.82	2.17	0.53	0.20	.0430	Check dam & Nala bund
7	LSW7	101.86	58.25	.00178	0.43	1.73	0.72	0.38	.0012	Check dam
8	MSW1	230.38	79.32	.0033	0.34	1.75	0.83	0.46	.0230	Percolation Tank
9	MSW2	222.00	85.53	.00306	0.36	1.82	0.61	0.38	.0300	Check dam
10	MSW3	304.54	101.2	.0030	0.30	2.29	0.64	0.37	.0280	Check dam
11	MSW4	145.4	65.23	.00231	0.32	1.66	0.83	0.43	.0122	Percolation Tank
12	MSW5	76.51	58.83	.00271	0.17	2.00	0.61	0.28	.0070	Nil

On the basis of the site suitability map (Figure 5.12) and morphometric study, best site was identified for artificial recharge structures in each sub-watershed. Total 22 suitable locations for artificial recharge sites were identified. During field visit, 4 sites were verified that match with the identified location. Figure 5.13 shows the proposed and already existing sites (check dam) for soil and water conservation structures. That shows RS and GIS was found to be an effective tool for integrating hydrological, LULC and morphometric parameters as per user defined criteria to identify suitable artificial recharge sites. Table 5.12 presents the result of morphological analysis and proposed structures for soil and water conservation. Already existing sites and proposed sites were verified during the field visit, as well as from Google Earth site and data collected from various organizations.

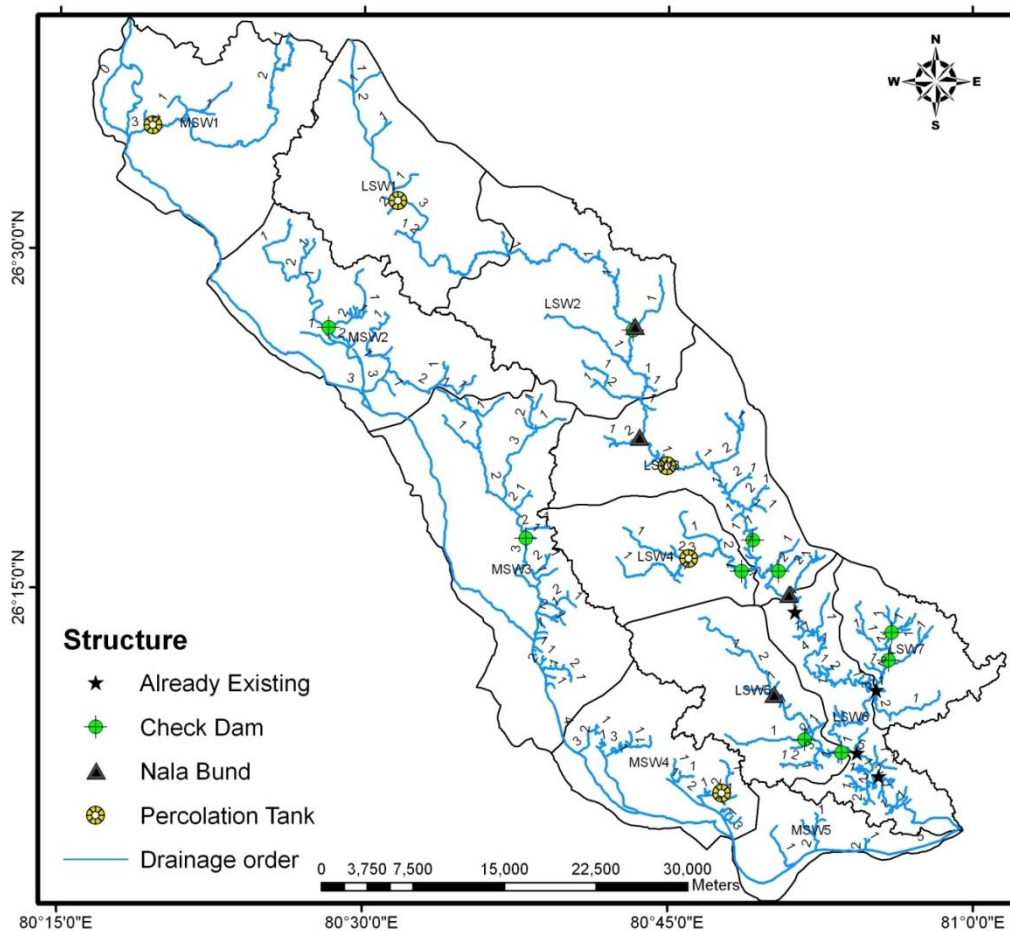


Fig. 5.13: Location of proposed and already existing artificial recharge structures

5.7 CONCLUDING REMARKS

In this study, groundwater potential and recharge zones map is delineated using RS, GIS and MCDM techniques. The AHP is MCDM technique that is used to determine the weights of various themes and their classes for identifying the groundwater potential zones.

These thematic layers were integrated by weighted linear combination method in a GIS environment to generate groundwater potential zones which were verified using the available well yield data from 40 pumping wells. The study area is classified into five zones, viz., 'very poor', 'poor', 'good', 'very good' and 'excellent'. It has been concluded that the area falling in excellent groundwater potential is about 150.93 km² (7.06% of the total study area), However, the area having very poor groundwater potential is about 372.03 km² (17.42% of the total study area), the area having poor, good and very good groundwater potential is about 815.39, 594, 202.94 km², respectively. The verification of the groundwater potential map using well yield data was found to be satisfactory. The developed groundwater potential zones map may be helpful to the decision makers in identifying suitable locations for drilling production wells and/or monitoring wells as well as in protecting the vital groundwater resources.

The study also reveals that remotely sensed data and GIS based approach is more appropriate than the conventional methods for the evaluation of drainage morphometric parameters and their influence on landforms, soils and eroded land characteristics at sub-watershed level. The conventional methods of morphometric analysis are not so accurate as well as time consuming. Interpretation of multi-spectral satellite sensor data is of great help in analysis of drainage parameters and morphometric characteristics which could be used for accurate delineation of distinct geological and landform units. The results of morphometric analysis show that sub-watershed LSW6 falls under highest priority, and therefore it is prone to relatively high erosion and soil loss. Hence, suitable control measures or structures are urgently required in this sub-watershed to preserve the land from further degradation.

Rainfall-runoff modeling was carried out in GIS environment where major inputs were derived from topographic maps, satellite images and field data. Fairly accurate classification of LULC types from satellite images helped in computing the CN values distributed over the sub-watershed required for SCS-CN model. The morphometric analysis of different sub-watersheds shows their relative characteristics with respect to hydrologic response of the watershed, which can serve as a guiding tool in decision-making process for planning different water and soil conservation structures in each sub-watershed. GIS is found to be an effective tool for integrating hydrological, LULC and morphometric parameters as per user defined criteria to identify suitable artificial recharge structures. The study assesses the necessity of having a particular kind of artificial recharge structure in each sub-watershed. It not only

indicates the suitability of the structures, but also helps whether a particular sub-watershed requires treatment or not in terms of water harvesting structures.

CHAPTER 6

ANALYSIS OF GROUNDWATER CONDITION AND ESTIMATION OF DYNAMIC GROUNDWATER RESOURCE

6.1 PROLOGUE

Quantification of natural groundwater recharge is a basic pre-requisite for effective management of these resources and is particularly vital in those areas where shallow groundwater is mostly polluted to highly toxic elements. GWD has declined in study area continuously due to overexploitation and mismanagement of water resources, which led to severe problem in study area. Groundwater occurs under unconfined condition of thick zone of alluvial sedimentation. Geo-statistics and geographical GIS are the efficient technology to manage the groundwater resources.

The groundwater resource estimation deals with the quantity of water recharged annually from the rainfall and other sources. Precipitation is the main source of groundwater recharge as well as other sources, which replenish the groundwater are seepage from canal system, recharge from the river system, return flow from the surface and groundwater irrigation, sub-surface inflow from the adjacent regions, etc. The present chapter outlines the procedure of groundwater resources estimation and trend analysis of GWD using GEC guidelines (MOWR-1997 & 2011) on block basis after that Mann Kendall's test are applied with GIS technology to understand the spatio-temporal behavior of groundwater level of wells. In the present study, pre and post monsoon GWD data of 40 monitoring wells of last 25 years (1984-2009) are used to detect the trend and also identifies the causes of change. The groundwater resources estimated in the study area based on the GEC guidelines, has been indicates that the net annual groundwater availability in command and non command are about 82339.72 ham

Hydrogeologically, it is a part of the central Ganga alluvial plain mainly constituted of clay, silt, sand, gravel and kankar sediments of quaternary age (Kumar *et al.*, 2011). These alluvial deposits of the area may be broadly classified into newer and older litho-units on the basis of sedimentary constitution, depositional and developmental geological history. The generalized sub-surface geological sequence is as follows, and shown in Table 6.1.

The Older Alluvium is made up of massive beds of clay of a pale reddish brown colour, very often yellowish with kankar (calcrete) present in between the clay layers. Its occupies large part in study area and its topographically high land so this area is not flooded by Ganga river whereas the newer alluvium occupies the area of low relief along the courses of the Ganga river and is susceptible to flooding during period. The upper layer of alluvium is composed of sandy loam and clayey loam. Sub-surface geology of the area is revealed from the study of strata logs of boreholes drilled by Central Ground Water Board (CGWB), which is given in Appendix – I.

Table 6.1: Sub-surface geology

Age	Litho-Unit	Sedimentary Constitution
-----Disconformity-----		
Holocene	Newer Alluvium	Channel Alluvium Lavee Alluvium
-----Unconformity-----		
Middle to Upper Pleistocene	Varanasi Older Alluvium	Clayey Facies Sandy Facies

Drilling has been carried out to a maximum depth of 569.27 m at Panna Lal Park, Unnao Town by the CGWB for a deposit well during 1975 which was abandoned due to the absence of promising water bearing granular zone. The bed rock was not encountered in above any of the boreholes in the study area.

6.2 GROUNDWATER SUBSURFACE CONDITION

The subsurface investigations are comparatively expensive, but it is essential for groundwater occurrence study. The small hole is drilled to find out the groundwater level and geological substrata. The different geological information has distinct physical properties that affect the flow of groundwater and determined the yield of a well. The lithology and the extension of aquifer both laterally and vertically are best revealed from the available litholog data of exploratory bore wells drilled by the CGWB. On the basis of subsurface lithology of seventeen exploratory bore wells, the lithologs of individual well has been prepared that shows the characteristics of aquifer/water bearing formation. In this study area, depths of exploratory bore wells are upto 450 meter. To understand aquifer geometry and the nature of sediments, three hydro geological cross sections along line AA', BB' and A'C' were prepared that cover the entire area in

which two sections run from west to east and one section AA' from north west to south east. The location of wells and cross sections are shown in Figure 6.1.

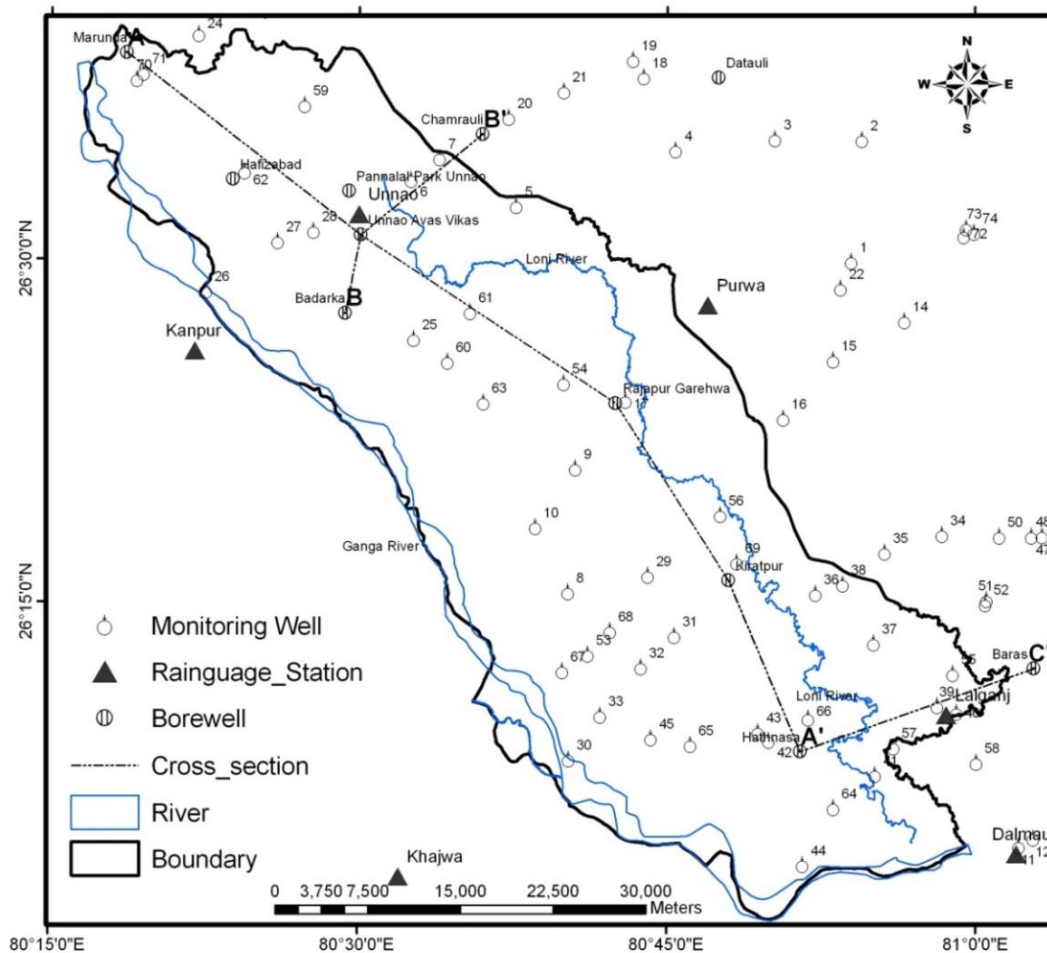


Fig. 6.1: Location of wells and rain gauge stations

Section A-A' (Marunda – Unnao Avas Vikas – Rajpur Garehwa – kiratpur – Hathnasa):

The section covers the area between Marunda in North West and Hathnasa in south west direction of the study area. A perusal of section shows that the thickness of granular zone gradually increases in central part and then it gradually increases towards south east. The subsurface geological formation comprises of clay, clay mixed with sand and sand.

The borehole drilled at Marunda down to the depth of 452 m has encountered with layers of impermeable and permeable granular materials with granular zone of 133.52 m thickness, the granular zone of 28.64 m thickness is encountered in the borehole drilled at Unnao Avas Vikas down to the depth of 452 m, the borehole drilled at Rajapur Garehwa down to the depth of 455 m

with granular zone of 135.48 m thickness, the borehole drilled at Kiratpur down to the depth of 484.94 m has been encountered with layers of impermeable and permeable granular materials having granular zone of 31.95 m thickness, the granular zone of 180.70 m thickness is encountered in the borehole drilled at Hathnasa down to the depth of 412.33 m.

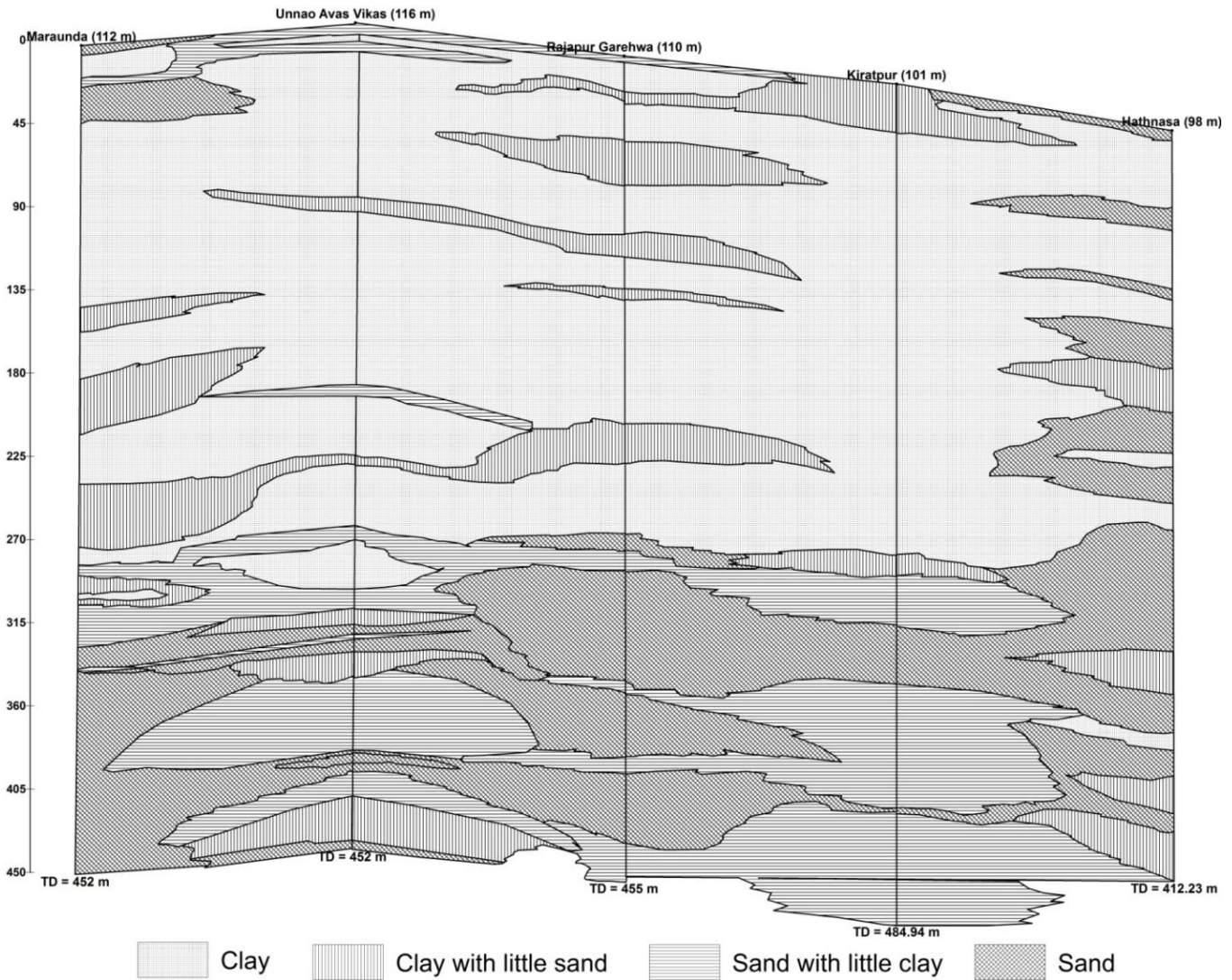


Fig. 6.2: Hydrogeological cross section along line AA'

Section B-B' (Badarka – Unnao Avas Vikas – Chamrauli):

The section covers the area between Badarka in west north and Chamrauli in east north direction of the study area. A perusal of section show that the thickness of granular zone gradually increases towards west north. The subsurface geological formation comprises of clay, clay mixed with sand and sand.

The borehole drilled at Badarka down to the depth of 437.50 m has encountered with layers of impermeable and permeable granular materials with granular zone of 137.55 m thickness, the granular zone of 28.64 m thickness is encountered in the borehole drilled at Unnao Avas Vikas down to the depth of 452 m, the borehole drilled at Chamrauli down to the depth of 454.28 m with granular zone of 40.6 m thickness.

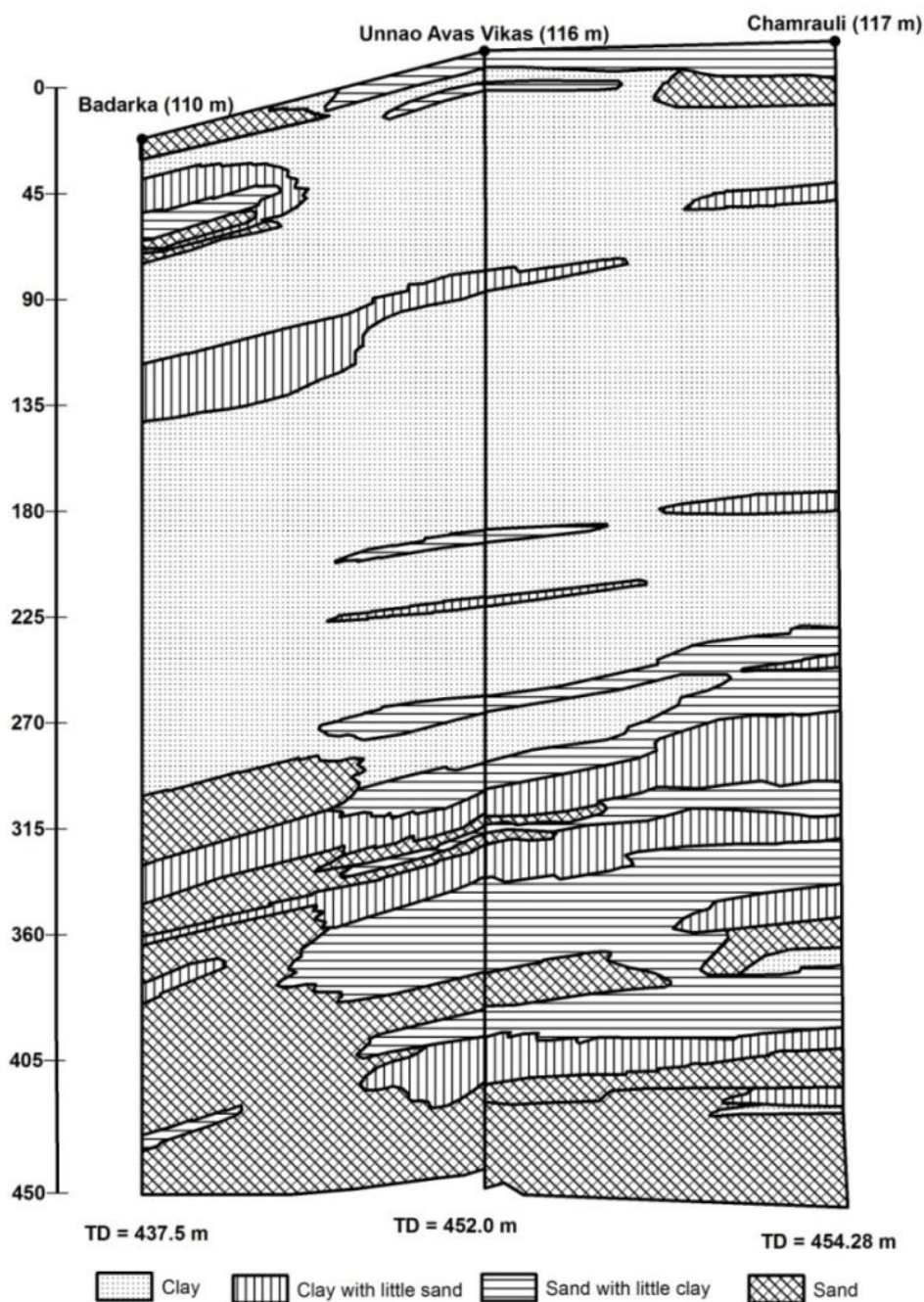


Fig. 6.3: Hydrogeological cross section along line BB'

Section A'-C' (Hathnasa – Baras):

The section covers the area between Hathnasa in south west and Baras in south east direction of the study area. A perusal of section show that the thickness of granular zone gradually increases towards west north. The subsurface geological formation comprises of clay, clay mixed with sand and sand.

The borehole drilled at Hathnasa down to the depth of 412.33 m has encountered with layers of impermeable and permeable granular materials with granular zone of 180.70 m thickness, the granular zone of 198.25 m thickness is encountered in the borehole drilled at Baras down to the depth of 378 m.

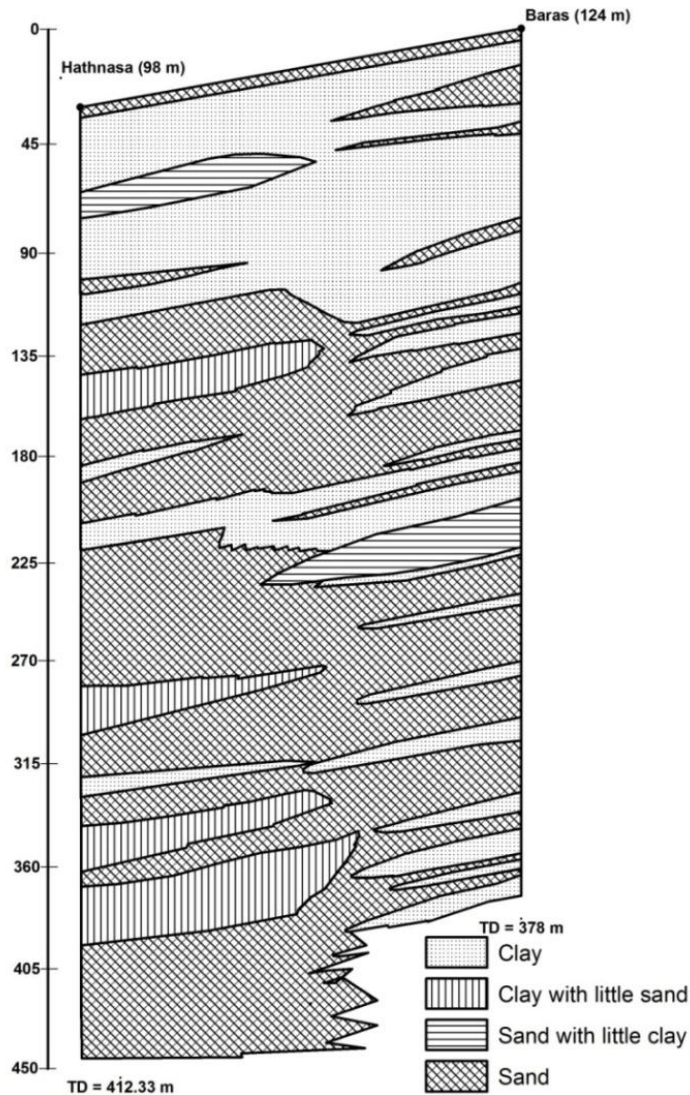


Fig. 6.4: Hydrogeological cross section along line CC'

6.3 METHODOLOGY FOR GROUNDWATER ASSESSMENT USING GEC

The detailed methodology for groundwater resource assessment is shown in Figure 6.5.

6.3.1 Groundwater Draft Estimation

Groundwater draft is estimated seasonally, on the basis of unit draft method as per GEC norms. In this method irrigation draft has been computed using unit draft of various structures, adopted through field studies, and is multiplied with the number of structures according to the Minor Irrigation Census report. Domestic & industrial draft has been taken as 5% of total irrigation draft. Monsoon and non_monsoon drafts have been shown in Table 6.2 and Figure 6.6 (a) & (b).

Table 6.2 Gross groundwater draft

S. No	Name of GWA Unit	Current gross GW draft in hecatres meters (ham) during for all uses			Area in hactares of the sub-unit	Current annual gross GW draft for all uses in subunit area per unit area in mm
		Monsoon Season	Non-Monsoon Season	Annual		
(a)	(b)	(c)	(d)	(e) = (c) + (d)	(f)	(g) = (e)/(f) *1000
1	Bichhiya	1634.86	4953.43	6588.29	30923.17	213.05
2	Bighapur	1800.41	5455.01	7255.43	28524.97	254.35
3	Khiron	1655.65	4966.95	6622.60	20269.82	326.72
4	Lalganj	1531.89	4595.96	6127.84	21947.01	279.21
5	Purwa	1443.71	4374.83	5818.53	25303.46	229.95
6	Sareni	1774.22	6403.97	8178.19	28516.71	286.79
7	Sikandarpur Karan	2380.46	7212.63	9593.08	36979.24	259.42
8	Sikandarpur Sarausi	1761.35	5336.69	7098.04	31540.80	225.04
9	Sumerpur	1210.67	3668.44	4879.11	26465.70	184.36
	TOTAL	15193.22	45887.90	61081.11	250470.89	2221.02

6.3.2 Estimation of Annual Groundwater Recharge

Groundwater is annually replenished or recharge through many sources such as precipitation, seepage from canal system, return flow from surface and groundwater irrigation, subsurface inflow from the adjoining region, recharge from the river system etc. Out of these precipitation is the main sources of groundwater recharge. Groundwater recharge has been computed separately for monsoon and non-monsoon seasons.

The annual replenishable groundwater recharge includes the following components (Kumar, 1992):

Total annual recharge = Rainfall recharge during monsoon & non-monsoon season + Recharge from other sources (Seepage from canals + Return flow from irrigation + Inflow from influent rivers etc. + Recharge from submerged lands, lakes etc.)

To estimate the rainfall recharge firstly we calculate the recharge from other sources

6.3.2.1 Recharge from other sources

The total recharge from other sources during monsoon and non-monsoon period is shown in Table 6.3.

6.3.2.1.1 Recharge due to canal seepage

Canal recharge has been calculated on the basis of GEC guidelines, when realistic data is not available. To calculate the recharge due to canal seepage following norms are used.

- (i) For unlined canals, where sandy soil with some clay contents is recharged 15 to 20 ham/day/million sq.m of wetted area of canal and if only sandy soil its recharged 25 to 30 ham/day/million sq.m of wetted area of canal.
- (ii) For lined canals, the seepage losses may be taken as 20% of the above values.

6.3.2.1.2 Recharge from surface water & groundwater irrigation

Return flow due to groundwater irrigation contributes to groundwater recharge. Irrigation water applied by groundwater irrigation during a given season is considered to be same as the gross groundwater draft for irrigation during that season. Return flow factor for paddy and non paddy is as per specific norms.

6.3.2.1.3 Recharge from ponds and tanks

1.4 mm/day for the period in which the ponds and tank has filled by water, based on the average water spread area. If the average area of water spread data is not available, then we take 60% of the maximum water spread area instead of average water spread area.

For recharge assessment during monsoon period, two types of approaches can be adopted: recharge by groundwater fluctuation method (WTF) and recharge by Rainfall infiltration factor method (RIF).

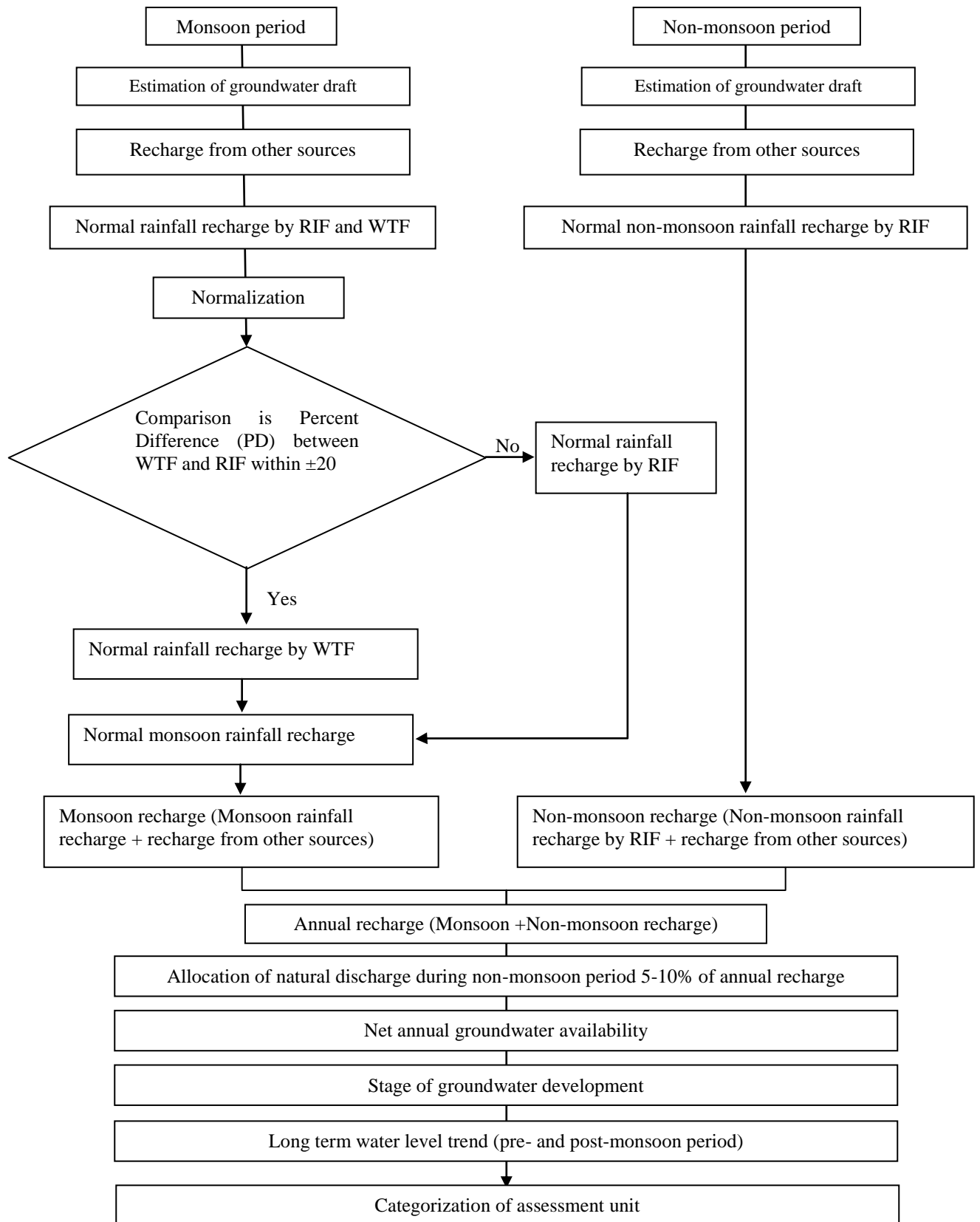


Fig. 6.5: Methodology for groundwater assessment using GEC (1997 & 2011) guidelines

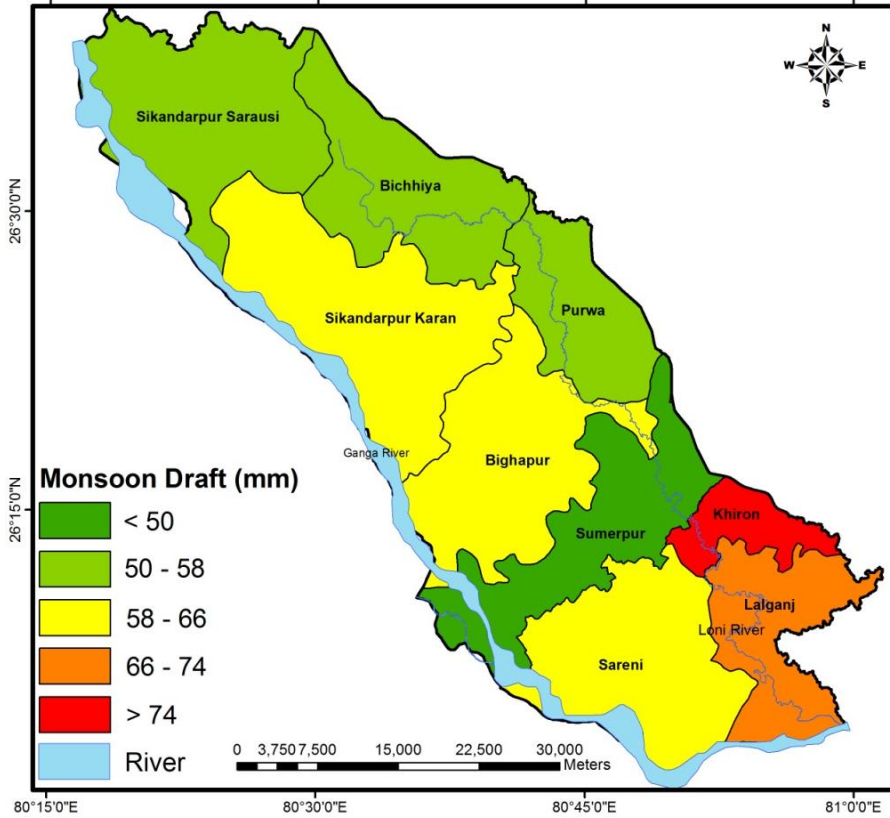


Fig. 6.6 (a): Groundwater draft in monsoon season (2004)

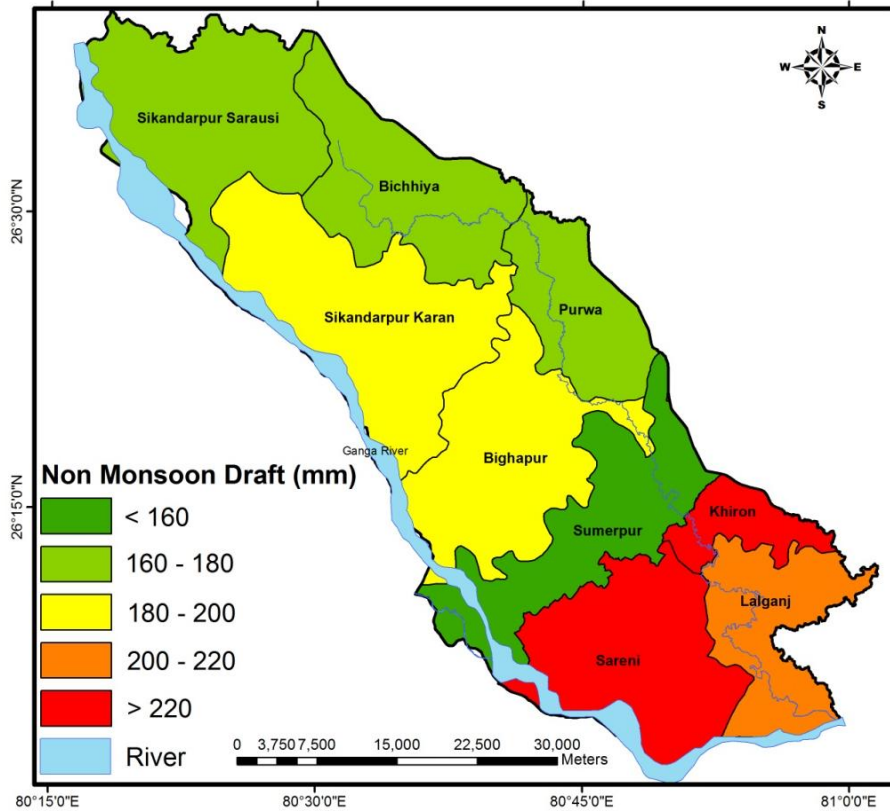


Fig. 6.6 (b): Groundwater draft in non-monsoon season (2004)

6.3.2.2 *Water Table Fluctuation (WTF) method*

The water table fluctuation method provides actual field evidence of recharge in an aquifer corresponds to the rainfall of observation year. The rainfall data should be corrected and normalized by using the average rainfall of last several years.

For calculating the annual recharge during monsoon period, the following formula is adopted (GEC, 1997) (Table 6.4):

$$R_{rf} = (S + DW - R_s - R_{igw} - R_{is}) \times \left(\frac{NMR_f}{AMR_f} \right) + R_s + R_{is} \quad (6.1)$$

where,

$$S = \text{Area (sq. km.)} \times \text{Water level fluctuation (m)} \times S_y \quad (6.2)$$

DW = Groundwater draft in monsoon period

R_s = Gross recharge from canal seepage in monsoon period.

R_{igw} = Recharge from groundwater irrigation in monsoon period.

R_{is} = Recharge from surface water irrigation in monsoon period.

NMR_f = normalized monsoon rainfall (meter).

AMR_f = annual monsoon rainfall (meter).

S_y = specific yield

The areas (such that high hills area and saline area) are not suitable for recharge so they should be excluded.

6.3.2.3 *Rainfall Infiltration Factor (RIF) method*

Rainfall recharge during monsoon as well as non-monsoon periods has been computed using, normal monsoon rainfall (data obtained from IMD), rainfall infiltration factors and area. The equation used for computation of recharge is (Table 6.5):

$$R_{rf} = F * A * \text{Normal rainfall during monsoon season} \quad (6.3)$$

R_{rf} = Recharge from rainfall

F = Rainfall infiltration factor (taken 0.20 in alluvial plain as per GEC norms)

A = Area of rainfall recharge

From the above two methods, which method is used for calculating monsoon rainfall recharge is based upon Percentage difference (PD). PD is the difference between WTF and RIF estimate expressed as percentage of RIF estimate. It is used the following criteria (Table 6.6).

- (a) If PD is in $\pm 20\%$, $R_{rf}(\text{normal}) = R_{rf}(\text{WTF})$
- (b) If PD is $< -20\%$, $R_{rf}(\text{normal}) = 0.8 * R_{rf}(\text{RIF})$
- (c) If PD is $> 20\%$, $R_{rf}(\text{normal}) = 1.2 * R_{rf}(\text{RIF})$

Non-monsoon rainfall recharge has been computed by rainfall infiltration factor (RIF) method. The total annual recharge for monsoon and non-monsoon periods is shown in Figure 6.7 (a) and (b).

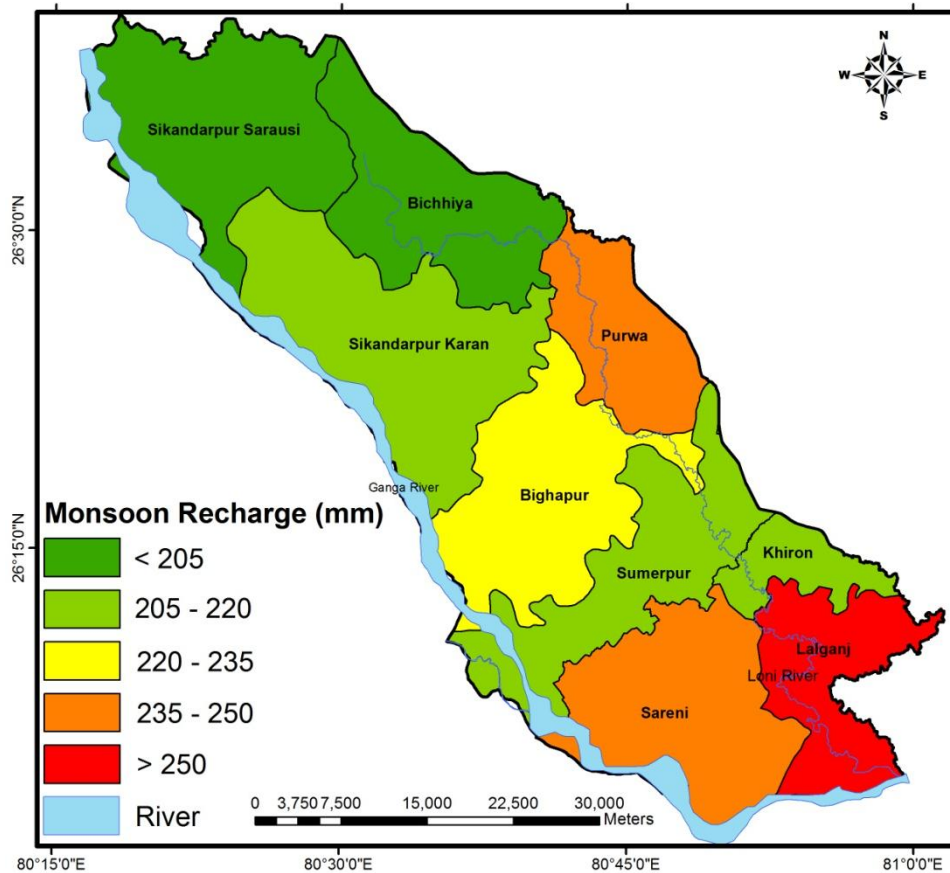


Fig. 6.7 (a): Groundwater recharge in monsoon season (2004)

Table 6.3 Total recharge from the other sources

S. No.	Name of GWA Unit	Area (ham)	Recharge from other sources										Annual recharge from other sources in ham
			Canal (ham)		Irrigation water applied by surface water irrigation (ham)		Irrigation water applied by GW irrigation (ham)		Tanks & ponds (ham)		Total Recharge (ham)		
			Monsoon Season	Non-Monsoon Season	Monsoon Season	Non-Monsoon Season	Monsoon Season	Non-Monsoon Season	Monsoon Season	Non-Monsoon Season	Monsoon Season	Non-Monsoon Season	Monsoon Season
1	Bichhiya	30923.17	2360.96	3930.04	0.00	0.36	735.69	1238.36	67.00	79.29	3163.65	5248.04	8411.69
2	Bighapur	28524.97	919.17	2044.73	0.00	0.00	810.19	1363.75	43.88	51.92	1773.24	3460.40	5233.64
3	Khiron	20269.82	675.66	1216.18	263.03	295.5	662.26	1490.09	50.82	79.11	1651.77	3080.88	4732.65
4	Lalganj	21947.01	382.04	687.67	248.98	257.40	612.75	1378.79	56.44	107.87	1300.21	2431.73	3731.94
5	Purwa	25303.46	1458.42	2269.05	18.90	7.92	649.67	1093.71	67.75	80.18	2194.74	3450.86	5645.59
6	Sareni	28516.71	331.37	596.47	227.02	297.60	709.69	1597.19	76.52	146.24	1344.59	2637.50	3982.09
7	Sikandarpur Karan	36979.24	790.38	1605.41	148.50	52.00	1071.20	1081.89	33.50	39.64	2043.58	2778.95	4822.53
8	Sikandarpur Sarausi	31540.80	732.76	1538.41	0.00	0.60	792.61	1334.17	32.15	38.05	1557.52	2911.24	4468.75
9	Sumerpur	26465.70	598.61	1324.78	44.10	16.08	544.80	917.11	19.25	22.77	1206.76	2280.74	3487.50

Table 6.4 Rainfall recharge by water table fluctuation method

S.No	Name of GWA Unit	Monsoon Season rainfall	Depth to water table below ground level (m) in the observation well		Specific yield	Groundwater balance during monsoon season						
			Pre-monsoon	Post-monsoon		Area (ha.)	Recharge from other sources (ham)	Gross GW draft (ham) for all uses	Water table fluctuation (m) during	Change in water storage during	Rainfall recharge (ham) by WTF	Normalized rainfall recharge (ham)
(a)	(b)	(c)	(d)	(e)	(f)	(g)	(h)	(i)	$j=(d)-(e)$	$k=(f)*(g)*(j)$	$(k)+(i)-(h)$	
1	Bichhiya	399.4	3.59	2.98	0.12	30923.17	3163.65	1634.86	0.61	2272.85	744.06	1103.58
2	Bighapur	640	6.04	5.00	0.12	28524.97	1773.24	1800.41	1.04	3544.51	3571.69	5062.33
3	Khiron	269.2	6.49	5.80	0.14	20269.82	1651.77	1655.65	0.69	1958.06	1961.95	2209.84
4	Lalganj	209.2	9.92	9.34	0.14	21947.01	1300.21	1531.89	0.58	1785.51	2017.19	4770.05
5	Purwa	596	4.46	2.78	0.12	25303.46	2194.74	1443.71	1.68	5091.06	4340.03	3808.46
6	Sareni	277.41	11.09	10.82	0.14	28516.71	1344.59	1774.22	0.27	1084.59	1514.21	5564.60
7	Sikandarpur Karan	437.23	8.28	7.05	0.12	36979.24	2043.58	2380.46	1.23	5467.01	5803.88	9253.53
8	Sikandarpur Sarausi	486.8	8.38	7.59	0.12	31540.80	1557.52	1761.35	0.79	2999.53	3203.37	9661.771
9	Sumerpur	475	5.47	3.86	0.12	26465.70	1206.76	1210.67	1.61	5121.11	5125.02	9258.05

Table 6.5 Rainfall recharge by Rainfall Infiltration Factor (RIF) method

S. No	Name of GWA Unit	Normal Rainfall			Normal non-monsoon season rainfall as a percentage of annual normal rainfall	Rainfall Infiltration Factor (RIF) from field studies as a fraction	Area (ha.)	If normal non-monsoon rainfall as a % of Normalised annual rainfall >10	Rainfall recharge by RIF method (ham) during	
		Monsoon	Non-Monsoon	Annual					Monsoon	Non Monsoon
		(c)	(d)	(e)					$f = (d)/(e)*100$	(g)
1	Bichhiya	576.25	55.35	631.6	8.76	0.22	30923.17	No	3920.29	0.00
2	Bighapur	642.94	55.34	698.28	7.93	0.22	28524.97	No	4034.77	0.00
3	Khiron	817.9	149.3	967.2	15.44	0.21	20269.82	Yes	3481.52	635.52
4	Lalganj	817.9	149.3	967.2	15.44	0.21	21947.01	Yes	3769.60	688.10
5	Purwa	642.94	55.34	698.28	7.93	0.22	25303.46	No	3579.09	0.00
6	Sareni	817.9	149.3	967.2	15.44	0.21	28516.71	Yes	4898.00	894.08
7	Sikandarpur Karan	576.25	55.35	631.6	8.76	0.22	36979.24	No	4688.04	0.00
8	Sikandarpur Sarausi	576.25	55.35	631.6	8.76	0.22	31540.80	No	3998.59	0.00
9	Sumerpur	642.94	55.34	698.28	7.93	0.22	26465.70	No	3743.49	0.00

Table 6.6 Rainfall recharge during monsoon season

S. No	Name of GWA Unit	GW year	Rainfall recharge during monsoon (ham)		Percentage Difference (PD)	Rainfall recharge (ham)
			WTF	RIF		
(a)	(b)	(c)	(d)	(e)	$f = ((d) - (e)) / (e) * 100$	(g)
1	Bichhiya	2004	1103.57	3920.29	-71.85	3136.23
2	Bighapur	2004	5062.33	4034.77	25.47	4841.72
3	Khiron	2004	2209.84	3481.52	-36.53	2785.22
4	Lalganj	2004	4770.05	3769.60	26.541	4523.52
5	Purwa	2004	3808.467	3579.09	6.415	3808.46
6	Sareni	2004	5564.60	4898.00	13.61	5564.60
7	Sikandarpur Karan	2004	9253.53	4688.04	97.38	5625.65
8	Sikandarpur Sarausi	2004	9661.77	3998.59	141.63	4798.30
9	Sumerpur	2004	9258.04	3743.49	147.31	4492.18

* GW is Groundwater, GWA is Groundwater Assessment, WTF is Water Table Fluctuation, RIF is Rainfall Infiltration Factor, ham is hectare meter and mm is millimeter.

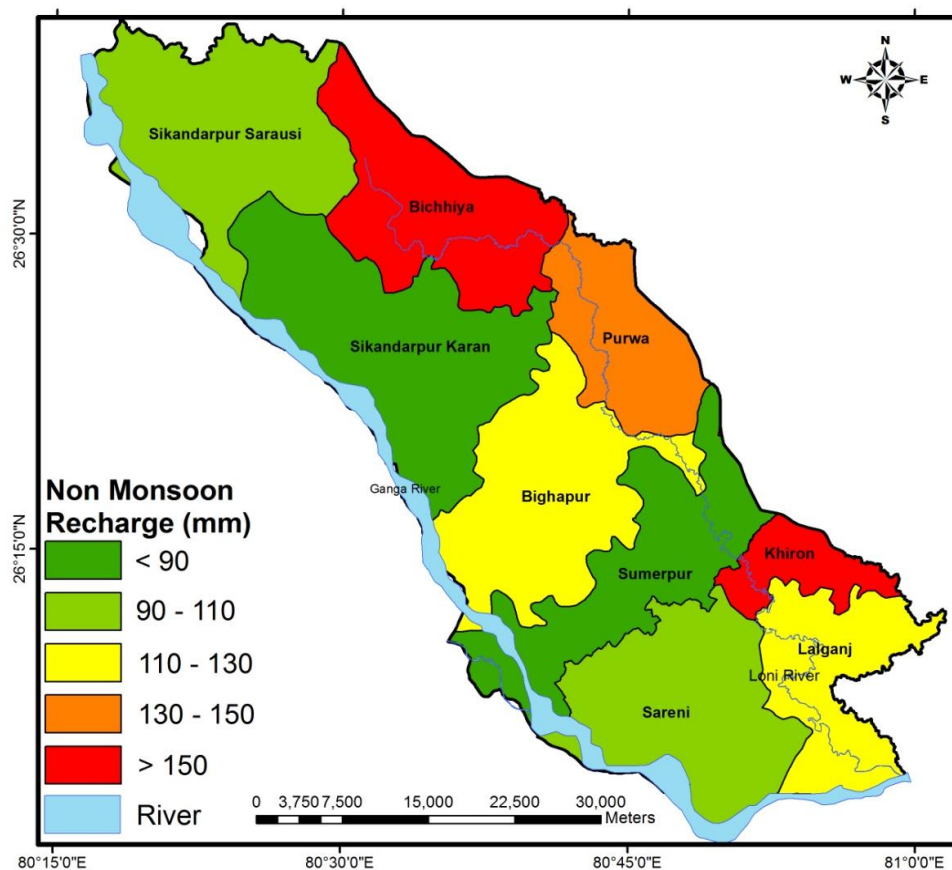


Fig. 6.7 (b): Groundwater recharge in non-monsoon season (2004)

6.3.3 Net Annual Groundwater Availability

The total annual groundwater potential obtained for the unit refers to the available annual recharge after allowing for natural discharge in the monsoon season in terms of base flow and subsurface inflow/outflow. This annual groundwater potential includes the existing groundwater withdrawal, natural discharge due to base flow and subsurface inflow/outflow in the non-monsoon season, and availability for future development.

As the groundwater development progresses, the natural discharge gets suitably modified. However, while deciding on the groundwater available for future development, some provision needs to be kept for natural discharge in the non-monsoon season. In the water level fluctuation method, a significant part of base flow is already accounted by taking the post monsoon water level one month after the end of rainfall. The base flow in the remaining non-monsoon period is likely to be small. However, detailed data for quantitative assessment of the natural discharge is not generally available. Considering these factors, it is recommended that 5 to 10% of the total annual groundwater potential may be assigned to account for natural discharges in the non-monsoon season (MOWR, 2007). The balance will account for existing groundwater withdrawal for various uses and potential for future development. This quantity is termed as the net annual groundwater availability (Table 6.7).

Table 6.7: Net annual groundwater availability

S. No	Name of GWA Unit	Annual recharge from rainfall (ham)	Annual recharge from other sources (ham)	Total annual GW recharge		Is rainfall recharge during monsoon season computed by WTF method (Y/N)	Unaccounted annual natural discharge		Net annual GW availability in the sub-unit	
				(ham)	per unit area (mm)		In ham [if response to (9) is Yes=0.05*(7) else 0.1*(7)]	per unit area (mm)	(ham)	Per unit area (mm)
1	Bichhiya	3136.23	8411.69	11547.92	373.44	No	841.17	27.20	10706.75	346.24
2	Bighapur	4841.72	5233.64	10075.36	353.21	No	523.36	18.35	9551.99	334.86
3	Khiron	3420.74	4732.649	8153.39	402.24	No	473.26	23.35	7680.12	378.89
4	Lalganj	5211.62	3731.94	8943.56	407.51	No	373.19	17.00	8570.37	390.50
5	Purwa	3808.46	5645.59	9454.05	373.63	Yes	282.28	11.16	9171.77	262.07
6	Sareni	6458.69	3982.09	10440.78	366.13	Yes	199.10	6.98	10241.67	362.47
7	Sikandarpur Karan	5625.65	4822.53	10448.18	282.54	No	482.25	13.04	9965.93	359.14
8	Sikandarpur Sarausi	4798.30	4468.75	9267.06	293.81	No	446.87	14.17	8820.18	279.64
9	Sumerpur	4492.19	3487.50	7979.69	301.51	No	348.75	13.18	7630.94	288.33

6.3.4 Categorisation of Areas for Groundwater Development

6.3.4.1 Stage of groundwater development

The stage of Groundwater development is percentage of total groundwater draft for all uses and the net annual groundwater availability

Stage of Groundwater development (%) =

$$\frac{\text{Existing gross groundwater draft for all uses}}{\text{Net annual groundwater availability}} \times 100 \quad (6.4)$$

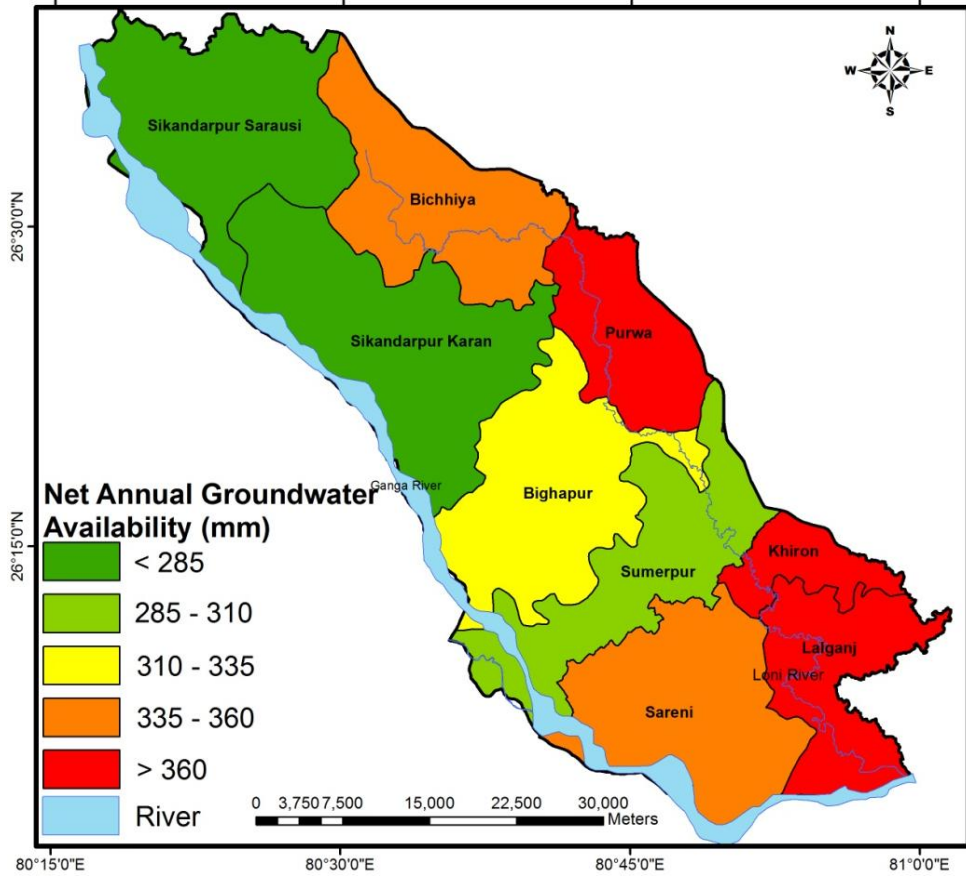


Fig. 6.8: Net annual groundwater availability (2004)

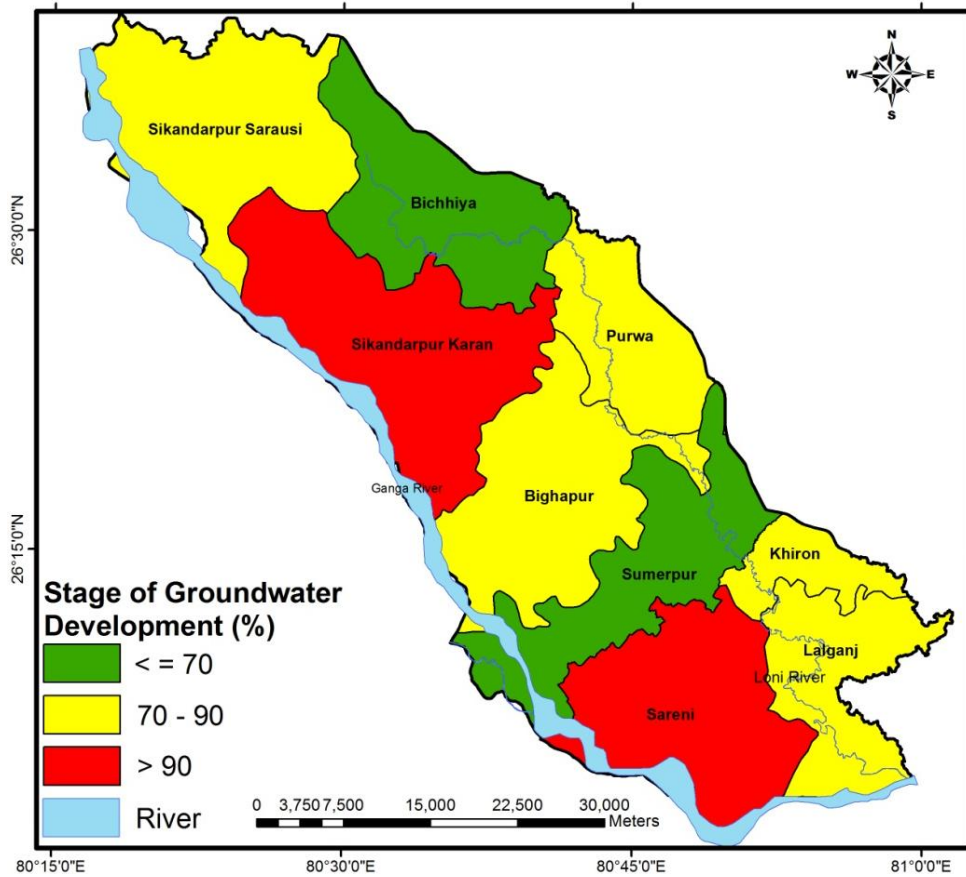


Fig. 6.9: Stage of groundwater development (2004)

6.3.4.2 Long term groundwater level trend

The stage of groundwater development is an index that measures balance between the groundwater availability and its utilization (draft). As the stage of development is nearby 100%, it indicates that future groundwater development prospects are scarce. However, the assessment based on the stage of groundwater development has inherent uncertainties. The numerator in equation 6.4, namely groundwater draft has uncertainties due to its estimation that are based on indirect assessment, such as electricity consumption, well census, and area irrigated from groundwater. The denominator in eqn. 6.4, namely net annual groundwater availability also has uncertainties due to limitations in the assessment methodology, as well as uncertainties in the data. In view of this, it is desirable to provide an alternate index of the present status of groundwater management, which is based on long term trend of groundwater levels.

It is recommended that in addition to obtaining an assessment of net annual groundwater availability and stage of groundwater development, as part of the groundwater assessment, the long term trend of groundwater levels in the unit should be presented. A steady and regular movement in a time series in which the values are, either increasing or decreasing is termed as trend. Long term trends are more appropriate for the study of hydrologic time series, for which historical data should be available for a longer period (Thakur, 2011). An ability to understand and interpret changes in groundwater levels is essential for management of groundwater resources. Various statistical methods have been developed to explain trends of groundwater level (Ferdowsian, 2009). Statistical methods are used in this study to analyze the spatial variations and temporal trends of the extreme water level series are linear regression method and Mann-Kendall's test.

Linear regression method: This method requires a set of ordered pairs of data on x_i and y_i for $i = 1$ to n , where 'n' refers to the number of pairs of data, x_i refers to the year and y_i refers to the depth to water table below ground level during the pre-monsoon and post-monsoon interval. The value of x_i for $i = 1$ is 1, and this corresponds to the earliest groundwater year for which water table data is available. If water table data is available for the next groundwater year, the value of x_i for $i = 2$ is 2. However, if water table data is available only after a gap of one groundwater year, the value of x_i for $i = 2$ is 3. A similar procedure is followed and the complete set of ordered pairs of data on x_i and y_i are obtained. The estimation of GWL trend is based on the following assumptions:

(a) The variation in groundwater level over successive groundwater years is linear. Let x be successive years and y be the groundwater level in metres. The relation between x and y is,

$$y = ax + b \quad (6.5)$$

where 'a' and 'b' are the regression constants

Thus, the value of 'a' obtained by linear regression analysis multiplied by 100 gives the trend of groundwater level in cm per year. Let this be designated as 'Z' (GEC, 2011).

$$Z = \frac{(n \sum_{i=1}^n x_i y_i) - (\sum_{i=1}^n x_i \sum_{i=1}^n y_i)}{(n \sum_{i=1}^n x_i^2) - (N \sum_{i=1}^n x_i)^2} \times 100 \quad (6.6)$$

The water table shows a falling trend if 'Z' is positive and rising trend if 'Z' is negative. The absolute value of 'Z' gives the rise or fall of water table in cm per year.

(b) As discussed in 'a' above, the water table shows a neither rising nor falling trend only if 'Z' is equal to zero. However, from a practical point of view it is necessary to adopt a range of values for 'Z' within which the water table can be considered to show a neither rising nor falling trend. With this consideration in mind, the water table trend is assumed to be,

- i) 'Rising' if 'Z' < -5 cm/year
- ii) 'Falling' if 'Z' > +5 cm/year
- iii) 'Neither Rising nor Falling' if 'Z' is between -5 and +5 cm/year

Mann-Kendall's test: Mann (1945) originally used this test and Kendall (1975) subsequently derived the test statistic distribution. The Mann-Kendall is a non-parametric trend test, which does not require any particular distribution of data (Gilbert, 1987) and has been widely used to test for randomness against trends in hydrology and climatology (Hirsch *et al.*, 1982). The Mann Kendall's test considers only the relative values of all terms in the series $X = \{x_1, x_2, \dots, x_n\}$ to be analyzed. In this test, the null hypothesis H_0 states that the series X is a sample of n independent and identically distributed random variables having no trend (Yu *et al.*, 1993). The alternative hypothesis H_1 of a two-sided test is that the distribution of x_k and x_j are not identical for all $k; j \leq n$ with $k \neq j$:

The Mann Kendall's test statistic S is given by:

$$S = \sum_{i=1}^{n-1} \sum_{j=i+1}^n \text{sgn}(x_j - x_i) \quad (6.7)$$

Where x_j and x_k are the sequential data values and n is the number of data points, and

$$\text{sgn}(x_j - x_i) = \begin{cases} +1 & \text{if } (x_j - x_i) > 0 \\ 0 & \text{if } (x_j - x_i) = 0 \\ -1 & \text{if } (x_j - x_i) < 0 \end{cases}$$

Under the null hypothesis of no trend, and the assumption that the data are independent and identically distributed, the zero mean and variance of the S denoted is computed as:

$$\text{Var}(S) = \frac{1}{18} \left[n(n-1)(2n+5) - \sum_{p=1}^q n_p(n_p-1)(2n_p+5) \right] \quad (6.8)$$

where n is the number of observations, q is the number of tied groups and n_p is the number of data in the p^{th} tied group (Gilbert, 1987). For sample size n is larger than 10 (Douglas *et al.*, 2000; Kahya 2004; Bihrat 2002), the standard normal variant Z is used for hypothesis testing, and is computed as follows:

$$Z = \begin{cases} \frac{S-1}{\sqrt{\text{Var}(S)}} & S > 0 \\ 0 & S = 0 \\ \frac{S+1}{\sqrt{\text{Var}(S)}} & S < 0 \end{cases} \quad (6.9)$$

Thus, in a two-tailed test for trend, the null hypothesis H_0 is either rejected or accepted depending on whether the calculated Z is more than or less than the critical value of Z obtained from the normal distribution table at significance level of α . Therefore, the values of Z are computed and it is seen that if the values lies in the limits -1.96 and 1.96, the null hypothesis that the series have no trend cannot be rejected at 5% level of significance using a two-tailed test.

Figures 6.10 (a-i) are prepared using the pre- and post-monsoon groundwater levels data of 25 years (1985-2009). Both pre- and post-monsoon water level trends may be shown on the same figure for ensuring conciseness in presentation and clarity in interpretation, it should be treated as an integral component of groundwater assessment. In Figure 6.10 (b, c, d, f), sudden falls has been occurred in year 1989 and 1990, due to data is not available of that time period.

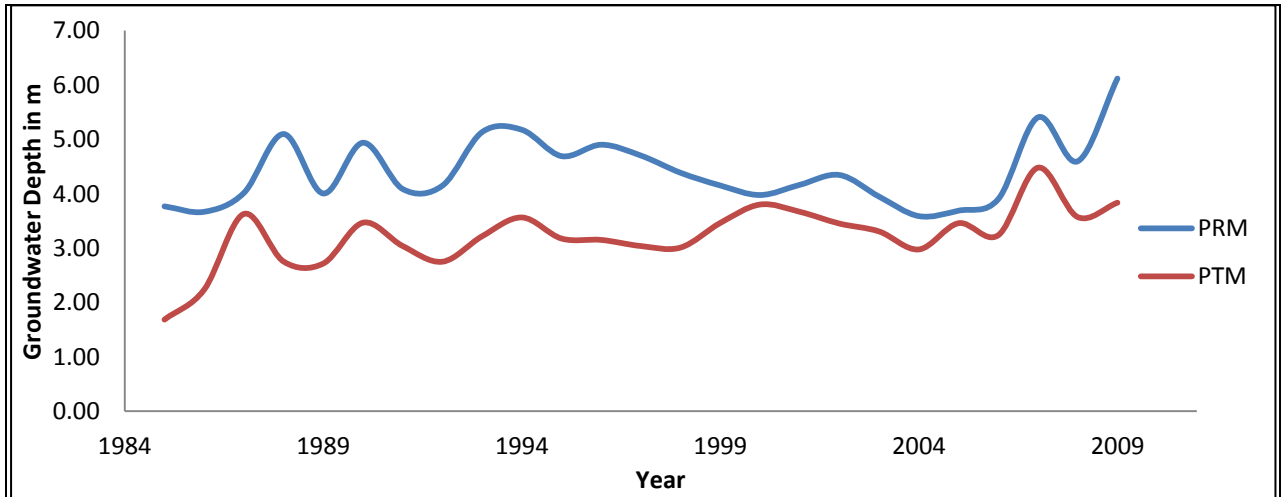


Fig. 6.10 (a) Groundwater level trend in Bichhiya block

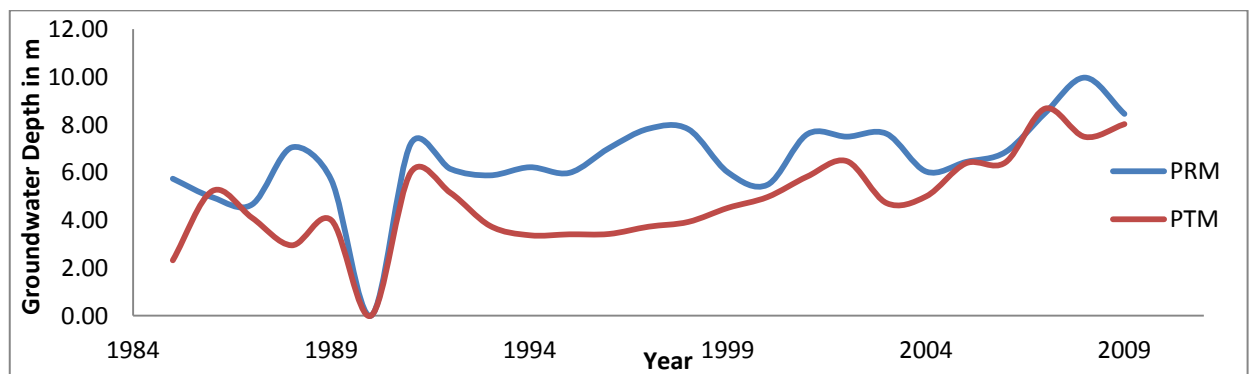


Fig. 6.10 (b) Groundwater level trend in Bighapur block

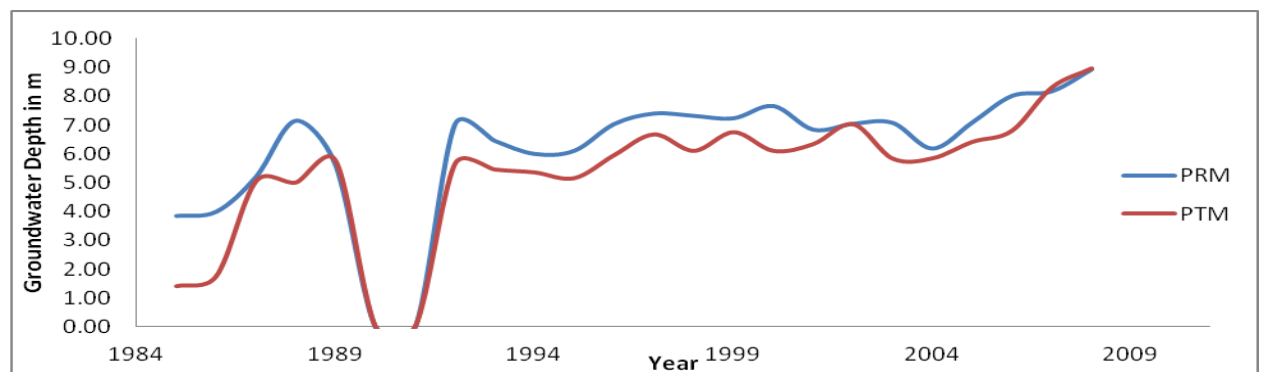


Fig. 6.10 (c) Groundwater level trend in Khiron block

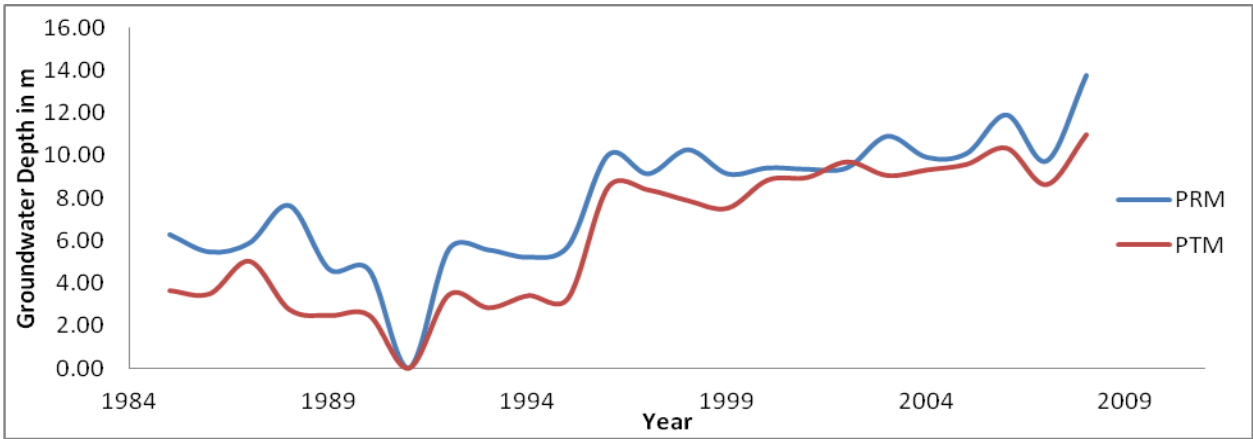


Fig. 6.10 (d) Groundwater level trend in Lalganj block

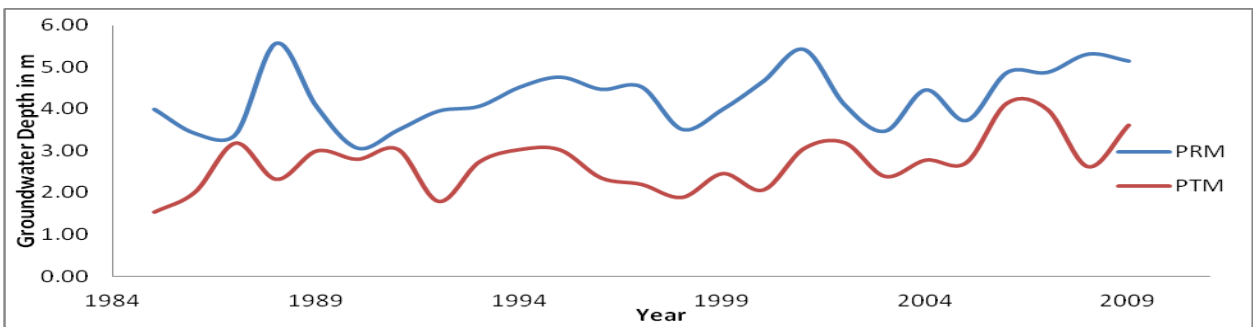


Fig. 6.10 (e) Groundwater level trend in Purwa block

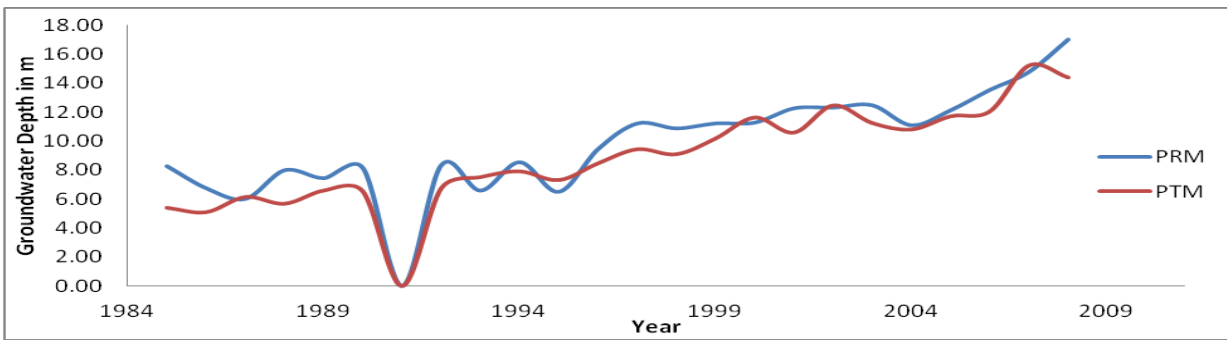


Fig. 6.10 (f) Groundwater level trend in Sareni block

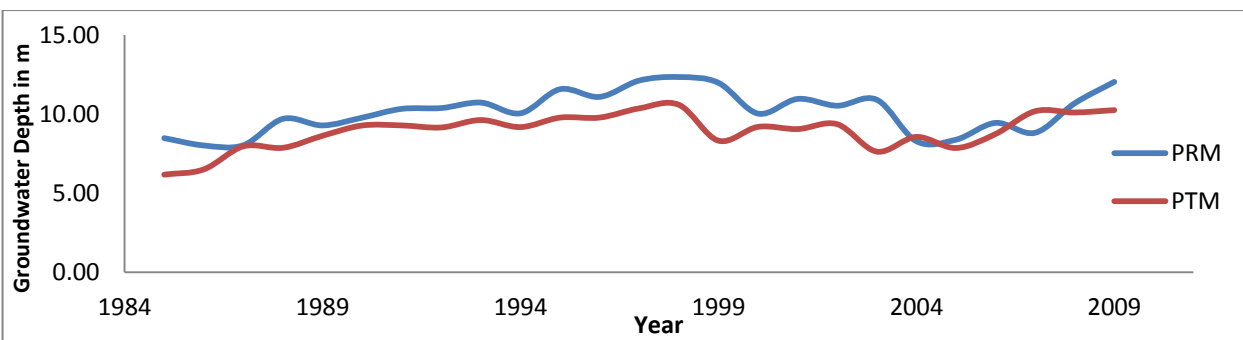


Fig. 6.10 (g) Groundwater level trend in Sikandarpur Karan block

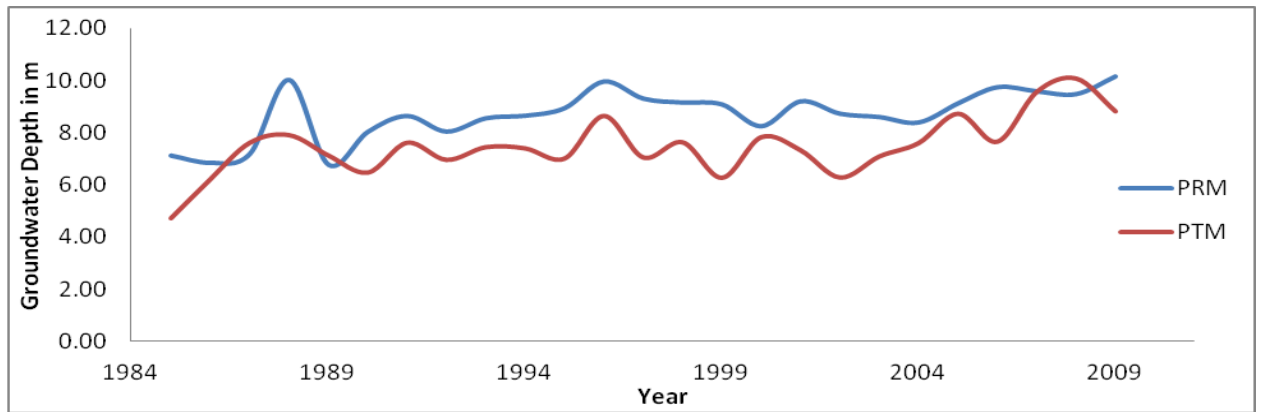


Fig. 6.10 (h) Groundwater level trend in Sikandarpur Sarausi block

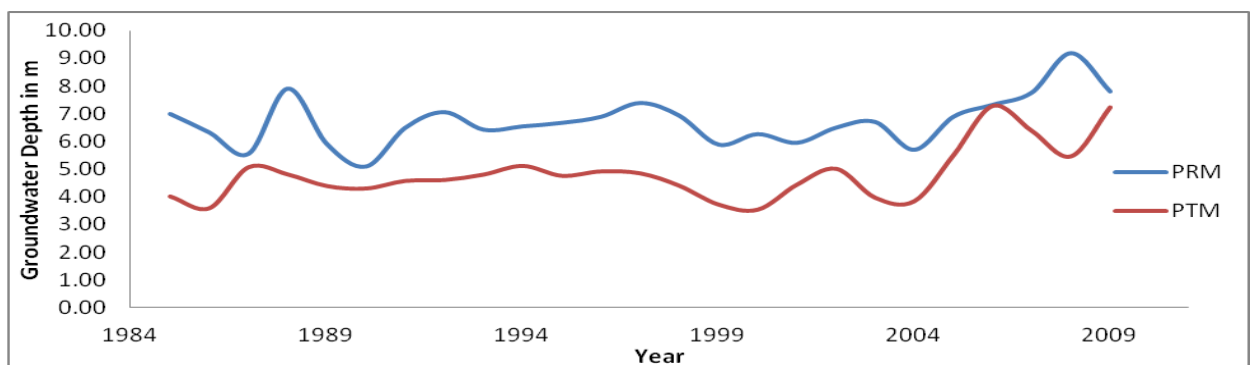


Fig. 6.10 (i) Groundwater level trend in Sumerpur block

If the groundwater resource assessment and the trend of long term water levels contradict each other, this anomalous situation requires a review of the groundwater resource computation, as well as the reliability of groundwater level data. The nature of groundwater level trend is shown in Table 6.8.

6.3.5 Categorization of Areas for Groundwater Development

The units of assessment can be categorized for groundwater development based on the stage of groundwater development (eqn.6.4) and the long term trend of pre- and post-monsoon groundwater levels. The following categorization is proposed based on these two factors and is shown in Figure 6.11 and Table 6.8.

6.3.5.1 Safe areas with potential for development

It is defined as the areas, where groundwater development is 70% or lower and there is no significant long termed declining trend of pre or post-monsoon groundwater levels or groundwater development is between 70–90% and also there is no significant long term

declining trend of pre- or post-monsoon groundwater levels. However, in these areas, caution may be exercised in planning future development with regard to quantum of additional groundwater withdrawal.

6.3.5.2 *Semi-critical areas for cautious groundwater development*

It is defined as the areas, where groundwater development is between 70–90% and significantly long termed declining trend of ground water levels in either pre- or post- monsoon season.

6.3.5.3 *Critical areas*

It is defined as the areas, where groundwater development is between 90–100% and significantly long term declining trend of groundwater levels in either pre- and post-monsoon seasons or groundwater development is less than 100% but long term declining trend of groundwater levels in both seasons or groundwater development is higher than 100% but significantly long termed declining trend of ground water levels in either pre and post monsoon season.

6.3.5.4 *Over-exploited areas*

It is defined as the areas where groundwater development is 100% or higher and significantly long term declining trend of groundwater levels in pre- and post-monsoon season.

Table 6.8: Categorization of groundwater assessment unit

Block	GW level trend		Stage of GW development in %	Category of GWA unit
	Pre monsoon	Post monsoon		
Bichhiya	no	no	61.54	Safe
Bighapur	yes	yes	75.96	Semi-Critical
Khiron	yes	yes	86.23	Semi-Critical
Lalganj	yes	yes	71.50	Semi-Critical
Purwa	no	no	87.74	Safe
Sareni	yes	yes	96.78	Semi-Critical
Sikandarpur Karan	yes	yes	96.26	Critical
Sikandarpur Sarausi	yes	yes	80.47	Semi-Critical
Sumerpur	no	yes	63.94	Safe

* GW is Groundwater, GWA is Groundwater Assessment.

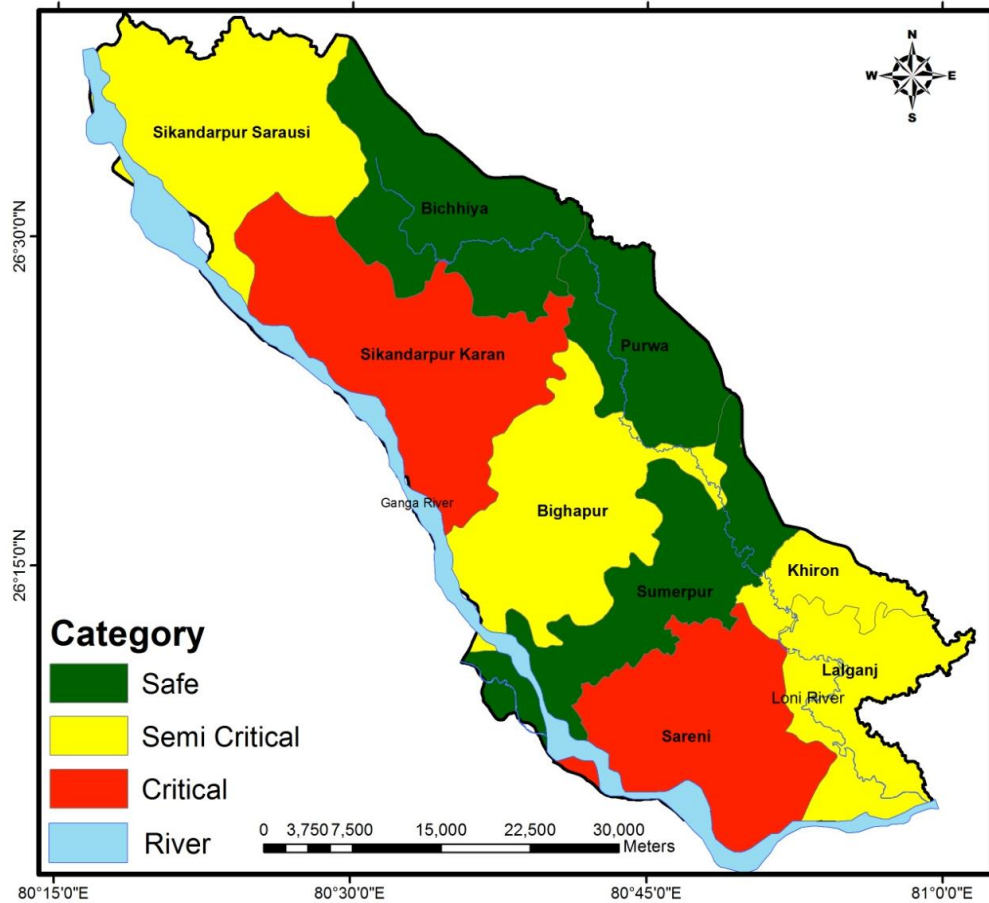


Fig. 6.11: Categorization of areas for groundwater development (2004)

6.3.6 Well Wise Trend Analysis

Mann Kendall’s trend test and linear regression method has been used to investigate the trend in groundwater level for a network of 40 observation wells obtained from CGWB for both pre- and post-monsoon seasons. The trend of individual well has been calculated to identify the reason and overcome the problem of groundwater depletion, water logging and soil salinity, that causes gradual fall and rise in groundwater level. The results of the Mann Kendall’s test and linear regression for pre- and post-monsoon groundwater level are summarized in Tables 6.9 & 6.10 and found that most of the wells have declining trend. The spatial variations of groundwater level trends for different observation wells during pre- and post-monsoon seasons is shown in Figures 6.12 & 6.13.

As for the results, in pre-monsoon season, 58% wells showed decreasing (falling) trends which can be due to high pumpage of water and less recharge, while about 5% wells showed increasing (rising) trends, most of which are located near pond and canal. In post-monsoon season, 63% wells showed decreasing (falling) trends and about 7% wells showed increasing (rising) upward trends. However, 61% wells showed decreasing (falling) trends and 6% showed

increasing (rising) trends trend in both pre- and post-monsoon seasons. These results are very helpful for sustainable groundwater development.

Table 6.9: Analysis of groundwater level trends in pre-monsoon season using the Mann-Kendall test for wells for a period 1985-2009

S. No	Well name	Data period	S	Z	Inference
1	Achal Ganj	1985-2009	89	2.06	Decreasing
2	Ajab Khera	1985-2009	165	3.83	Decreasing
3	Asgarganj	1985-2009	154	3.58	Decreasing
4	Babu Khera	1985-2009	-83	-1.92	No trend
5	Bahaee	1996-2008	17	0.98	No trend
6	Baksar	1985-2009	-44	-1.0	No trend
7	Bara	1993-2009	34	1.36	No trend
8	Bhagwant Nagar	1985-2009	132	3.07	Decreasing
9	Bhitargaon	1996-2006	36	2.73	Decreasing
10	Bichhiya	1985-2009	-72	-1.66	No trend
11	Bighapur Gauri	1985-2009	20	0.44	No trend
12	Bisenmau	2000-2009	19	1.61	No trend
13	Chanda	1996-2005	9	0.72	No trend
14	Dundi	1985-2009	-33	-0.75	No trend
15	Gajauli	1985-2009	89	2.06	Decreasing
16	Gandhi Nagar	1985-2009	185	4.31	Decreasing
17	Ganga Ghat	1985-2009	172	4.0	Decreasing
18	Gaziapur	1985-2002	119	4.47	Decreasing
19	Kheron	1996-2007	-20	-1.3	No trend
20	Lalganj-2 Ow	1994-2006	46	2.75	Decreasing
21	Lalganj Piezo	1985-2008	204	5.04	Decreasing
22	Lalkuwan	1999-2009	31	2.34	Decreasing
23	Magarwara	1985-2002	102	3.83	Decreasing
24	Mudian Khera	1985-2009	-93	-2.15	Increasing
25	Murtaza Nagar	1985-2009	-78	-1.80	No trend
26	Naraindas Khera	1985-2009	-184	-4.27	Increasing
27	Nihastha	1995-2004	23	1.97	Decreasing
28	Pahon	1985-2009	63	3.07	Decreasing
29	Paliyaveer Singhpur	1985-2008	218	5.38	Decreasing
30	Pathak Khera	1994-2006	-4	-0.18	No trend
31	Purwa	1985-2009	59	1.35	No trend
32	Raghuraj Singh	1985-2008	67	3.61	Decreasing
33	Ralpur	1985-2005	204	6.13	Decreasing
34	Rawatpur	1985-2009	104	2.41	Decreasing
35	Sareni	1985-2005	21	1.56	No trend
36	Sareni Piezo	1985-2009	172	3.99	Decreasing
37	Saraiya	1985-2009	-76	-1.75	No trend
38	Singraushi	1985-2002	119	4.47	Decreasing
39	Sumerpur	1985-2009	118	2.73	Decreasing
40	Tej Gaon Piezo	1999-2008	43	3.76	Decreasing

Table 6.10: Analysis of groundwater level trends in post-monsoon season using the Mann-Kendall test for wells for a period 1985-2009

S.No	Well name	Data period	S	Z	Inference
1	Achal Ganj	1985-2009	147	3.42	Decreasing
2	Ajab Khera	1985-2009	127	2.94	Decreasing
3	Asgarganj	1985-2009	219	5.10	Decreasing
4	Babu Khera	1985-2009	-96	-2.22	Increasing
5	Bahaee	1996-2008	66	3.97	Decreasing
6	Baksar	1985-2009	46	1.05	No trend
7	Bara	1993-2009	96	3.91	Decreasing
8	Bhagwant Nagar	1985-2009	150	3.49	Decreasing
9	Bhitargaon	1996-2006	37	2.8	Decreasing
10	Bichhiya	1985-2009	-81	-1.87	No trend
11	Bighapur Gauri	1985-2009	64	1.47	No trend
12	Bisenmau	2000-2009	27	2.33	Decreasing
13	Chanda	1996-2005	15	1.25	No trend
14	Dundi	1985-2009	-59	-1.35	No trend
15	Gajauli	1985-2009	123	3.68	Decreasing
16	Gandhi Nagar	1985-2009	188	4.64	Decreasing
17	Ganga Ghat	1985-2009	209	4.87	Decreasing
18	Gaziapur	1985-2002	129	4.85	Decreasing
19	Kheron	1996-2007	-40	-2.67	Increasing
20	Lalganj-2 Ow	1994-2006	45	2.69	Decreasing
21	Lalganj Piezo	1985-2008	203	5.01	Decreasing
22	Lalkuwan	1999-2009	29	2.18	Decreasing
23	Magarwara	1985-2002	84	3.15	Decreasing
24	Mudian Khera	1985-2009	-84	-1.94	No Trend
25	Murtaza Nagar	1985-2009	-11	-0.23	No trend
26	Naraindas Khera	1985-2009	-181	-4.21	Increasing
27	Nihastha	1995-2004	23	1.97	Decreasing
28	Pahon	1985-2009	55	2.67	Decreasing
29	Paliyaveer Singhpur	1985-2008	220	5.43	Decreasing
30	Pathak Khera	1994-2006	3	0.12	No trend
31	Purwa	1985-2009	-27	-0.61	No trend
32	Raghuraj Singh	1985-2008	67	4.04	Decreasing
33	Ralpur	1985-2005	204	6.13	Decreasing
34	Rawatpur	1985-2009	125	2.9	Decreasing
35	Sareni	1985-2005	47	1.39	No trend
36	Sareni Piezo	1985-2009	204	5.04	Decreasing
37	Saraiya	1985-2009	19	0.42	No trend
38	Singraushi	1985-2002	102	3.83	Decreasing
39	Sumerpur	1985-2009	102	2.36	Decreasing
40	Tej Gaon Piezo	1999-2008	31	2.68	Decreasing

The trend of groundwater level derived as a result of Mann Kendall's test and linear regression analysis indicate that most of the wells have decreasing trend while increasing, while no trend is found in some of the wells. Both decreasing and increasing trends in groundwater

levels have so many adverse impacts on the environment. Variation in groundwater levels can be due to the natural climate changes and human activities. Groundwater level has declined; it may be due to rapid urbanizations and industrialization as well as due to modern irrigation practices.

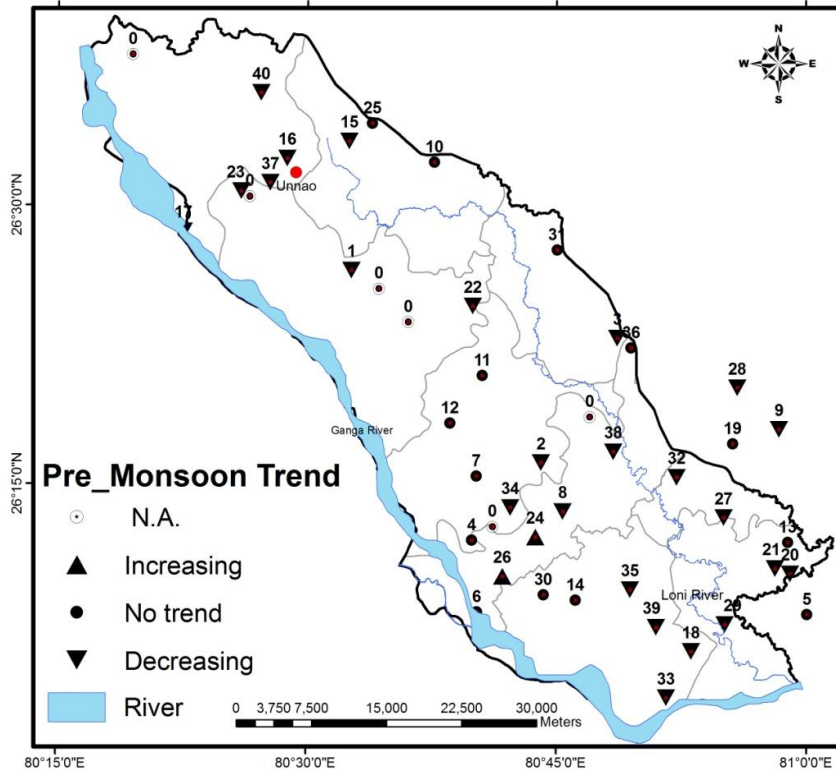


Fig. 6.12: Spatial variation GWL trend in pre-monsoon season (1985-2009)

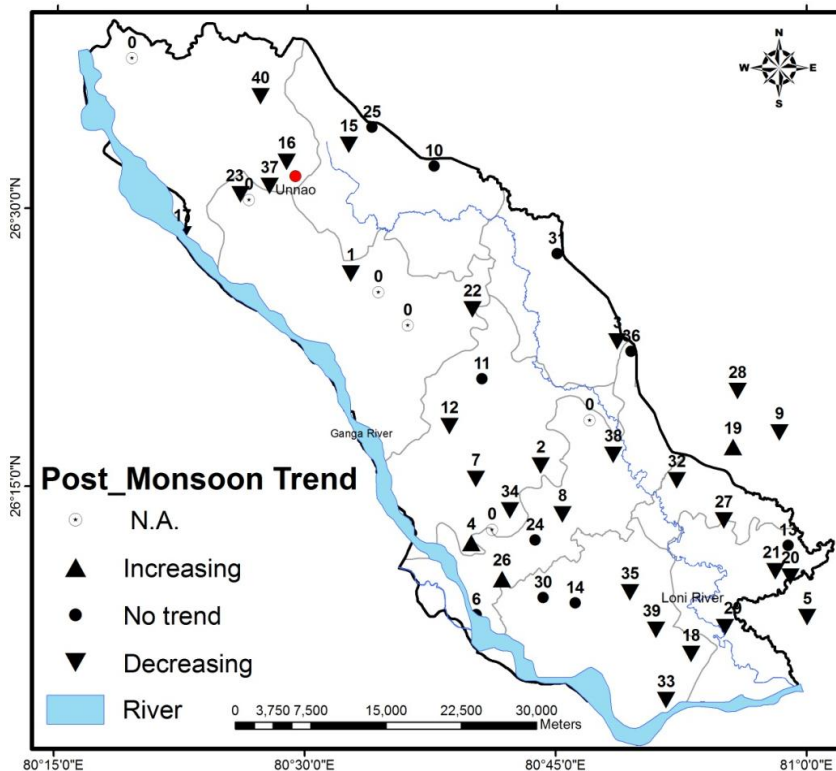


Fig. 6.13: Spatial variation GWL trend in post-monsoon season (1985-2009)

6.3.7 Analysis of Salt Affected Area

In this region, groundwater level has declined in some areas but near canals has it high water table, which increases the salt-affected area. To analyze this problem, LULC map was generated using Landsat TM image of April for the year 1989 and 2010. Initially, it has been classified into eight classes namely; agriculture land, fallow land, barren land, sand, urban, water logged area, water body and salt-affected area. During classification some portion of sand was also classified as salt affected area, and therefore to eliminate the sandy area from salt-affected class mask of canal was used.

After that salt-affected area has been extracted from the LULC map and the remaining classes were masked out. The extracted salt-affected maps are shown in Figures 6.14 and 6.15. These were interpreted and the salt-affected area has been found to decreased upto 50% in year 2010. This may be due to projects (UP Sodic Land Reclamation) which has been started by Government of Uttar Pradesh has been implemented in the various districts of Uttar Pradesh including Unnao, Rae Bareilly, Sultanpur, Hardoi, Barabanki districts. In these projects, salt-affected or degraded lands are being used for cultivation using gypsum in the soils.

6.4 CONCLUDING REMARK

It is concluded that most of the exploratory wells are drilled upto 455 m depth. On the basis of groundwater recharge modeling using GEC guidelines, it was found that Sikandarpur Karan and Sareni blocks fall in critical category and remaining blocks in semi-critical and safe category but most of the blocks have significantly decline in groundwater level.

The results of Mann Kendall's test and linear regression for pre- and post-monsoon groundwater levels indicate that most of the wells have a declining trend. For protecting groundwater from further depletion, the groundwater development needs to be taken up in a planned manner in order to prevent adverse impact on groundwater. The artificial recharge can be implemented to avoid the declining trend in groundwater levels. Water-logging and soil salinity problems, resulting from gradual rise of groundwater levels, were observed in study area. These are due to the surface water irrigation without environmental consideration of environmental conditions. So, there is a great need to adopt the conjunctive water use strategy in the area experiencing water logging problems.

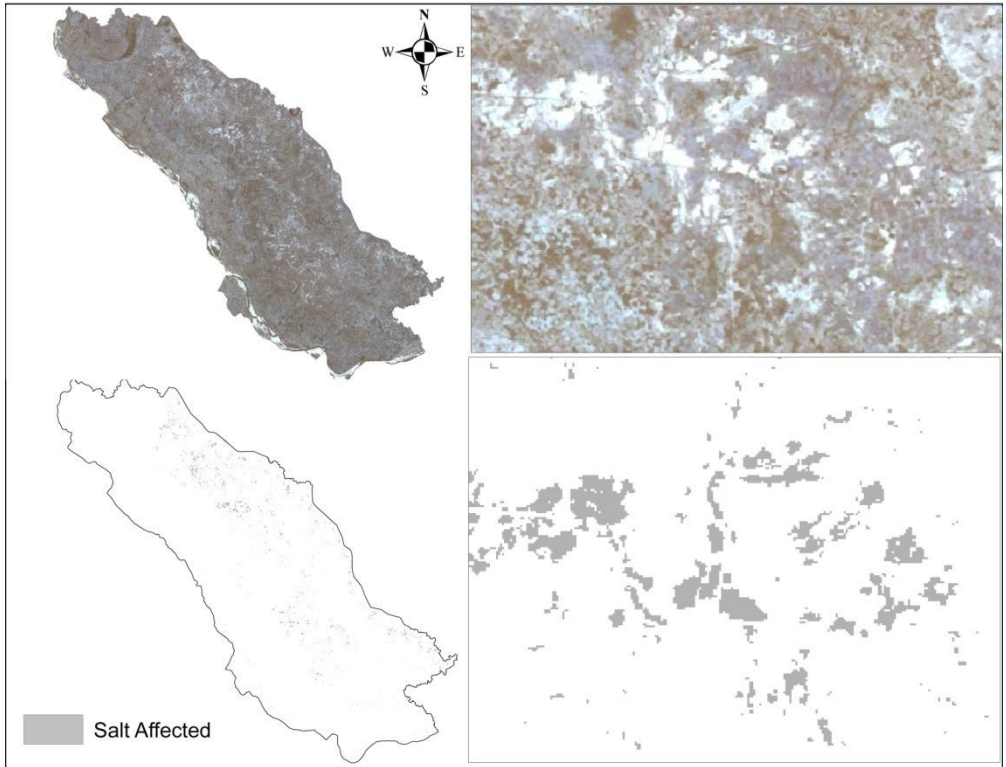


Fig. 6.14: Landsat TM image and salt-affected area for year 1989

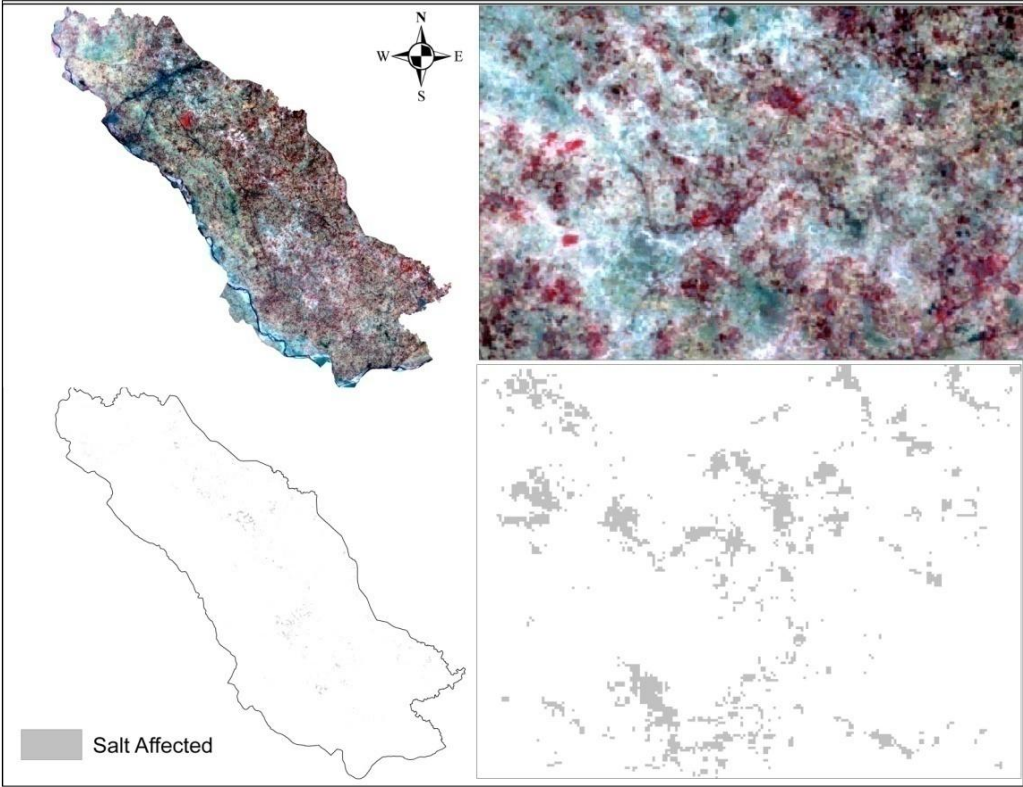


Fig. 6.15: Landsat TM image and salt-affected area for year 2010

7.1 PROLOGUE

In general, the models are conceptual description that describes the physical system using mathematical equations, which are approximate description of the physical system. Groundwater flow modeling is the process of description of groundwater movement of an area through the mathematical equations (Kumar *et al.*, 1992).

In this chapter, the basic concept of groundwater flow modeling and the procedure of development of numerical groundwater flow model using GIS and RS data for the alluvial aquifer are described. There are various approaches developed and used for groundwater modeling in alluvial aquifers in the past (Wolf *et al.*, 2008). In the present study, Processing Modflow (PMWIN) software has been used to implement the groundwater flow model for the study. Various aspects of model conceptualization, such as parameterization, boundary conditions and integration with GIS are presented. Further, the model calibration and validation aspects are discussed. Finally, the sensitivity analysis has been carried out and the simulation results presented.

7.2 GROUNDWATER MODELING

Groundwater flow models are used to calculate the rate of flow and the direction of movement of groundwater through aquifers and confining units in sub-surface. Groundwater models describe the groundwater flow using mathematical equations that are based on certain assumptions. Because of the simplifying assumptions used by the mathematical equations and many other uncertainties involved the input data, a model can give an approximation and not a replication of exact field conditions. Following features and assumptions are usually considered while using ground water flow models (Willis and Yeh, 1987).

1. The one aquifer system is modeled with only one storage coefficient in vertical direction.
2. The aquifer is bounded at the bottom by an impermeable layer.
3. Ratio of horizontal and vertical conductivity is 10.

4. The upper boundary of the aquifer is either an impermeable (confined aquifer), or a slightly permeable layer (semi-confined aquifer) or a free water table (unconfined aquifer).
5. Darcy's law (head loss varying with apparent velocity of flow) and Dupuit's assumptions (negligible vertical flow) are applicable.
6. The aquifer has head controlled, flow controlled, and/or zero-flow boundaries: the first two of the boundaries may vary with time, and
7. The process of infiltration and percolation of rain and surface water and of capillary rise and evaporation, taking place in the unsaturated zone of aquifer (above the water table), can't be simulated. This means that net recharge of the aquifer must be calculated separately and prescribed in the model.

The equation that describes the groundwater flow process may be solved by using different types of models. Some models may provide exact solution to equations that describe very simple flow (analytical model) while others may be approximation of equations that describe very complex conditions (numerical model). In selecting a model for use at a site, it is necessary to determine whether the model equations account for the key process occurring at the site. Analytical models provide an exact solution of a specific, often greatly simplified, groundwater flow equation. Specifically, these simplifications result in reducing the groundwater flow to one dimension. This results in changes to the model equations that include one dimensional uniform groundwater flow, simple uniform aquifer geometry, homogeneous and isotropic aquifers, uniform hydraulic properties and simple flow boundaries. Analytical models are typically steady state and one dimensional groundwater flow models. Because of the simplifications inherent with analytical models, it is not possible to account for field conditions that change with time or space. This includes variations in groundwater flow rate or direction, variation in hydraulic properties changing hydraulic stresses, or complex hydro-geologic boundary conditions (Mandle, 2002).

Numerical models are capable of solving the more complex equations that describe groundwater flow. These equations generally describe multi-dimensional groundwater flow, although there are one-dimensional numerical models. Numerical models use approximations (e.g., finite differences, or finite elements) to solve the differential equation describing the groundwater flow. These approximations require that the model domain and time be discretised. In the discretisation process, the model domain is represented by a network of grid cells

or elements while the time of simulation is represented by time steps. The accuracy of numerical model is dependent upon the accuracy of model input data, size of the space and time discretisation and numerical method used to solve the equation. Unlike analytical model, numerical models have the capability of representing a complex multi-layered hydro-geologic framework. This is accomplished by dividing the framework into discrete cells or elements. In addition to complex 3D groundwater flow problems, numerical models may be used to simulate very simple flow, which may easily be simulated using an analytical model. However, numerical models are generally used to simulate problems which cannot be accurately described using analytical models (Mandle, 2002).

Since the process of describing and solving a numerical groundwater model is problem independent, many commercial and public domain software area available for this purpose, like PMWIN. The simulations of groundwater flow using any model require a thorough understanding of hydro-geologic characteristics of the aquifer. The hydro-geologic investigations should include a complete characterization of the following:

1. Sub-surface extent and thickness of aquifers and confining units (hydro-geological framework),
2. Hydrologic boundaries (also referred as boundary conditions), which control the rate and direction of movement of groundwater,
3. Hydraulic properties of aquifers and confining units,
4. A description of the horizontal and vertical distribution of hydraulic heads throughout the modeled area for beginning (initial conditions), equilibrium (steady state condition) and transitional condition, when hydraulic head may vary with time (transient condition), and
5. Distribution of magnitude of recharge, pumping or injection of groundwater, leakage to or from surface water bodies etc. (sources or sinks, also referred as stresses). These stresses may be constant (not varying with time) or may change with time (transient).

7.2.1 General Equation of Groundwater Flow

There are two basic equations which govern the flow through porous media: (a) Darcy's law and (b) Continuity equation (law of mass conservation). Various partial differential equations, which themselves may be models for various situations of groundwater flow, are some kind of combination of Darcy's law and Continuity equation. Only selected equations of

groundwater flow are presented in this section. The equation representing the piezometric head distribution in a 3d flow through non homogeneous and anisotropic medium is expressed as (Bear, 1979):

$$\frac{\partial}{\partial x} \left(k_{xx} \frac{\partial h}{\partial x} \right) + \frac{\partial}{\partial y} \left(k_{yy} \frac{\partial h}{\partial y} \right) + \frac{\partial}{\partial z} \left(k_{zz} \frac{\partial h}{\partial z} \right) = S_0 \frac{\partial h}{\partial t} \quad (7.1)$$

Where k_{xx} , k_{yy} and k_{zz} are permeabilities of the medium (L/T) measured along the principal axis X, Y and Z respectively and vary with space coordinates (x, y, z), h is the piezometric head which is a function of both space and time i.e., $h = f(x, y, z, t)$ and S_0 is the specific storativity of the porous medium (L^{-1}). Specific storativity of the porous medium of an aquifer is defined as the volume of water released from storage (or added to it) in a unit volume of aquifer per unit decline (or rise) in the piezometric head.

Equation 7.1 is a simple combination of Darcy's law and basic mass balance equation. The derivation of this equation involves the following assumptions (Bear, 1979: Sharma 1987):

1. The velocity of solids is too small (in comparison to the actual velocity of fluid i.e., v_s/n) that v_s may still be expressed by Darcy's law,
2. Permeabilities may vary with space and independent of the variability of density of the fluid (ρ),
3. Storativity and permeability coefficients are unaffected by the variation in porosity (n) due to matrix deformability. It is assumed that these variations are small relative to the initial value of n. The same is true for ρ ,
4. Spatial variation in ρ is much smaller than local and temporal ones,
5. Permeability coefficient must be continuous and has a continuous first derivative everywhere in the flow domain is considered, and
6. First and second derivative of the piezometric head should also be continuous in the considered flow domain.

7.2.2 Flow in a Confined Aquifer

The groundwater flow is an anisotropic and non-homogeneous, non-leaky confined aquifer is expressed by the following partial differential equation:

$$\frac{\partial}{\partial x} \left(T_{xx} \frac{\partial h}{\partial x} \right) + \frac{\partial}{\partial y} \left(T_{yy} \frac{\partial h}{\partial y} \right) = S_0 \frac{\partial h}{\partial t} + q(x, y, z, t) \quad (7.2)$$

Where T_{xx} and T_{yy} are aquifer transmissivities in the principal direction X and Y and unit is (L^2/T) . $T_{xx} = T_{xx}(x, y)$, $T_{yy} = T_{yy}(x, y)$, $q(x, y, z, t)$ represents the distributed sink function and is defined as excess of outflow over inflow per unit area per unit time (L/T) , S is the storativity of confined aquifer (dimensionless). Aquifer transmissivity is defines as the rate of flow per unit width through the entire thickness of aquifer per unit hydraulic gradient. The derivation of this equation involves the following assumptions (Sharma, 1987):

1. Equation 7.2 essentially represents horizontal flow i.e., combined aquifer flow is treated as two dimensional flow in the horizontal plane, and
2. Variables h , T and S are the average value of piezometric head, aquifer transmissivity and aquifer storativity, respectively. The averages are taken along a vertical line extending from the bottom and the top of confined aquifer.

Assumptions discussed in previous section (i.e. 7.2.1) are also applicable in equation 7.2.

7.2.3 Flow in an Unconfined Aquifer

Groundwater flow problems in unconfined aquifer are generally analyzed based on the Dupuit-Forchheimer assumptions. The continuity equation and Darcy's law are combined with free surface boundary condition to obtain the partial differential equation of groundwater flow. The governing differential equation for a two-dimensional transient flow in anisotropic and heterogeneous unconfined aquifer may be written as (Willis and Yeh, 1987):

$$\frac{\partial}{\partial x} \left(k_{xx} h \frac{\partial h}{\partial x} \right) + \frac{\partial}{\partial y} \left(k_{yy} h \frac{\partial h}{\partial y} \right) = S_y \frac{\partial h}{\partial t} + q(x, y, z, t) \quad (7.3)$$

Where S_y is the storativity of unconfined aquifer, which is nothing but specific yield of the aquifer medium i.e., $S = S_y$. This equation is also called Boussinesq equation. In the present work, aquifer of the study area is unconfined in nature. Therefore, equation 7.3 is applicable for modeling of groundwater system of the chosen study area.

7.3 GROUNDWATER FLOW MODEL DESIGN

The groundwater flow model consists of the following stages (Anderson and Woessner 1992):

- i. Development of concept, which is the most important part of the modeling and the basis for all further activities.
- ii. Selection of mathematical model.
- iii. Defining the geometry of model (i.e. model boundary, grid, position and number of layers).
- iv. Definition of boundary array, i.e. cell types (active, inactive and constant head cells).
- v. Input hydro-geological parameters for each cell such as hydraulic conductivity, storage properties.
- vi. Defined the boundary conditions.
- vii. Definition of initial conditions (distribution of hydraulic heads).
- viii. Definition of stresses acting on the system such as recharge, pumping etc.
- ix. Model run.
- x. Model calibration, which is probably the lengthiest and most important part of modeling.
- xi. Verification of model validity. The calibrated model is checked against another set of field data that was not used in model design.
- xii. Sensitivity analysis, which is used to quantify the uncertainty in the calibrated model caused by the estimate of the aquifer parameters, stress and boundary conditions.
- xiii. Derivation of results.

Stepwise procedure followed in the present study is shown in Figure 7.1.

7.4 CONCEPTUALIZATION OF GROUNDWATER SYSTEM

The formulation of conceptual model is most important task that is necessary prior to develop a numerical model. Model conceptualization is the process whereby data describing field conditions are assembled in systematic way to represent the groundwater flow process at a site (Anderson and Woessner 1992). The conceptual model is shown in Figure 7.2.

Firstly, a conceptual model is defined as the geological framework that includes thickness, lithology and structure of any aquifers and confining units. Data for the geological framework are typically obtained from geological maps, bore logs, geophysics and additional field mapping. Establishment of the geological framework then permits the hydrological

framework to be defined involving four important steps; (i) identifying the hydrological boundaries, (ii) hydro-stratigraphic units, (iii) preparing a water budget and (iv) defining the flow system.

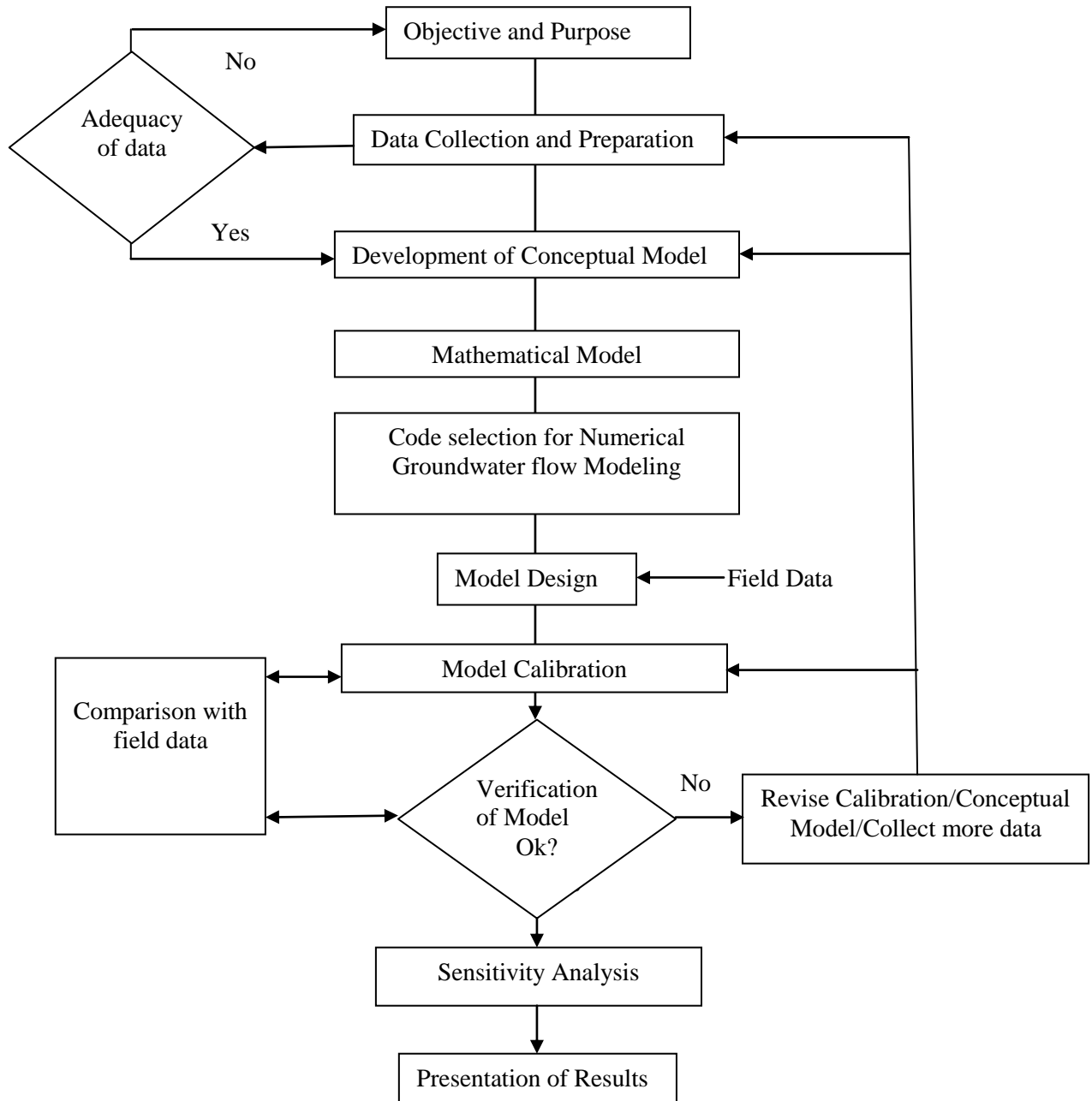


Fig. 7.1: Steps in groundwater flow modeling

The boundaries of a model must be identified first so that all the following steps can proceed within their framework. Boundaries can be either natural hydro-geological boundaries including the surface of the water table, groundwater divides and impermeable contacts

between different geological units, or may need to be unnatural such as cadastral boundaries. The type of boundary selected will depend on the modeling scope and requirements, and affect how the boundaries are represented within MODFLOW, however for simplicity; natural boundaries should be used wherever possible.

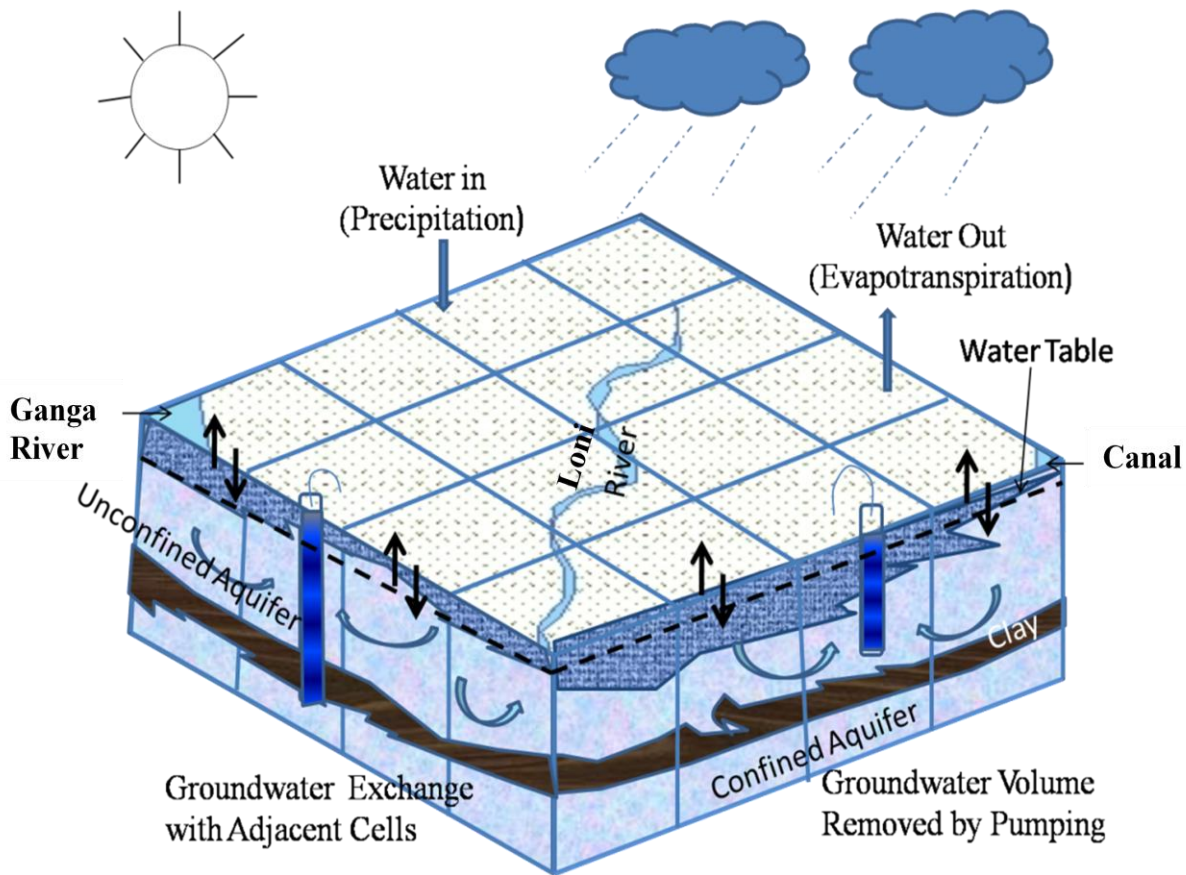


Fig. 7.2: Conceptual model of study area

7.4.1 Grid Designing

Discretisation of the model domain plays an important role in the modeling. The model area is sub-divided into square or rectangular regions called block or cells that are associated with node points. The network of cells or nodes is called as grid. The nodal grid forms the framework of mathematical model. In finite difference approximation method, either block or mesh centered grid technique is used. These techniques refer to the relationships between nodes and grid lines. If head is computed at the center of cell are called block centered approach whereas it is computed at the intersection of lines called as mesh centered approach. To discretise the problem domain, it is necessary to approximate variation of internal properties, boundaries, and stresses of the system.

In the present study, block centered approach has been adopted. The grid has been prepared by importing the boundary shapefile of the desired area. A finite difference grid is designed by manipulating rows, column and layers of cells. The size of grid depends on the availability of data and area. In the current study, the model domain was discretised into 149 columns and 144 rows using the 500 x 500 m grid spacing, resulting in twenty one thousand four hundred fifty six grids cells (Figure 7.3). All the grid cells are not active, cells falling outside the no flow boundaries are designated as inactive cells using IBOUND array in MODFLOW Software. Thus, the active grid cells are eight thousand three hundred eight. These dimensions are reasonable to minimize numerical errors occurred from a variety of sources (Anderson and Woessner, 1992).

Model domain in the vertical direction has been defined in the form of two surfaces (layers). First layer is represents the ground surface. Second layer represents the bottom of the alluvial aquifer. Digital Elevation Model and aquifer thickness map prepared in GIS are import to define the model boundary in Z direction. The model grid in X-Y domain has been shown in Figure 7.3.

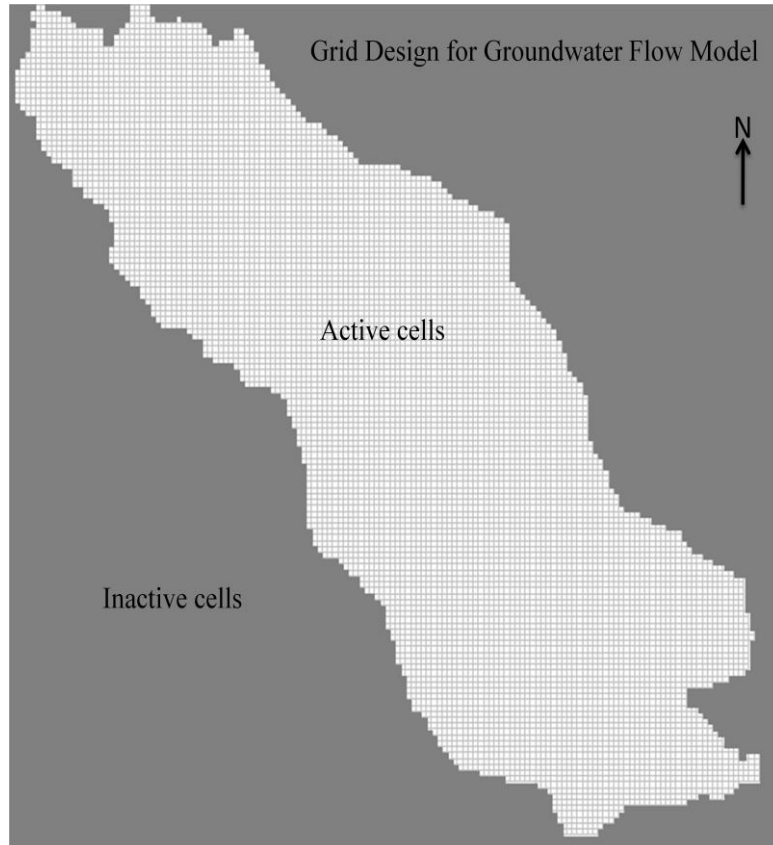


Fig. 7.3: Grid design of groundwater flow model

7.4.2 Time Discretisation

Time discretisation is the time step adopted in the simulation of groundwater flow. In the present study, monthly time step has been used for simulation. Model has been calibrated for eight years period (1997-2004) and validated for three years period (2005-2007). Time discretisation for different input parameters is given in Table 7.1.

Table 7.1: Time discretisation adopted for different parameters

Parameter	Time discretisation
Recharge (Rainfall, Irrigation return flow, canal seepage)	Seasonal
Ganga river (River boundary)	Seasonal
Specified head boundaries	Seasonal
Groundwater withdrawal	Seasonal
Simulation time step	Seasonal
Water zone budget	Seasonal
Piezometric head	Seasonal
Calibration period	8 years
Validation period	3 years

7.4.3 Model Parameterisation

Transmissivity (T) and storage coefficient (S) values are the two parameters which define the physical framework of an aquifer, and control the movement and storage of groundwater. Various aquifer parameters (e.g., hydraulic conductivity and specific yield) can be estimated and assigned to different layers based on previous studies (e.g. Bhatnagar *et al.*, 1982).

7.4.3.1 Hydraulic parameters

For hydro-geological formation, two hydraulic parameters (i.e., saturated hydraulic conductivity (K) and specific storativity or specific yield (S_y) for unconfined aquifer) have been defined on the cell basis using GIS database. Initially, hydraulic conductivity value is taken from the published report of CGWB. These values were assigned to nine distinct zones using the Thiessen Polygon method (Figure 7.4). Thiessen polygon method is used where data points are sparse. The hydraulic conductivity values in the study ranged between 15.75 to 89.22 m/day. The value of specific yield was taken as 0.12 as per GEC guidelines (GEC, 1997) for the entire study area.

7.4.3.2 Groundwater levels

Groundwater level data of 40 wells were collected from Uttar Pradesh State Ground Water Board (UPSGWB) and Central Ground Water Board (CGWB) are used in the study area. Seasonal (pre and post-monsoon) water levels have been obtained for all the wells for a period of 23 years (1985-2007). Rainfall data is available from 1997-2004 only. So groundwater flow modeling is simulated from 1997-2007. Pre-monsoon water levels are measured at the end of May. Post-monsoon water levels are measured at the end of November. Location of observation wells are shown in Figure 6.1.

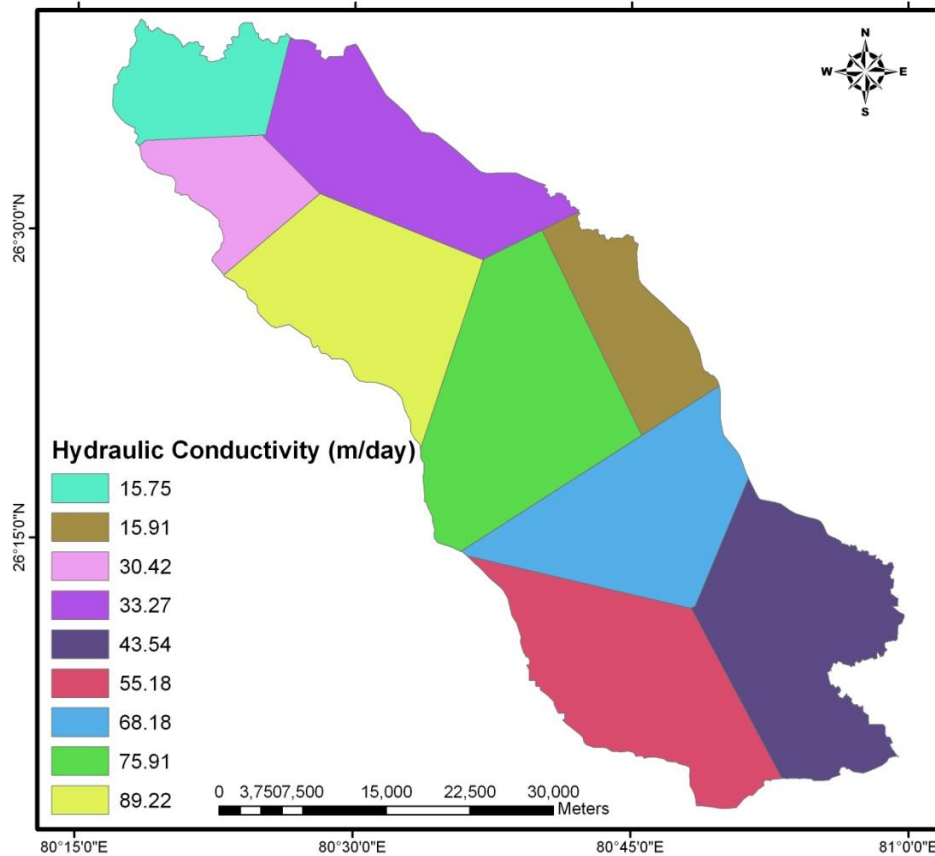


Fig. 7.4: Spatial distribution of hydraulic conductivity of study area alluvial aquifer

Water levels of all wells have been used to prepare the water level contours in GIS both pre and post-monsoon periods. Further, horizontal and vertical distribution of hydraulic heads have been defined throughout the modeled area for beginning (initial condition), equilibrium (steady state condition) and transitional condition using the water level contour of respective time periods. Pre-monsoon water level of year 1997 has been used to define the initial head distribution (initial condition). Water level contours have been supplied from GIS in the form of shapefile. Groundwater level surface has been generated using IDW interpolation technique

to assign the head value on initial model grid. For transient simulation, the initial conditions were the piezometric heads predicted in steady state simulation. Groundwater level of observation wells located in the study area has been used for calibration (transient state) and validation of model.

7.4.3.3 Groundwater recharge & withdrawal

Groundwater is recharged from many sources, such as rainfall recharge, Irrigation return flow (IRF) and canal seepage. Groundwater withdrawal depends on number of wells, tube wells and pumpage time. All the above recharge and withdrawal have been calculated on the basis of GEC guidelines and detailed methodology of recharge and withdrawal calculation is already described in chapter 6.

7.4.3.4 Boundary conditions

To obtain a solution of groundwater flow equation of an area, boundary conditions must be specified along the entire boundary of three dimensional flow domains. Three boundary conditions can be applied to cells in a finite difference grid such as MODFLOW including (a) Dirichlet, (b) Neuman, and (c) Cauchy.

(a) Dirichlet condition: the head at the boundary is known, examples are the water table in an unconfined aquifer, or a river or lake in contact with an unconfined aquifer, all under steady state conditions. Dirichlet conditions are also used when simulating unnatural boundaries such as cadastral boundaries of a hydro-geological system which are often defined for the purposes of the modeling investigation. In a natural hydro-geological system an aquifer may continue onwards past the boundary and therefore must be accounted for by placing a fixed or specified head cell or cells, in which the allocated head is known. All applications of Dirichlet boundaries require some form of head measurement on or very near the boundary.

(b) Neuman condition: the flux across a boundary is known, examples include no flow boundaries between geological units, interactions between groundwater and surface water bodies, spring flow, underflow, and seepage from bedrock into alluvium. The simulation of Neuman boundaries requires the measurement or estimation of one of the above fluxes, which is often inaccurate. The most commonly applied form of a Neuman boundary is a no-flow or impermeable boundary, often occurring between a highly permeable unit and a unit of much lower permeability. A difference in hydraulic conductivity of two orders of magnitude or

greater between two adjacent units can be used to justify the placement of a no-flow boundary (Anderson and Woessner 1992).

(c) *Cauchy condition*: the flux across the boundary is dependent on the magnitude of the difference in head across the boundary, with the head on one side of the boundary being input to the model and the head on the other side being calculated by the model. Examples of a Cauchy boundary include leakage from a surface water body where the flux is dependent on the difference in elevation between the surface water and groundwater level and the vertical hydraulic conductivity of the boundary; and evapo-transpiration where the flux is proportional to the depth of the water table in an unconfined aquifer. A Cauchy boundary has the advantage over a Neuman boundary in that its flux can be calculated by the model if given sufficient input data.

7.4.3.5 Time step

Time step selection for numerical computation is purely based on the purpose of study, data availability and the desired accuracy. In the present study, one year period is divided into two seasons (monsoon and non-monsoon) for groundwater modeling. Seasonal time step has been adopted for defining the initial and boundary conditions.

7.4.3.6 Tolerance criteria

The selection of tolerance level (i.e., convergence and model termination) depends upon the acceptable standards of accuracy in the results. The adoption of large convergence threshold leads to relatively less accurate results. On the other hand, small threshold will increase the computational time. In the present investigation, WHS solver has been used for solving the governing partial differential equations. Maximum number of inner and outer iteration, head change in successive iteration, residual, relative residual criteria have been used as the convergence thresholds. Details adopted are presented in Table 7.2.

7.5 DIRECT AND INVERSE PROBLEM

Simulations of the aquifer response to a deterministic pattern of stresses (groundwater withdrawal and recharge) are known as direct problem (Figure 7.5 a) in groundwater hydrology. To simulate the response of aquifer, appropriate initial and boundary condition are imposed with known aquifer parameters. To carry out this type of study, transmissivity (T) and storage coefficient (S)/specific yield (S_y) are required.

Table 7.2: Convergence threshold adopted in solver (WHS)

S. No.	Tolerance criteria	Threshold value
1.	Maximum number of outer iterations	50
2.	Maximum number of inner iterations	100
3.	head change between successive iterations	0.01 m
4.	Residual	0.01 m
5.	Relative residual	0.00 m

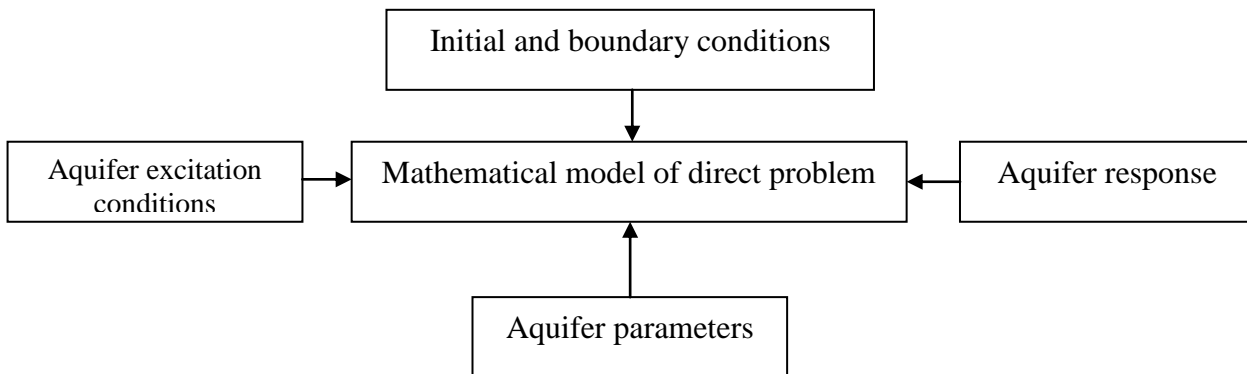


Fig. 7.5 (a): Direct problem in groundwater hydrology

Pumping test is most popular method that is used for estimating these parameters. It involves generating the aquifer response to the pumping in a single well. The generated data are analyzed to arrive at the estimate of aquifer parameters. The aquifer parameters so obtained represent only that portion of the aquifer which lies within the radius of influence of the well used for the test pumping.

Another approach for estimating S_y and T , known as inverse problem, is to employ the historical data of aquifer response and the corresponding aquifer excitations (Figure 7.5 b). The aquifer excitations can be either in the form of vertical acceleration (pumping or recharge) or change in boundary conditions. The model is first calibrated against historical data. The calibration process invariably requires adjustment in the aquifer parameters. The estimation of these parameters is thus an inverse problem where in these parameters are calculated from the historical excitations response and the associated initial and boundary condition data. The system in this case is represented by the equation correlating the response to excitation.

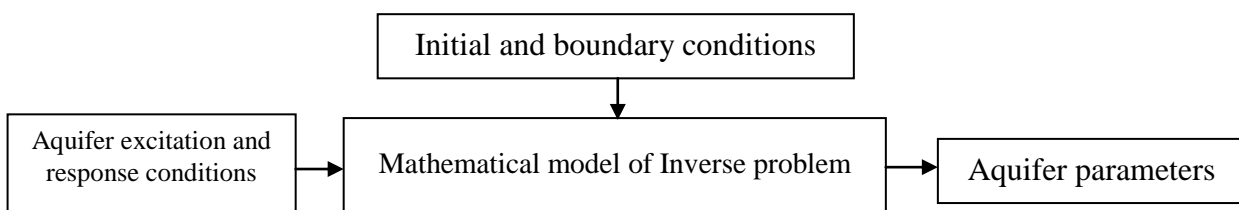


Fig. 7.5 (b): Inverse problem in groundwater hydrology

7.6 CALIBRATION OF GROUNDWATER FLOW MODEL

Model calibration is the process of modifying one or more model parameters until the results of the simulation match the measured data. Calibration of an inverse problem involves modifying the boundary conditions, hydraulic properties etc until the simulated values closely match the observed values, typically the case with real world hydro-geologic systems. Calibration of a forward problem involves working from an existing set of boundary conditions, hydraulic properties and stresses to estimate heads, which is usually the case with a theoretical system (Anderson and Woessner, 1992). This study uses an inverse problem. A steady state calibration is performed to water levels that represent steady state conditions, such as long term mean water levels, mean annual water levels, or mean seasonal water levels for a particular season. Transient calibration is performed to water levels that represent the aquifer's response to stresses such as recharge and extraction over time, and consequently it is essential to have some handle on the magnitude of these fluxes for the duration of the modeling period in order to achieve accurate calibration.

Two methods may be employed to reduce the non uniqueness of the calibrated solution. Firstly, the model should be calibrated with field measured parameters, e.g., aquifer properties determined from pumping tests. Secondly the model should be calibrated to multiple distinct hydrological conditions, to demonstrate that the parameters chosen are capable of reproducing the system behavior under different hydrological stresses. The different hydrological conditions used can be natural such as a dry period and a wet period, or artificial such as variable extraction (Murray Darling Basin Commission, 2000).

To qualitatively gauge the efficiency of the calibration, contour plots of heads may be constructed. To quantitatively assess the calibration, the difference between observed and calculated heads, otherwise known as residuals, may be compared graphically and statistically. When the mean of the residuals is reduced to as close to zero as possible and the standard deviation is reduced as much as possible, the model is calibrated. Plots of observed and calculated heads over time can be used to graphically compare the differences between the two head datasets during the course of the model simulation. The calibration should also be evaluated by a standard statistical method such as the Root Mean Square (RMS) error, which is the average of the squared differences in measured and simulated heads.

In the present study model is calibrated using PEST (Parameter Estimation) module of PMWIN that is developed by Dr. Jhon Doherty (Doherty, 1994). Model has been calibrated for both steady state and transient state. Initially, model is calibrated for steady state to verify the aquifer parameters obtained from various sources. Finally, modeled is calibrated for transient state (for a duration of 8 years, 1997-2004) using the narrow range of aquifer parameters obtained from various agencies and verified from steady state calibration. Further, model results have been validated corresponding to the observed data of three years (2005-2007). Further, validated model has been used for the prediction of groundwater response under different excitation/stresses.

7.6.1 Parameter Optimization using PEST

The PEST is a non- linear parameter estimation program which is used for estimation of parameter (Doherty, 1994) by inverse modeling approach. The Gauss-Marquardt-Levenberg algorithm (Levenberg, 1944; Marquardt, 1963) is used in PEST for parameter optimization.

PEST is supplied with initial values of the parameters to be optimized and the set of observations, which PEST can compare with the model outputs. Initially, PEST executes the given initial parameter values and outputs are compared with the given set of observed data and estimate the objective function. Then the PEST starts minimizing the objective function by adjusting parameters. In case of linear models, generally optimization can be achieved in one step while non-linear models required iterative process to optimize its parameters. At the beginning of the each iteration process the relationship between model parameters and model generated outputs are linearised to obtain currently estimated best parameter set. Then it is solved for a better parameter set and this new set of these parameters are tested again by running the model. Then the code compares the objective function of the current iteration with the previous one and decides whether it is worth undertaking iteration (Doherty, 1994). The procedure of automatic calibration is shown in Figure 7.6.

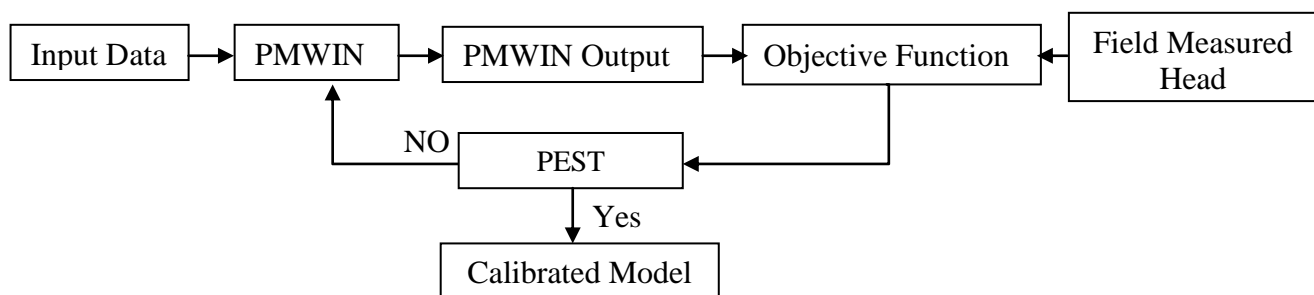


Fig. 7.6 Steps in automatic calibration

Automatic calibration yield results, not only parameter estimates and heads simulated for the model, but also confidence intervals for both the estimated parameters and the heads, which are convenient for conveying the reliability of the results to regulators. Sensitivities, parameter standard deviations and correlations, and prediction standard deviations can be used to evaluate whether model parameter estimates and predictions are reliably calculated with the available data and what additional data could be most useful in improving the model. Moreover, benefits of PEST include expedited determination of best fit parameter values and quantification of the quality of calibration, confidence limits on parameter estimates and predictions. Further, the inverse modeling has an ability to automatically calculate parameter values that produce the best fit between observed and simulated hydraulic heads. Knowing that the parameter values are producing the best possible fit for a given conceptual model is crucial to the conclusive comparison of alternative models.

7.6.2 Calibration Parameters

For a ground water model, the calibration parameters may include hydraulic conductivity and storage capacity of the porous media. In the present study, saturated hydraulic conductivity, specific yield and recharge (rainfall recharge, irrigation return flow and canal seepage) factors have been taken for calibration. The study area has been divided into various zones of homogeneous hydraulic parameters, and selected parameters have been calibrated for each defined zones. Model was run several times with different initial values of selected parameters, as given in Table 7.3. Initial values of hydraulic parameters have been taken from CGWB report.

Table 7.3: Range of initial values of hydraulic parameters used in the calibration process

Formation	Hydraulic conductivity (m/day)				Specific yield (for initial, lower and upper limit)	
	Initial		Lower limit	Upper limit	From	To
	From	To				
Alluvium	11	99	1	100	0.001	0.12

7.6.3 Control Parameters of PEST

Calibration process has been controlled in the "WINPEST" by defining the different parameters related to Marquardt lambda, parameter change constraints and termination criteria. Limiting values of these parameters have been adopted as suggested by Doherty (1994). Different controlling parameters adopted in the present study for the calibration of groundwater model have been presented in Table 7.4.

Finally, the model is calibrated in transient state from year 1997-2004 using the narrow range of aquifer parameters obtained from various agencies and verified from steady state calibration. Further, model results have been validated corresponding to the observed data of three years (2005-2007). Validation of hydraulic parameters have been used for further analysis

7.6.4 Statistical Approach for Error Criteria

Calculating the error associated with each target (head, drawdown, concentration, flux) and then computing simple statistics on the population targets will be useful in evaluating the merits of calibration. The error is called residuals, and it is the difference between observed and simulated target value. Negative residuals means the model is calculating the dependent values too high and positive residual means too low. The type of statistics computed could include the following:

- i. *Mean Error (ME)*: It is the mean of difference between observed and calculated heads

$$ME = \frac{1}{n} \sum_{i=1}^n (h_o - h_c)_i \quad (7.4)$$

- ii. *Mean Absolute Error (MAE)*: It is mean of absolute value of the difference between observed and calculated heads.

$$MAE = \frac{1}{n} \sum_{i=1}^n |(h_o - h_c)_i| \quad (7.5)$$

- iii. *Root Mean Square (RMS) error*: It is the average of the squared differences between observed and calculated heads.

$$RMS = \left[\frac{1}{n} \sum_{i=1}^n (H_o - H_c)_i^2 \right]^{0.5} \quad (7.6)$$

where

n = number of model observations

h_o = observed head for each observation

h_c = calculated head for each observation

Table 7.4: Initial setting is used in Parameter Estimation (PEST) calibration

S. No.	Parameter	Value
1.	Initial lambda	10.0
2.	Lambda adjustment factor	2.0
3.	Sufficient new/old phi ratio per optimisation iteration	0.3
4.	Limiting relative phi reduction between lambdas	0.01
5.	Maximum trial lambdas per iteration	8
6.	Maximum relative parameter change (relative-limited changes)	10
7.	Maximum factor parameter change	10
8.	Fraction of initial parameter values used in computing change limit for near-zero parameters	0.001
9.	Relative phi reduction indicating convergence	0.01
10.	Number of phi values required within this range	3
11.	Maximum number of consecutive failures to lower phi	3
12.	Negligible relative change	0.01
13.	Maximum “no change” iterations	3
14.	Overall iteration	50

7.6.5 Steady State Simulation

In a steady state groundwater model, all flows in and out of the model are equal, and there is no net change in storage; consequently no storage terms are required in the input parameters. A steady state model may be run for different times and the outcome will be the same as time is irrelevant under steady state conditions.

Steady state simulated hydraulic heads were used to calibrate the model with the measured hydraulic heads distribution serving as the basis for comparative evaluation. The hydraulic heads of June 1997 (pre-monsoon period) from 40 observation wells were used as initial condition for steady state simulation. The hydraulic heads show a stable trend over this steady state period. Initially, steady state calibration has been done manually to know the modeling mechanism and afterwards PEST module of PMWIN model has been used by using the criteria shown in Table 7.3 for calibration. After the calibration, simulations were carried out to evaluate the sensitivity of the model results to variation in hydrologic parameters and modeling assumptions.

Initially, model is calibrated for steady state condition for one year period (June 1997 to June 1998) to verify the range of hydraulic parameters (for aquifer). Model is calibrated corresponding to pre-monsoon groundwater levels of year 1997. It is run several times for different conditions i.e., initial value of calibration parameters. In the calibrated run, most of the wells had compatibility with reference to observed and calculated heads. Hydraulic

parameters have been found within the range of reported values for similar hydro-geological formations. Figure 7.7 shows a map of the spatial distribution of the measured and simulated heads. Simulated head which is higher than the measured head indicates residual less than zero and simulated head which is lower than the measured head indicates residual greater than zero. The scattergram of the model output shows a comparison between the observed and calculated hydraulic heads about the line to perfect fit (Figure 7.8). The final calibration shows a reasonable agreement between observed and calculated heads.

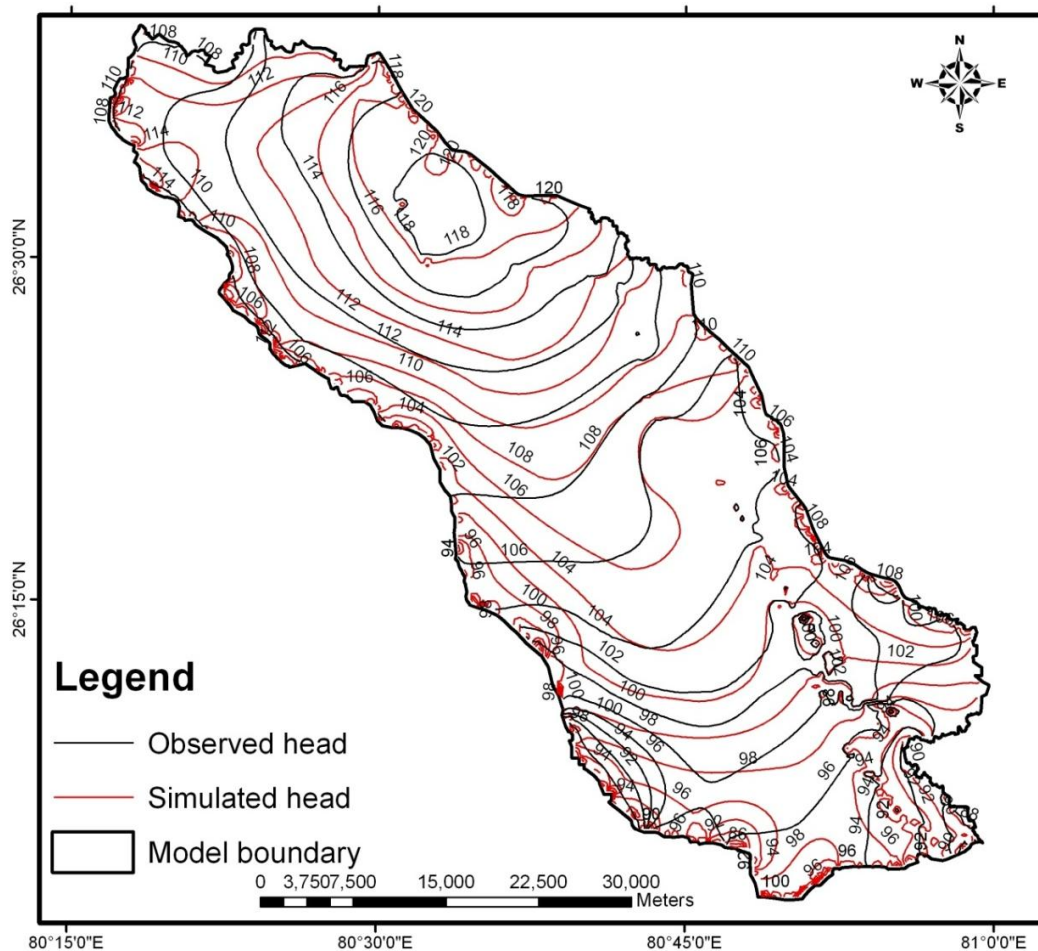


Fig. 7.7: Equipotential map of simulated and observed hydraulic heads

7.6.6 Transient State Simulation

After checking the stability of the model in steady state simulation and by knowing the range of hydraulic parameters, one can go for the transient state. A transient groundwater model simulates the stresses on an aquifer over time, and is therefore divided into stress periods which are further divided into time steps. The number of stress periods can be input by the user and should reflect any temporal stress on the aquifer, such as recharge or extraction. Initial

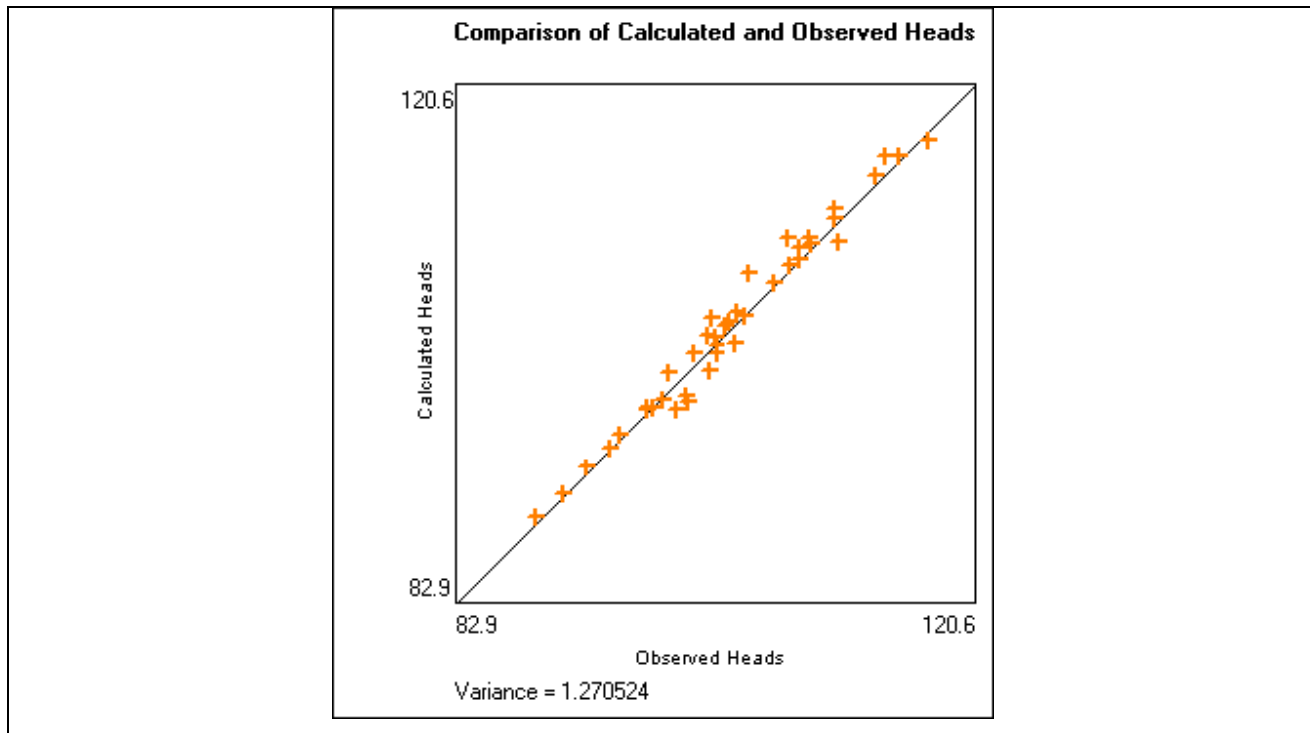
hydraulic heads must be input before running the simulation. In transient state, heads are the result of a steady state simulation. Heads at fixed head cells must be real values, and therefore should be interpolated from the nearest observation bore well. Model calibration should include comparisons between model simulated conditions and field conditions for hydraulic heads, groundwater flow directions, and water mass balance. Further, calibration process can be judged using various criteria, which include residual mean (difference between observed and calculated heads), absolute residual mean, root mean square error, and correlation coefficient determined for the simulated versus observed hydraulic heads as shown in Figure 7.9. At the end, calibration statistics is generated, which includes different criterion to judge the calibration quality.

Groundwater flow model has been calibrated in transient state for a period of 8 years (1997-2004). Calibration has been performed in several trials with different initial values of calibration parameter (Table 7.3). Accuracy has been judged by comparing RMS error, residual mean and absolute residual mean.

Calibration statistics has been generated at seasonal time steps. Parameter optimization algorithm has been run several times with different set of initial, lower and upper bounds of calibration parameters to check the consistency of the calibration process and to eliminate the chance of over calibration. The over-calibration is stage at which results in a model appears to be calibrated but has been based on datasets that is not supported by field data i.e., not within the range of reported values. In the present study, over calibration has been restricted by placing the lower and upper bounds of the calibration parameters for each zone separately.

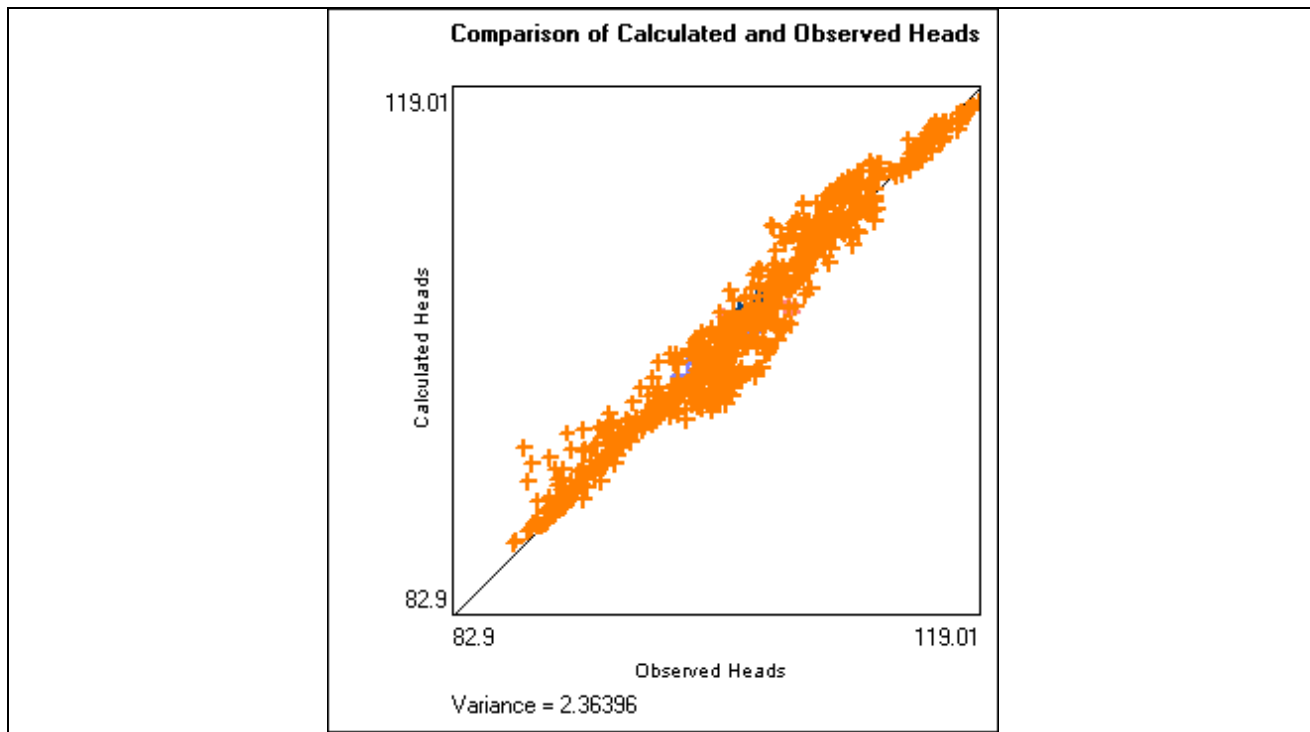
The calibrated and validated statistics for different time steps are shown in Figure 7.10. The RMS error has been found in a range of 1.24 m to 1.63 m throughout the calibration period, which is unacceptable range. Residual mean has been found to lie within range of -0.49 m to 0.49 m, absolute residual mean within a range of 0.9 m to 1.25 m throughout the calibration period. Further, average calibration errors have been determined and presented in Table 7.5.

Average value of RMS error of calibration has been found to 1.47 m, which is within satisfactory range. Average absolute mean residual and mean residual has been found to be 1.07 m and 0.14 m.



Number of wells	40	M.E.	-0.32 (m)
M.A.E	0.88 (m)	R.M.S.E	1.127 (m)
R²	0.975		

Fig. 7.8: Scattergram between observed and calculated heads, steady state simulation



Number of wells	40	M.E.	0.01 (m)
M.A.E	1.10 (m)	R.M.S.E	1.53 (m)
R²	0.953		

Fig. 7.9: Scattergram between observed and calculated heads, transient state simulation

Table 7.5 Average errors of calibration and validation time periods

Stage	Period (Days)	RMS (m)	MAE (m)	ME (m)
Calibration (1997-2004)	0 - 2920	1.47	1.07	0.14
Validation (2004-2007)	2920 - 4015	1.66	1.20	-0.33
Whole period (1997-2007)	0 - 4015	1.52	1.11	0.01

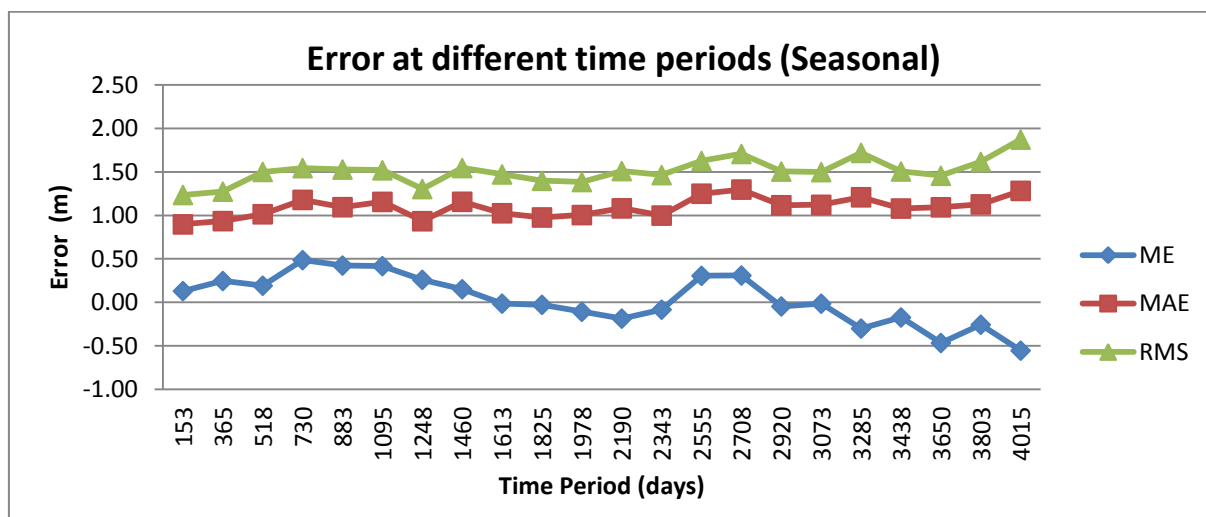


Fig. 7.10: Errors (seasonal) during the calibration period (0-2920 days) and Validation period (2920 – 4015 days)

Further, simulated and observed water table elevations have been compared over the entire calibration and validation period. Simulated and observed water table elevations are shown in figures 7.11 (a) to 7.11 (u). Results indicated that a good match occurs between observed and predicted groundwater levels. In the beginning, water levels were not matching well, which may be due to the effect of initial unsteady state conditions because of the initial hydraulic head adopted at the beginning of calibration.

7.7 VALIDATION OF GROUNDWATER FLOW MODEL

A calibrated model uses defined value of hydro-geological parameters and boundary conditions to match with the field conditions for specific time periods. In addition, the model was verified with the historical data.

In the present study, calibrated model has been validated over a period of three years (2005-2007) to further check its consistency. Calibrated model has been used to simulate the aquifer under stressed conditions i.e., with new set of data (stresses and boundary conditions). Aquifer parameter and recharge factor have been kept constant during the process.

Further, various error statistics have been generated along with the simulated groundwater levels. Average RMS error has been found to be 1.65 m and average absolute mean residual has been found to be 1.2 m (Table 7.5). Validation results (Figures 7.11 (a) to 7.11 (u)) reveal that there is a good agreement between simulated and observed groundwater levels, and there is as such no need for further calibration or refinement. As model has successfully reproduced the measured changes in field conditions, for both calibration and validation (history matching) time periods, it is ready for prediction the future scenario. Further, the velocity vectors of the groundwater also confirm the model calibration condition.

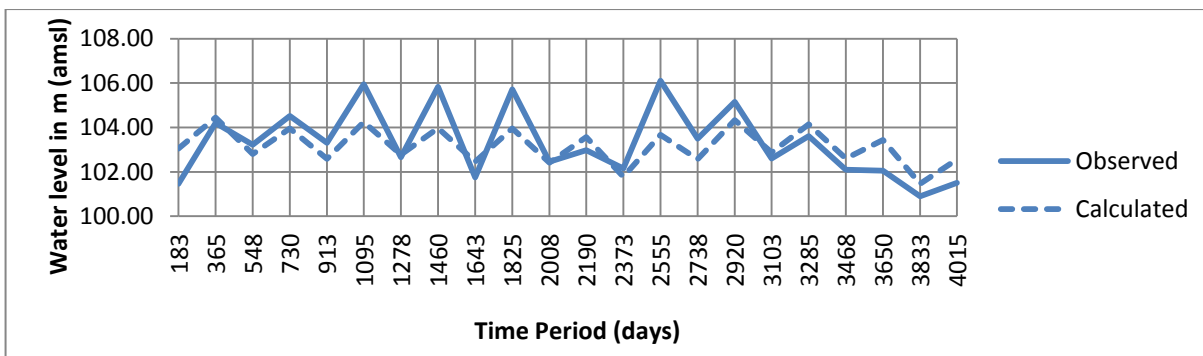


Fig.7.11 (a): Groundwater level elevations for Ajabkhera well after calibration and validation

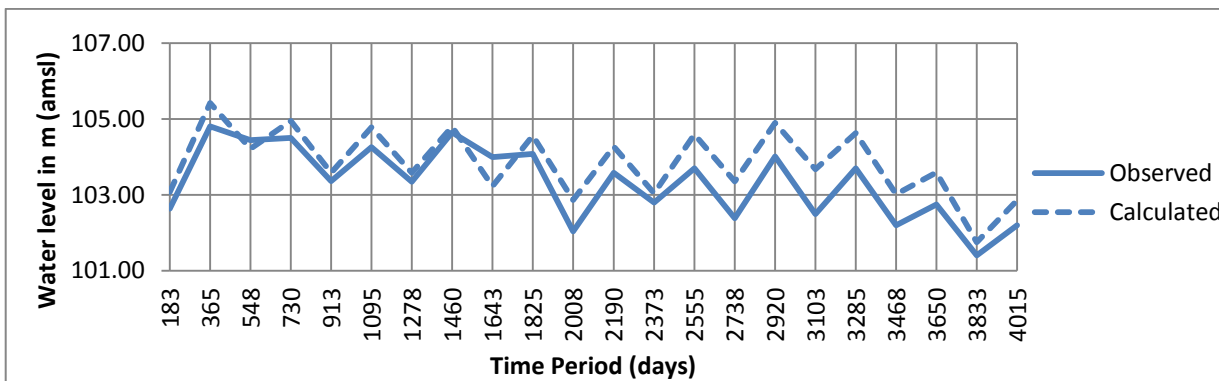


Fig. 7.11 (b): Groundwater level elevations for Asgarganj well after calibration and validation

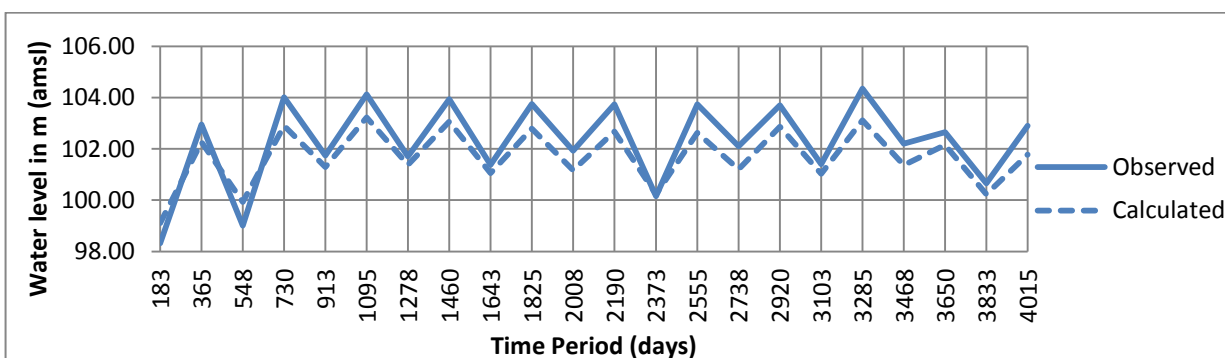


Fig. 7.11 (c): Groundwater level elevations for Babu Khara well after calibration and validation

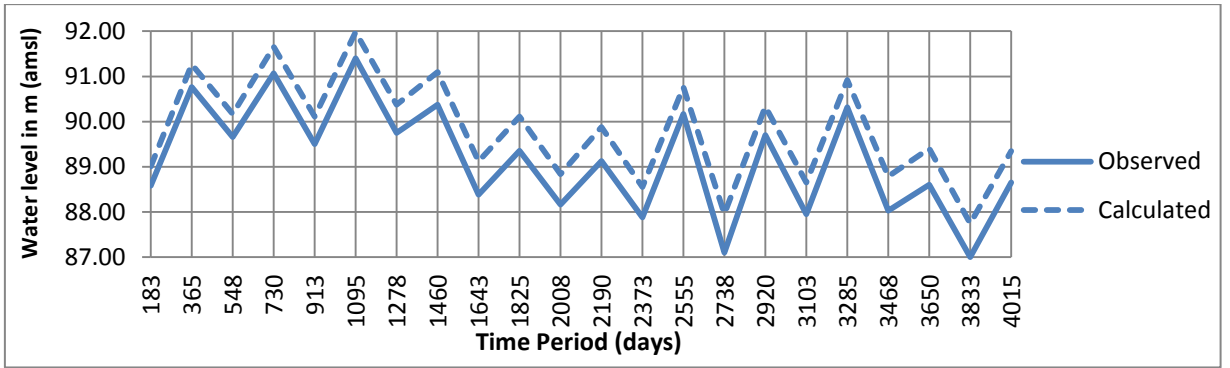


Fig. 7.11 (d): Groundwater level elevations for Baksar well after calibration and validation

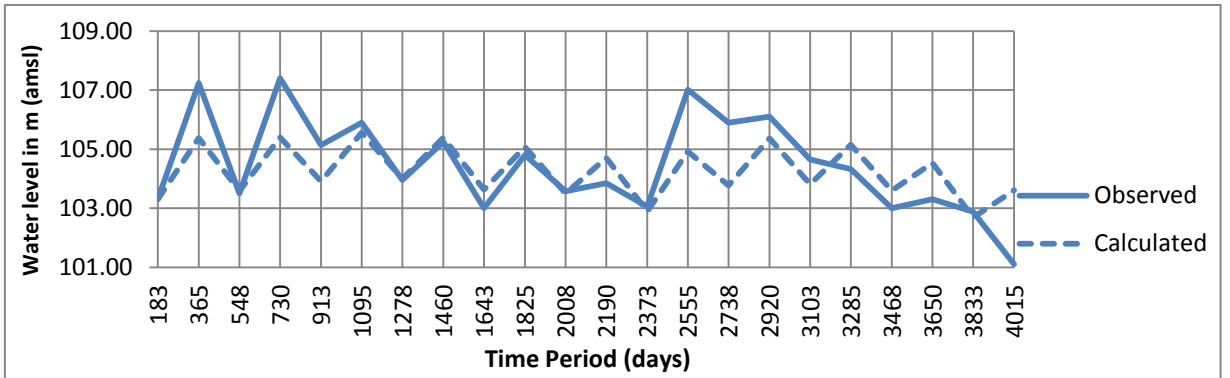


Fig. 7.11 (e): Groundwater level elevations for Bara well after calibration and validation

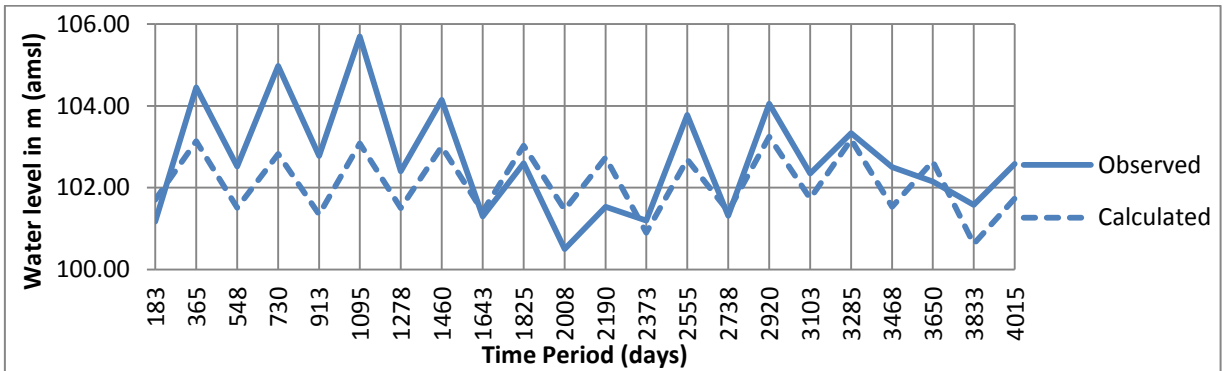


Fig. 7.11 (f): Groundwater level elevations for Bhagwant Nagar well after calibration and validation

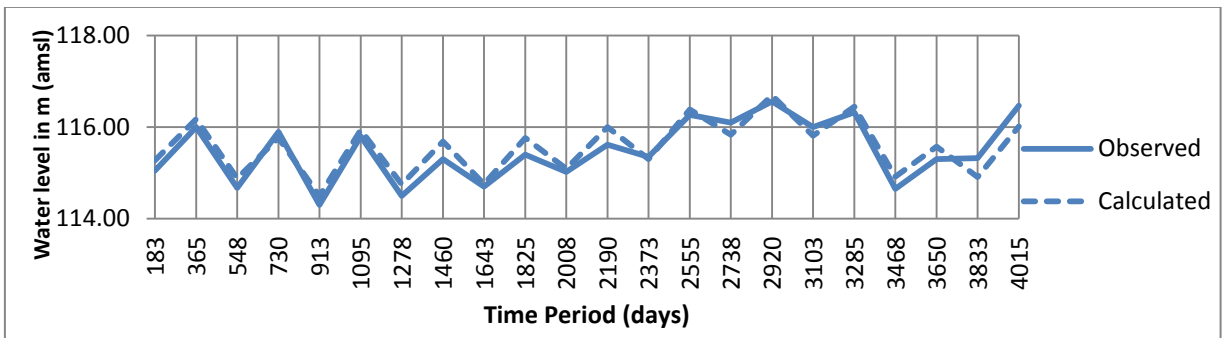


Fig. 7.11 (g): Groundwater level elevations for Bichhiya well after calibration and validation

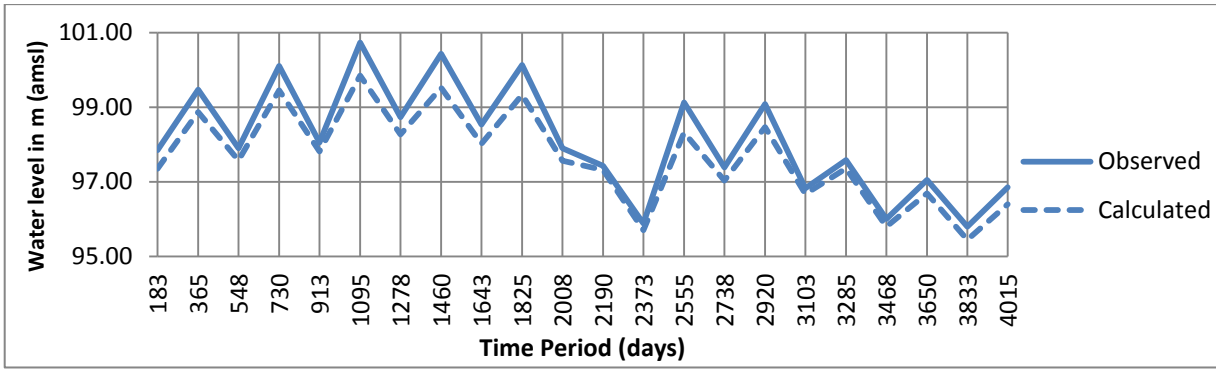


Fig. 7.11 (h): Groundwater level elevations for Chanda well after calibration and validation

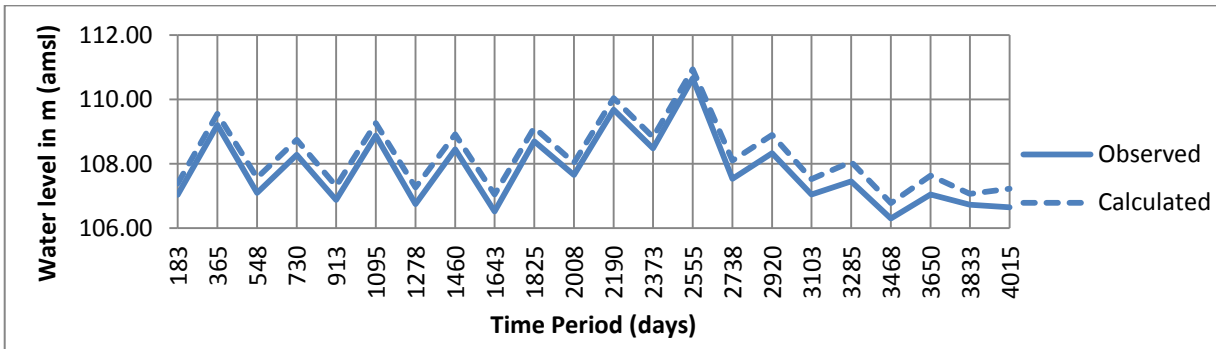


Fig. 7.11 (i): Groundwater level elevations for Gangaghat well after calibration and validation

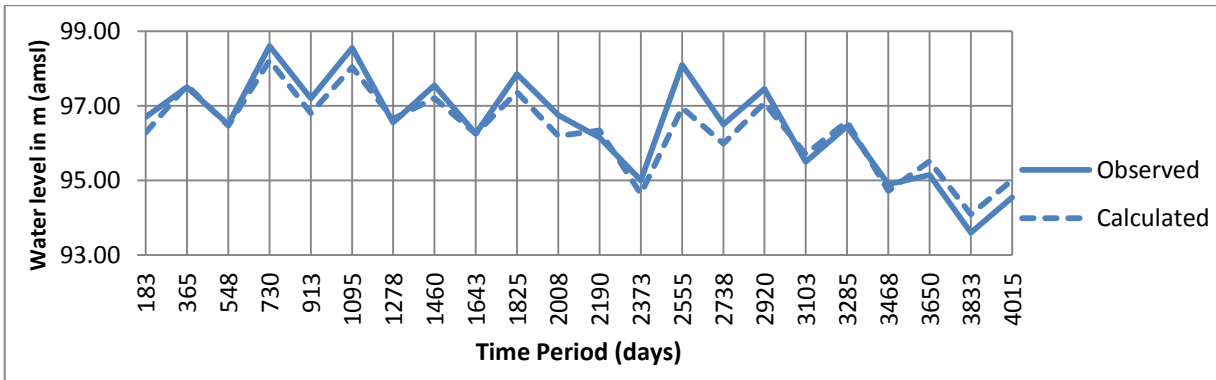


Fig. 7.11 (j): Groundwater level elevations for Lalganj Piezo well after calibration and validation

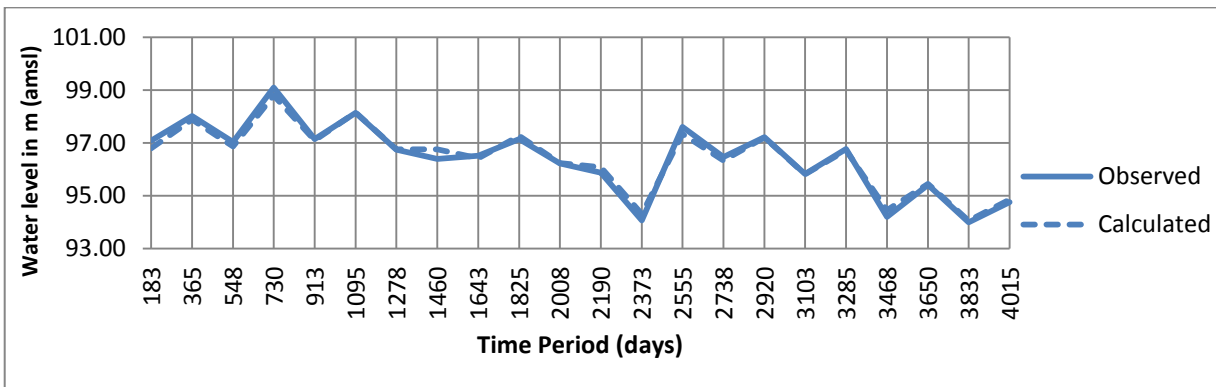


Fig. 7.11 (k): Groundwater level elevations for Lalganj-2 (OW) after calibration and validation

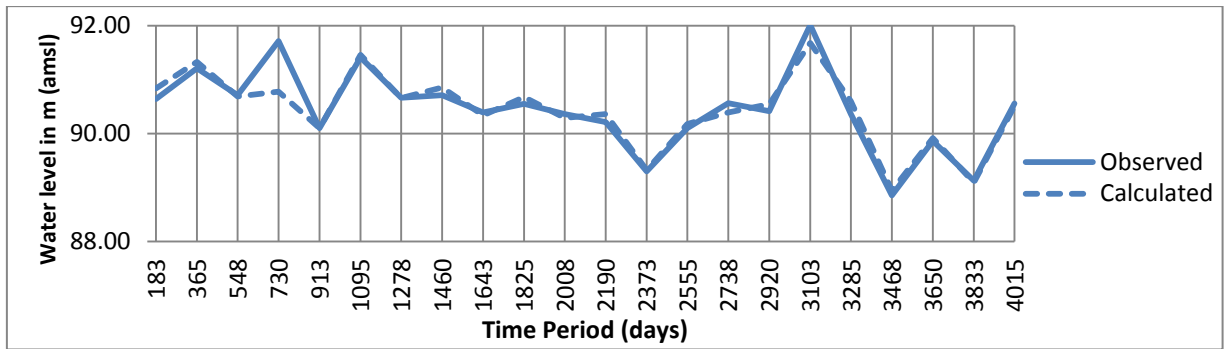


Fig. 7.11 (l): Groundwater level elevations for Paliyaveer Singhpur well after calibration and validation

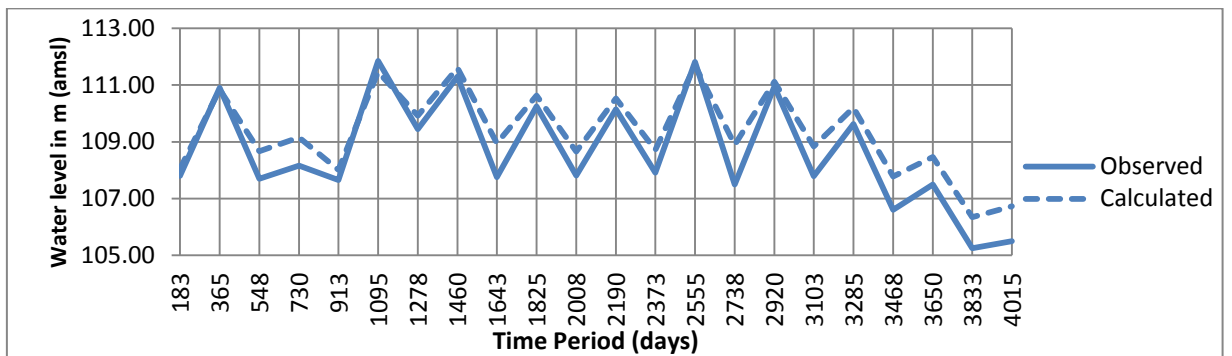


Fig. 7.11 (m): Groundwater level elevations for Pariyar well after calibration and validation

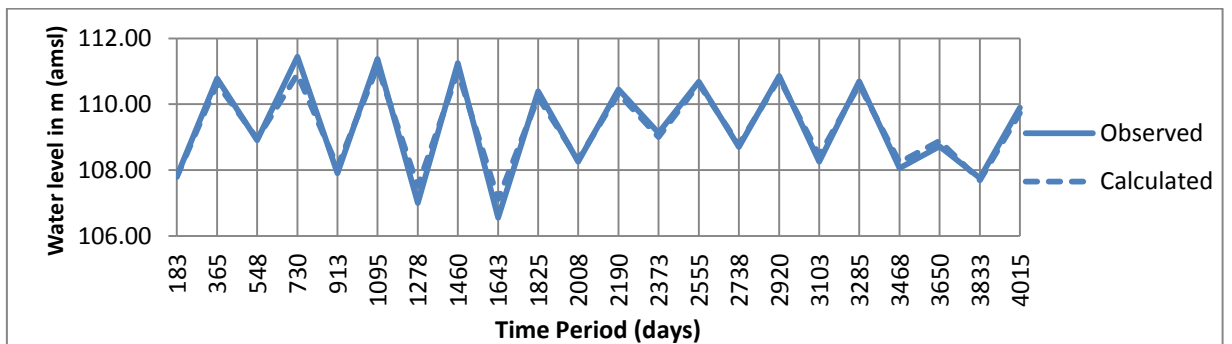


Fig. 7.11 (n): Groundwater level elevations for Purwa well after calibration and validation

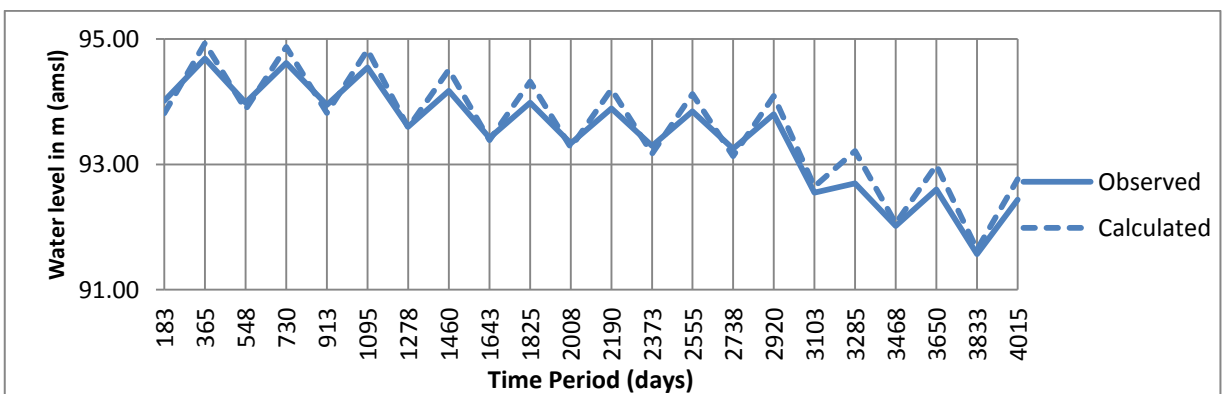


Fig. 7.11 (o): Groundwater level elevations for Ralpur well after calibration and validation

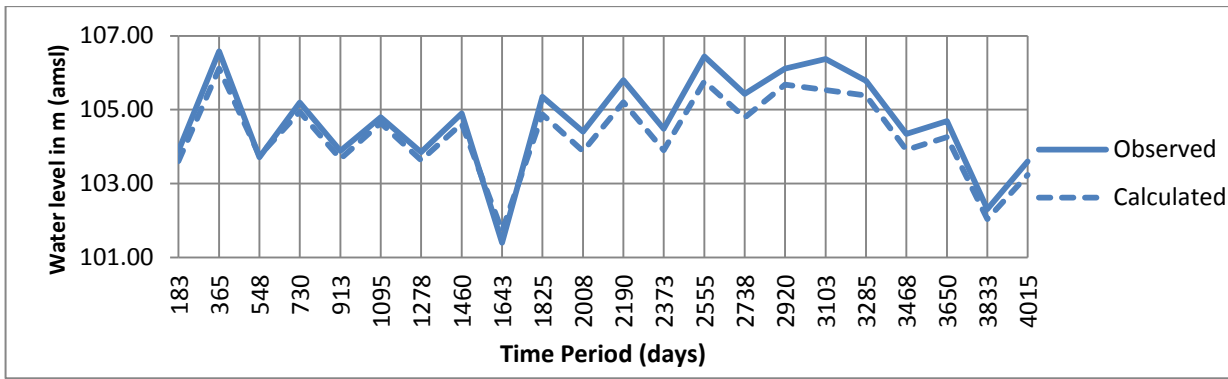


Fig. 7.11 (p): Groundwater level elevations for Saraiya well after calibration and validation

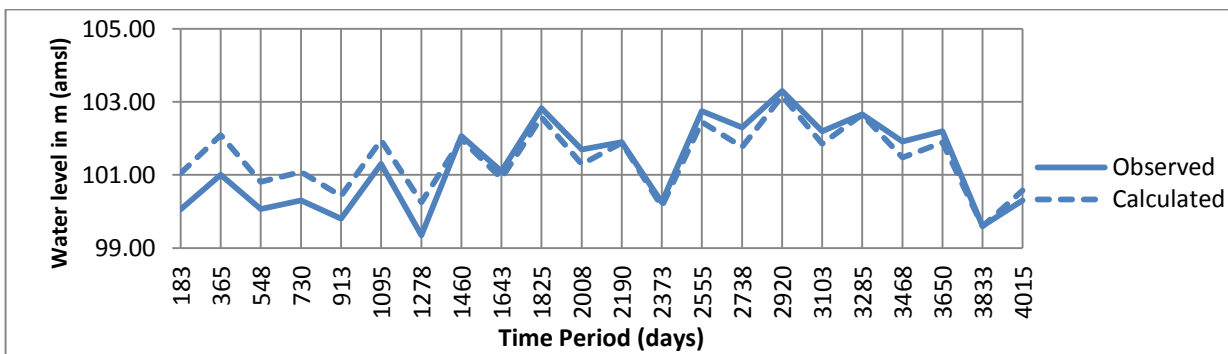


Fig. 7.11 (q): Groundwater level elevations for Sumerpur well after calibration and validation

7.8 RESULTS AND DISCUSSIONS

7.8.1 Calibrated Aquifer Parameter & Recharge

After calibration and validation of the model by observing the calibrated aquifer parameters, hydraulic conductivity values lies between 15.4 and 93.1 m/day in the area (Figure 7.12). Specific yield is in the range of 0.002 to 0.12 in different zones of area (Figure 7.13). Spatial distribution of calibrated hydraulic conductivity and specific yield has been used in GIS by exporting the modeling data into raster format.

7.8.2 Sensitivity Analysis

The purpose of sensitivity analysis is to quantify the uncertainty in the calibrated model caused by the estimate of the aquifer parameters, stress and boundary conditions. During this analysis, the calibrated value for the aquifer parameters and the boundary conditions are systematically changed with plausible range (Anderson and Woessner, 1992). The purpose of sensitivity analysis is to observe the model response to variation in uncertain parameters. The results can be used to identify sensitive input parameters for the purpose of guiding for the calibration.

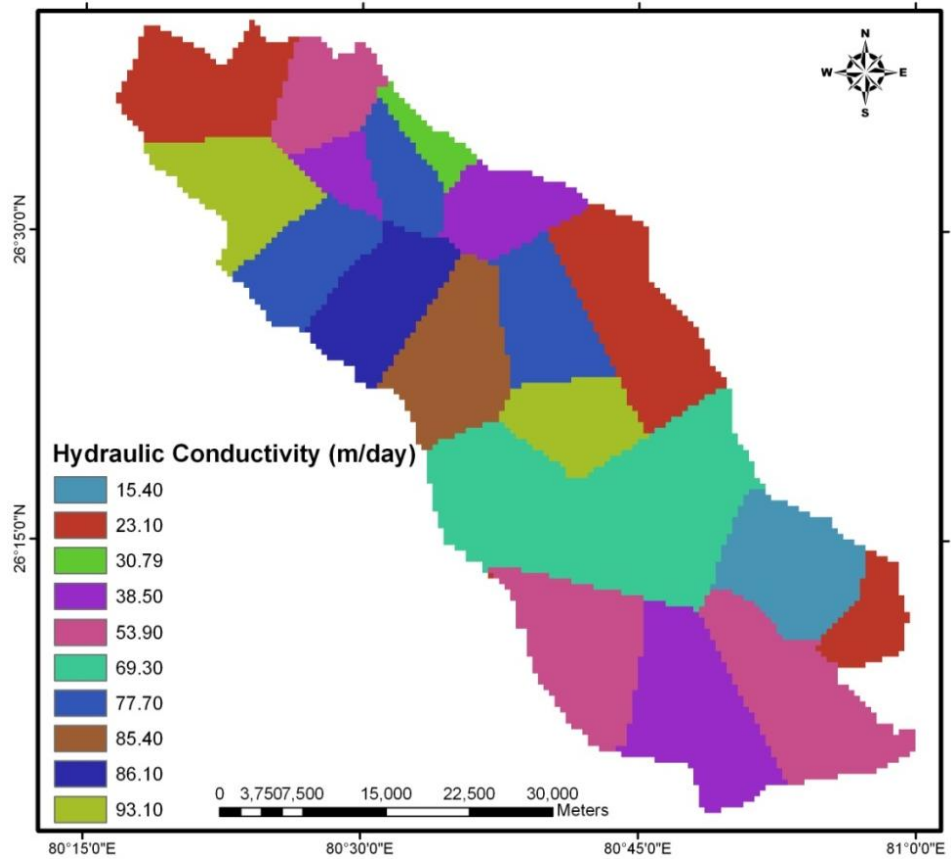


Fig. 7.12: Calibrated hydraulic conductivity of study area

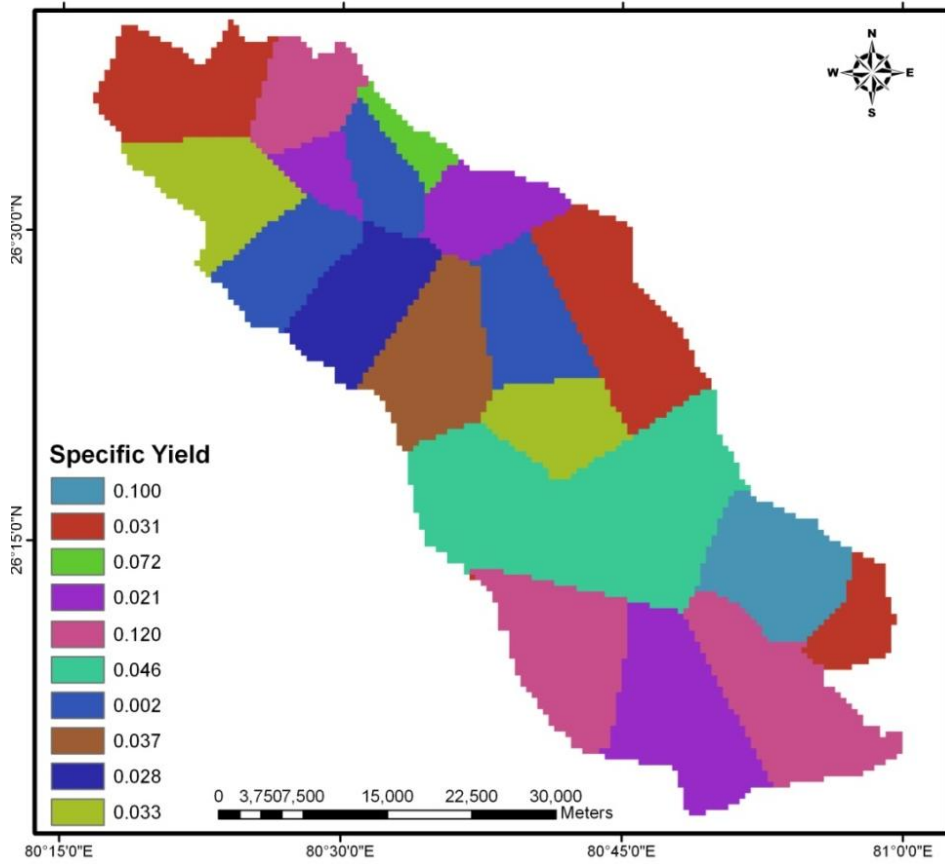


Fig. 7.13: Calibrated specific yield of study area

Hydraulic conductivity, storage parameters (specific yield) and recharge were selected as the most uncertain parameters. Sensitivity of the model was evaluated by ME, MAE and RMSE, after multiplying each parameter a time by a factor 0.2 to 1.8 of the initial value and running the model. The ME, MAE and RMSE related to each run were plotted against the multiplying factor are shown in Figures 7.14 to 7.16. The model has been found to be more sensitive to recharge and hydraulic conductivity as compared to specific yield, as indicated by the relative mobility in the mean errors between the mean errors corresponding to calibrated values. Errors have been tabulated in Tables 7.6 to 7.8. Changes in error with respect to change in aquifer parameters are shown in Figures 7.14 to 7.16.

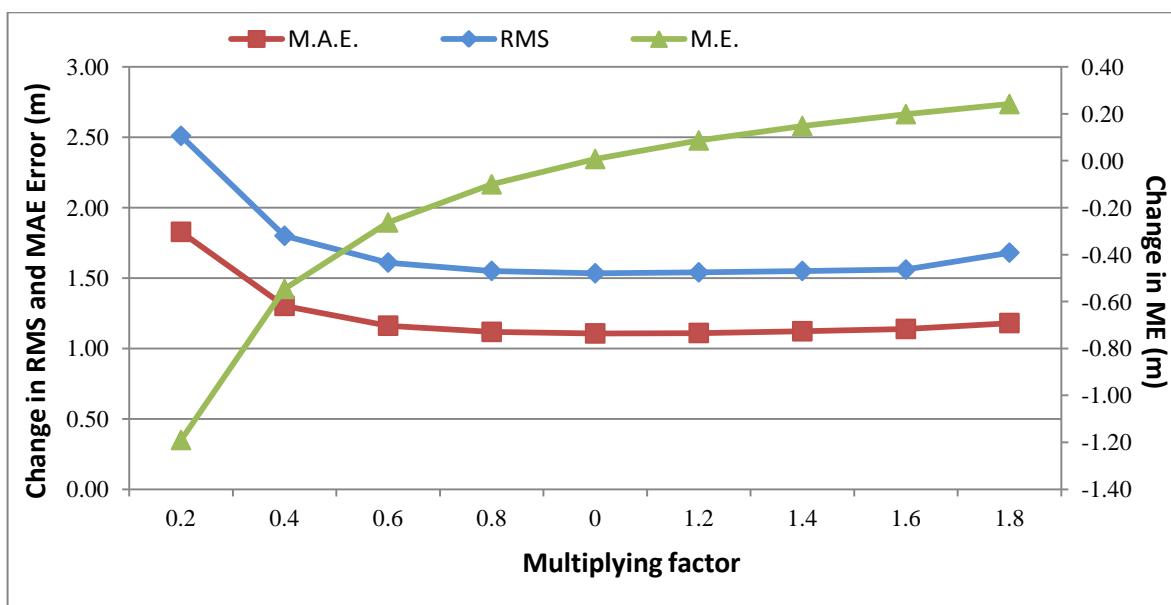


Fig. 7.14: Sensitivity analysis of hydraulic conductivity

Table 7.6: Changes in error during sensitivity analysis of hydraulic conductivity

Factor	M.E. (m)	M.A.E. (m)	RMS (m)
0.2	-1.19	1.83	2.51
0.4	-0.55	1.30	1.80
0.6	-0.26	1.16	1.61
0.8	-0.10	1.12	1.55
1.0	0.01	1.11	1.53
1.2	0.09	1.11	1.54
1.4	0.15	1.12	1.55
1.6	0.20	1.14	1.56
1.8	0.24	1.18	1.68

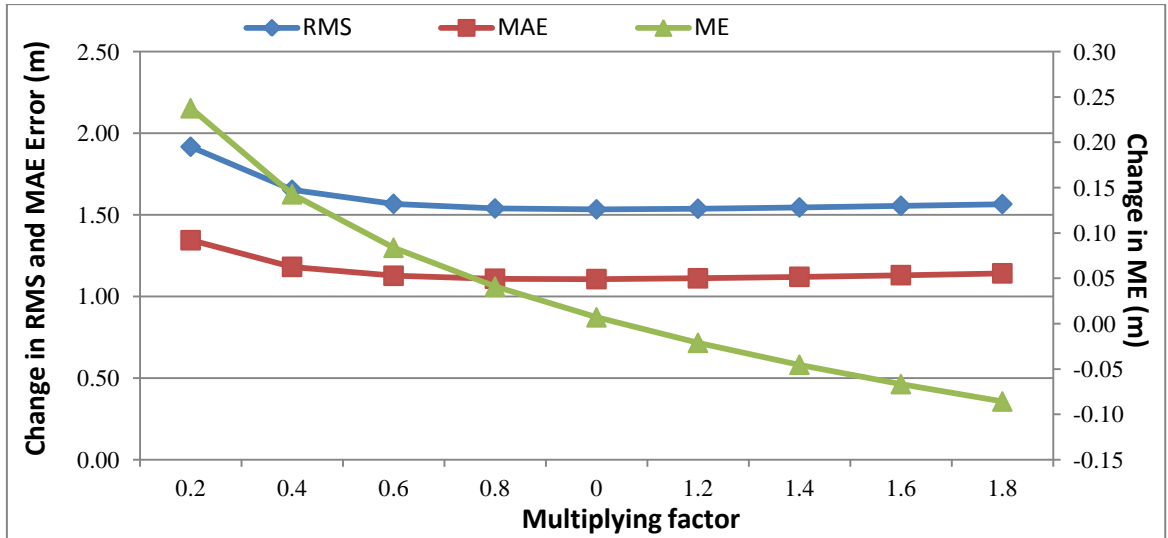


Fig. 7.15: Sensitivity analysis of specific yield

Table 7.7: Changes in error during sensitivity analysis of specific yield

Factor	M.E. (m)	M.A.E. (m)	RMS (m)
0.2	0.24	1.34	1.92
0.4	0.14	1.18	1.65
0.6	0.08	1.13	1.57
0.8	0.04	1.11	1.54
1.0	0.01	1.11	1.53
1.2	-0.02	1.11	1.54
1.4	-0.05	1.12	1.55
1.6	-0.07	1.13	1.56
1.8	-0.09	1.14	1.57

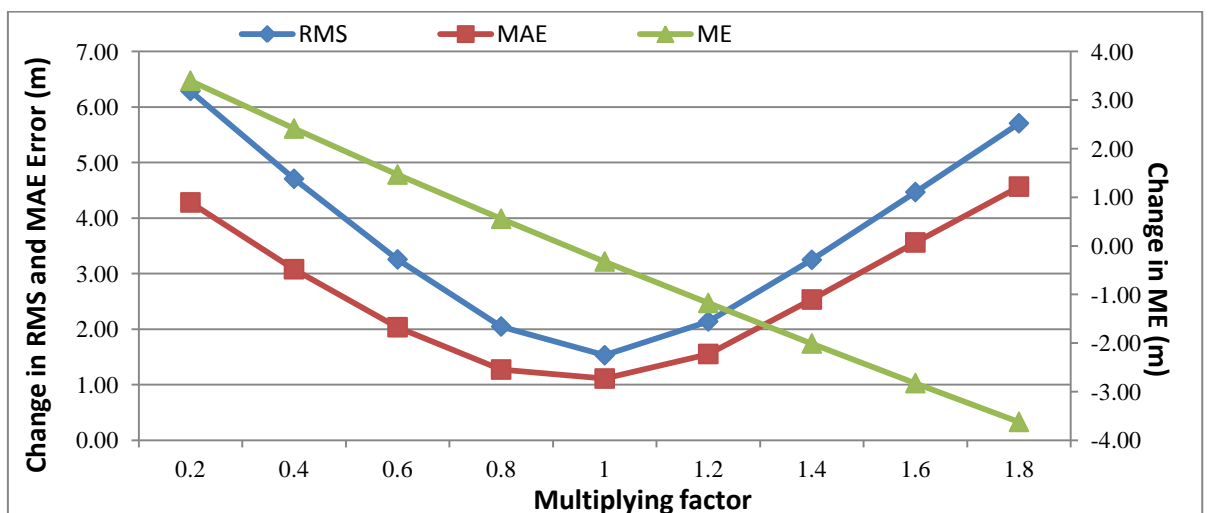


Fig. 7.16: Sensitivity analysis of recharge

Table 7.8: Changes in error during sensitivity analysis of recharge

Factor	M.E. (m)	M.A.E. (m)	RMS (m)
0.2	3.40	4.28	6.29
0.4	2.41	3.08	4.71
0.6	1.47	2.03	3.26
0.8	0.56	1.27	2.05
1	-0.32	1.11	1.53
1.2	-1.18	1.55	2.14
1.4	-2.01	2.53	3.25
1.6	-2.83	3.56	4.47
1.8	-3.62	4.57	5.71

It is seen that RMS error has increased by 1.6 times with a decrease in hydraulic conductivity by 80%, whereas it has increased by 1.1 times with an increase in hydraulic conductivity by 80%. For recharge, the model is more sensitive as compared to hydraulic conductivity. RMS error has increased by 4.1 times with a decrease in recharge by 80%, whereas it has increased by 3.7 times with an increase in recharge by 80%. In case of specific yield it is observed that small change as compared to recharge and hydraulic conductivity.

7.8.3 Zone Budget

Zone budget calculates the sub-regional water budget using results from steady state or transient state simulations. It calculates budget by tabulating the budget data that MODFLOW produces using cell by cell flow option. The user simply specifies the sub-regions for which budget will be calculated. These sub-regions are entered as zones analogues to way that properties, such as hydraulic conductivity, are entered. Simulation flow observations, such as base flow to a stream, or flux across a boundary, are very useful for calibrating a groundwater flow model against data other than just head measurements. The utilization of flow observations provides a stronger line of evidence to verify the model prediction, and particularly useful in models where the water table is relatively flat.

In this study, water budget from the model has been calculated of all the stress periods shown in Table 7.9. It is very helpful to know the available groundwater resources in a particular region.

Table 7.9 Water budget of the whole model for each stress period

Flow Term	Storage	Constant Head	Wells	Recharge	River Leakage	Head Dep Bounds	Sum	Discrepancy [%]
Period 1								
input	715486.38	6609.88	0	1052495.7	273817.44	229743.22	2278152.6	
output	6981.68	0	1499483.4	0	456966.41	314755.13	2278186.6	
in-out							-34	0
Period 2								
input	0	5688.68	0	1452781.4	286218	257041.92	2001730	
output	560958.19	0	697881.88	0	421203.1	321582.91	2001626.1	
in-out							103.92	0
Period 3								
input	716677.06	8017.36	0	1051971.2	292530.13	201184.02	2270379.8	
output	0	0	1494483.5	0	399304.34	376625.31	2270413.1	
in-out							-33.34	0
Period 4								
input	1963.34	8405.04	0	1452381.4	223777.55	296619.75	1983147.1	
output	382047.13	0	697881.88	0	566824.5	336289.69	1983043.3	
in-out							103.8	0.01
Period 5								
input	592011.94	10266.54	0	1052427.7	321488.25	224993.36	2201187.8	
output	13.06		1494483.4	0	359618.72	347105.13	2201220.3	
in-out							-32.5	0
Period 6								
input	0	0	0	1452781.4	279405.84	237895.47	1970082.8	
output	621598.75	7440.64	699738.88	0	352509.72	288688.51	1969976.5	
in-out							106.3	0.01
Period 7								
input	744762.75	12363.86	0	1050426.7	315177.01	202595.18	2325325.5	
output	0	0	1499521.4	0	435618.47	390216.97	2325356.8	
in-out							-31.3	0
Period 8								
input	3143.68	11739.71	0	1452643.4	277465	220695.88	1965687.6	
output	459617.47	0	699689.88	0	454148.09	352127.94	1965583.4	
in-out							104.2	0.01
Period 9								
input	795764.38	17078.41	0	1050487.7	317289.5	195789.98	2376409	
output	0	0	1499521.4	0	442241.5	434676.78	2376439.7	
in-out							-30.7	0
Period 10								
input	0	14931.91	0	1452643.4	276399.13	224415.73	1968390.1	
output	510901.72	0	699681.88	0	388456.88	369245.63	1968286.1	
in-out							104	0.01
Period 11								
input	655555.13	16648.06	0	1050487.7	279427.91	231323	2233441.8	
output	0	0	1499521.4	0	367541.41	366412.41	2233475.2	
in-out							-33.4	0
Period 12								
input	1356.36	15694.59	0	1438243.6	244258.88	215934.75	1915488	
output	404222.16	0	701327.28	0	439748.47	370086.42	1915384.3	
in-out							103.7	0.01
Period 13								
input	692868.44	21442.19	0	1050487.7	283127.5	234887.97	2282813.8	
output	0	0	1499521.4	0	412071.34	371254.06	2282846.8	
in-out							-33	0
Period 14								
input	0	16946.87	0	1438243.6	297662.27	273415.75	2026268.5	
output	595073.5	0	701327.28	0	407671.88	322090.84	2026163.5	
in-out							105	0.01
Period 15								
input	586104	16655.44	0	1049962.5	339860.84	268853.06	2261435.8	

output	2689.99	0	1500354.5	0	340127.61	418297.63	2261469.7	
in-out							-33.9	0
Period 16								
input	62.08	15496.48	0	1437485	270684.94	239606.62	1963335.1	
output	463994.2	0	701362.14	0	412787.91	385086.35	1963230.6	
in-out							104.5	0.01
Period 17								
input	677290.75	17264.84	0	1049962.5	336790.19	249630.56	2330938.8	
output	13904.9	0	1500354.5	0	395946.78	420765.05	2330971.2	
in-out							-32.4	0
Period 18								
input	10879.98	16073.05	0	1437485	261030.91	215039.38	1940508.3	
output	356750.47	0	701362.14	0	457351.51	424939.98	1940404.1	
in-out							104.2	0.01
Period 19								
input	764274	21209.85	0	1049962.5	308815.03	211413.46	2355674.8	
output	65.97	0	1500354.5	0	438383.03	416905.03	2355708.5	
in-out							-33.7	0
Period 20								
input	3358.64	19134.8	0	1437485	291758.16	205663.82	1957400.4	
output	306503.44	0	701362.14	0	513878.25	435551.87	1957295.7	
in-out							104.7	0.01
Period 21								
input	780087.56	24300.32	0	1049962.5	254285.39	214014.27	2322650	
output	0	0	1500354.5	0	437636.59	384691.14	2322682.2	
in-out							-32.2	0
Period 22								
input	3659.02	20491.29	0	1437485	243566.36	240538.15	1945739.8	
output	308889.5	0	701362.14	0	463313.91	472069.95	1945635.5	
in-out							104.3	0.01

7.9 CONCLUDING REMARKS

Groundwater model has been developed for the study area to determine the water table fluctuation in response to excitations in the form of pumping and recharge subject to initial and boundary conditions. The model has been calibrated for a period of eight years (1997-2004), and validated for a period of three years (2005-2007). In general, the model has successfully reproduced the groundwater elevations. Spatial variation of aquifer parameters has been obtained during the calibration process. These are found to be within the range of reported values in literature for similar hydro-geological formations. These values of specific yield, transmissibility and recharge factors are used for the prediction of future water levels in the study area.

8.1 PROLOGUE

Groundwater is a precious and valuable natural resource of water, so protection and management of this resource is vital for human evolution, socio-economic development and ecological diversity. Its vulnerability assessment is also necessary because human health and economic impacts are associated with groundwater contamination. In this chapter, a detailed study is carried out using the DRASTIC model with slight modification on an ArcGIS platform for assessing groundwater vulnerability.

In DRASTIC model, seven layers (depth of water, net recharge, aquifer media, soil media, impact of vadose zone, topography and hydraulic conductivity) are used out of these layers topography of the aquifer is not included in computing the final DRASTIC index for potential contamination, as the terrain is almost flat. In groundwater management, LULC pattern plays an important role so it has been added as a new parameter in the DRASTIC approach. The resulting groundwater vulnerability map was then integrated with the LULC map as an additional parameter in the DRASTIC model to assess the potential risk of groundwater to contamination in the study area. The final modified DRASTIC model is called DRASIC-LU which was tested using hydro-chemical data of the aquifer

8.2 METHODOLOGY

The detailed methodology of development of groundwater vulnerability map using modified approach DRASIC-LU is shown in Figure 8.1. All the layers were created in GIS environment. These layers and their individual features have been assigned suitable weights as per relative importance to groundwater vulnerability map. The AHP technique was used to normalize the weight of individual thematic layer and their different features, which is shown in Table 8.1. The detailed methodology of AHP is already explained in previous section 5.2.

After deriving the normalized weights, all the thematic layers were integrated in the GIS environment using equation 8.1 that was proposed by Malczewski (1999):

$$GWV = \sum_{w=1}^m \sum_{i=1}^n (w_j \times x_i) \quad (8.1)$$

Where, GWV = Groundwater Vulnerability, x_i = normalized weight of the i^{th} class/feature of theme and w_j = normalized weight of the j^{th} theme, m = total number of themes, and n = total number of classes in a theme.

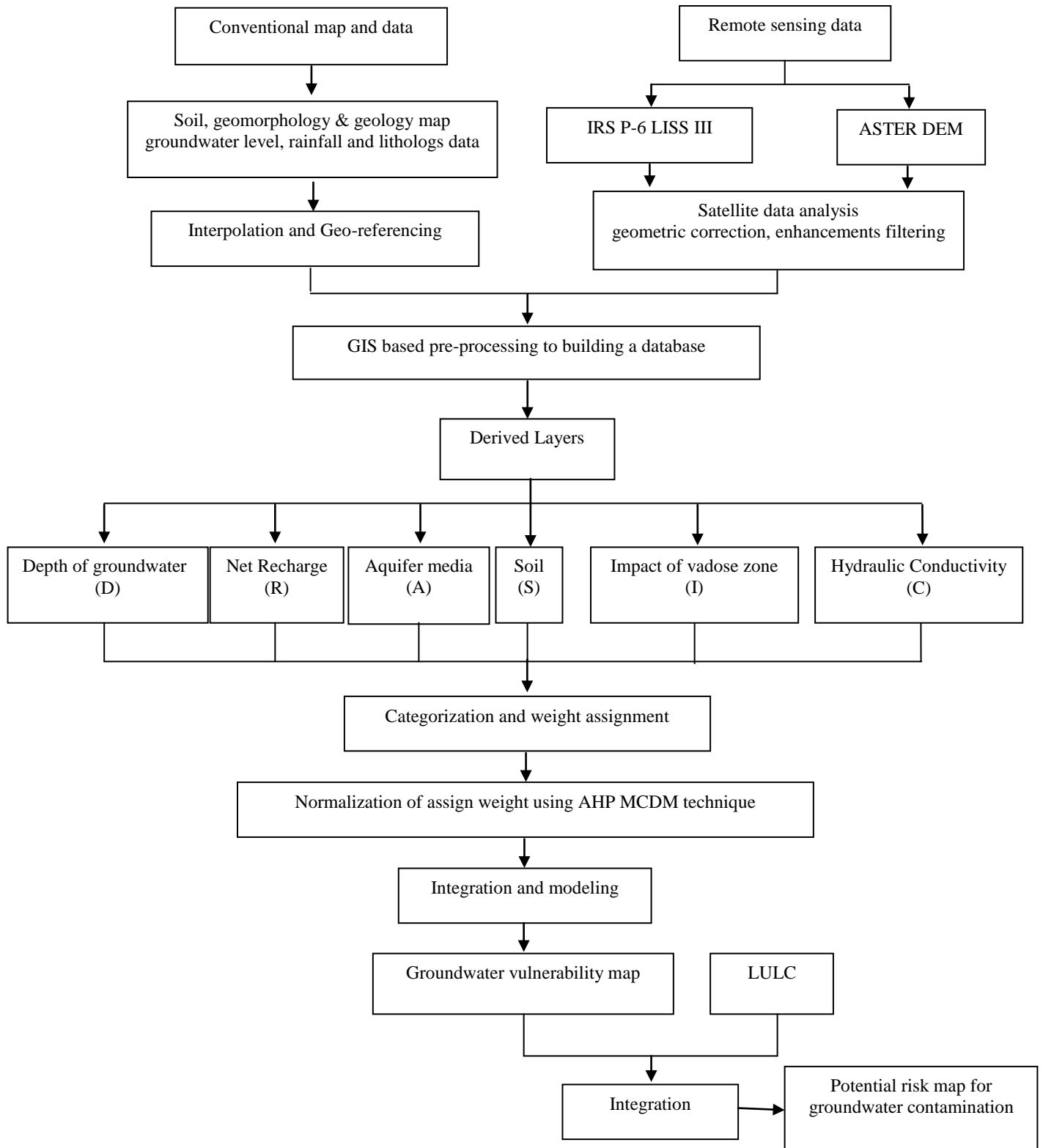


Fig. 8.1 Methodology for DRASIC-LU model

Table 8.1 DRASIC-LU parameters normalized weights

Parameters	Weights	Sub_classes	Weights
Depth of Groundwater (D)	0.23	< 6	0.34
		6 - 9	0.23
		9 -12	0.19
		12 - 15	0.13
		> 15	0.11
Net Recharge (R)	0.17	< 165	0.10
		165 - 180	0.16
		180 - 195	0.19
		195 - 210	0.25
		> 210	0.30
Aquifer Media (A)	0.15	Coarse Sand	0.43
		Sand Fine to Medium	0.32
		Fine Sand	0.25
Soil (S)	0.11	Sand	0.31
		Sandy loam	0.21
		Silt loam & Loam	0.19
		Silt loam	0.19
		Silty clay loam & Clay loam	0.10
Impact of Vadose Zone (I)	0.19	Clay	0.23
		Sand	0.47
		Sand & Little clay	0.29
		River	0.01
Hydraulic Conductivity (C)	0.15	< 35	0.10
		35 - 50	0.16
		50 - 65	0.19
		65 - 80	0.25
		> 80	0.30

8.3 RESULTS AND DISCUSSIONS

8.3.1 Depth to Water Layer

It determines the depth of groundwater level, and its most important layer used in groundwater vulnerable studies. Shallow water tables were more conducive for contamination as compared to deep water table under similar surface conditions. The average pre- and post-monsoon groundwater level data of year 2006 are used to prepare depth to water layer. A map has been generated by using IDW interpolation technique. The depths vary from 2.3 to 18.6 m, and are classified into five categories i.e. < 6, 6 - 9, 9 -12, 12 -15 and > 15 m, as shown in Figure 8.2. The major area ($\approx 45\%$) falls within 6-9 m depth.

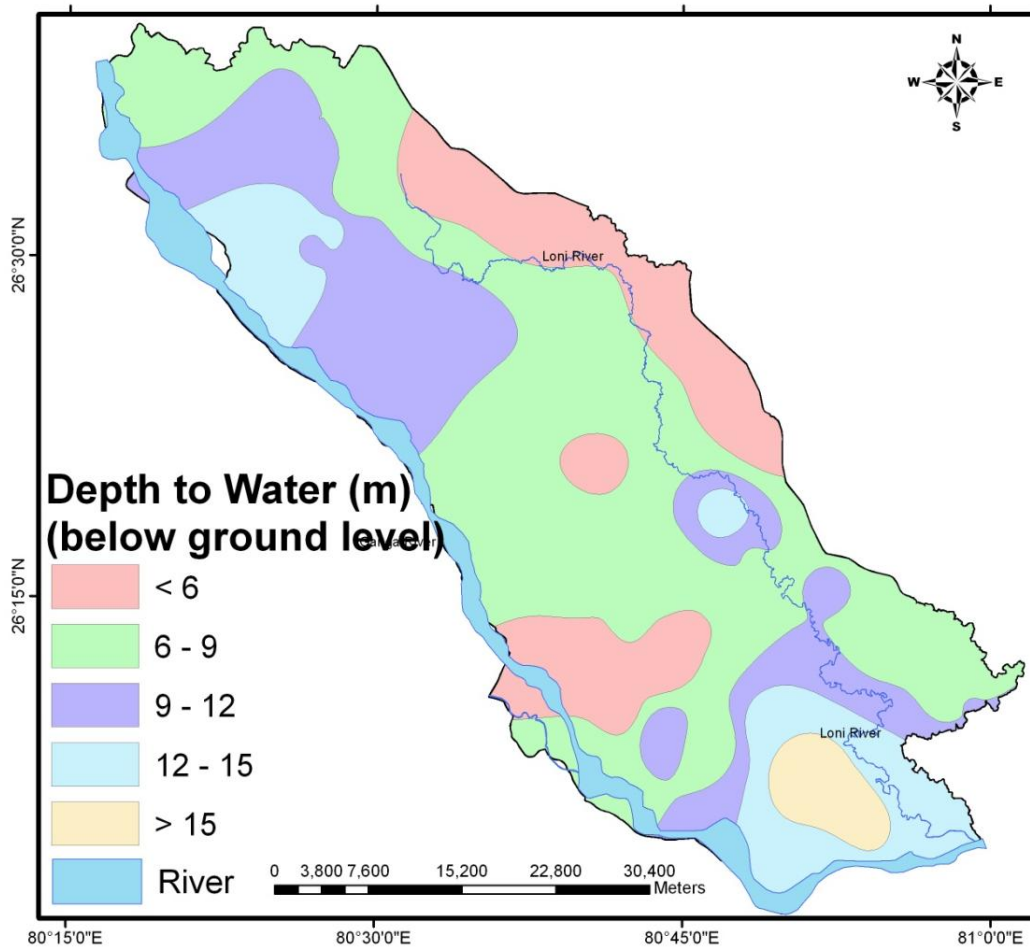


Fig. 8.2: Average depth to water layer from (1985-2007)

8.3.2 Net Recharge Layer

The primary source of groundwater recharge is precipitation, canal seepage and irrigation seepage that infiltrate through unsaturated zone to water table. Net recharge represents the amount of water that percolates per unit area of land surface to the water table on annual basis. The recharge water has the ability to carry the contaminants to water table and within the aquifer. Hence, a great recharge corresponds to a high potential for groundwater pollution. The pollution potential of an area with confined aquifer is lesser than that of an unconfined one because of the presence of a confining layer. Net recharge component was estimated using GEC norms, (Ministry of Water Resources, 1997 and 2011) based on the ground water balance method. The net recharge map was classified into five classes, i.e., < 270, 270 – 295, 295 - 320, 320 - 345 and > 345, as shown in Figure 8.3. The lowest recharge is found in Sikandarpur Karan and Purwa blocks and highest recharge occurs in Bichhiya and Lalganj blocks.

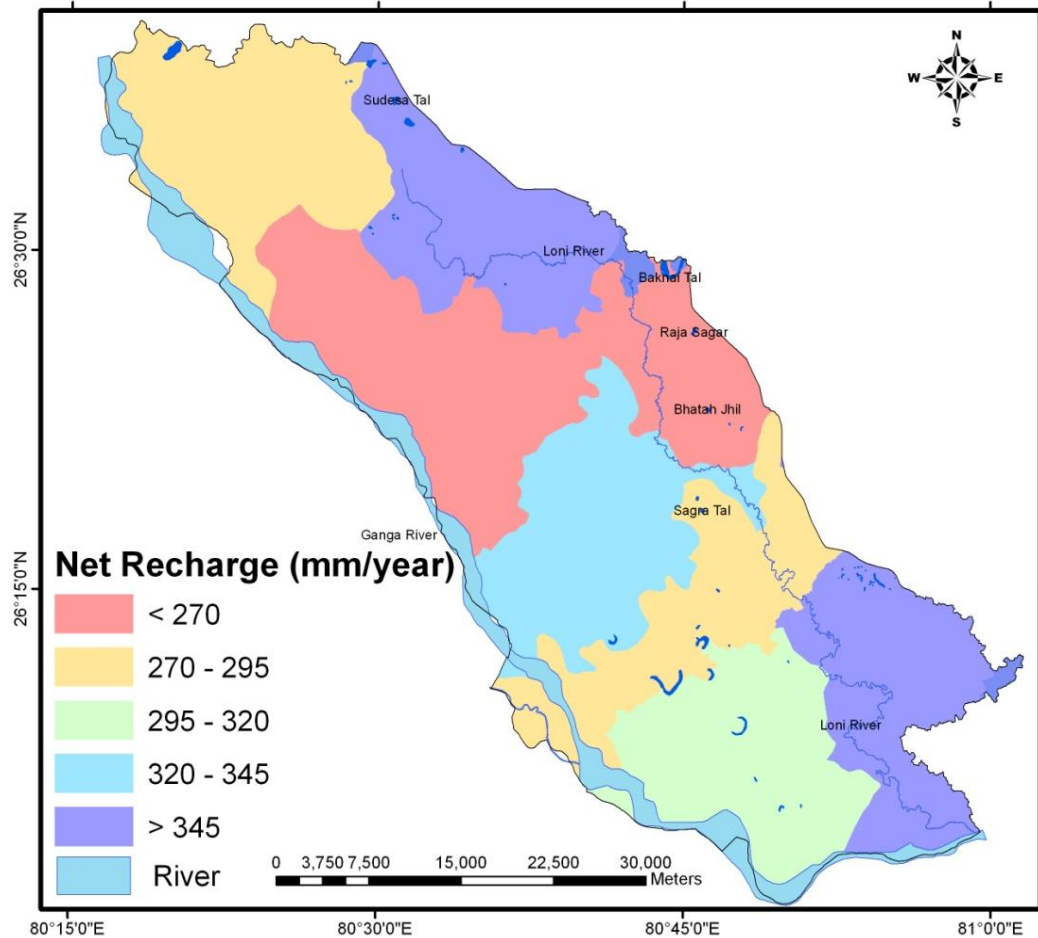


Fig. 8.3: Net recharge layer (1997-2004)

8.3.3 Aquifer Media Layer

The consolidated and unconsolidated rock formation is referred to as aquifer media, as it stores and yields sufficient quantity of water for use (Chandrashekar *et al.*, 1999). In consolidated formation, the rating is based on the amount of primary and secondary porosity along with fractures and bedding planes. In unconsolidated formation, the rating is based on the amount of fine material within the aquifer. It exerts major control over the route and path length that a contaminant travels and it is an important control, in addition to hydraulic conductivity and gradient, in determining the time available to contamination processes and the effective surface area of materials contacted in the aquifer (Aller *et al.*, 1987). In general, large grain size and high permeability will yield greater pollution potential. The aquifer media map (Figure 8.4) was prepared from the field studies, borehole data from 58 hydro-geological boreholes, geomorphology and topographical maps. Ratings for the aquifers range from 1 to 9 which were normalized using AHP analysis, as shown in Table 8.1.

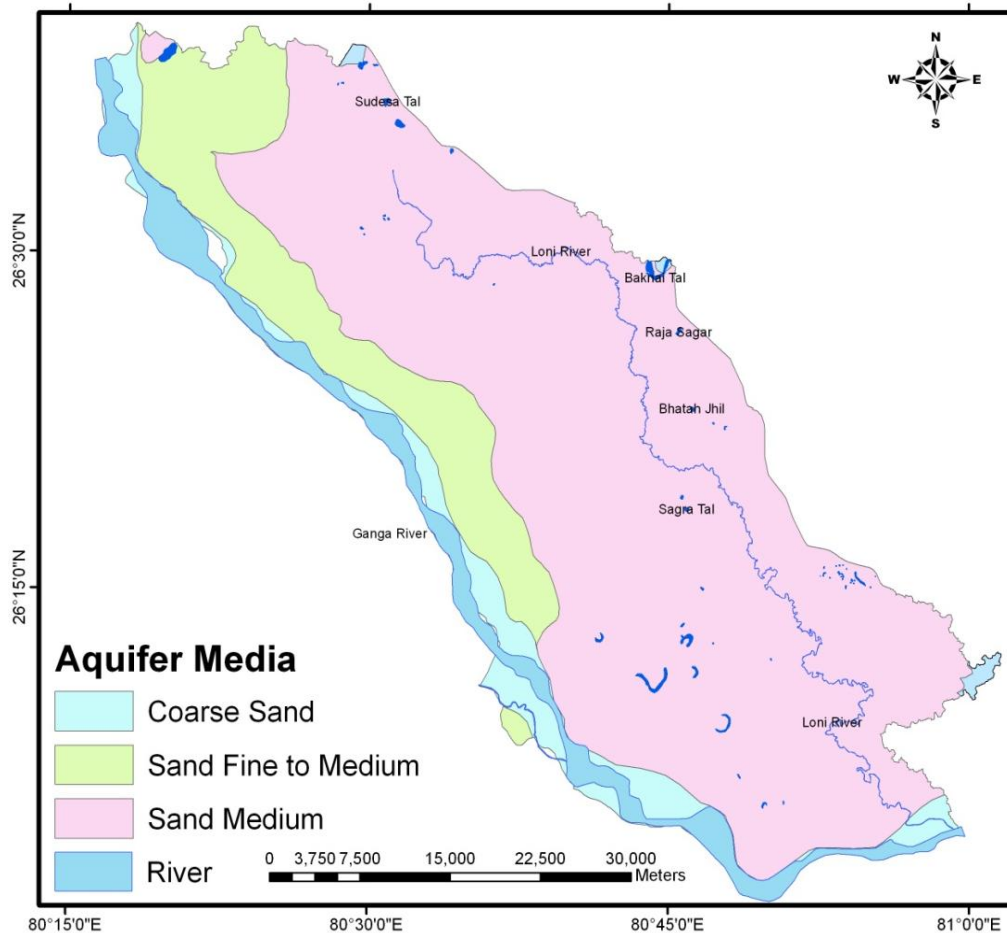


Fig. 8.4: Aquifer media layer

8.3.4 Soil Layer

It is the topmost layer of the Earth surface, which averages ≤ 2 m in thickness below the ground surface. In general, the pollution potential of soil was largely affected by the type of soil present and the grain size of the soil. The quantity of organic material present in the soil may also be an important factor. It has a significant impact on the amount of recharge that can infiltrate into the ground. The grid layer for soil media (permeability) was determined from the soil map developed by NBSS&LUP, Nagpur. The soil map is shown in Figure 4.12. Mainly five types of soils (Sand, Sandy loam, Silt loam, Silt loam and Silty clay loam & clay loam) are present. The soil map is assigned the ratings, as recommended by DRASTIC method, and it was further normalized using AHP.

8.3.5 Impact of Vadose Zone Layer

It is lying between water table and earth surface; also called as unsaturated zone. The texture or material of vadose zone determines the travel time of contamination through it. In surficial aquifers, the ratings for the vadose zone are generally the same as the aquifer media.

Sometimes, however, a lower rating is assigned if the aquifer media is overlain by a less permeable layer, such as clay. The impact of the vadose zone grid layer was prepared from the field studies, borehole data from 58 hydro-geological boreholes, soil and topographical maps. Ratings for the aquifers range from 1 to 9 which were normalized using Analytical Hierarchical Process (AHP) analysis, as shown in Figure 8.5.

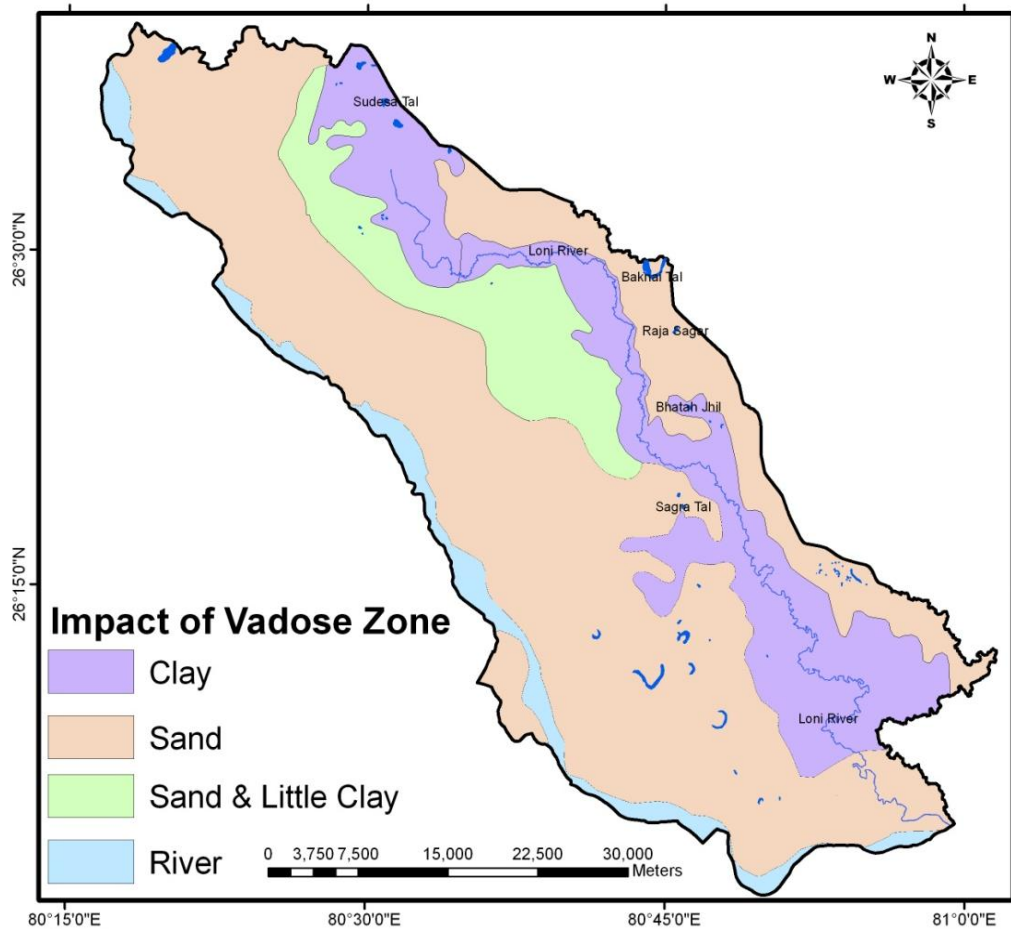


Fig. 8.5: Impact of vadose zone layer

8.3.6 Hydraulic Conductivity of the Aquifer (C)

It defines as the rate of flow of contaminant in saturated zone horizontally through an aquifer. If rate of flow is high in aquifer then the chance of vulnerability is also high. The hydraulic conductivity is calculated on the basis of transmissivity data measured during the pumping test. The hydraulic conductivity data have been calibrated using groundwater flow modeling and found to lie between 15.4 to 93.1 m/day. The calibrated hydraulic conductivity is classified into five classes, as shown in Figure 8.6. Ratings for the aquifers in this study range from 1 to 9 which were then normalized using AHP analysis, as shown in Table 8.1.

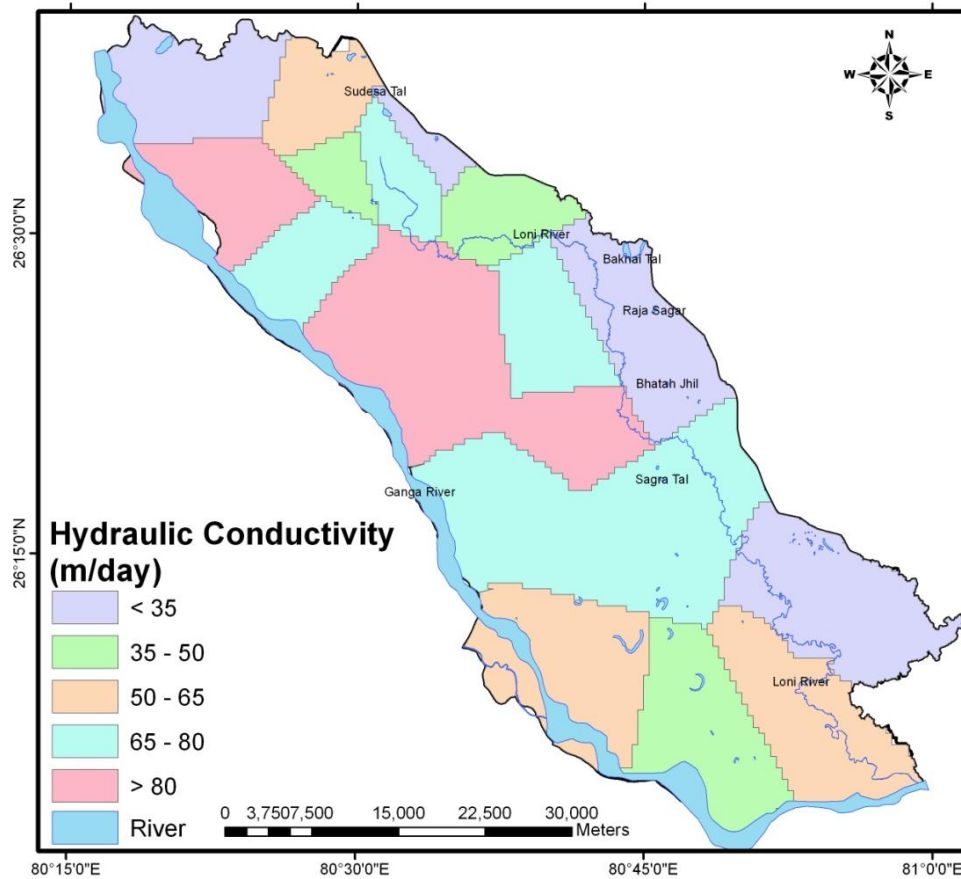


Fig. 8.6: Hydraulic conductivity layer

8.3.7 LULC Layer

Groundwater quality has been deteriorating due to industrial and sewage pollution in study area (Singh *et al.*, 2007). The land use pattern has strong bearing on groundwater quality. Therefore, land use pattern is taken into account in vulnerability mapping. In the present study, analysis of groundwater, surface water and trace elements, and subsequent interpretation indicate that urban Land use (industrial and sewage pollution) has maximum impact followed by rural land use. A similar study was conducted by Hussain *et al.*, (2006), utilizing land use pattern in DRASTIC approach, for vulnerability mapping. Based on these observations, qualitative ratings were proposed for the different types of land use categories.

8.3.8 Groundwater Vulnerability Map

Groundwater vulnerability map was calculated using equation (8.1) utilizing all developed input parameters in GIS framework. Figure 8.7 shows the degree of groundwater vulnerability to contamination in term of normalized DRASTIC index, where values vary from 0.21 to 0.96. Groundwater vulnerability map was categorised into four classes: low, moderate, high and very high, considering as the higher the index, the greater the relative pollution

potential. A high index corresponds to easiest to be polluted and consequently need to be managed more closely. Low index indicates that groundwater is protected from contaminant leaching by natural environment.

The output of DRASTIC method indicates that 13.44% area is categorized as very high vulnerable zone, while 32.56% and 19.95% of the areas are categorized as moderate and high vulnerable, respectively. Similarly, 34.05% of the total area is classified as low vulnerable zone. The combination of the model parameters that is pertinent to groundwater vulnerability like very shallow depth to water table (< 6 m) in the most part of study area with almost flat area ($< 2\%$ slope) and high to very high recharge rate in study area led to this high pollution potential index.

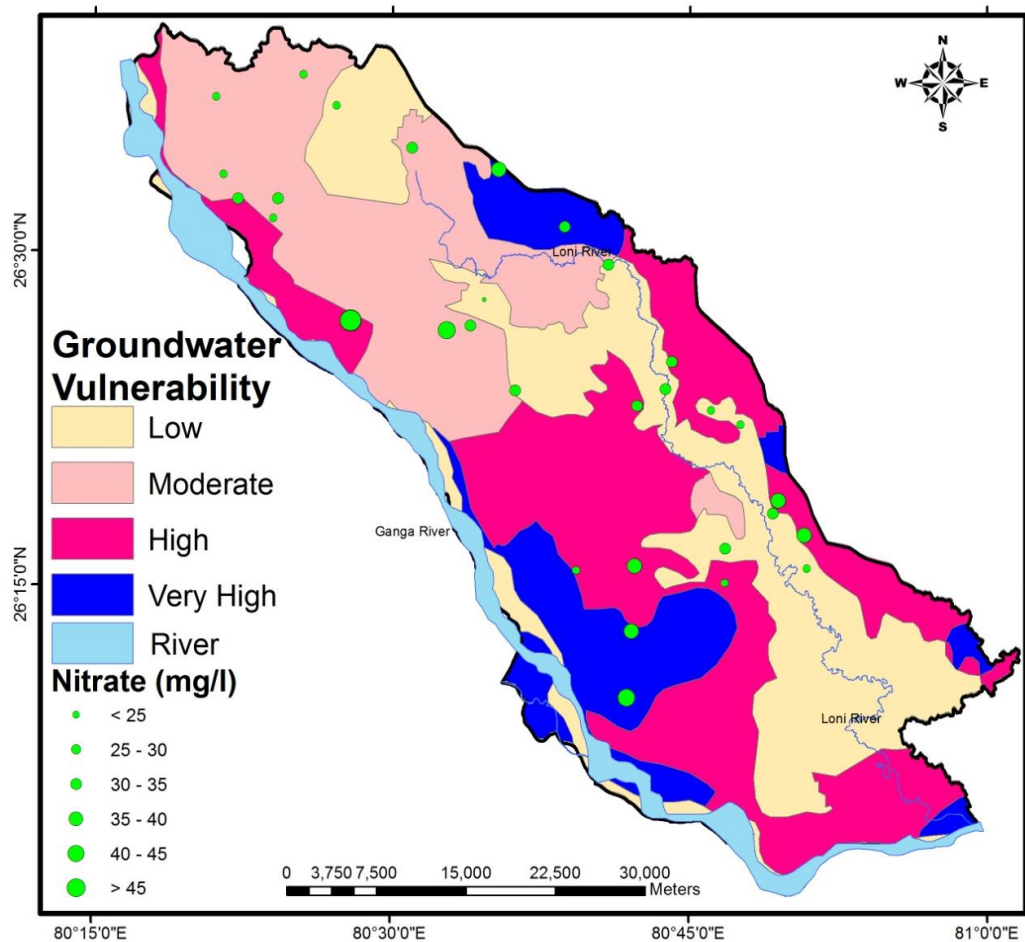


Fig. 8.7: Groundwater vulnerability map overlaid with nitrate data

8.3.9 Validation of Groundwater Vulnerability Map

In this study, the output of vulnerability model was tested using the measured nitrate and fluoride data of 40 different locations collected from UP Jal Nigam, Unnao. All the tested

samples of nitrate are in permissible range as per BIS, 2012 except a few samples, which were fall nearby Unnao city and western south part of the study area. However, most of the tested samples of fluoride are not in permissible range as per BIS, 2012. Firstly, nitrate data was overlaid on the groundwater vulnerability map using GIS in order to study how many wells with high concentration of nitrate are found within different vulnerable zones. Groundwater vulnerability map developed in this study based on aquifer characteristics does not consider contaminants sources, loading and transport mechanism into groundwater systems. Nevertheless, it was encouraging to find that majority of sampled sources which violated BIS, 2012 limit values of nitrate are located in high to very high vulnerable zones (Figure 8.7).

Secondly, for further validation, fluoride data was also overlaid on the groundwater vulnerability map using GIS. It was and found that most of the wells with high fluoride contents fall in very high and high vulnerable zones (Figure 8.8).

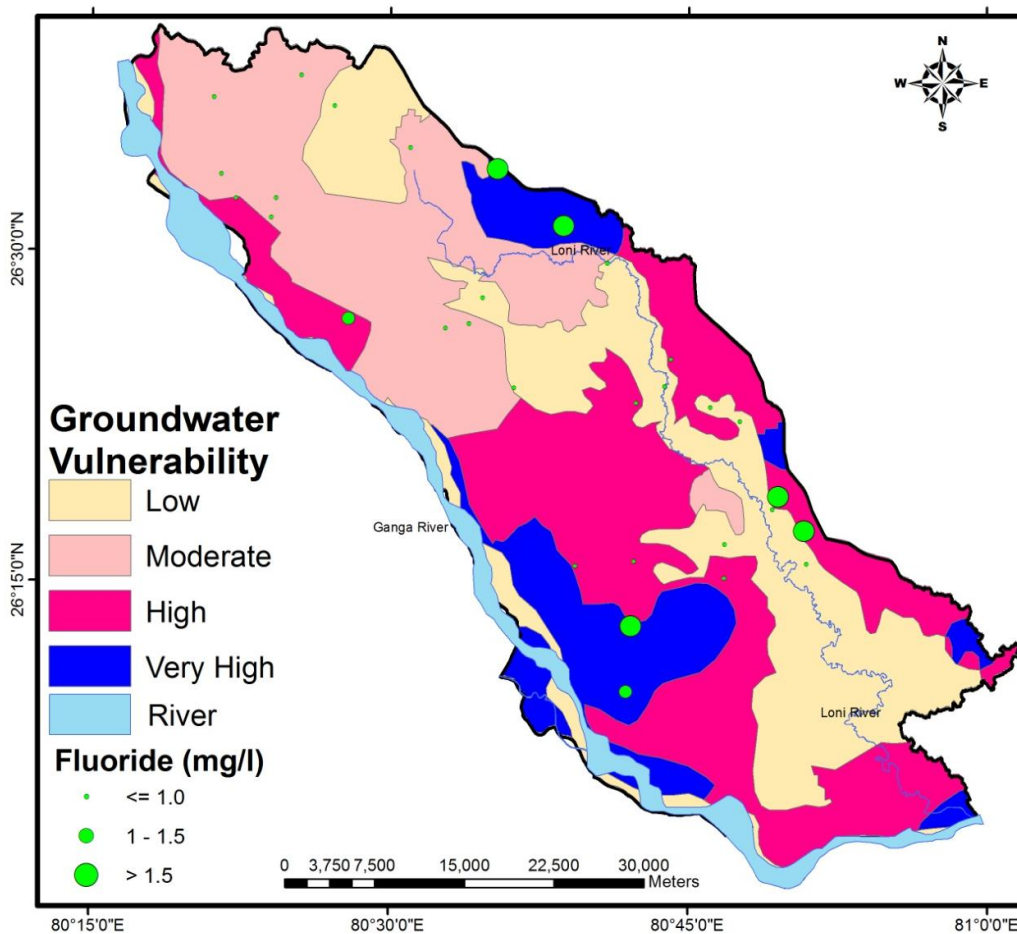


Fig. 8.8: Groundwater vulnerability map overlaid with fluoride data

In addition, the relationship between nitrate and groundwater depth (one of the important parameters that is pertinent to groundwater vulnerability to contamination) was established. It was found that concentration of nitrate was higher in shallow water table as compared to deeper water table (Figure 8.9).

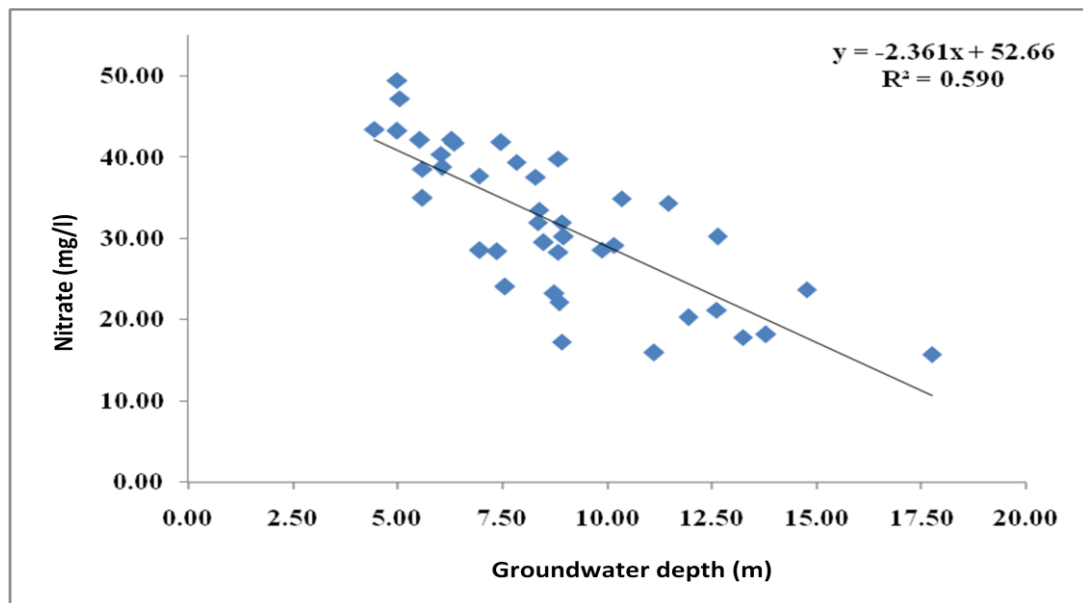


Fig. 8.9: Relationship between groundwater depth and nitrate in shallow aquifer

8.4 CONCLUDING REMARK

The modified DRASTIC model DRASIC-LU has been used to identify groundwater vulnerable zones in Loni and Morahi watersheds. The value of normalized DRASTIC index varied between 0.21 and 0.96, which was divided on the basis of histogram into four classes; low, moderate, high and very high, considering higher the index, the greater is the relative pollution potential. Out of the total area, 13.44% are a falls in very high vulnerable zone.

The result was validated using nitrate and fluoride data, and found that majority of sampled sources which violated BIS, 2012 limit value of nitrate and fluoride are located in high to very high vulnerable zones. This confirms that the model results are satisfactory.

9.1 PROLOGUE

Groundwater is considered as a purest resource of water that is used for drinking, irrigation and industrial activities but from past few decades' high usage of fertilizers in irrigation practices and rapid industrialization have contaminated it (Remesan and Panda, 2008). Groundwater contamination not only reduces the quantity of safe drinking water, but also it affect on public health. The main aim of this chapter is: (a) to assess spatial distribution of various chemical parameters affecting ground water quality (b) to statistically correlate the concentrations of measured parameters (c) to derive the water quality index to evaluate the suitability of water for drinking purpose, and (d) to analyze the suitability of groundwater for irrigation purpose.

9.2 METHODOLOGY

The overall methodology adopted to delineate the groundwater quality index (GWQI) for drinking purpose and its suitability for irrigation is shown in Figure 9.1. Data of 40 monitoring wells have been used for statistical and GIS based analysis. The IDW raster interpolation technique is used to generate the spatial distribution maps for the parameters, such as pH, chloride, fluoride, calcium, magnesium, sulphate, total dissolved solids (TDS), nitrate, bicarbonate and sodium. These parameters were compared and classified on the basis of guidelines suggested by Bureau of Indian Standards (BIS, 2012) as per suitability of groundwater for drinking purposes. A GWQI map was prepared to determine the overall suitability of groundwater for drinking purposes. Suitability of groundwater for irrigation was determined on the basis of salinity hazard diagram, sodium percentage, sodium adsorption ratio and electrical conductivity.

9.3 RESULTS AND DISCUSSIONS

9.3.1 Spatial Variation of Groundwater Quality

The statistics of various water quality parameters that were analyzed are given in Table 9.1, and the spatial distribution of the water quality parameters (pH, total dissolved solids (TDS), magnesium (Mg), calcium (Ca), chloride (Cl), nitrate (NO_3^-), fluoride (F), sodium (Na), sulfate (SO_4^{2-}), and bicarbonate (HCO_3^{2-})) are discussed below:

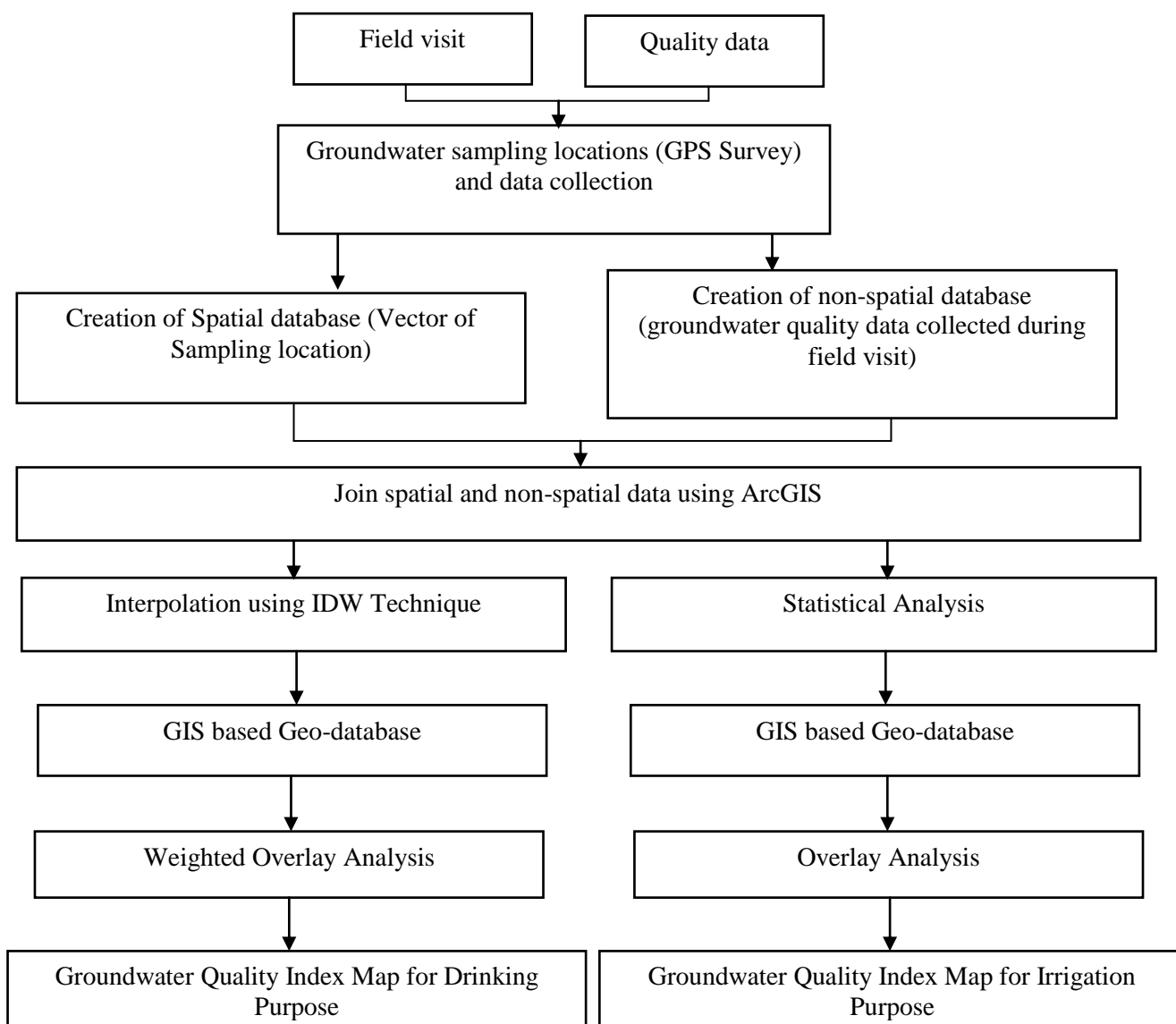


Fig. 9.1: Flowchart used for preparing GWQI

Table 9.1: Statistical analysis of physical and chemical groundwater quality parameters

Parameter (mg/l)	Min. value	Max. value	Mean value	Std. deviation	BIS, Indian Standards (IS 10500:2012)		WHO Standard
					Desirable limit	Permissible limit	Maximum allowable Concentration
pH*	7.98	8.70	8.32	0.12	6.5-8.5	No relaxation	6.5-8.5
TDS	783.41	2208.00	1581.55	276.35	500	2000	500
Ca	50.51	238.88	75.93	10.69	75	200	75
Mg	28.45	127.85	81.22	12.42	30	100	50
Cl	138.31	406.00	304.08	53.65	250	1000	250
NO ₃ ⁻	15.53	53.00	28.91	2.90	-	45	100
F	1.12	6.20	2.41	1.05	1.0	1.5	1.0
SO ₄ ²⁻	130.47	289.91	52.45	19.03	200	400	400
HCO ₃ ²⁻	112.08	300.49	249.23	38.78	30	-	150

9.3.1.1 pH layer

The high pH values in water samples cause a bitter taste of water and water using appliances become encrusted. It also lowers the effectiveness of the disinfection of chlorine, so additional chlorine is needed when pH is high. Low pH value in water will corrode or dissolve metals and other substances.

In the study area, value of pH lies between 7.98 - 8.7 as shown in Table 9.1, which is almost within the acceptable range, as suggested by BIS (2012). Table 9.2 and Figure 9.2 show the area statistics and quality map of pH layer, respectively. On the basis of table and figure, we conclude that 12% area falls in not permissible range and out of these the most of the area falls in Sikandarpur Karan, Sumerpur and Bichhiya blocks.

Table 9.2: Area statistics of pH layer

S. No.	Range	Class	Area (Km ²)	Area (%)
1	7.5-8.5	Maximum Permissible	1932.41	88.0
2	> 8.5	Not Permissible	263.51	12.0

9.3.1.2 Total Dissolved Solids (TDS) layer

TDS is described as the inorganic salts and small amounts of organic matter present in solution of water. Principally, it is a constituent of Ca, Mg, Na & K cations and HCO₃²⁻, Cl, SO₄²⁻ & NO₃⁻ anions. The tastiness of drinking water has been rated by panel of tasters in relation to its TDS level. Water with extremely low concentrations of TDS may also be unacceptable because of its flat, insipid taste. At a high TDS concentration, water becomes saline. The values of TDS between 783.41 to 2208 mg/l as shown in Table 9.1, and these are classified into three classes namely; desirable, maximum permissible and not permissible, on the basis of drinking water guidelines suggested by BIS, 2012 as shown in Figure 9.3 and Table 9.3. From the figure and table, it is concluded that 25.4% of area is not suitable for drinking, out of these, most of the area falls in Sikandarpur Karan and Bichhiya blocks.

Table 9.3: Area statistics of TDS layer

S. No.	Range (mg/l)	Class	Area (Km ²)	Area (%)
1	< 500	Desirable Limit	10.76	0.50
2	500-2000	Maximum Permissible	1590.28	74.11
3	> 2000	Not Permissible	544.88	25.39

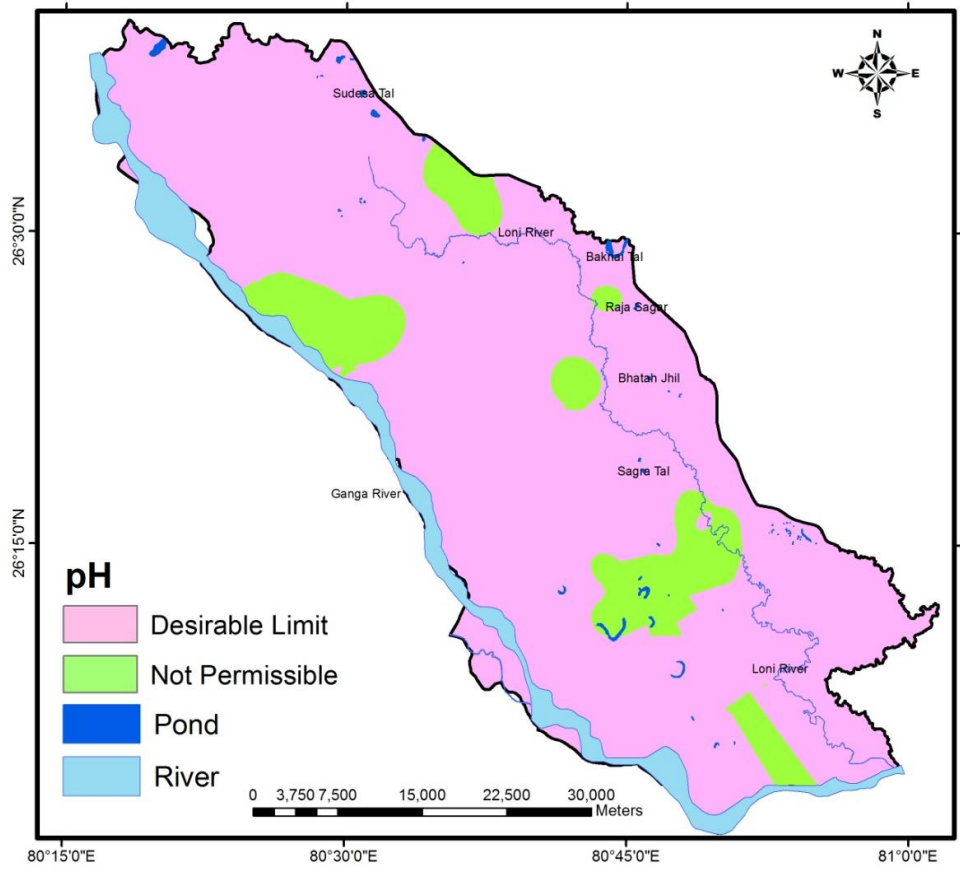


Fig. 9.2: pH layer

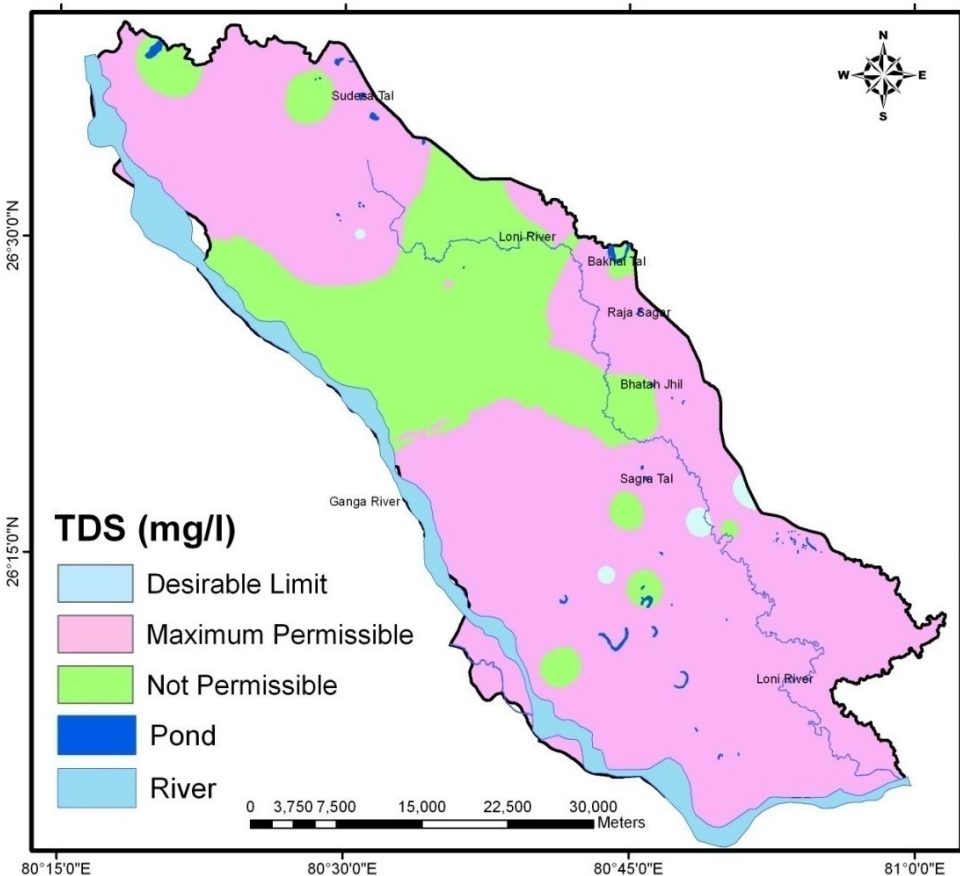


Fig. 9.3: TDS layer

9.3.1.3 Calcium (Ca) layer

Calcium is present in water naturally, due to its passes through mineral deposits and rock strata, it contributes in total hardness (Karavoltos *et al.*, 2008). The analytical data showed that the concentration of calcium in the water samples during the study period ranged from 50.5 to 238.88 mg/l with an average of 75.93 mg/l. The spatial distribution map and area statistics of calcium is shown in Figure 9.4 and Table 9.4 respectively. From figure and table, it is concluded that 16.3% of area falls in not permissible range, out of these most of the area falls in Sikandarpur Karan and Sumerpur blocks.

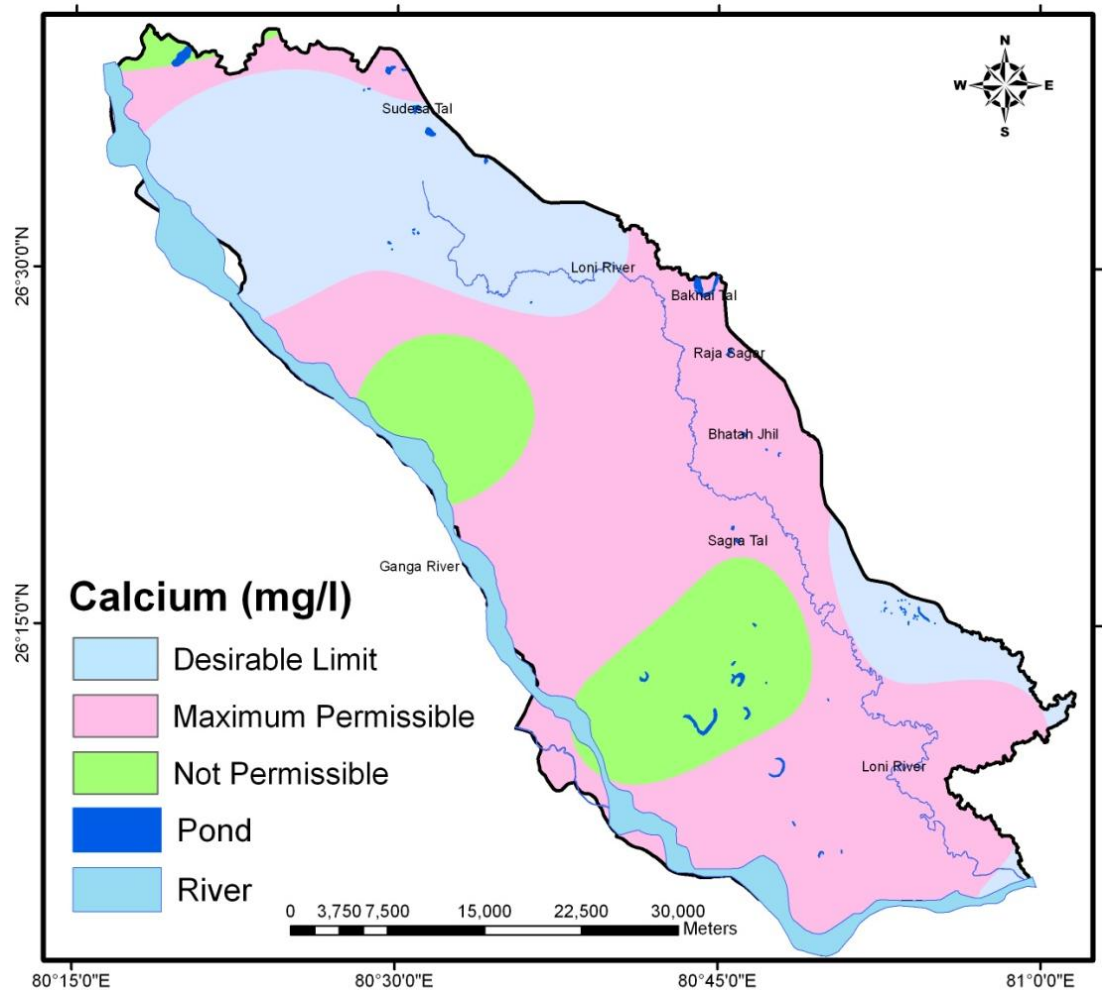


Fig. 9.4: Calcium layer

Table 9.4: Area statistics of calcium layer

S. No.	Range (mg/l)	Class	Area (Km ²)	Area (%)
1	< 75	Desirable Limit	555.30	25.88
2	75-200	Maximum Permissible	1240.53	57.81
3	> 200	Not Permissible	350.10	16.31

9.3.1.4 Magnesium layer

Magnesium is present in water naturally due to its passes through mineral deposits and rock strata, it also contribute in total hardness (Karavoltzos *et al.*, 2008). The analytical data showed that the concentration of magnesium in the water samples during the study period ranged from 28.45 to 127.85 mg/l with an average of 82.22 mg/l. The spatial distribution map and area statistics of magnesium is shown in Figure 9.5 and Table 9.5, respectively. From the figure and table, it is concluded that 6.6% of area falls in not permissible range, out of these are most of the falls in Sikandarapur Karan blocks. The reason of high magnesium in this area may be due to high usage of $MgSO_4$ as a fertilizer, which may lead to return flow into well water (Kelly *et al.*, 1996).

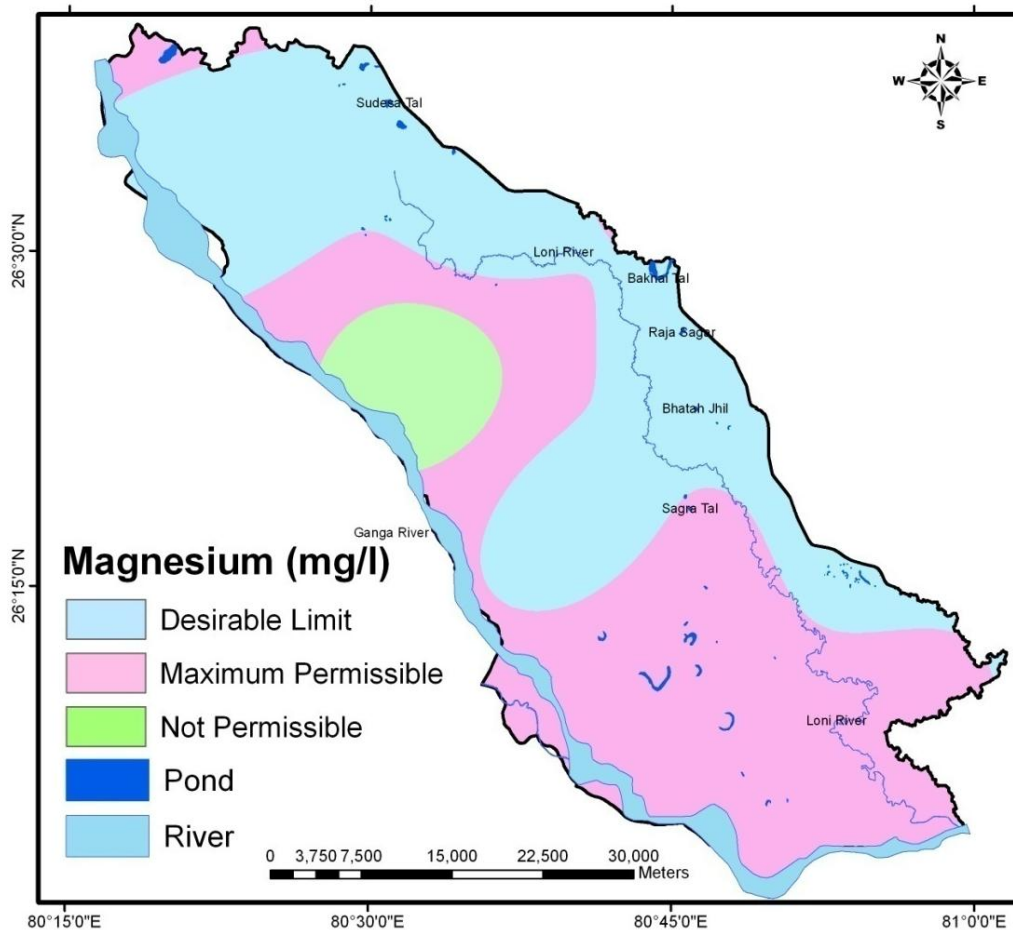


Fig. 9.5: Magnesium layer

Table 9.5: Area statistics of magnesium layer

S. No.	Range (mg/l)	Class	Area (Km ²)	Area (%)
1	< 30	Desirable Limit	930.34	43.35
2	30-100	Maximum Permissible	1074.36	50.07
3	> 100	Not Permissible	141.22	6.58

9.3.1.5 Chloride layer

Almost all natural water contains chloride ions. Its concentrations vary as per mineral content of the earth in any given area. In small amounts they are not significant but in large concentrations, they persists problems. The analytical data showed that the concentration of chloride in the water samples during the study period ranged from 138.31 to 406 mg/l, with an average of 304.08 mg/l, as shown in Table 9.1. Figure 9.6 and Table 9.6 show the area statistics and spatial distribution map of chloride, respectively. From figure and table, it is concluded that all the water samples fall in permissible range as per BIS 2012.

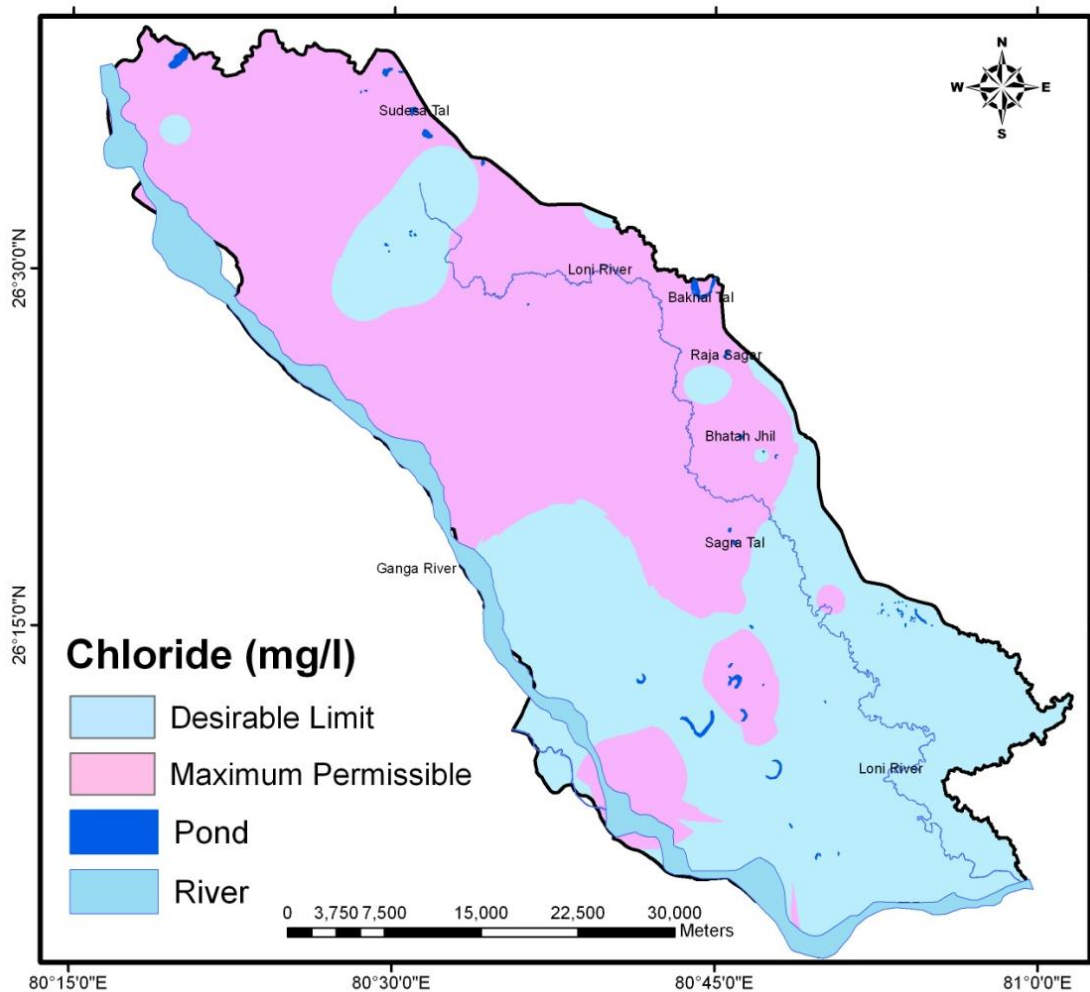


Fig. 9.6: Chloride layer

Table 9.6: Area statistics of chloride layer

S. No.	Range (mg/l)	Class	Area (Km ²)	Area (%)
1	< 250	Desirable Limit	961.90	44.82
2	250-1000	Maximum Permissible	1184.02	55.18

9.3.1.6 Nitrate layer

Nitrogen (N) is an essential input for the sustainability of agriculture. The problem of groundwater contamination by nitrate leaching in agricultural land use areas are faced by many countries around the world. It not only affects the drinking water quality, but also it disturbs the ecology of surface water. High concentration of nitrate in drinking water can cause blue baby disease (Methamoglobinemia) in infants and stomach cancer in adults (Anayah and Almasri, 2009). Sources of nitrates include sewage, fertilizers, air pollution, landfills and industries (CPCB, 2008). In the study area, nitrate lies between 15.53 to 53 mg/l with a mean of 28.91 mg/l. It was found that most of the area (about 91.5%) is in permissible limit as suggested by BIS (2012), and remaining 8.5% is above the permissible limit as shown in Table 9.7. The spatial distribution map of nitrate is shown in Figure 9.7. On the basis of figure and table we conclude that Northwestern portion of Sikandarpur Karan block is highly susceptible to nitrate pollution as compared to other places. It may be due to the presence of high number of leather industries that are situated in Sikandarpur Karan block.

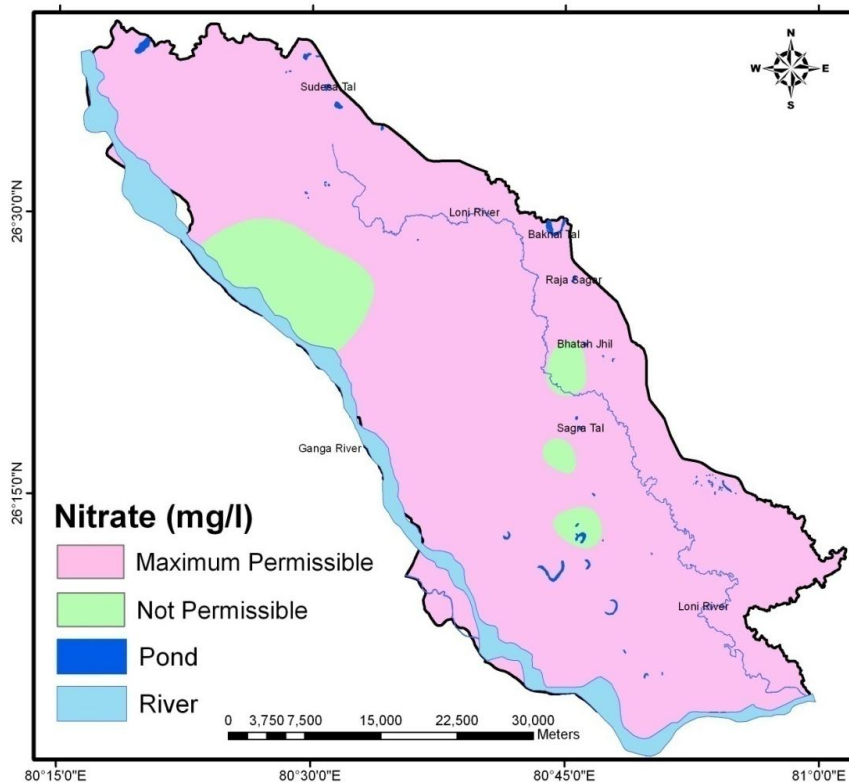


Fig. 9.7: Nitrate layer

Table 9.7: Area statistics of nitrate layer

S. No.	Range (mg/l)	Class	Area (Km ²)	Area (%)
1	< 45	Maximum Permissible	1962.04	91.43
2	> 45	Not Permissible	183.88	8.57

9.3.1.7 Fluoride layer

Fluoride, the most common occurring form of fluorine, is the natural contaminant of water. Groundwater usually contains fluoride dissolved in geological formation. Fluoride has long been recognized as one of the most significant natural groundwater quality problems affecting arid and semi-arid regions of India. Fluoride is known to contaminate groundwater reserves globally. The occurrence of fluoride in groundwater is a natural phenomenon that not only influences by the local, regional geological settings and hydrological conditions but it also depends upon on the retention and leaching of fluoride in soil (Verma, 2008; Jha *et al.*, 2010).

The fluoride intake in permissible range helps to prevent dental caries and strengthen the bones, but in exceeding limit it causes many diseases, such as dental fluorosis, decreased birth rates, skeletal fluorosis, kidney stones, and increased rates of bone fractures, impaired thyroid function and lower intelligence in children (Fordyce *et al.*, 2007). The analytical data showed that the concentration of fluoride in the water samples during the study period ranged from 1.12 to 6.2 mg/l, with an average of 2.41 mg/l, as shown in Table 9.1. The area statistics and spatial distribution map of fluoride is shown in Table 9.8 and Figure 9.8, respectively. From the table and figure it is concluded that 28.77% of area falls in not permissible for drinking as per BIS 2012 and most of the contaminated area lies in Sumerpur, Sareni, Khiron and Lalganj blocks.

Table 9.8: Area statistics of fluoride layer

S. No.	Range (mg/l)	Class	Area (Km ²)	Area (%)
1	< 1.5	Maximum Permissible	1528.48	71.23
2	> 1.5	Not Permissible	617.44	28.77

9.3.1.8 Sulfate layer

Sulfate is an essential plant nutrient, and is not toxic for plants or animals at lower concentrations, but at higher concentrations in drinking water it can cause noticeable taste and may cause laxative effect in unacquainted consumers (Subramani *et al.*, 2005). The analytical data showed that the concentration of sulfate in the water samples during the study period ranged from 130.47 to 289.91 mg/l, with average of 52.45 mg/l, as shown in Table 9.1. The Figure 9.9 and Table 9.9 show the spatial distribution map and area statistics of sulfate layer respectively. As per table, we conclude that all the groundwater samples falls in permissible limit as per BIS 2012.

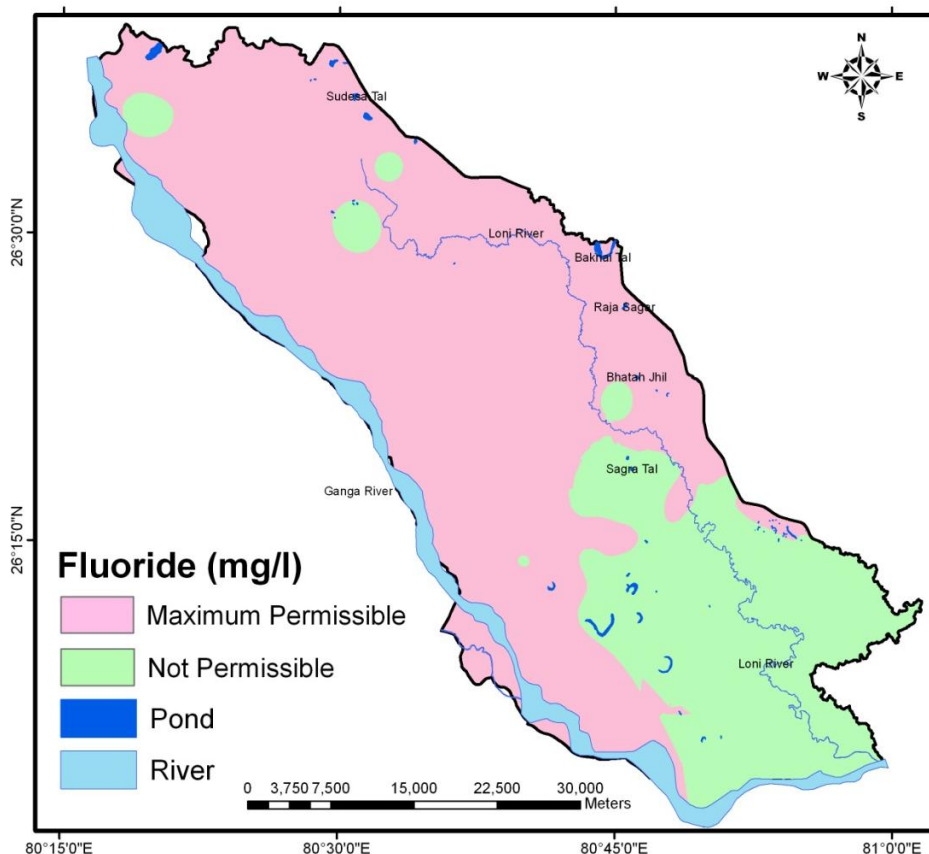


Fig. 9.8: Fluoride layer

Table 9.9: Area statistics of sulfate layer

S. No.	Range (mg/l)	Class	Area (Km ²)	Area (%)
1	< 200	Desirable Limit	1394.30	64.97
2	200-400	Maximum Permissible	751.62	35.03

9.3.1.9 Bicarbonate layer

The main source of bicarbonate ions in groundwater is the dissolved carbon dioxide in rainwater. When rainwater passes through soil and rocks, it generates bicarbonate ions (Anbazhagan and Nair, 2004). Its concentration in water lies between 112-300 mg/l with an average of 38.78 mg/l. The bicarbonate map is classified on the basis of WHO's standard because BIS 2012 has not defined. The spatial distribution of bicarbonate layer are divided into two classes permissible (<150 mg/l) and not permissible (>150 mg/l), as shown in Figure 9.10, and its area statistics is shown in Table 9.10. The most of the area (about 82%) falls in not permissible range

Table 9.10: Area statistics of bicarbonate layer

S. No.	Range (mg/l)	Class	Area (Km ²)	Area (%)
1	<150	Maximum Permissible	380.23	17.72
2	> 150	Not Permissible	1765.69	82.28

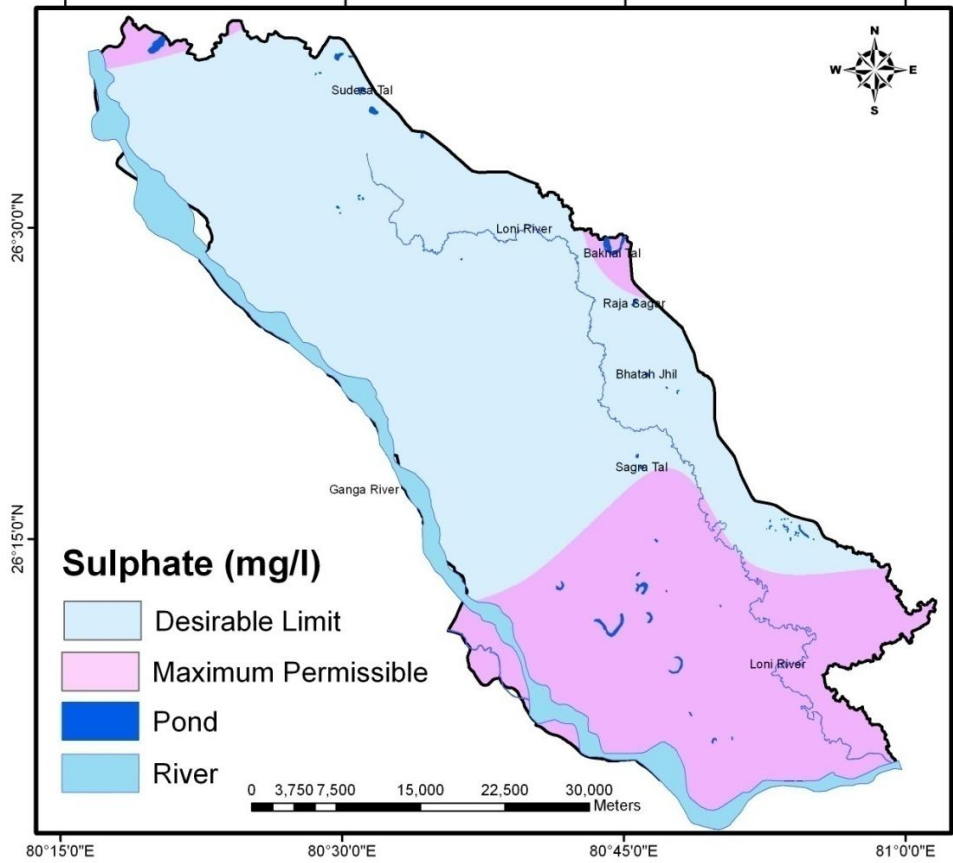


Fig. 9.9: Sulfate layer

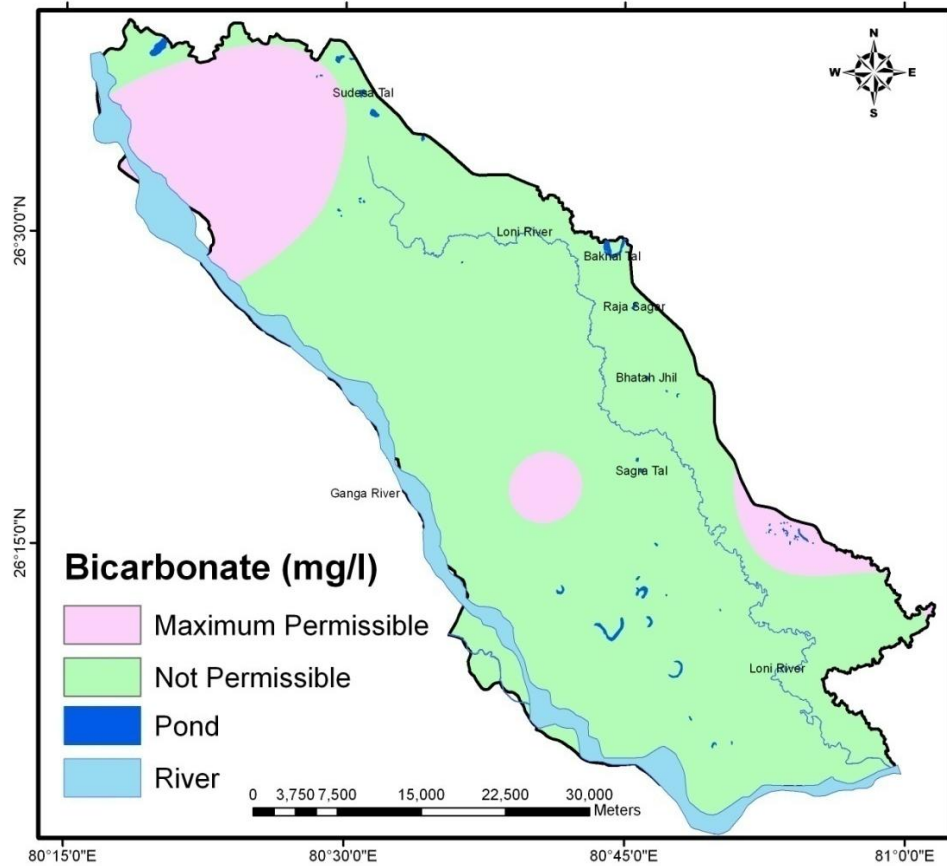


Fig. 9.10: Bicarbonate layer

9.3.2 Statistical Correlation among various Quality Parameters

In addition to analyze the groundwater quality parameters of desired area, correlations between various parameters were established which are presented in Table 9.11. It was found that almost all constituents are positively correlated to each other except nitrate. The positive correlation value ($r^2 > 0.8$) between EC and TDS, Na, Cl, and SO_4 , indicates that the conductivity depends on TDS and the main constituents of TDS in water are Na, Cl and SO_4 . Very high correlation ($r^2 = 0.997$) was observed between EC and TDS, which indicates that TDS values are derived from EC.

A significant correlation ($r^2 = 0.728$) between Na and HCO_3 , indicates that the sampling water is mainly composed of Na- HCO_3 . Also, the high correlation between Na and Cl, Mg and Cl, Na and SO_4 , & Mg and SO_4 , indicates that these soluble salts are predominant in water samples. Significant positive correlation between NO_3 with SO_4 and Ca indicates that they are originated from identical source in the watershed.

Table 9.11: Correlation matrix for groundwater quality variables

Parameters	EC	pH	TDS	Cl	HCO_3	SO_4	Fl	NO_3	Ca	Mg	Na
EC	1										
pH	0.704	1									
TDS	0.997	0.719	1								
Cl	0.907	0.746	0.932	1							
HCO_3	0.556	0.315	0.844	0.677	1						
SO_4	0.864	0.660	0.971	0.948	0.775	1					
F	0.210	0.323	0.300	0.157	0.381	0.096	1				
NO_3	0.148	-0.417	0.107	-0.173	0.554	0.011	0.356	1			
Ca	0.687	0.244	0.670	0.559	0.755	0.639	0.137	0.480	1		
Mg	0.742	0.413	0.723	0.774	0.715	0.787	0.211	0.229	0.803	1	
Na	0.879	0.614	0.956	0.938	0.728	0.954	0.231	0.097	0.567	0.761	1

9.3.3 Hydrogeochemical Facies

It is an important interpretation tool that is used for determining the flow pattern and origin of chemical histories of groundwater. It is also used to express similarity and dissimilarity in major cations and anions (Piper, 1953). To know the hydro-geochemical regime, plot the analytical samples in Piper trilinear diagram. This diagram contains two triangles one for plotting cations and other for anions. The cations and anion fields are combined to show a single point in a diamond shaped field from which inference is drawn on the basis of the hydro-geochemical facies concept. The Piper trilinear method is very useful to

find the chemical relationship among various quality parameters in more definite term as compared to other methods. The piper trilinear plot is drawn of major cations and anions to know the hydrochemistry of groundwater aquifer of alluvium region. All the cations and anions are expressed in meq/l. The trilinear plot of cations expresses abundance of each species (Ca, Mg and Na+K) as a percentage of their sum. The same rationale applies to the trilinear plot of anions (CO_3+HCO_3 , SO_4 and Cl). The trilinear plots of the major cations and anions in the groundwater of the study region are shown in Figure 9.11. These plots suggest that among the cationic species, the univalent cations (Na and K) dominate in the aquifer of this region, which tends to shift towards magnesium. On the other hand, bicarbonate is the major anion showing dominance over others. Thus, majority of groundwater samples belong to the sodium/potassium-bicarbonate type. Weathering of Na-K bearing minerals, cation-exchange process and industrial and/or agricultural activities are responsible for the dominance of Na-K in ground water in the study area.

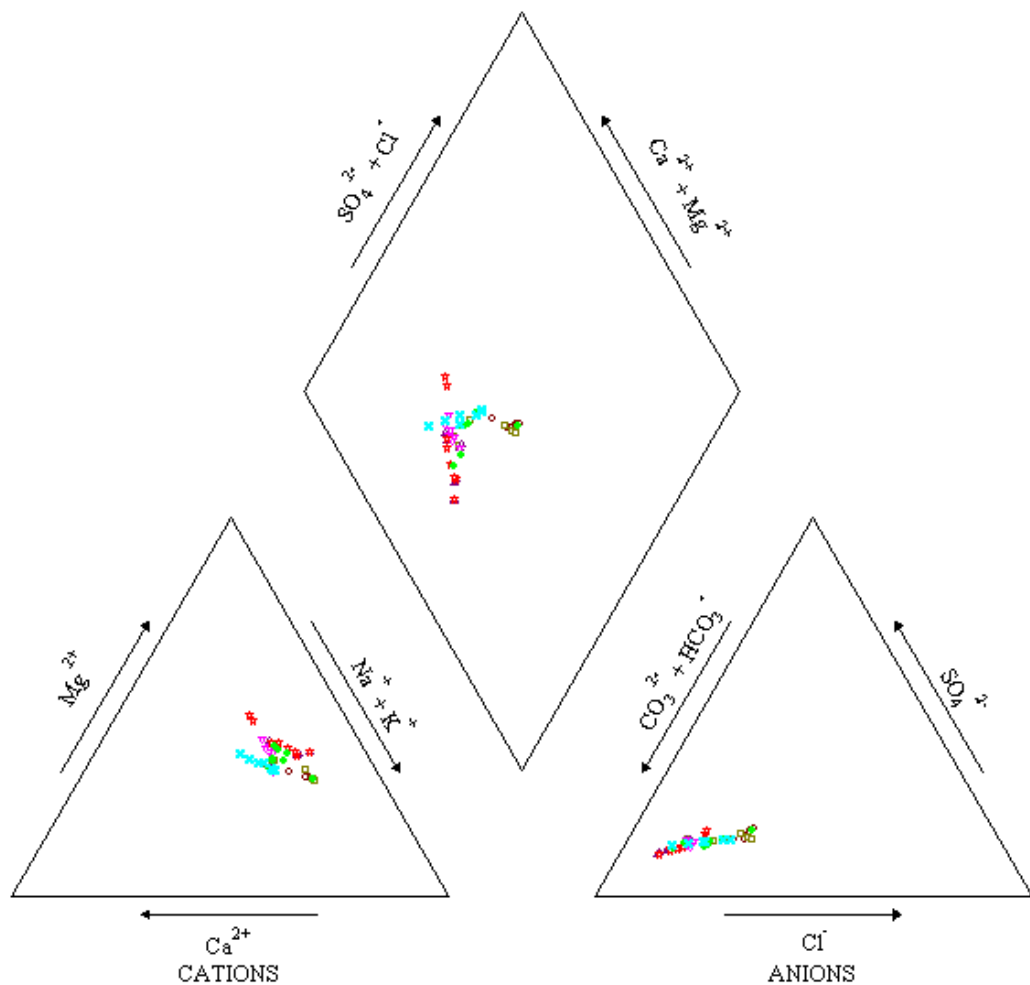


Fig. 9.11: Piper trilinear diagram

9.3.4 Evaluation of Groundwater Quality Index (GWQI)

GWQI is a very useful and efficient method for assessing the drinking water quality. To determine the suitability of the groundwater for drinking purposes, GWQI is computed using the following steps.

- 1) In the first step, assigned a weight (w_i) is assigned to each quality parameter according to its relative importance in the overall quality of water for drinking purposes.
- 2) In the second step, the relative weight (W_i) is computed using the following equation:

$$W_i = \frac{w_i}{\sum_{i=1}^n w_i} \quad (9.1)$$

where, W_i is the relative weight of all the quality parameters, w_i is the weight of each parameter and n is the number of parameters.

- 3) A quality rating scale (q_i) for each parameter is assigned by dividing its concentration in each water sample by its respective standard according to the guidelines laid down in the BIS, 2012 and the results are multiplied by 100:

$$q_i = \frac{C_i}{S_i} \times 100 \quad (9.2)$$

where, q_i is the quality rating, C_i is the concentration of each chemical parameter in each water sample in mg/l (milligram/litre), and S_i is the Indian drinking water standard for each chemical parameter in mg/l, according to the guidelines of the BIS (2012).

- 4) For computation of the GWQI, firstly determines the SI value for each chemical parameter is determined, which is then used to determine the GWQI, as per the following equation:

$$SI_i = W_i \times q_i \quad (9.3)$$

$$GWQI = \sum SI_i \quad (9.4)$$

Where SI_i is the sub index of i^{th} parameter; q_i is the rating based on concentration of i^{th} parameter and n is the number of parameters.

The groundwater quality index has been categorized into five classes namely; excellent, very good, good, poor and unfit for drinking, as shown in Figure 9.12. It is found that the area falling in excellent groundwater quality is about 240.6 km² (11.2% of the total study area), which covers central portion of Bighapur block and Eastern south part of study area that lies in Sumerpur and Khiron blocks. However the area having unfit for drinking is about 117 km² (5.46% of the total study area), which falls in western part of Sikandarpur block and is nearby the Unnao city and industrial area of Unnao district. The area having very good, good and poor groundwater quality is about 761.9 (35.51%), 652.39 (30.41%), 373.9 (17.42%) km², respectively.

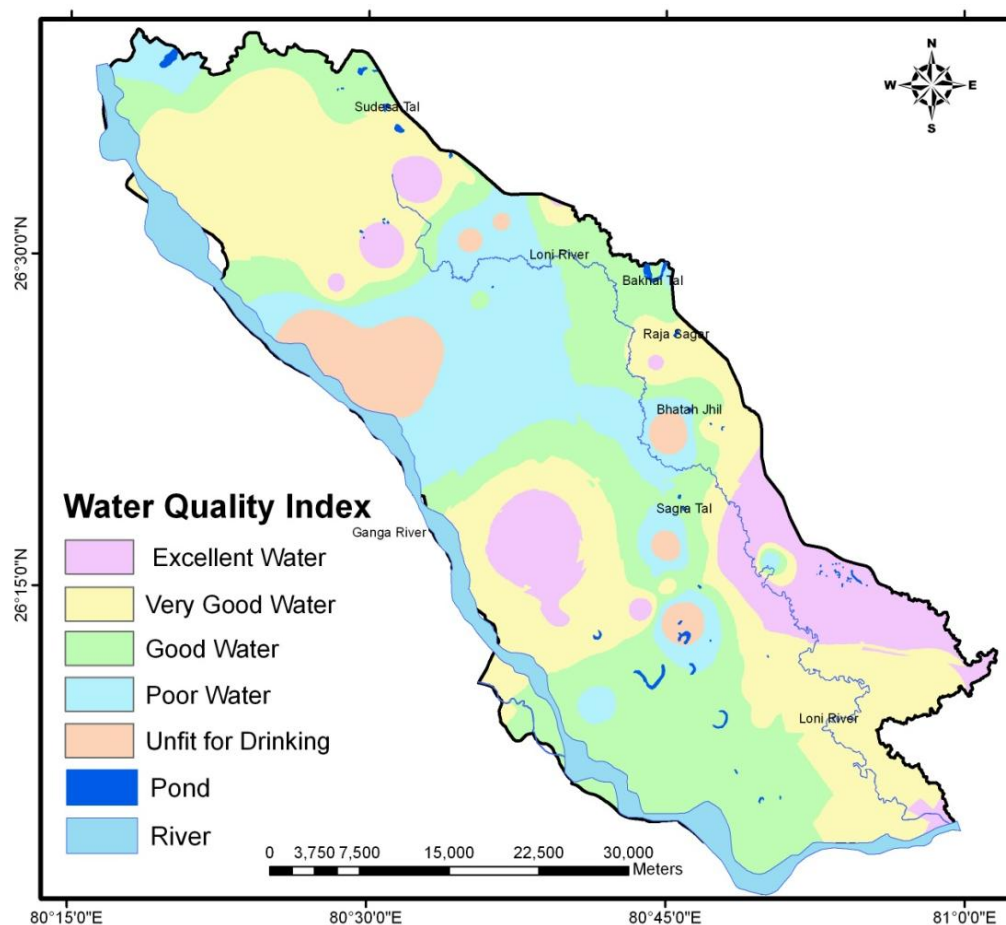


Fig. 9.12: Groundwater quality index map

9.3.5 Groundwater Quality Analysis for Irrigation

Groundwater has been intensively used for irrigation in the study area. Its quality plays an important role for irrigation practice. If the water is not suitable for irrigation, it affects plants and agriculture soils, physically and chemically, that reduces the productivity. Physically it lowers the osmotic pressure in structural cells of plants. The low osmotic pressure prevents

water from reaching branches and leaves. Chemically, it interrupt plant metabolism. Suitability of groundwater for irrigation purposes has been judged graphically using the following indices, salinity, chlorinity, sodicity (Mills. 2003). It is also analyzed using GIS analysis of groundwater quality layers viz. Electrical Conductivity (EC), Sodium percent (Na%), Sodium Adsorption Ratio (SAR) and Residual Sodium Carbonate (RSC). Indices, which can be developed to verify the suitability, as follows:

9.3.5.1 Salinity

It is computed using Electrical conductivity (EC) values of field groundwater samples. Water exhibiting low to moderate salinity (classes I and II) is not considered very harmful to soils or crops, whereas, water exhibiting high salinity (class III) is suitable for irrigating the medium and high salt tolerant crops. High salinity water (class IV) is suitable for irrigating high salt tolerant crops, whereas, water of salinity class V or above is generally unsuitable for irrigation. Majority of the groundwater samples (63%) in the study region are categorized as class I or II, and thus, may be considered as suitable for irritation. However, about 12% of the water samples are found to exhibit very high to extremely high salinity (classes IV–VI), and may not be suitable for irrigation (Figure 9.13). Spatial variation map of EC is classified on the basis of salinity hazard classes C1 to C5 as shown in Figure 9.14, and its area statistics is given in Table 9.12.

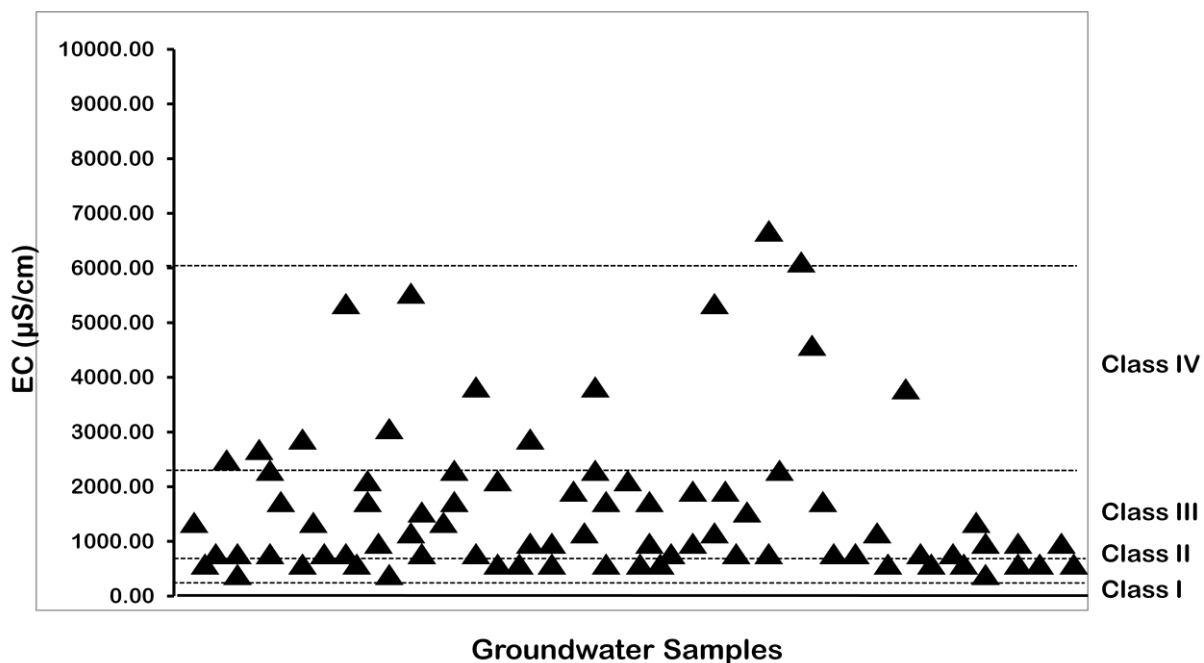


Fig. 9.13 Salinity index for the groundwater samples of the study region

Table 9.12: Suitability of groundwater for irrigation based on electrical conductivity

S. No.	Range	Salinity Hazard	Class	Area (Km ²)	Area (%)
1	< 250	C1	Excellent	379.80	17.70
2	250-750	C2	Good	703.10	32.76
3	750-2250	C3	Doubtful	1010.10	47.08
4	> 2250	C4 & C5	Unsuitable	52.92	2.46

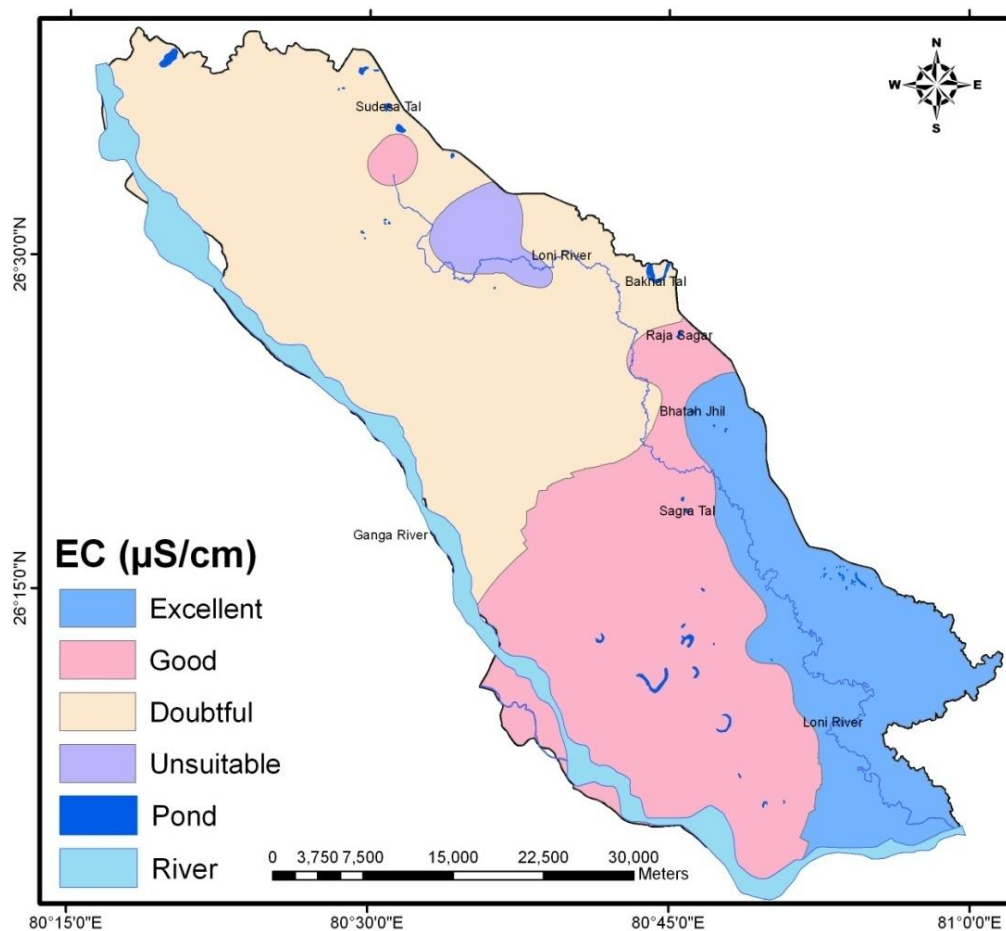


Fig. 9.14: Electrical conductivity layer

9.3.5.2 Chlorinity

Low salt tolerance crops are usually chloride sensitive. The chlorinity index of the groundwater sources was calculated using measured chloride ion concentration in water (Figure 9.15). All the groundwater samples are falls in classes I and II, both the classes are suitable for irrigation.

9.3.5.3 Sodium Adsorption Ratio (SAR) layer

Another important factor for water quality is the sodium concentration to express reaction with the soil and know reduction in its permeability. High sodium-depositing waters

are generally not suitable for irrigating the soils, as higher deposition of sodium may deteriorate the soil characteristics. Therefore, SAR is considered as a better measure of sodium (alkali) hazard in irrigation, as SAR of water is directly related to the adsorption of sodium by soil and is a valuable criterion for determining the suitability of the water for irrigation.

Excessive sodium content relative to calcium and magnesium reduces soil permeability and thus inhibits the supply of water needed for the crops. The SAR measures the relative proportion of sodium ions to those of calcium and magnesium in a water sample. The SAR is used to predict the sodium hazard of high carbonate waters, especially if it contains no residual alkali. The excess sodium or limited calcium and magnesium content are evaluated by SAR (Kalra and Maynard 2012), which is computed as:

$$SAR = \frac{Na^+}{\sqrt{(Ca^{2+} + Mg^{2+})/2}} \quad (9.5)$$

where all cationic concentrations are expressed in mg/l.

Spatial variation map of SAR is classified on the basis of alkalinity hazard classes, S1 to S4 as shown in Figure 9.16, and its area statistics is given in Table 9.13.

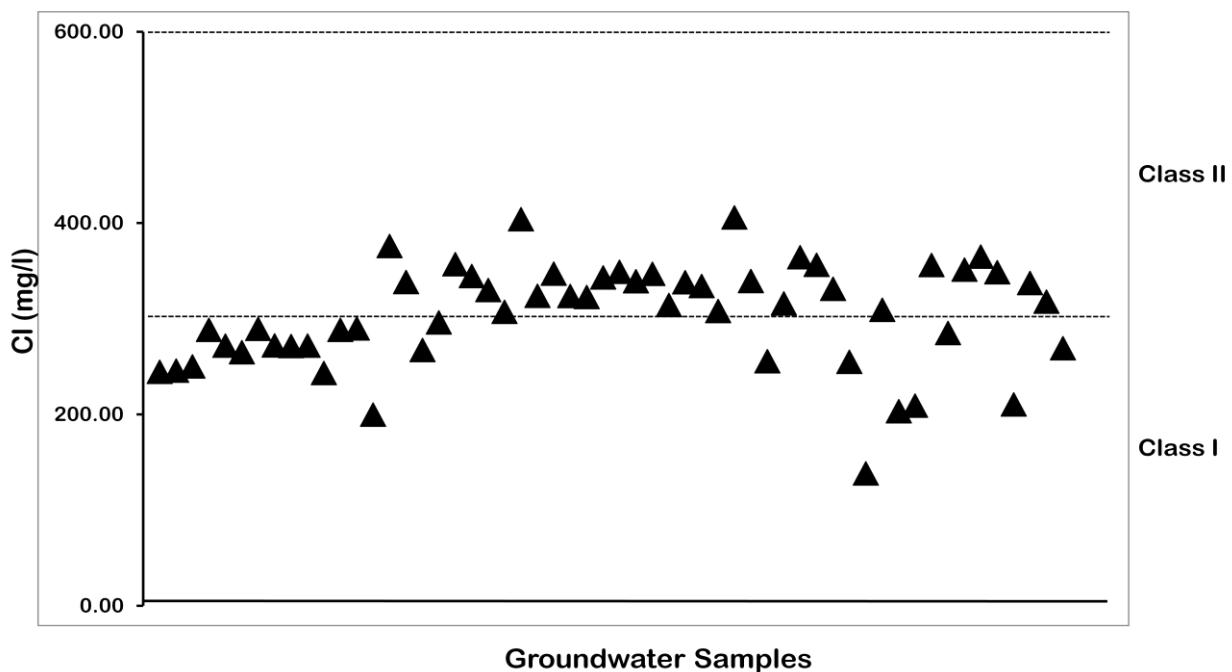


Fig. 9.15: Chlorinity index for the groundwater samples of the study region

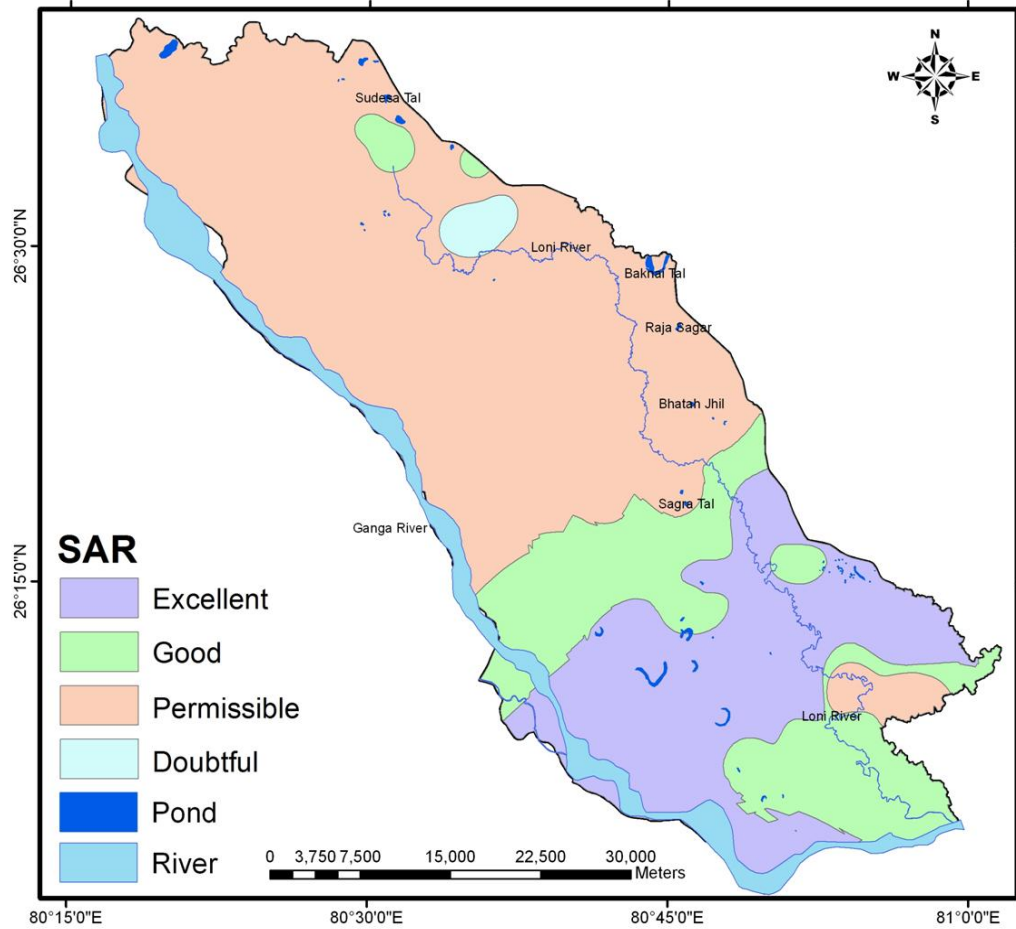


Fig. 9.16: Sodium adsorption ratio layer

Table 9.13: Suitability of groundwater for irrigation based on sodium adsorption ratio

S. No.	Range	Alkalinity Hazard	Class	Area (Km ²)	Area (%)
1	< 10	S1	Excellent	495.67	23.10
2	10-18	S2	Good	402.84	18.77
3	18-26	S3	Permissible	1223.15	57.00
4	>26	S4	Doubtful	24.26	1.13

9.3.5.4 Sodium percent (Na %) layer

Na % is calculated using the formula given below:

$$\text{Na}(\%) = \frac{(\text{Na}^+ + \text{K}^+) \times 100}{(\text{Ca}^{2+} + \text{Mg}^{2+} + \text{Na}^+ + \text{K}^+)} \quad (9.6)$$

where all the concentration are expressed in mg/l.

When the concentration of sodium is high in irrigation water, sodium ions tend to be absorbed by clay particles, displacing Mg²⁺ and Ca²⁺ ions. This exchange process of Na⁺ in

water for Ca^{2+} and Mg^{2+} in soil reduces the permeability and eventually results in soil with poor internal drainage. Hence, air and water circulation is restricted during wet conditions, and such soils become usually hard when dry (Saleh *et al.*, 1999). On the basis of Table 9.14 and Figure 9.17, we conclude that all the groundwater samples are in permissible range, so it is considered to be suitable for irrigation.

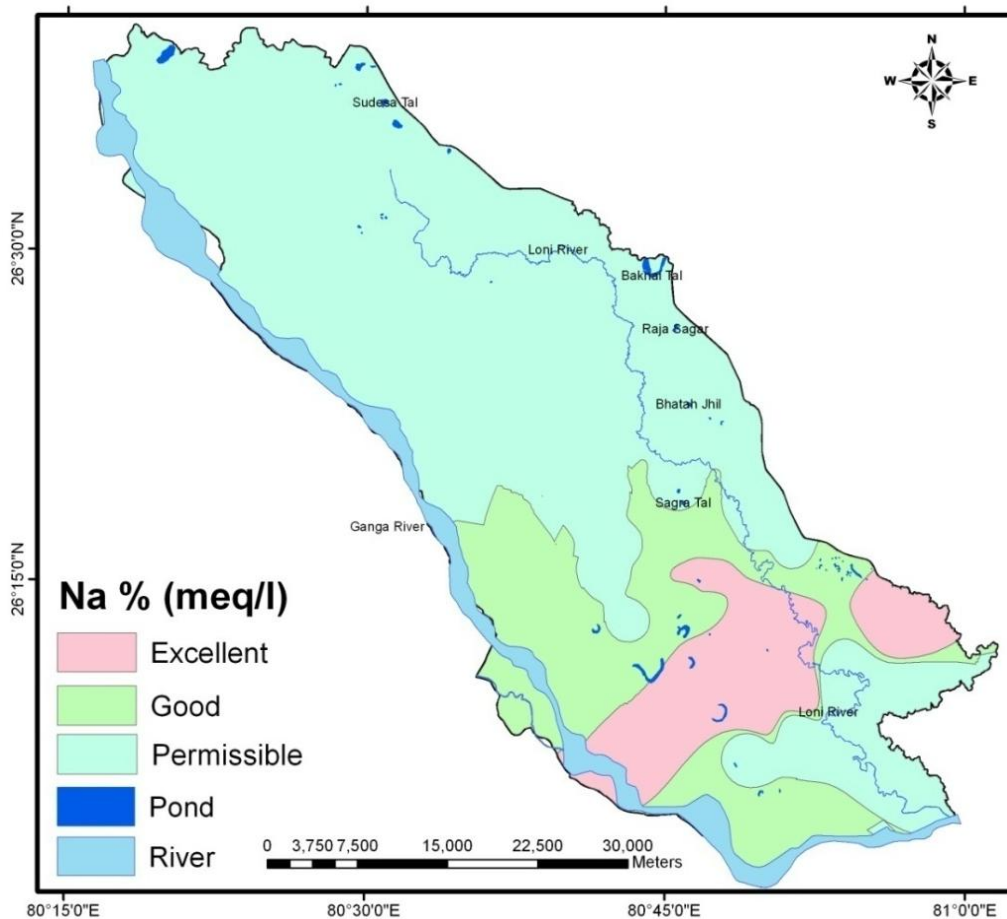


Fig. 9.17: Sodium percent layer

Table 9.14: Suitability of groundwater for irrigation based on sodium percent

S. No.	Range	Class	Area (Km ²)	Average (%)
1	< 20	Excellent	249.27	11.6
2	20-40	Good	452.35	21.1
3	40-60	Permissible	1444.3	67.3

9.3.5.5 Groundwater quality index for irrigation

To delineate groundwater quality map for irrigation purpose all the GIS layers (EC, SAR, Chloride, Sulfate and Na%) were integrated in ArcGIS 9.3 using overlay analysis tool, and categorized into four classes namely: excellent, good, permissible and doubtful as shown in

Figure 9.18. It was found that most of the area (about 99%) is suitable for irrigation, except few areas (about 1%) in Bichhiya block that are in doubtful range.

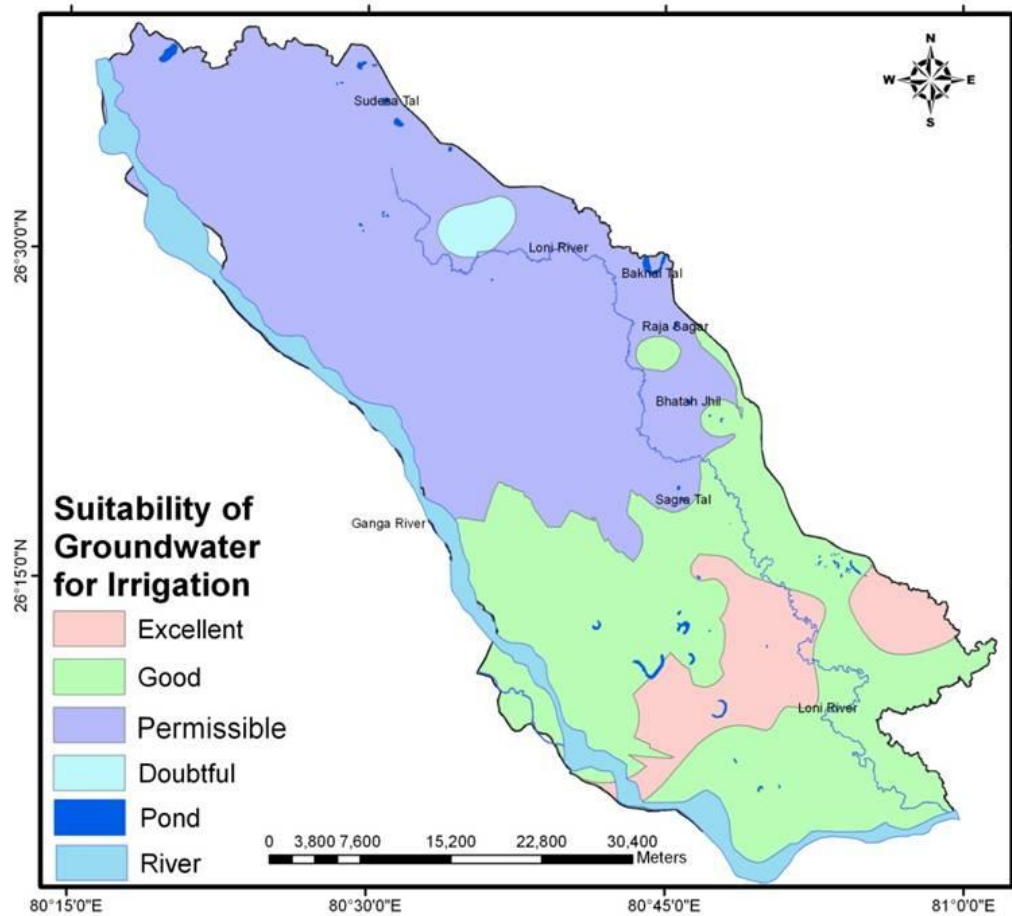


Fig. 9.18: Groundwater quality index map for irrigation purpose

9.4 CONCLUDING REMARKS

It is concluded that the most of the area is suitable for drinking purposes, except few area (5.46% of the total study area), which falls in western part of Sikandarpur block, and nearby the Unnao city and industrial area of Unnao district. On the basis of groundwater quality map for irrigation purposes, it was found that most of the area (about 99%) is suitable for irrigation, except few areas (about 1%), which falls in Bichhiya block.

CHAPTER 10

OPEN SOURCE WEB GIS TOOL FOR GROUNDWATER RESOURCE MANAGEMENT

10.1 PROLOGUE

A GIS is a computerized system that are designed to capture, store, manipulate, analyze, manage and present all types of spatial or geographical data. GIS converts diverse datasets into the form of easily accessible and readable maps and information (Agarwal and Gupta, 2014). The technologies that facilitate the widespread use and dissemination of spatial information among greater audiences are Web-based Geographic Information System (Web GIS).

The advantage of Web GIS is real-time accessibility, ensured its potential as an important medium for the dissemination of GIS functions and data. It promoted the participation of the public and customers, and resulted in the increased scale and profitability of many GIS projects (Cheng, 2006). A Web GIS system can be modeled using the client-server architecture. It is an integrated client/server network system where web browser application provides Internet users to access GIS application software residing at server end. The client on web can work with GIS data interactively, using web browser without owning GIS software on his/her local machine. In the field of GIS, the Internet has played a significant role in the development of new facets of the technology that open many doors for expanding the options for building spatially-enabled web applications.

Growing trend of the adoption of open source technologies for Web GIS is largely due to the fact that many successful Open Source Software (OSS) projects have proven under many circumstances to perform at acceptable and sometimes exceptional levels as compared to proprietary products. In the present chapter, the development of a web enabled geoportal using open source GIS technology is briefly outlined.

10.2 GEOPORTAL

A geoportal is a type of web portal, which are used to find and access geographic information (geospatial information) and associated geographic services (display, editing, analysis, etc.) via the internet. Geoportals are important for effective use of GIS and a key element of Spatial Data Infrastructure (SDI). Its architecture illustrates web browser, clients and server mechanism. The dataset is organized into database server as a repository. In this

study, a geoportal is developed using MapGuide OSS, which is based on three tier (client, web and server) architecture (MapGuide, 2010). Figure 10.1 illustrates the general architecture.

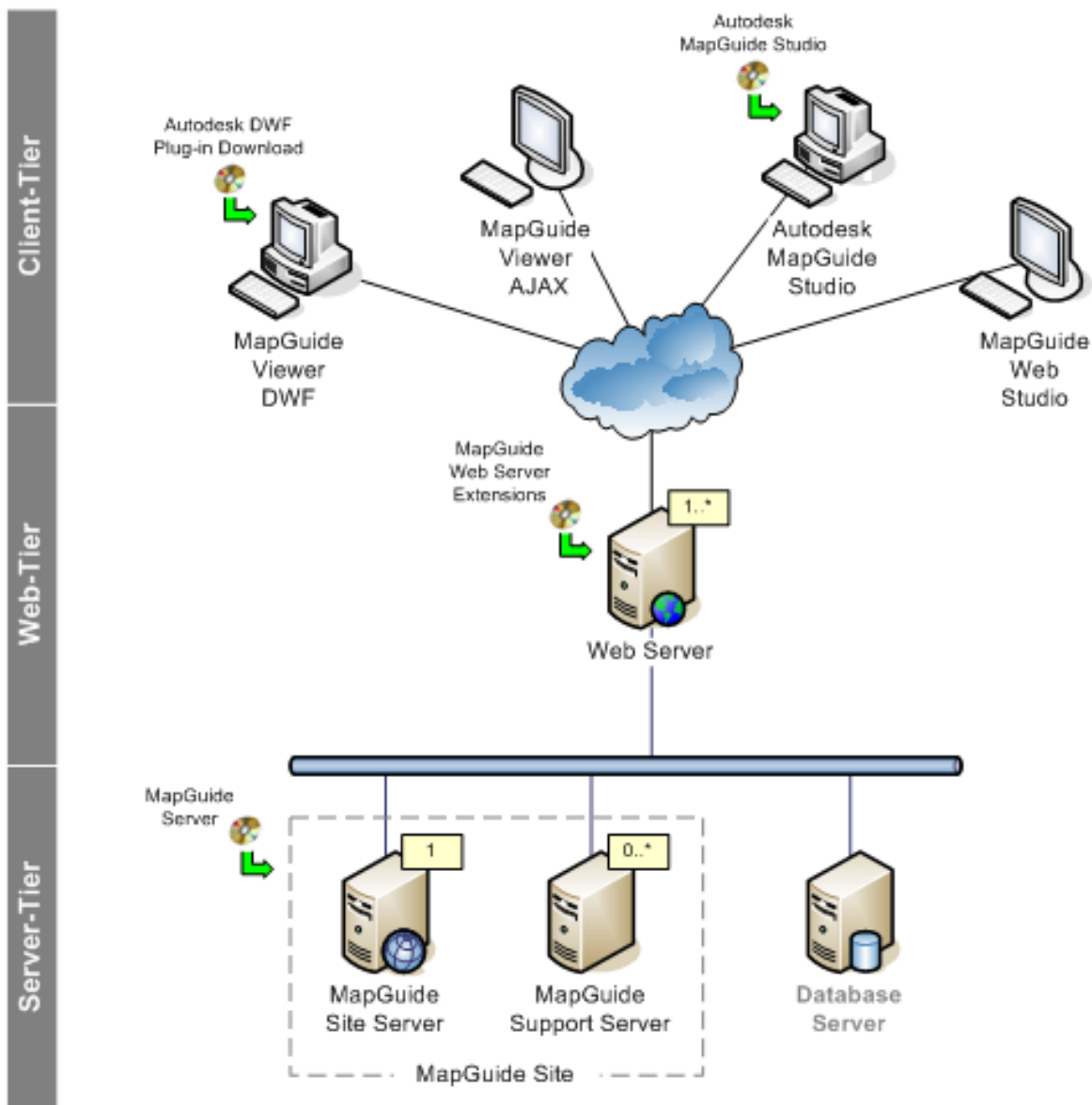


Fig. 10.1: The architecture of MapGuide open source (MapGuide, 2010)

10.3 METADATA

The significance of metadata with geospatial dataset has been recognized due to demand perspective. The metadata can be defined as information about data. The advantage of metadata is to enlarge the opportunities of interoperability. Interoperability comprises accessing and sharing data across multiple information sources. The interoperability can be achieved by open standards and protocols such as Open Geospatial Consortium (OGC) services (Web Map Services (WMS), Web Feature Service (WFS), Catalogue Service for Web (CSW)) and

Geography Markup Language (GML), Z39.50 etc., for the development of the interoperable metadata catalogue framework.

10.4 METHODOLOGY USED

The conceptual flow elaborates the processes involved in geoportal and its metadata creation using open source tools and technology is shown in Figure 10.2, and illustrated in the following steps:

Step1: Coordinate transformation

A GIS database is created in ArcGIS software, and converted into standard projected coordinate system (UTM WGS 84 and 44 N zones).

Step2: Data capture

The entire GIS database has been clipped using clip tool to develop a geoportal for the desired area.

Step 3: Tool selection for creation a website

On the basis of trials (explorations) of several open source GIS software, emphasizing mainly on ease of use ended in favor of Mapguide open source. It allows users to quickly develop and deploy web mapping applications and geospatial web services to a web-based platform. It is a powerful viewer that provides support which includes:

- For feature selection
- Measuring
- Map tips
- Buffering
- Basic queries
- Property inspection

Thus Mapguide OSS was selected to deploy the maps on web. Mapguide open source was downloaded freely from internet, and then installed and configured to Apache HTTP Server and PHP using the bundle configuration options. The service name for Apache is Apache MapGuide that listens on port 80 and it does not conflict with any existing web server, by default, port is 8008. The development environment is then selected as PHP.

Step 4: Selecting the authoring tool

Mapguide Maestro is an authorized tool of MapGuide, which is used to upload feature and raster data. It is also used for creation and designing of GIS layers as well as creation of maps.

Step 5: Creating a folder structure

In this step, folder structure is created to define the thesis. In this thesis we created the folders for data, layers, maps and layout.

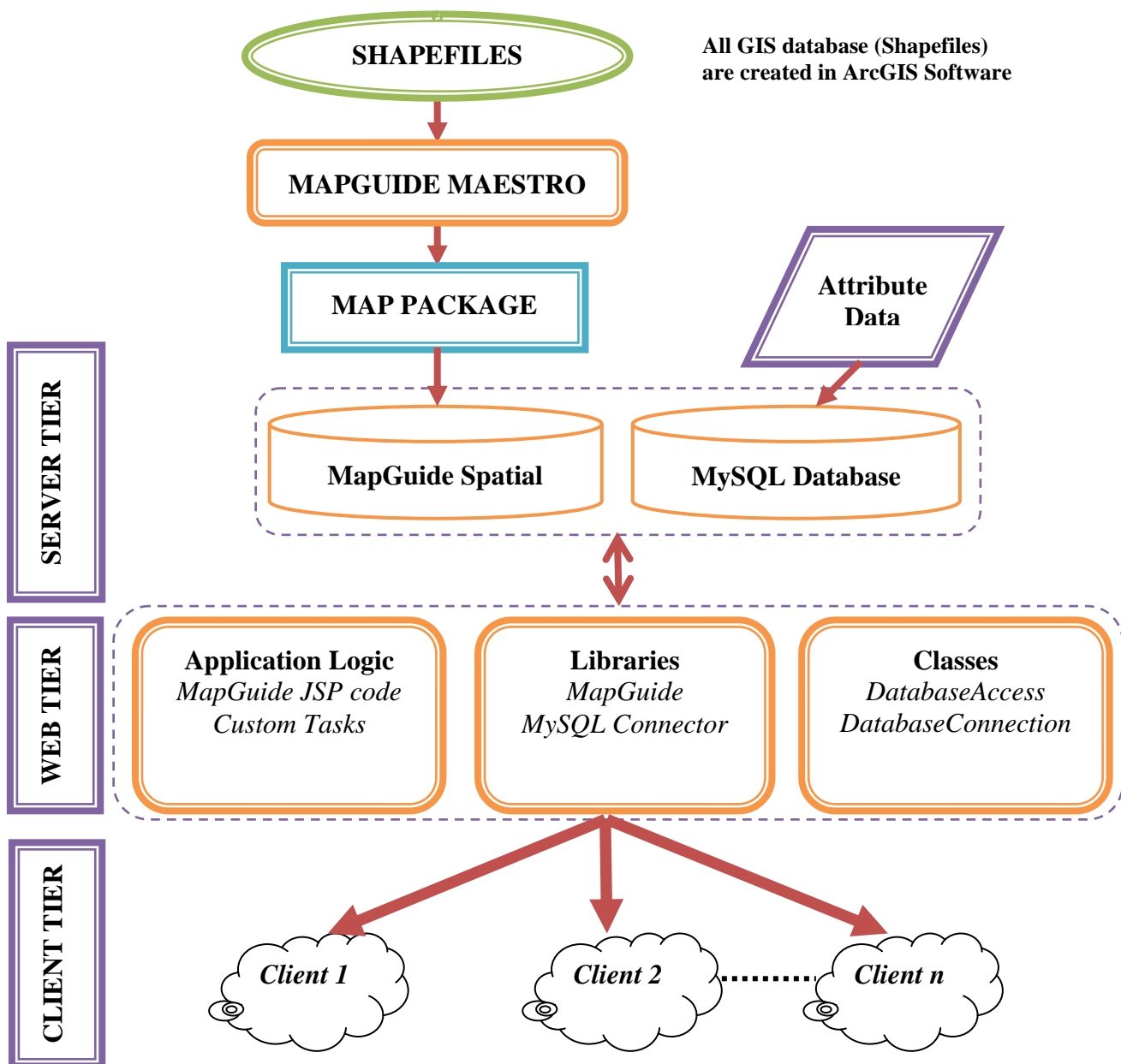


Fig. 10.2: Methodology used

Step 6: Connect to an MYSQL database

Instead of connecting all the shapefiles directly via MapGuide Maestro as described above, we loaded all the spatial data to the MySQL database, and then connected it to MapGuide application using MapGuide Maestro and its MySQL FDO provider. This approach was not pursued as this data is likely to remain relatively static, and therefore placing them on a relational database would create an unnecessary overhead due to database connection and querying. Instead, we used MySQL to simply store all the attribute data.

Step 7: Setting the style for Layer

In this step, we styled the feature layers (point, polylines and polygon) using styling tool to makes layers more interactive and understandable form to the user.

Step 10: Creation of new map

This step involved creating new maps and setting its properties. The basic description of the map was entered here leaving the coordinate system section blank because the map automatically added the coordinate system of the first layer that was added to it. Those layers are added that we wanted to display in geoportal.

Step 11: Organize the layers in a map

The layers are organized in an appropriate manner (It means starting with point feature then polyline feature then polygon feature) so that viewers can see all the features clearly. Labels were also generated on the map.

Step 12: Adding tooltips

To improve on the usability of the system, tooltips were included on the map Tooltips are pop-up boxes that contain information about the features in the map. Users will be able to view the tooltips in the web browser. When a user points the mouse to a given feature, a tool tip appears describing, briefly, the specific feature under scrutiny. Whenever a user places the mouse cursor on a feature, the information set on the tool tips would appear automatically.

10.5 RESULTS AND DISCUSSIONS

The main page of website contains menu bar, side bar and map window, as shown in Figure 10.3. Menu bar contains different modules such as Home, GIS database, artificial recharge sites, groundwater modeling, groundwater vulnerability, groundwater quality and

geoportal. Side bar contains information about the study area and field photographs of study area. Map window shows the study area location. All the modules contain static maps that are generated using GIS, related to study area except the geoportal.

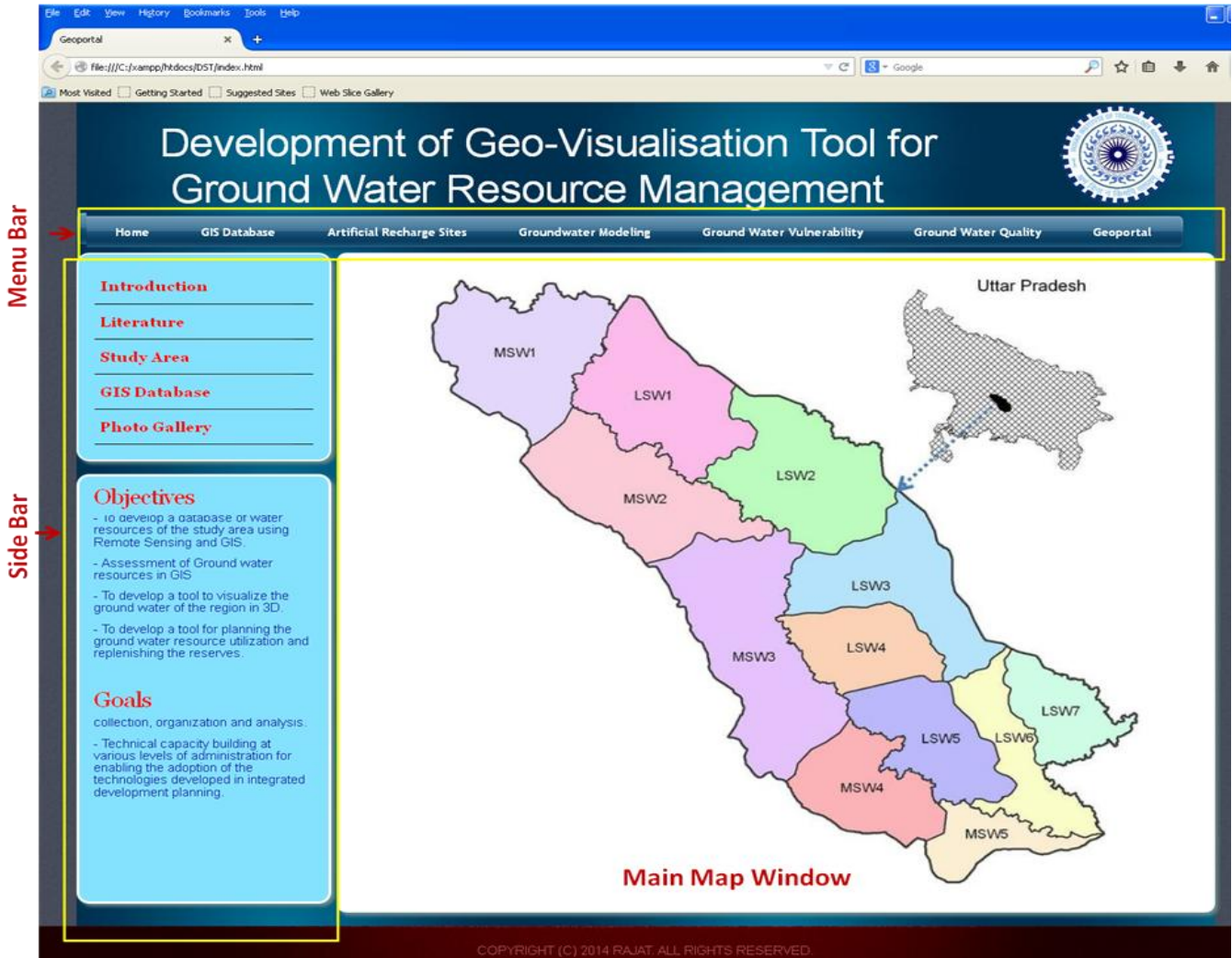


Fig. 10.3 Website main page

Geoportal is a tool that contains the dynamic maps its metadata information of study area. Its layout is described as toolbars, legend panels, tool bars and map window, as illustrated in Figure 10.4. The toolbar is used to control the map functionality, such as zoom in, zoom out, fit to extent querying and buffer analysis etc. The layer control is performed by the legend panel. At the bottom, it shows the scale bar, which contains the scale information as well as geographic coordinates of the area.

The feature, such as canal, drainage, geomorphology, blocks, sub-watersheds, geology, soil, and all the GIS layers and their output such as groundwater quality index, groundwater

potential zones etc., are created in previous chapters are deployed in geoportal. Some functionality of tools on different layers is presented in Figures 10.5 to 10.15.

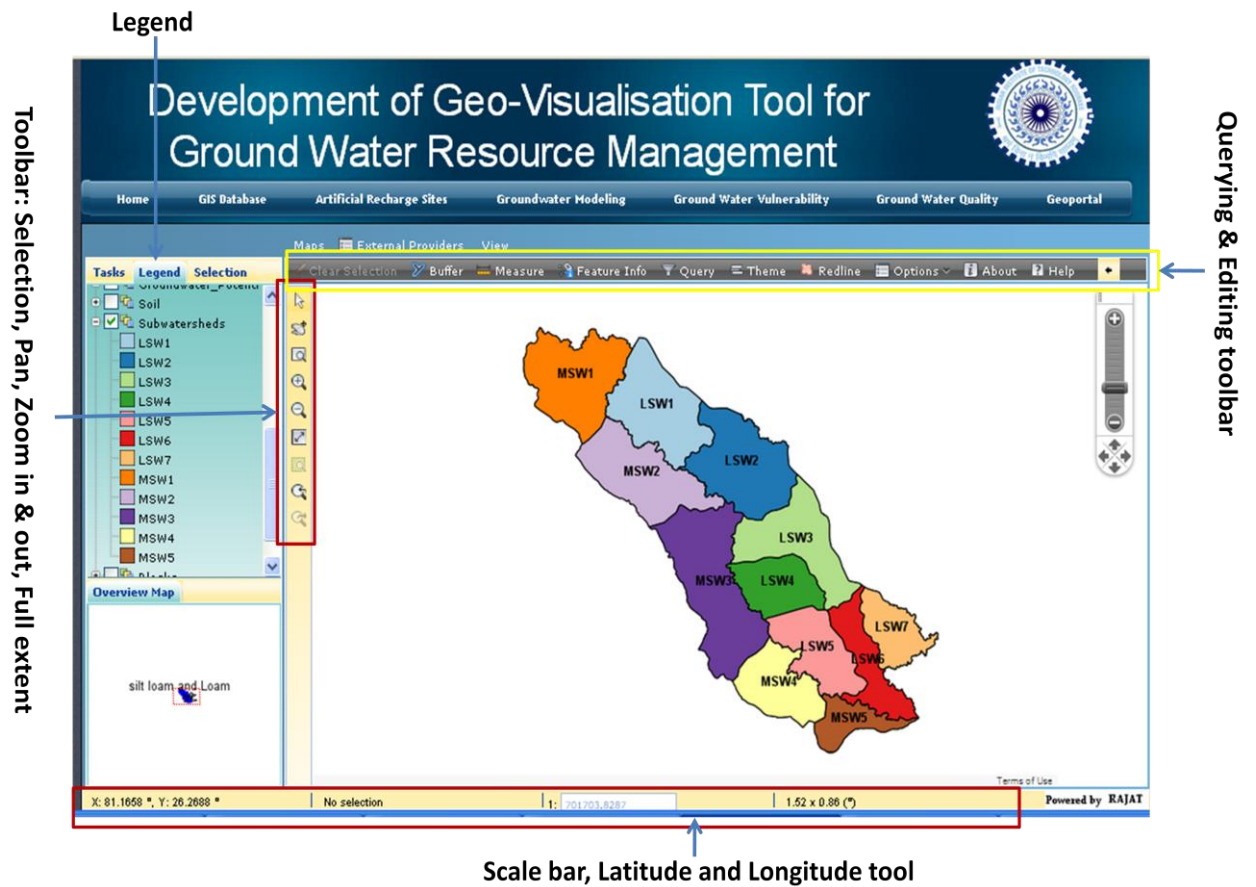


Fig. 10.4: Geoportal main page

A group of features can collectively be selected within a particular layer. The extent of select is defined by a polygon, rectangle or point. Feature info tool is very important tool that displayed all the information of selected or desired layer on single click. In Figure 10.5, we showed the application of feature info tool to display the information of canal layer. The application also allows the user to print the content of the map area by using print button respectively from the menu bar. It also shows the scale of plot and the date of plot, though the information plotted will be relative to how frequently the information is updated.

The user can perform spatial and non-spatial queries, and enquire for more information other than what is presented in the property pane. Most of the common GIS analysis can be performed with this application, thereby informing users on their decisions relating to customary land within the study area. Some of the analyses that can be performed are:

- Buffer analysis
- Measurements
- Non – spatial selection
- Spatial selection

Using buffer analysis, the user can define a region of interest marked by a fixed distance relative to a particular feature. The buffer analysis may be used in selecting a suitable location relative to the position of another feature by defining a buffer region around the feature. In the example below, Figure 10.6 creates a buffer of 1 km along the canal, which is shown in green. The buffer region is added as a new layer which can be printed but will be lost when the browser is closed or the page refreshed. The region is made transparent to the user's specification.

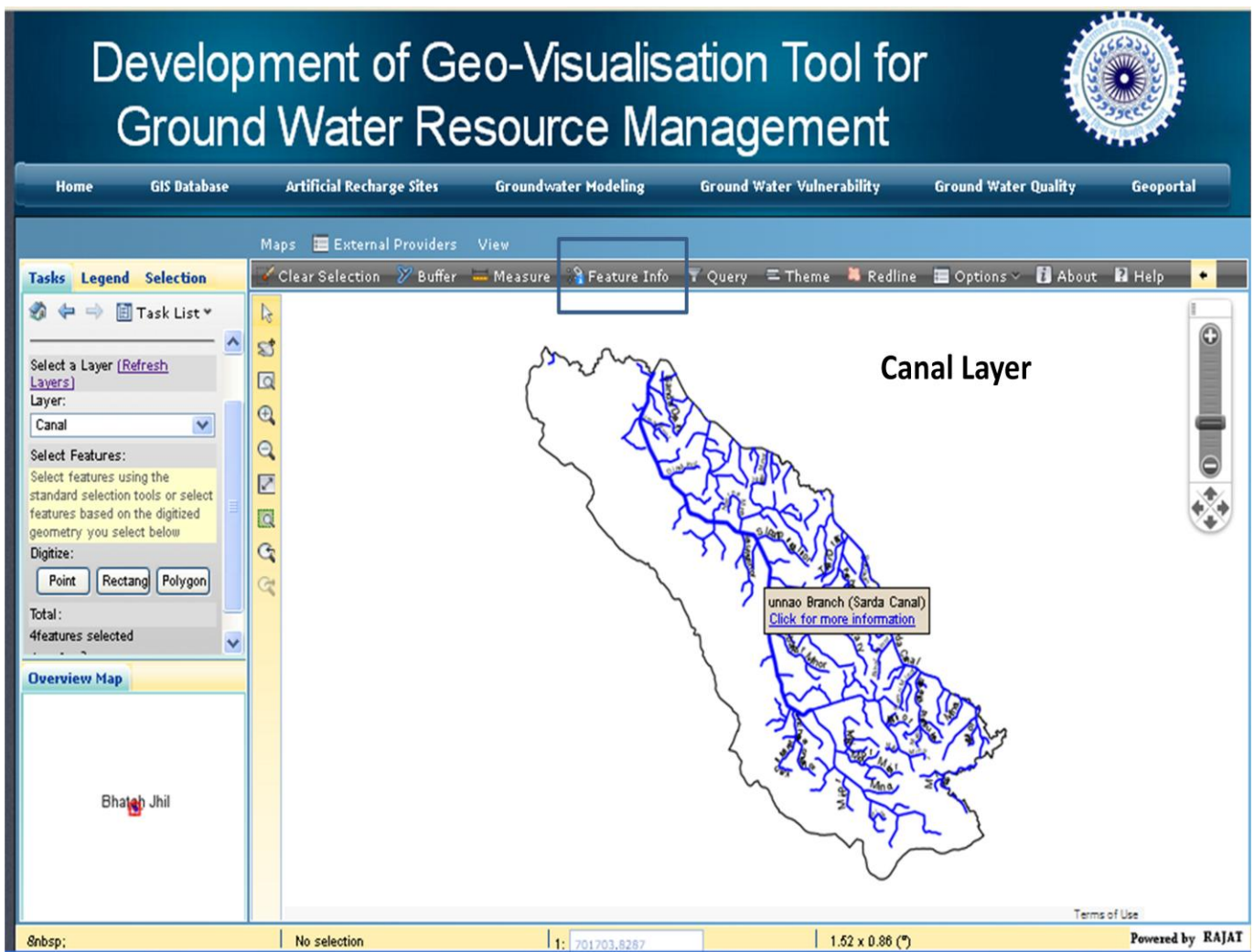


Fig. 10.5: Feature information using identify tool

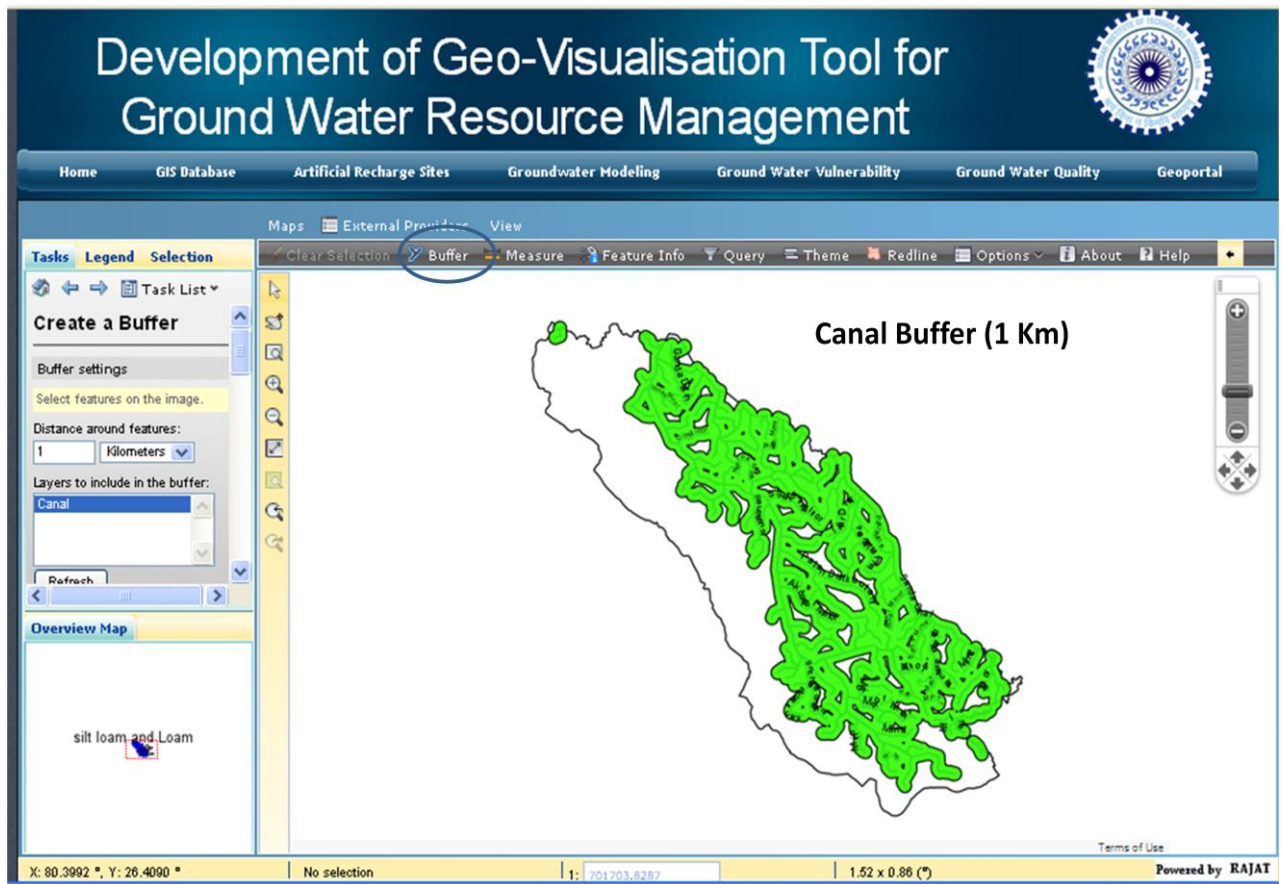


Fig. 10.6: Coverage analysis using buffer tool

Measurement of distances and areas can also be done by using the measure tool. The system gives the distance estimation between two points after clicking on the points of interest when the measure tool is selected. The system automatically estimates an area for the user if the network of points forms a polygon. A series of measurements that has been done with the area of the polygon formed estimated.

There are so many tools are also available in tool that have different-2 applications. The user not only seen the thematic layers that are previously designed by author (Figure 10.7 & 10.8) he/she can prepare thematic layer on the basis of the attribute information of the layer. In Figure 10.9, we show that simple lined geomorphology map is converted into thematic map on the basis of geo-morphological landforms. A new thematic layer of geomorphology is created layer which can be showed temporarily, it will be lost when the browser is closed or the page refreshed.

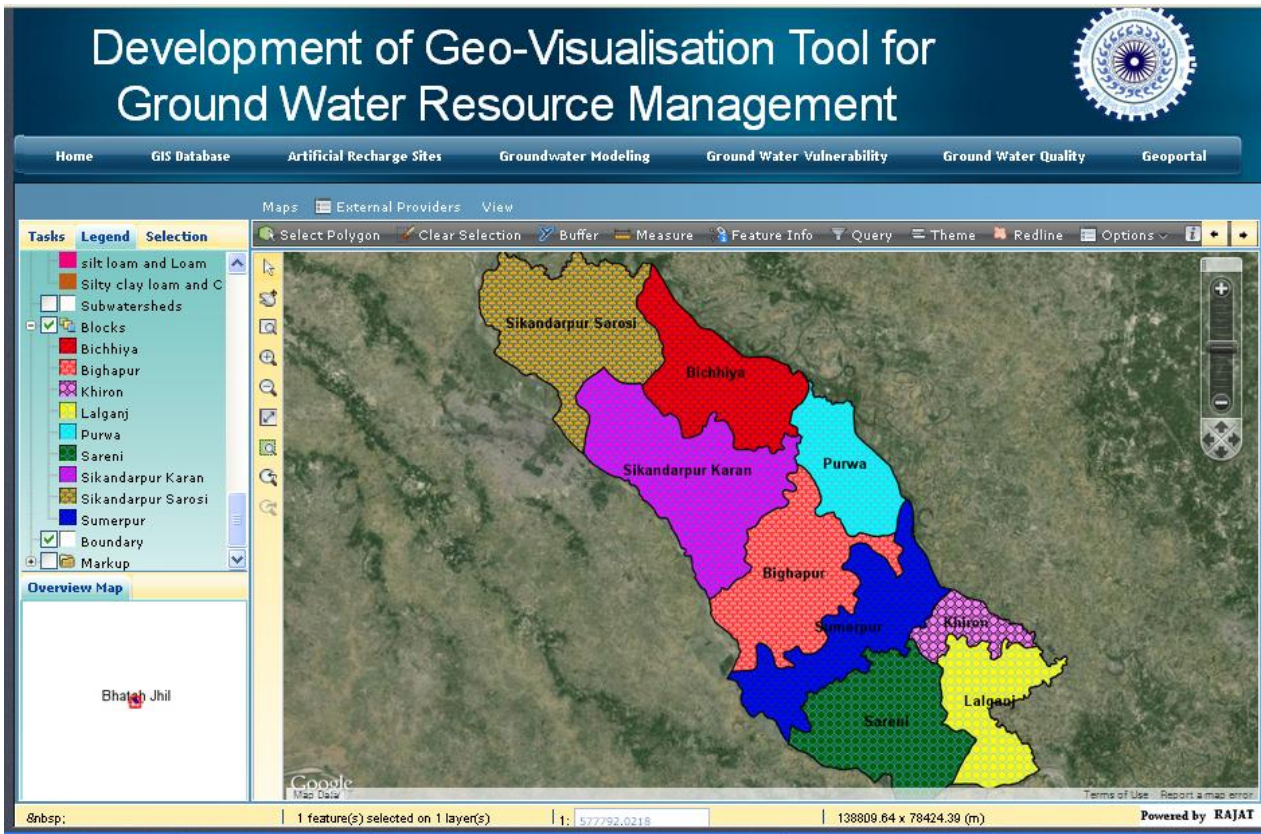


Fig. 10.7: Thematic map of block layer

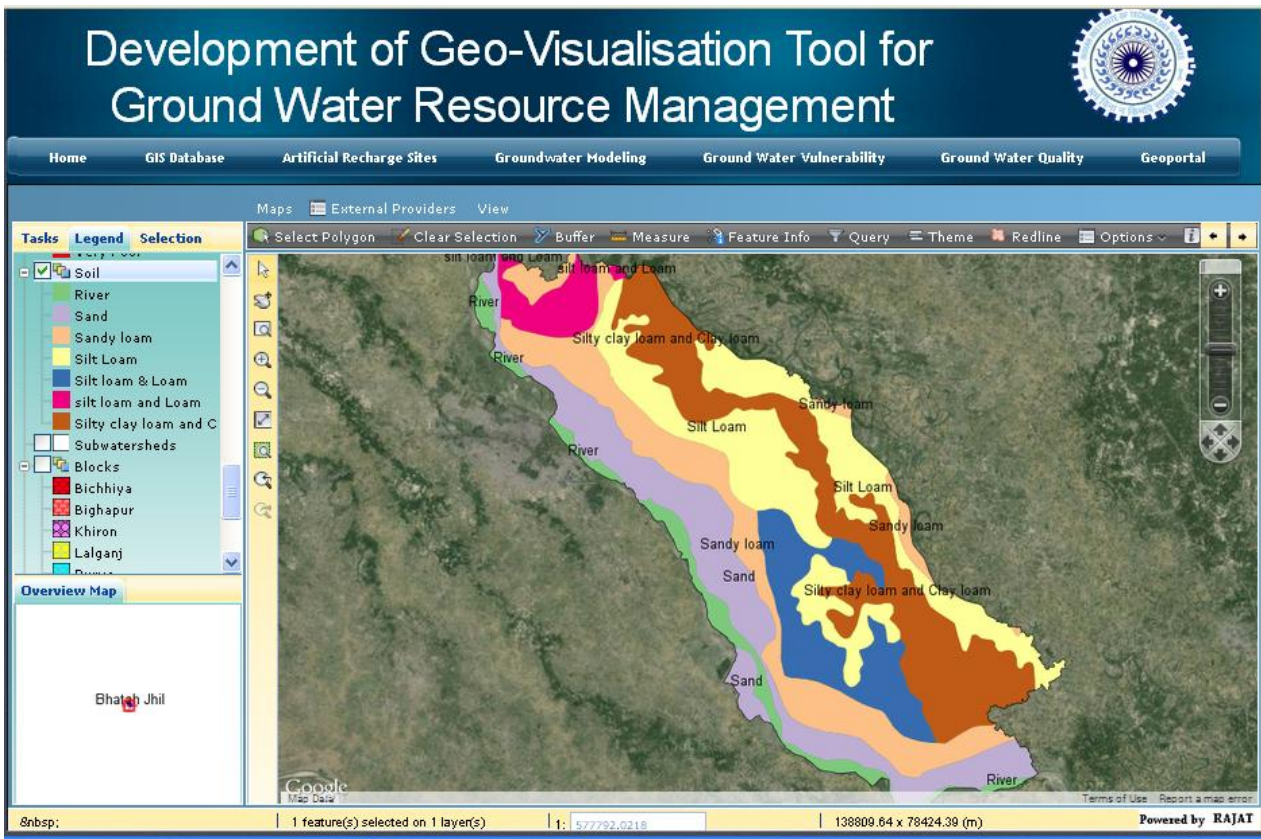


Fig. 10.8: Thematic map of soil layer

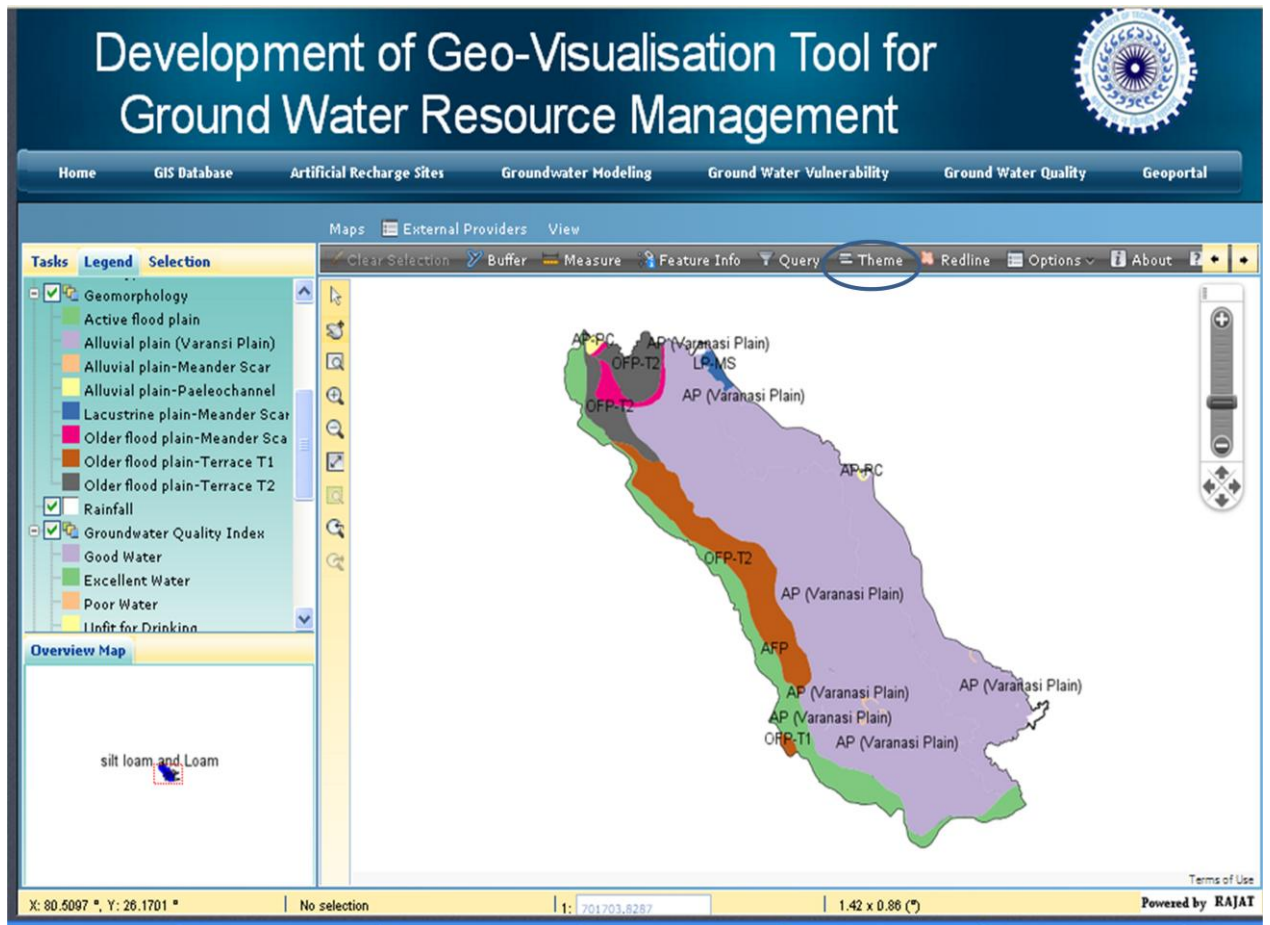


Fig. 10.9: Thematic map of geomorphology layer

The groundwater regional data of the Loni and Morahi watershed was created at 1:50,000 scale. The metadata was generated for entire groundwater dataset and attached with thumbnails using open source software. In Figure 10.10 (a) and 10.10 (b) showed the sample of groundwater metadata creation of soil layer. In Figure 10.10 (a) we showed the attribute data by clicking on view data tool of portal and in Figure 10.10 (b) displayed the feature layer by clicking on view feature tool in portal. Similarly, we can extract or view the metadata of all the GIS layers related to groundwater.

A mashup application is defined as the integration of publicly accessible information with owned privately created data sources. In this study we can add Google earth and Google map services in geoportal as shown in Figure 10.11 and 10.12. In Figure 10.11 sub-watershed layer is overlaid on Google earth image as well as road layer is overlaid on Google map.

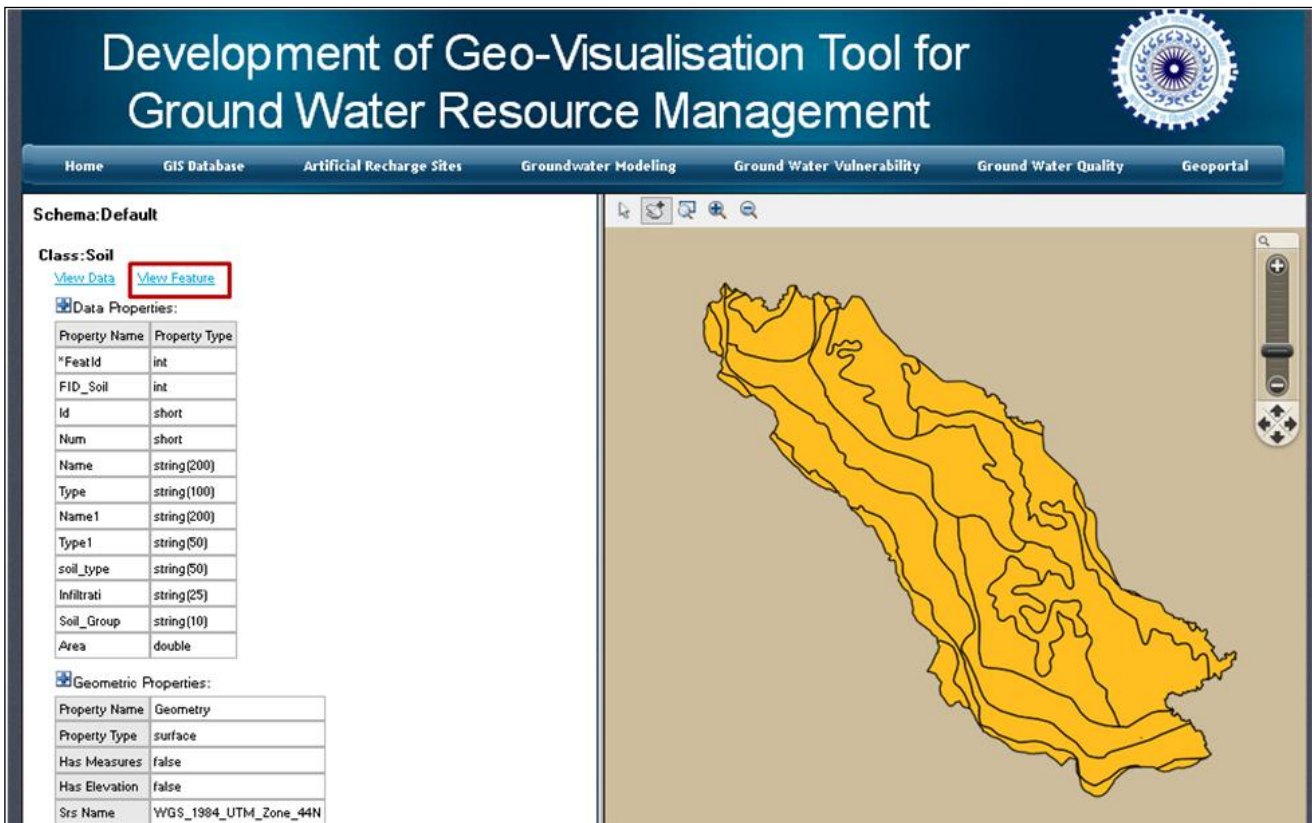


Fig. 10.10 a: Metadata of soil map (feature view)

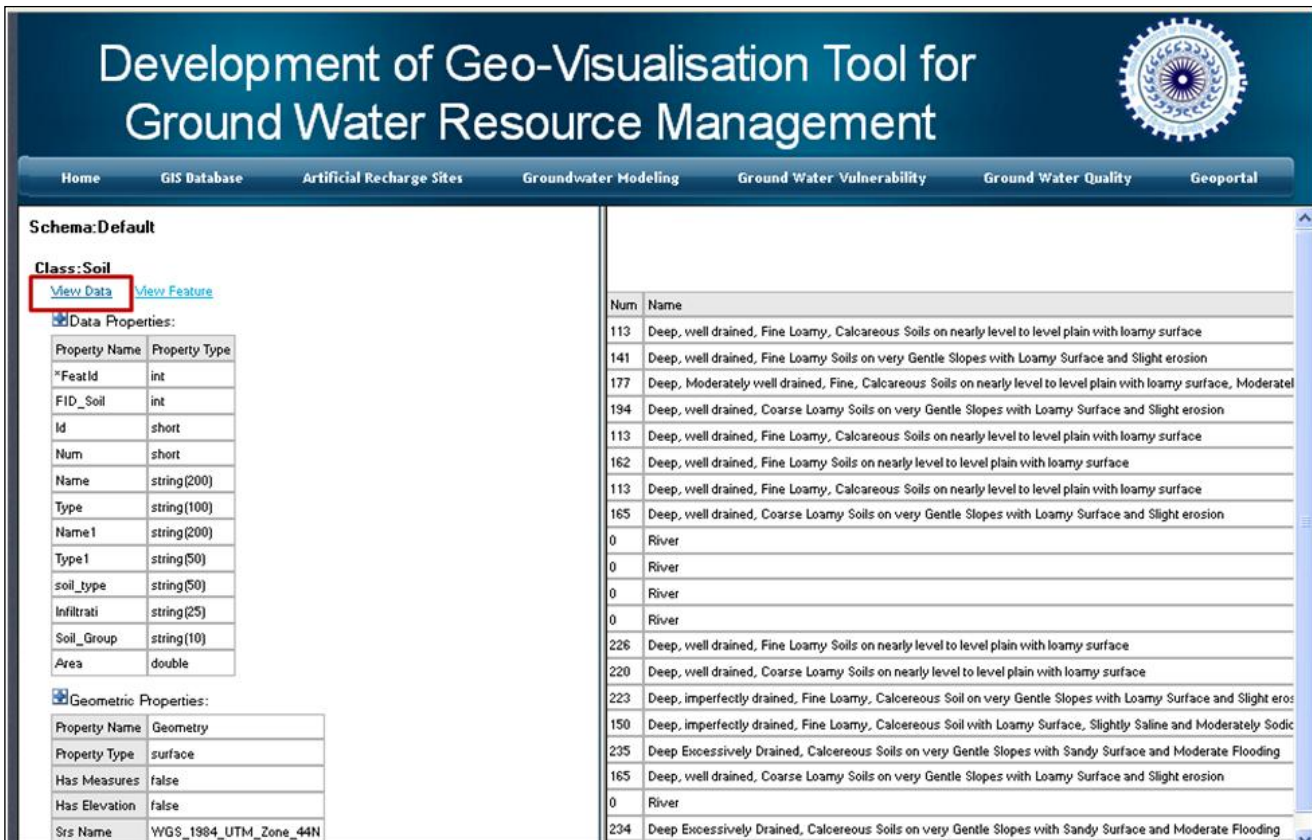


Fig. 10.10 b: Metadata of soil map (data view)

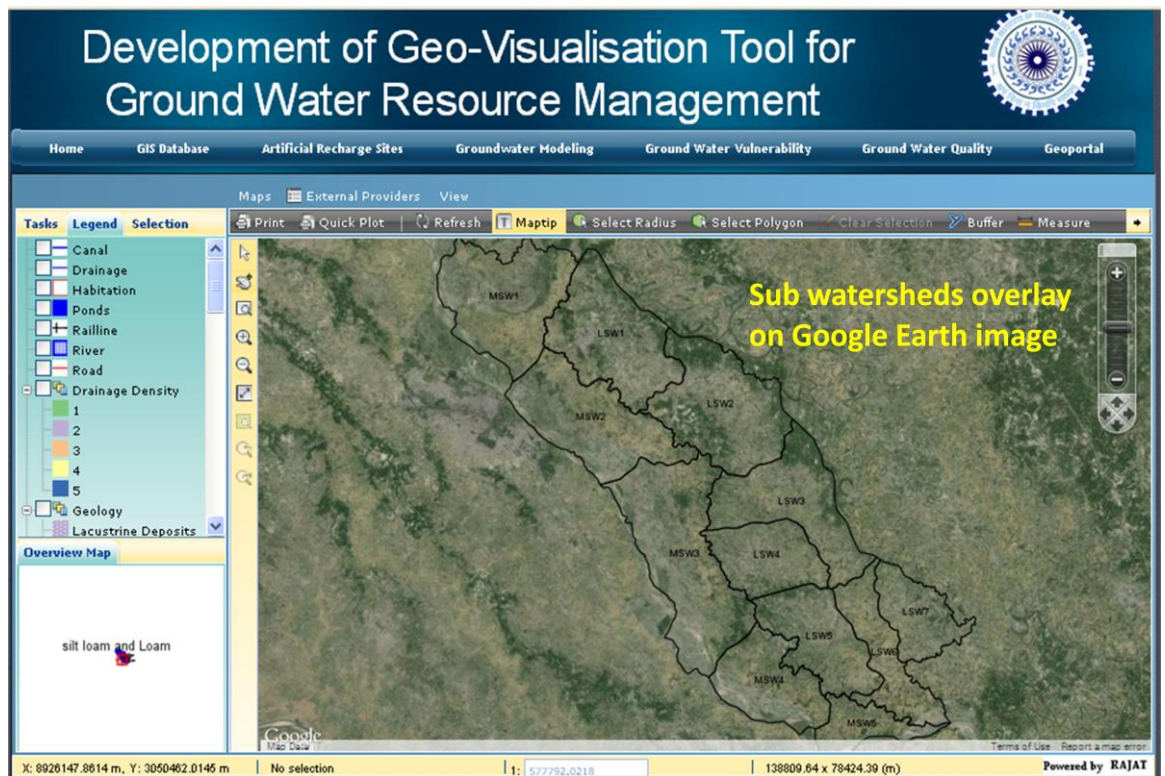


Fig. 10.11: Mashup application using web services (Sub-watershed overlaid on Google Earth image)

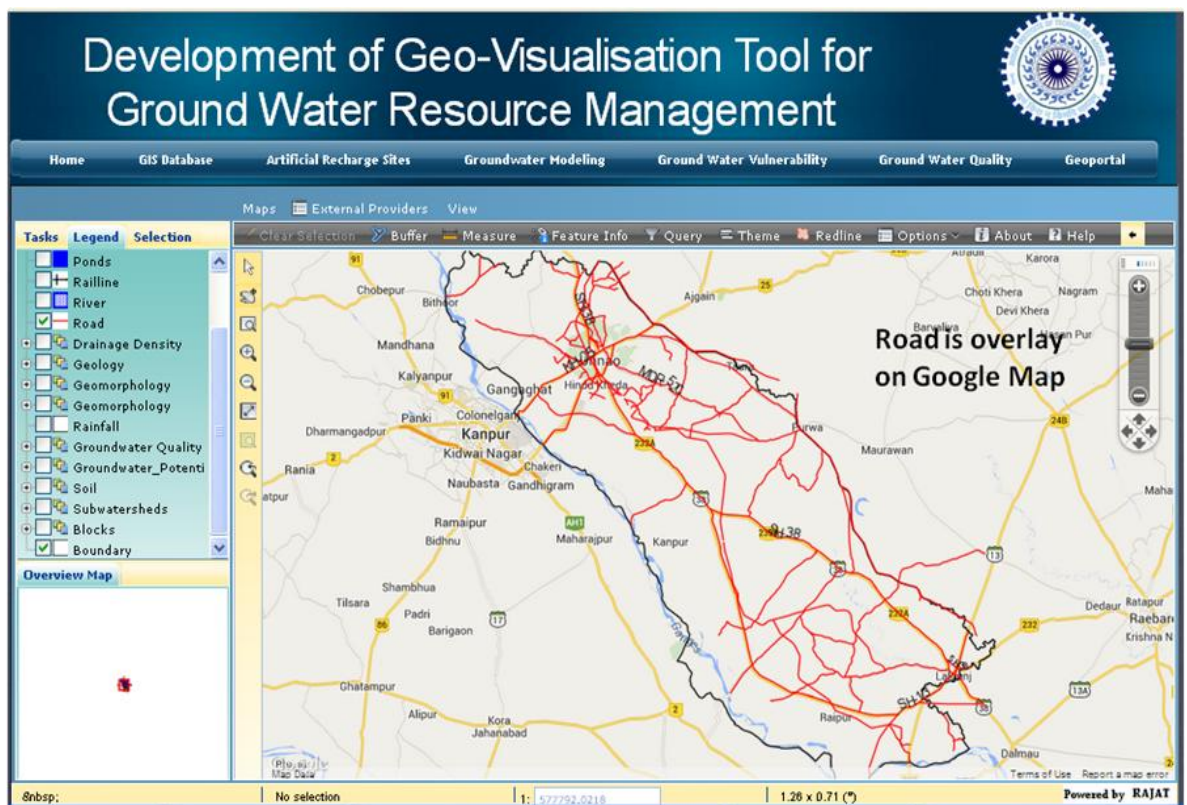


Fig. 10.12: Mashup application using web services (Road is overlay on Google map)

A non-spatial selection of a feature from the attribute data of features within a specific layer may also be done by using the query tool. The query tool presents the user with the option of defining the criteria for the query in a query dialogue box. When the criteria for the query are defined, the application queries the attribute data to find the features that satisfy the criteria defined by the users. In the example bellow, Figure 10.13 shows a query box with a criterion for selecting an unfit for drinking water area, to take remedial measures.

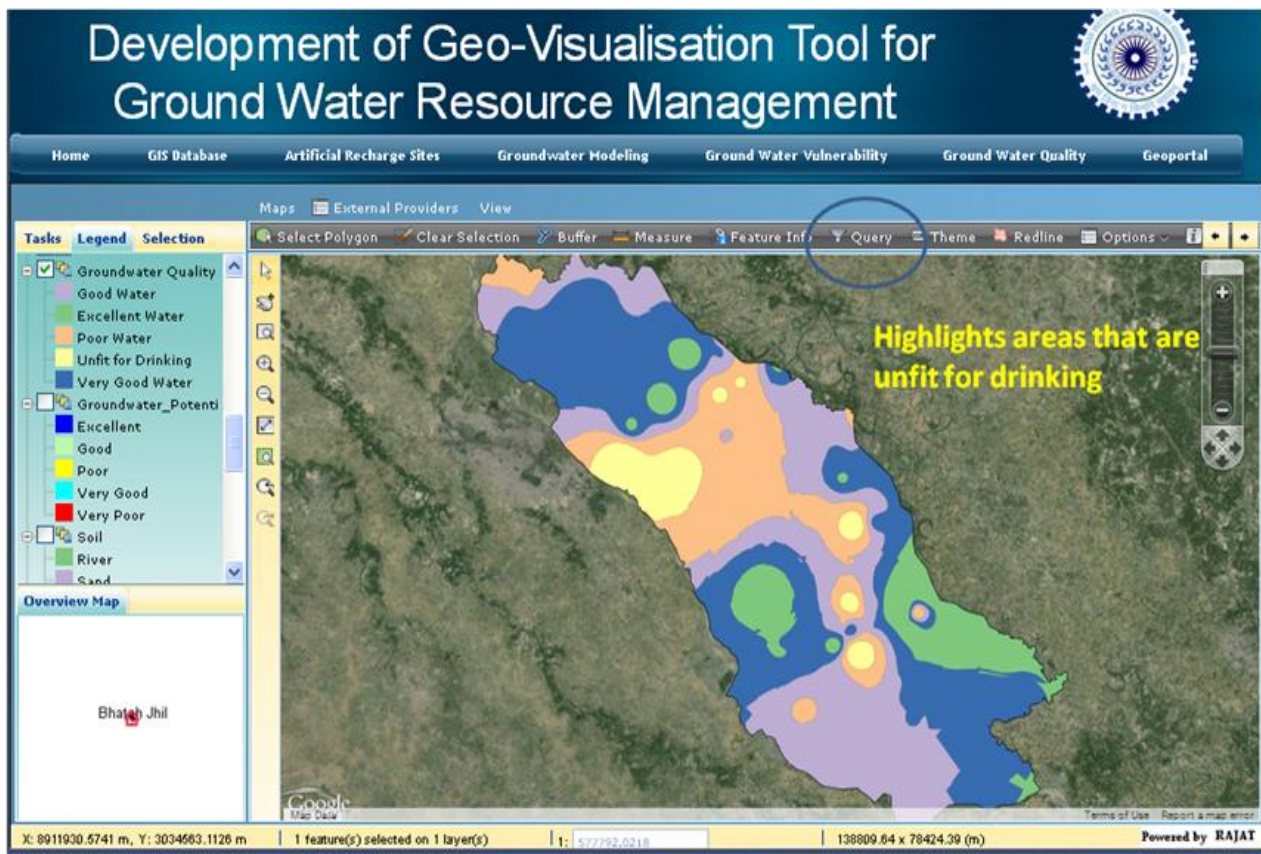


Fig. 10.13 (a): Spatial query

The more layers can be added from local GeoServer or remote GIS server by adding URL of the particular server. Remote server add all the layers mentioned in the repository. The advantage is that single geoportol can access the data from multiple remote server using web services technology.

We can not only extract all the information of complete study area, It will be extracted subwatershed wise and village wise also. For example Figure 10.14 shows the groundwater database of Loni sub-watershed 1. Similarly we can see information of all the other sub-watershed.

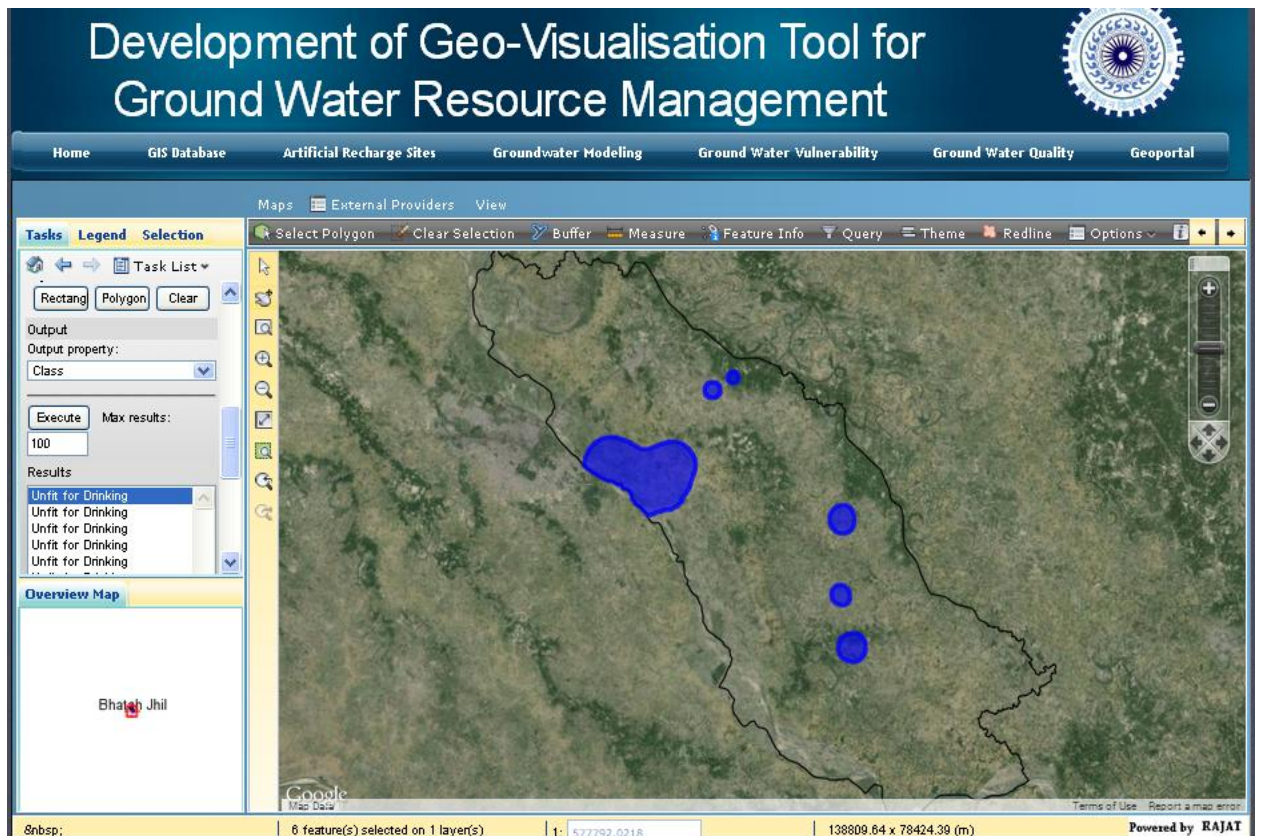


Fig. 10.13 (b): Result of spatial query

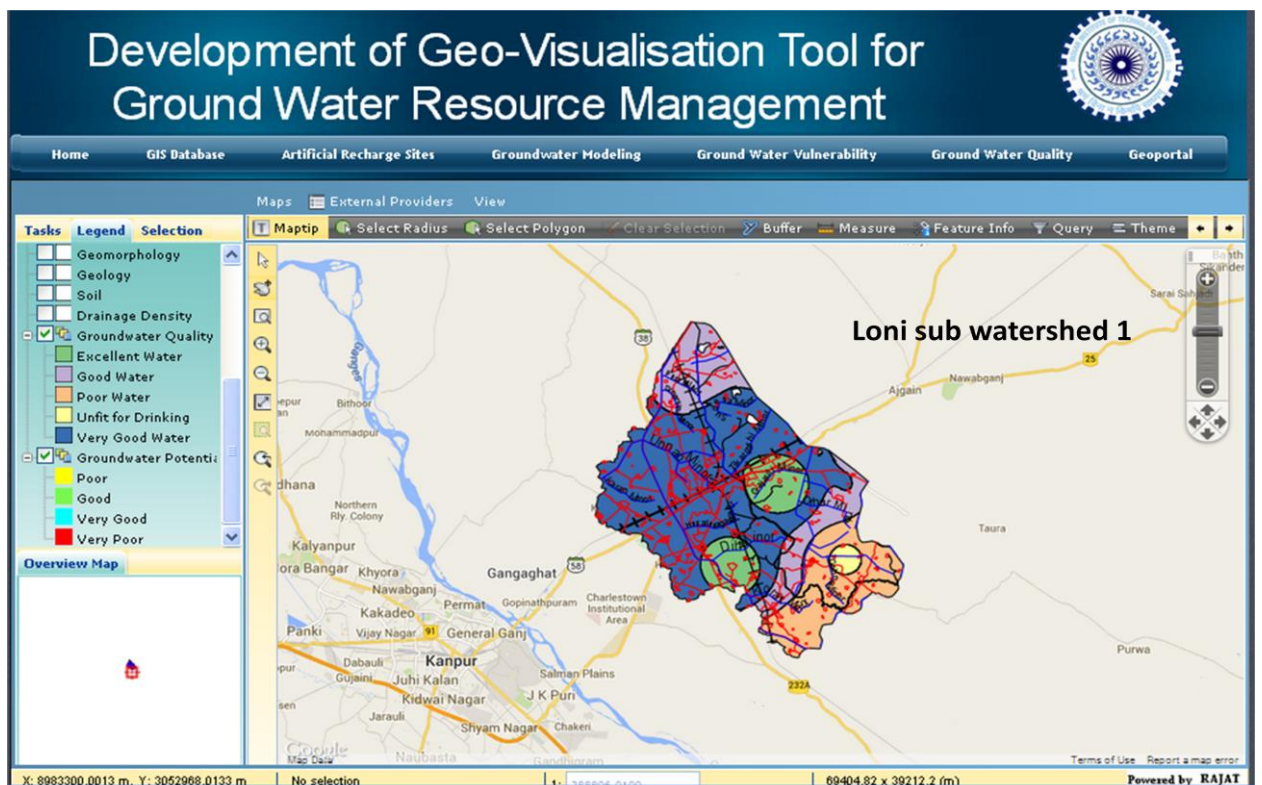


Figure 10.14: Groundwater quality of Loni sub-watershed 1

10.6 CONCLUDING REMARK

The open source web based geoportal has been developed that demonstrates the applicability of tool in groundwater management. The Geoprocessing in web GIS environment is emerging area where GIS researcher are trying to build a complete spatial decision support system (SDSS) and expert system to solve GIS based decision problem. This application can be enhanced to provide a complete GIS solution in web browser environment.

The study demonstrates the capability of RS and GIS technique in management of groundwater resources and development of web enabled tool using open source technology. On the basis of this study, we conclude the following points.

11.1 CONCLUSIONS

- Groundwater potential zones map was created in GIS environment, and it was found that very poor areas lies southern east portion of Loni watershed.
- Groundwater fluctuation layer indicates that it is low in central part and gradually increases towards northern west and southern corners, and reaches up to 4 m.
- Rainfall-runoff modeling reveals that 19 % of the study area has 1.71 to 2.02 mm/day (high) runoff depth potential. It is also found that for 40 mm/day storm event, runoff depth estimates range between 23.87 mm/day and 4.4 mm/day.
- RS and GIS greatly helped in extraction of morphometric parameters faster and accurate which were used to prioritize the watersheds. Watershed LSW6 (Loni Sub-Watershed 6) was found to have highest priority, and therefore it is prone to relatively high erosion and soil loss.
- Twenty two suitable sites were identified for artificial recharge structures, such as percolation tank (5), nala bund (4) and check dam (13). Out of the 13 check dams, 4 already exists which were found during the field visit. This study is important to identify the suitable locations for artificial recharge structures.
- On the basis of stage of ground water development and the study of long term trend, it was found that Sikandarpur block falls under critical category. Well-wise trend analysis indicates that most of the wells (upto 61%) have falling trend in both pre- and post-monsoon seasons.
- The steady state calibration of the model shows a close agreement between the simulated and observed heads with the residual mean of -0.32 m, variance 1.27 m and correlation coefficient as 0.975. In transient state, calibration of the model shows a close agreement between the simulated and observed heads with the residual mean of 0.01 m, variance 2.36 m and correlation coefficient as 0.953.
- The calibrated and validated statistics for different time steps of RMS error has been found in the range of 1.24 m to 1.63 m throughout the calibration period, which is

within the acceptable range. Residual mean has been found to lie within -0.49 m to 0.49 m, absolute residual mean within 0.9 m to 1.25 m throughout the calibration period.

- On the basis of calibration and validation of the model by observing the calibrated aquifer parameters, hydraulic conductivity was found to lie between 15.4 and 93.1 m/day in the area, and specific yield in the range of 0.002 to 0.12 in different zones of area.
- On the basis of DRASIC-LU model, it is indicated that 13.44% and 19.95% areas are categorized as very high and high vulnerable zones, respectively. It is further validated using nitrate and fluoride data and found to be satisfactory results.
- A relationship between nitrate and groundwater depth was established, and found that concentration of nitrate was higher in shallow water table as compared to deeper water table.
- GWQI indicates that area lying in unfit for drinking category is about 5.46% of the total study area, which falls in western part of Sikandarpur block, and nearby the Unnao city as well as industrial area of Unnao district.
- The web GIS based geoportal has been developed in this study for technology demonstration purpose. This portal provides a GIS based solutions in web browser environment. This geoportal may be quite useful to provide wealth of information to researchers, administrators and planners.

11.2 RESEARCH CONTRIBUTION

- Detailed GIS database has been created for the study area.
- Identification of areas, with poor groundwater potential zones, based on parameters on which groundwater depends.
- Identification of suitable sites for artificial recharge alongwith suitable type of water harvesting structure.
- Prioritisation of sub-watersheds to prevent these from high erosion and soil loss.
- Groundwater fluctuation map over a period which helps in to replenish the groundwater. Critical, semi-critical blocks have been identified. Groundwater flow modeling helps to predict the future groundwater level scenario as well as mitigate the flood and drought conditions.
- Groundwater vulnerable zones are identified, where possibility of groundwater contamination exists.

- Web based geoportal helps to share the geospatial information among large community, and additional benefits to planners and decision makers.
- Demonstrated that how geospatial techniques i.e. GIS and RS can be used in managing the water resources and hydrological processes which can serve as a useful reference to water resource professionals and researchers.

11.3 FUTURE RECOMMENDATIONS

- Groundwater potential map is required to be validated with more intense field data.
- Data from runoff modeling can be verified in the field before using them further in groundwater model.
- For better calibration and validation of the groundwater model, more pumping test data may be required.
- Network of observation wells should be distributed in large number over the whole area so that improved results from groundwater model could be derived. Detailed lithologs and borehole logging data would be required to improve the performance of this model which can be used for the implementation of groundwater development in the area through down scaling to sub-regional or local groundwater models.
- Spatial distribution of groundwater quality parameters can be used as general tool to evaluate the groundwater quality of the area since the chemical composition of groundwater also has significant temporal variation. It is also needed to consider temporal variation of the groundwater quality parameters within the study area.
- The geoportal module can further be enhanced by incorporating the advanced query system, beneficial for groundwater administrators and planners.

REFERENCES

1. Abdulla, F. and Al-Assa'd, T. (2006). "Modeling of groundwater flow for Mujib Aquifer, Jordan". *Journal of Earth System Science*, 115(3):289-297.
2. Agarwal, S. and Gupta, R. D. (2014). "Development and Comparison of Open Source based Web GIS Frameworks on WAMP and Apache Tomcat Web Servers". *The International Archives of the Photogrammetry, Remote Sensing and Spatial Information Sciences*, 4:1-5.
3. Adhikary, P. P., Chandrasekharan, H., Chakraborty, D. and Kambly, K. (2010). "Assessment of groundwater pollution in West Delhi, India using geostatistical approach". *Environ Monit Assess*, 167:599-615.
4. Adhikary, P. P., Dash, C. J., Chandrasekharan, H., Rajput, T. B. S. and Dubey, S. K. (2012). "Evaluation of groundwater quality for irrigation and drinking using GIS and geostatistics in a peri-urban area of Delhi, India". *Arabian Journal of Geosciences*, 5(6): 1423-1434.
5. Ahmadi, S. H. and Sedghamiz, A. (2007). "Geostatistical Analysis of Spatial and Temporal Variations of Groundwater Level". *Environ Monit Assess*, 129:277-294.
6. Alam, F., Umar, R., Ahmed, S. and Dar, F. A. (2014). "A new model (DRASTIC-LU) for evaluating groundwater vulnerability in parts of central Ganga plain, India". *Arab J. Geosci*, 7:927-937.
7. Al-Assa'd, T. A. and Abdulla, F. A. (2010). "Artificial groundwater recharge to a semi-arid basin: case study of Mujib aquifer, Jordan". *Environmental Earth Science*, 60:845-859.
8. Aller, L., Bennett, T., Lehr, J., Petty, R. (1987). "DRASTIC: a standardized system for evaluating ground water pollution". Doc. EPA/600/2-85/018, US EPA, Washington, DC, 157 pp.
9. Anayah, F. M. and Almasri, M. N. (2009). "Trends and occurrences of nitrate in the groundwater of the West Bank, Palestine". *Applied Geography*, 29(4):588-601.
10. Anbazhagan S. and Nair A. M. (2004). "Geographic information system and groundwater quality mapping in Panvel basin, Maharashtra, India", *Journal of Environmental Geology*, 45:753-761.
11. Anderson, M. P. and Woessner, W. W. (1992). "Applied Groundwater Modeling". Academic Press, Inc. San Diego, California.

12. Anon (1973). "A method for estimating volume and rate of runoff in small watersheds". Technical paper no. 149, Soil Conservation Service, USDA- SCS, Washington, D.C..
13. Asadi, S. S., Vuppala, P. and Reddy, A. M. (2007). "Remote Sensing and GIS Techniques for Evaluation of Groundwater Quality in Municipal Corporation of Hyderabad (Zone-V), India". *Int. J. Environ. Res. Public Health*, 4(1):45-52.
14. Atkinson, S. F., and Thomlinson, J. R. (1994). "An examination of groundwater pollution potential through GIS modeling". ASPRS/ACSM.
15. Babiker, I. S., Mohammed, A. A. M., Hiyama, T., Kato, K. and Ohta, K. (2004). "Assessment of groundwater contamination by nitrate leaching from intensive vegetable cultivation using geographical information system". *Environment International*, 29:1009-1017.
16. Babiker, I. S., Mohammed, A. A. M., Hiyama, T. and Kato, K. (2005). "A GIS-based DRASTIC model for assessing aquifer vulnerability in Kakamigahara Heights, Gifu Prefecture, central Japan". *Science of the Total Environment*, 345(1-3):127-140.
17. Babiker I. S., M. A. A. Mohamed and Hiyama, T. (2007). "Assessing groundwater quality using GIS", *Water Resour Manage*, 21:699–715.
18. Bachmat, Y. and Collin, M. (1990). "Management oriented assessment of groundwater vulnerability to pollution". Israel hydrological Service Report, Israel Hydrological Service, Jerusalem.
19. Barker, R. D., Rao, T. V. and Thangarajan, M. (2001). "Delineation of contaminant zone through electrical imaging technique". *Current Sciences*, 81(3):101-107.
20. Bear, J. (1979). *Hydraulics of Groundwater*, McGraw-Hill, New York.
21. Bear, J., Beljinb, M.S. and Rossc, R.R. (1992). "Fundamentals of Ground-Water Modeling". Ground Water Issue EPA/540/S-92/005.
22. Becker, M.W. (2006). "Potential for satellite remote sensing of groundwater". *Groundwater* 44(2):306-318.
23. Bekesi, G. and McConchie, J. (1999). "Groundwater recharge modelling using the Monte Carlo technique, Manawatu region, New Zealand", *Journal of Hydrology*, 224:137-148.
24. Bhatnagar, N. C., Agashe, R. M. and Mishra, A. K. (1982). "Subsurface Mapping of Aquifer System" Water balance study of Upper Yamuna Basin, Section-Hydrogeology, Technical report No.2, Upper Yamuna Project, CGWB, NW region, Chandigarh.
25. Bhunia, G. S., Chatterjee, N. and Pal, D. K. (2014). "Identification of groundwater potential zone of Nawada district, Bihar (India) – a study based on remote sensing and GIS platform. *Hydrology Research*, 45(4-5):631-644.

26. BIS (Bureau of Indian Standards) 10500, Indian standard for drinking water specification, 1991, first revision, p 1-8.
27. Biswas, S., Sudhakar, S. and Desai, V. R. (1999). "Prioritization of subwatersheds based on morphometric analysis of drainage basin: A Remote sensing and GIS approach". *J. Indian Soc. Remote Sensing*, 27(3):155-166.
28. Brahmabhatt, V. S., Dalwadi, G. B. Chhabra, S. B., Ray, S. S. and Dadhwal, V. K. (2000). "Land use/land cover change mapping in Mahi canal command area, Gujarat, using multi-temporal satellite data". *Journal of the Indian Society of Remote Sensing*, 28(4):221-232.
29. Bredehoeft, J. D. (2002). "The Water Budget Myth revisited: why hydrogeologists model". *Ground Water*, 40(4):340-345.
30. Brema, J. and Arulraj, G. P. (2012). "Identification of Sites Suitable for Artificial Recharging and Groundwater Flow Modeling in Noyyal River Basin, Tamilnadu, India". *OIDA International Journal of Sustainable Development*, 3(8):45-58.
31. Caldeweyher, D., Jinglan, Z., and Pham, B. (2006). "OpenCIS-open source GIS-based Web community information system". *International Journal of Geographical Information Science*, 20(8):885-898.
32. CGWB, 1999. *Report on Status of Groundwater exploration in Uttar Pradesh* [online]. Central Groundwater board, Ministry of Water Resources. Available from: <http://www.cgwb.gov.in> [Accessed 05 September 2010].
33. CGWB (2006). *Dynamic Groundwater Resources of India* [online]. Ministry of Water Resources. Government of India.
34. CGWB, Faridabad (2010). Ground water quality in shallow aquifers of India, Central Ground water board ministry of water resources government of India.
35. Chandrashekhar, H., Adiga, S., Lakshminarayana, V., Jagdeesha, C. J. and Nataraju, C. (1999). "A case study using the model 'DRASTIC' for assessment of groundwater pollution potential". In Proceedings of the ISRS national symposium on remote sensing applications for natural resources. June 19-21, Bangalore.
36. Chandrashekar, H., Ranganna, G. and Nataraju, C. (2000). "Assessment of groundwater pollution potential through remote sensing and GIS technique a case study for anekal taluk, bangalore urban district, India". *International Archives of Photogrammetry and Remote Sensing*. Vol. 33, Part B7 Amsterdam.
37. Chatterjee, R., Tarafder, G. and Paul, S. (2009). "Groundwater quality assessment of dhanbad district, Jharkhand, India". *Bull Eng Geol Environ*, 69:137-141.

38. Chenini, I. and Mammou, A. B. (2010). "Groundwater recharge study in arid region: An approach using GIS techniques and numerical modeling". *Computers & Geosciences*, 36:801-817.
39. Chenini, I., Mammou, A. B. and El May, M. (2010). "Groundwater Recharge Zone Mapping Using GIS-Based Multi-criteria Analysis: A Case Study in Central Tunisia (Maknassy Basin)". *Water Resources Management*, 24:921-939.
40. Chitale, V., Rao, V. V. S. and Sharma, V. (2000). "GIS-based Watershed Management for Sustainable Development in Rural Areas- a Pilot Study". *6th GeoAsia Pacific Conference*, Bangkok, Thailand.
41. Chowdary, V.M., Ramakrishnan, D., Srivastava, Y.K., Chandran, V. and Jeyaram, A. (2009). "Integrated water resource development plan for sustainable management of Mayurakshi watershed, India using Remote Sensing and GIS". *Water Resource Management*, 23:1581-1602.
42. Chowdhury, A., Jha, M. K., Chowdary, V. M. and Mal, B. C. (2009). "Integrated remote sensing and GIS-based approach for assessing groundwater potential in West Medinipur district, West Bengal, India". *International Journal of Remote Sensing*, 30(1):231-250.
43. Civita, M., De Maio M (2004) Assessing and mapping groundwater vulnerability to contamination: the Italian "combined" approach. *Geofis Int* 43(4):513–532
44. Clarke, J. I. (1966). "Morphometry from Maps, Essays in Geomorphology". New York, USA: Elsevier Publication Company.
45. Chavarriaga, E., and Macias, J. A. (2009). "A model-driven approach to building modern Semantic Web-Based User Interfaces". *Advances in Engineering Software*, 40(12):1329-1334.
46. Cuylenburg, R., Black, M., Arrowsmith, C. and Cartwright, W. (2005). "An Evaluation of OpenSource and Commercial Map/GIS Server Software", Proceedings of the Spatial Science Conference 2005 'Spatial Intelligence, Innovation and Praxis' The biennial conference of the Spatial Sciences Institute, September, 2005. Melbourne, Spatial Sciences Institute. ISBN 0-9581366-2-9.
47. Dar, I. A., Sankar, K. and Dar M. A. (2010). "Remote sensing technology and geographic information system modeling: An integrated approach towards the mapping of groundwater potential zones in Hardrock terrain, Mamundiyar basin". *Journal of hydrology* 394:285-295.
48. Debebe, A. and Amer, K. M. (2008). "Qatar Groundwater Resources Information System". *3rd International Conference on Water Resources and Arid Environments*.

49. Delleur, J. W. (1999). *The handbook of Groundwater Engineering*, CRC Press, Taylor and Francis Group, Florida.
50. Doherty, J., Brebber, L. and Whyte, P. (1994). *PEST - Model-independent parameter estimation. User's manual*. Watermark Computing, Australia.
51. Elango, L. and Sivakumar, C. (2008). "Regional Simulation of a Groundwater Flow in Coastal Aquifer, Tamil Nadu, India". *Groundwater Dynamics in Hard Rock Aquifers*, 234-242.
52. El Alfy, M. (2014). "Numerical groundwater modelling as an effective tool for management of water resources in arid areas". *Hydrological Sciences Journal*, 59(6):1259-1274.
53. El-Hames, A. S., Al-Ahmadi, M. and Al-Amri, N. (2010). "A GIS approach for the assessment of groundwater quality in Wadi Rabigh aquifer, Saudi Arabia". International conference on Environ Earth Science.
54. Elmahdy, S. I. and Mohamed M. M. (2014). "Groundwater potential modelling using remote sensing and GIS: a case study of the Al Dhaid area, United Arab Emirates. *Geocarto International*, 29(2):433-450.
55. El-Fadel, M., Tomaszkiwicz, M., Adra, Y., Sadek, S. and Abou Najm, M. (2014). "GIS-Based Assessment for the Development of a Groundwater Quality Index towards Sustainable Aquifer Management". *Water Resour Manage*, 28:3471-3487.
56. Erwig, M., Guting, R. H., Schneider, M. and Vazirgiannis, M. (1999). "Spatio-Temporal Data Types: An Approach to Modeling and Querying Moving Objects in Databases". *Geoinformatica*, 3(3):1-23.
57. Fashae, O. A., Tijani, M. N., Talabi, A. O. and Adedeji, O. I. (2013). "Delineation of groundwater potential zones in the crystalline basement terrain of SW-Nigeria: an integrated GIS and remote sensing approach". *Appl Water Sci.*, 4:19-38.
58. Fayeze, A. and Tamer Al-Assa'd, (2006). "Modeling of groundwater flow for Mujib aquifer, Jordan". *Journal of Earth System Science*, 115(3): 289-297.
59. Ferdowsian, R. and Pannell, D. J. (2009). "Explaining long-term trends in groundwater hydrographs". 18th World IMACS / MODSIM Congress, Cairns, Australia Source: <http://mssanz.org.au/modsim09>.
60. Fordyce, F. M., Vrana, K., Zhovinsky, E., Povoroznuk, V., Toth, G., and Hope, B. C. (2007). "A health risk assessment for fluoride in Central Europe". *Environ Geochem Health*, 29(2):83-102.

61. Foster, S.S. D. (1987). "Fundamental concepts in aquifer vulnerability, pollution risk and protection strategy". Proceedings and Information/TNO Committee on Hydrological Research 38:36-86.
62. Foster, S. S. D. (1998). "Groundwater recharge and pollution vulnerability of British aquifers: a critical overview". In: Robins, N.S. (ed.) *Groundwater Pollution, Aquifer Recharge and Vulnerability*. Geological Society, London, Special Publications, 130:7-22.
63. Fritch, T. G., McKnight, C. L., Yelderman Jr, J. C., and Arnold, J. G. (2000). "An aquifer vulnerability assessment of the paluxy aquifer, central Texas, USA, using GIS and a modified DRASTIC approach". *Environmental Management*, 25:337–345.
64. Freeze, R. A. and Cherry, A. J. (1979) *Groundwater*, Prantice Hall, Inc. New Jersey, pp 262- 265.
65. Gaaloul, N. (2014). "GIS-Based Numerical Modeling of Aquifer Recharge and Saltwater Intrusion in Arid Southeastern Tunisia". *Journal of Hydrologic Engineering*, 19(4):777-789.
66. Ganapurama, S., Kumar, G. T. V., Krishna, I. V. M., Kahya, E. and Demirel, M. C. (2008). "Mapping of groundwater potential zones in the Musi basin using remote sensing data and GIS". *Advances in Engineering Software*, 40(7):506-518.
67. Ghayoumian, J., Ghermezcheshme, B., Feiznia, S. and Noroozi, A. A. (2005). "Integrating GIS and DSS for identification of suitable areas for artificial recharge, case study, Meimeh Basin, Isfahan, Iran". *Environmental Geology* 47(4):493-500.
68. Ghosh, B. A. (2002). "Numerical modelling of salt–water intrusion due to human activities and sea-level change in the Godavari delta, India". *Hydrological Science Journal*, 47(S): 67-80.
69. Ghosh, D. K. and Singh, I. B. (1988). "Structural and geomorphic evolution of the northwestern part of Indo-Gangetic Plain". *Proc. Sem. Quat. Geol.*, Baroda, India, 164-175.
70. Gilbert, R.O. (1987) *Statistical methods for environmental pollution monitoring*. New York: Van Nostrand Reinhold.
71. Gnanasundar, D. and Elango, L. (2000). "Groundwater flow modeling of a coastal aquifer near Chennai city, India", *Journal of Indian Water Resources Society*, 20(4):162-171.
72. Gogu, R. C., Carabin, G., Hallet, V., Peters, V. and Dassargues, A. (2001). "GIS-based hydrogeological databases and groundwater modelling". *Hydrogeology Journal*, 9: 555-569.

73. Gogu, R. C., Hallet, V. and Dassargues, A. (2003). "Comparison of aquifer vulnerability assessment techniques, application to the Neblon river basin (Belgium)". *Environmental Geology*, 44(8):881-892.
74. Gopinath, G., Lovholt, F., Kaiser, G., Harbitz, C. B., Raju, K. S., Ramalingam, M. and Singh, B. (2014). "Impact of the 2004 Indian Ocean tsunami along the Tamil Nadu coastline: field survey review and numerical simulations". *Nat Hazards*, 72:743–769.
75. Gowd, S. S., Reddy, M. R. and Govila, P. K. (2010). "Assessment of heavy metal contamination in soils at Jajmau (Kanpur) and Unnao industrial areas of the Ganga Plain, Uttar Pradesh, India". *Journal of Hazardous Materials* 174:113-121.
76. Goyal, V., Jhorar, B. S., Malik, R. S. and Streck, T. (2009). "Simulation of groundwater recharge from an aquifer storage recovery well under shallow water table condition". *Current Science*, 96(3):376-385.
77. Geetha, K., Mishra, S. K., Eldho, T. I., Rastogi, A. K. and Pandey, R. P. (2007). "Modifications to SCS-CN Method for Long-Term Hydrologic Simulation". *Journal of Irrigation and Drainage Engineering*, 133(5):475-486.
78. Gleick P. H. (ed.), *Water in Crisis: A Guide to the World's Freshwater Resources*, 1993. Oxford University Press, New York.
79. Gupta, M. and Srivastava, P. K. (2010). "Integrating GIS and remote sensing for identification of groundwater potential zones in the hilly terrain of Pavagarh, Gujarat, India, *Water International*, 35(2):233-245.
80. Gupta, R.D. (2004). "Role of GIS as Decision Support System in Water Resources Planning and Management". *Journal Indian Cartographer*, 24.
81. Guting, R.H. (1994). "An Introduction to Spatial Database Systems". *VLDB Journal* 4: 357-399.
82. Handa, B.K., (1975). "Geochemistry and genesis of fluoride containing groundwater in India". *Groundwater*, 13:278-281.
83. Hashemi, H., Berndtsson, R., Kompani-Zare, M. and Persson, M. (2013). "Natural vs. artificial groundwater recharge, quantification through inverse modeling". *Hydrol. Earth Syst. Sci.*, 17:637-650.
84. Hearne, G. M., Wireman, A., Campbell, S., Turner, A. and Ingersall, G. P. (1992). "Vulnerability of the uppermost groundwater to contamination in the Greater Denver Area, Colorado". USGS water-resources investigations report 92-4143, pp.241.

85. Hendricks, H. J. F., Brunner, P., Kgotlhang, L., Bauer-Gottwein, P., and Kinzelbach, W. (2006). "How can Remote Sensing Contribute in Groundwater Modeling". *Hydrogeology Journal* 15: 5-18.
86. Horton R.E. (1932). "Drainage basin characteristics". *Trans. Amer. Geophys. Union*, 13: 350-361.
87. Horton, R. E. (1945). "Erosional development of streams and their drainage basins: hydrophysical approach to quantitative morphology". *Bull. Geological Society of America*, 5:275-370.
88. Hrkal, Z. (2001). "Vulnerability of groundwater to acid deposition, Jizerske Mountains, northern Czech Republic: construction and reliability of a GIS-based vulnerability map". *Hydrogeology Journal*, 9:348–357.
89. Huan, H., Wang, J. and Teng, Y. (2012). "Assessment and validation of groundwater vulnerability to nitrate based on a modified DRASTIC model: A case study in Jilin City of northeast China". *Science of the Total Environment*, 440:14-23.
90. Hussain, M. H., Singhal, D. C., Joshi, H. and Kumar, S. (2006). "Assessment of Groundwater vulnerability in a tropical alluvial interfluvies, India". *Bhu-Jal News Jour.*, No.1-4:31-43.
91. International Association of Hydrogeologists (1994). *Guidebook on Mapping Groundwater Vulnerability*, 16, Verlag Heinz Heise GmbH & Co KG, Hannover, 131 p.
92. IMSD (1995). "Integrated Mission for Sustainable Development (IMSD) Technical Guidelines". *NRSA: Hyderabad*.
93. Jain, P. K. (1998). "Remote sensing techniques to locate ground water potential zones in upper Urmil River basin, district Chattarpur-central India". *Journal of Indian Society of Remote Sensing*, 26(3):135-147.
94. Jaiswal, R. K., Mukherjee, S., Krishnamurthy, J. and Saxena R. (2003). "Role of remote sensing and GIS techniques for generation of groundwater prospect zones towards rural development—an approach". *International Journal of Remote Sensing*, 24(5): 993-108.
95. Jamrah, A., Futaisi, A. A., Rajmohan, N. and Al-Yaroubi, S. (2007). "Assessment of groundwater vulnerability in the coastal region of Oman using DRASTIC index method in GIS environment". *Environ Monit Assess.* doi:10.1007/s10661-007-0104-6
96. Jasrotia, A. S., Kumar, R. and Saraf, A. K. (2007). "Delineation of groundwater recharge sites using integrated remote sensing and GIS in Jammu district, India". *International Journal of Remote Sensing*, 28(22):5019-5036.

97. Jaworska-Szulc, B. (2009). "Groundwater flow modelling of multi-aquifer systems for regional resources evaluation: the Gdansk hydrogeological system, Poland". *Hydrogeology Journal*, 17:1521-1542.
98. Jha, S. K., Nayak, A. K. and Sharma, Y. N. (2010). "Potential fluoride contamination in the drinking water of Marks Nagar, Unnao district, Uttar Pradesh, India". *Environ Geochem Health*, 32:217-226.
99. Jin, H., Liu, H., Feng, L. and Xing, S. (2011). "Research Progress of a GIS-based DRASTIC Model". IEEE, DOI: [10.1109/MACE.2011.5987497](https://doi.org/10.1109/MACE.2011.5987497) 2524-2526.
100. Kahya, E. and Kalayc S. (2004). "Trend analysis of stream flow in Turkey". *Journal of Hydrology*, 289(1):128-144.
101. Kallioras, A., Pliakas, F. and Diamantis, I. (2010). "Simulation of Groundwater Flow in a Sedimentary Aquifer System Subjected to Overexploitation". *Water Air Soil Pollution*, 211:177-201.
102. Kalinski, R. J., Kelly, W. E., Bogardi, I., Ehrman, R. L., & Yamamoto, P. D. (1994). "Correlation between DRASTIC vulnerabilities and incidents of VOC contamination of municipal wells in Nebraska". *Groundwater*, 32(1): 31–34.
103. Kaliraj, S., Chandrasekar, N. and Magesh, N. S. (2013). "Identification of potential groundwater recharge zones in Vaigaiupper basin, Tamil Nadu, using GIS-based analytical hierarchical process (AHP) technique". *Arab J Geosci.*, DOI 10.1007/s12517-013-0849-x.
104. Kamaraju, M. V. V., Bhattacharya, A., Sreenivasa, G. R., Rao, G. G., Murthy, G. S. and Rao, T. C. M. (1996). "Groundwater potential evaluation of West Godavari District, Andhra Pradesh State, India—a GIS approach". *Ground Water*, 34:318-325.
105. Kappas, M. (2014). "Aerial Photogrammetry for Glacial Monitoring". *Encyclopedia of Earth Sciences Series*, pp 4-15.
106. Katiyar, S. K. and Dikshit, O. (2011). "GCP database development methodology for remote sensing and GIS using GPS and SOI topographic maps". *Journal of Geomatcis*, 5(2):101-106.
107. Khodapanah, L., Sulaiman, W. N. A. and Khodapanah, N. (2009). "Groundwater Quality Assessment for Different Purposes in Eshtehard District, Tehran, Iran". *European Journal of Scientific Research*, 36(4):543-553.
108. Karanth, K. R. (1987). "Groundwater assessment, development and management, Tata McGrawHill Publishing Company Limited, New Delhi, pp 576-638.

109. Karavoltsova, S., Sakellaria, A., Mihopoulos, N., Dassenakisa, M. and Scoullosa, M.J. (2008). "Evaluation of the quality of drinking water in regions of Greece". *Desalination*, 224:317-329.
110. Kendall, M.G. (1975) Rank Correlation Methods. Charles Griffin, London, 202
111. Kim, S., Arrowsmith, C. A. and Handmer, J. (2009). "Assessment of socioeconomic vulnerability of Coastal Areas from an indicator based approach". Proceedings of the 10th International Conference on GeoComputation, University of New South Wales.
112. Krishnamurthy, J. and Srinivas, G. (1995). "Role of geological and geomorphological factors in ground water exploration: a study using IRS LISS data". *International Journal of Remote Sensing*, 16(14):2595-2618.
113. Krishnamurthy, J., Kumar, N. V., Jayaraman, V. and Manivel, M. (1996). "An approach to demarcate groundwater potential zones through remote sensing and a geographic information system". *International Journal of Remote Sensing*, 17(10): 1867-1884.
114. Kumar, C. P. (1992). "Groundwater Modelling— In. Hydrological Developments in India since Independence. A Contribution to Hydrological Sciences". National Institute of Hydrology, Roorkee, pp. 235-261.
115. Kumar, S., Thirumalaivasan, D. and Radhakrishnan, N. (2014). "GIS Based Assessment of Groundwater Vulnerability Using Drastic Model". *Arab J Sci Eng*, 39:207-216.
116. Kumar, V. and Sharma, V. (2006). "Overcoming 64kb data size limit in handling large spatial data in GISNIC while cleaning and building topology". *International Journal of Information Technology and Management*, 5(1):77-86.
117. Lake, I. R., Lovett, A. A. and Hiscock, K. M. (2003). "Evaluating factors influencing groundwater vulnerability to nitrate pollution: developing the potential of GIS". *J Environ Manage*, 68:315-328.
118. Langbein, W. B. (1947). "Topographic characteristics of drainage basins". *US Geological Survey Water-Supply paper*, 986 (C):157-159.
119. Lee, S. (2003). "Evaluation of waste disposal site using the DRASTIC system in southern Korea". *Env Geol*, 44:654-664.
120. Levenberg, K. (1944). "A Method for the Solution of Certain Problems in Least Squares". *Quart. Appl. Math.* 2, 164-168.
121. Lima, M. L., Zelaya, K. and Massone, H. (2011). "Groundwater vulnerability assessment combining the DRASTIC and Dyna-Clue model in the Argentina Pampas". *Environmental Management*, 47:828-839.

122. Linsley, R. K., Kahler, M. A. and Paulhus, J. L. H. (1958). "Hydrology for Engineers". New York: McGraw-Hill Book company
123. Lobo-Ferreira, J.P. and Oliveira, M.M. (1993). "Desenvolvimento de um Inventário das Águas Subterrâneas de Portugal. Caracterização dos recursos Hídricos Subterrâneos e Mapeamento DRASTIC da Vulnerabilidade dos Aquíferos de Portugal, Laboratório Nacional de Engenharia Civil, Relatório 179/93 - GIAS, Lisboa.
124. Lynch, S. D., Reynders, A. G. and Schulz, R. R. (1994). "Preparing input data for a national-scale groundwater vulnerability map of Southern Africa", 6th National Hydrological Symposium, SANCIAHS, Pietermaritzburg, South Africa 20:239-246.
125. Machiwal, D., Mishra, A., Jha, M. K., Sharma, A. and Sisodia, S. S. (2012). "Modeling Short-Term Spatial and Temporal Variability of Groundwater Level Using Geostatistics and GIS". *Natural Resources Research*, 21(1):117-136.
126. Magesh, N. S., Chandrasekar, N. and Soundranayagam, J. P. (2012). "Delineation of groundwater potential zones in Theni district, Tamil Nadu, using remote sensing, GIS and MIF techniques". *Geoscience Frontiers*, 3(2):189-196.
127. Mahmoud, S. H. (2014). "Delineation of potential sites for groundwater recharges using a GIS -based decision support system". *Environ. Earth Sci.*, 72:3429-3442.
128. Malczewski, J. (2006). "GIS-based multicriteria decision analysis: a survey of the literature". *International Journal of Geographical Information Science*, 20(7):703-726.
129. Mandle, R. J. (2002). "Groundwater Modeling Guidance". Groundwater Modeling Program, Michigan Department of Environmental Quality, 54 p.
130. Mann, H.B. (1945). "Nonparametric tests against trend". *Econometrica*, 13:245-259.
131. Margat, J. (1968). "Groundwater vulnerability to contamination". Publication 68, BRGM, Orleans, France.
132. Marquardt, D. (1963). "An Algorithm for Least Squares Estimation of Nonlinear Parameters". *SIAM J. Appl. Math.* 11:431-441.
133. Martínez-Santos, P., Pedritti, P., Martínez-Alfaro, P. E., Conde, M. and Casado, M. (2010). "Modelling the Effects of Groundwater-Based Urban Supply in Low-Permeability Aquifers: Application to the Madrid Aquifer, Spain", *Water Resources Management*, 24: 4613-4638.
134. McBride, S., Bellman, C. and Arrowsmith, C. (2003). "Developing space-time models and representation for GIS" proceedings of the Spatial Sciences Coalition Conference, Canberra.

135. Menani, M. R. (2001). "Evaluating and mapping the groundwater pollution susceptibility of the El Madher alluvial aquifer, eastern Algeria, using the Drastic method". *Science et changements planétaires/Secheresse* 12(2):95-101.
136. Mendoza, J. A. and Barmen, G. (2006). "Assessment of groundwater vulnerability in the Río Artiguas basin, Nicaragua". *Env Geol*, 50:569-580.
137. Miller, V.C. (1953). "A quantitative geomorphic study of drainage basin characteristics in the Clinch Mountain area, Virginia and Tennessee". Project NR 389042, Tech. Rept. 3., Columbia University, Department of Geology, ONR, Geography Branch, New York.
138. Mills, B. (2003). *Interpreting Water Analysis for Crop and Pasture*, File No. FS0334, DPI's Agency for Food and Fibre Sciences, Toowoomba.
139. Ministry of Water Resources (1997) Report of the groundwater resource estimation committee-Groundwater resource estimation methodology, Government of India, New Delhi.
140. Ministry of Water Resources (2011) Report of the groundwater resource estimation committee-Groundwater resource estimation methodology, Government of India, New Delhi.
141. Mondal, N. C., Saxena, V. K. and Singh, V. S. (2005). "Assessment of Groundwater Pollution due to Tanneries in and around Dindigul, Tamilnadu, India. *Environment Geology*, 48(2):149-157.
142. Mondal, N. C., Singh, V. S., Puranik, S. C. and Singh, V. P. (2009). "Trace elements concentration in groundwater of Pesarlanka island, Krishna delta, India". *Environ. Monit Assess.*, 163(1-4):215-227.
143. Mukherjee, S. Veer, V. Tyagi, S. K. Sharma, V. (2007). "Sedimentation Study of Hirakud Reservoir through Remote Sensing Techniques". *Journal of Spatial Hydrology*, 7(1):122-130.
144. Muracevic, D. and Orucevic, F. (2008). "Development of web spatial applications based on MapGuide open source". Paper presented at the *Proceedings of the 30th International Conference on Information Technology Interfaces*. Dubrovnik, Croatia.
145. Murthy, K. S. R. (2000). "Ground water potential in a semi-arid region of Andhra Pradesh - a geographical information system approach". *International Journal of Remote Sensing*, 21(9):1867-1884.
146. Murthy, K. S. R. and Mamo, A. G. (2009). "Multi-criteria decision evaluation in groundwater zones identification in Moyale-Teltele sub-basin, South Ethiopia". *International Journal of Remote Sensing*, 30(11):2729-2740.

147. Nag, S. K. (1998). "Morphometric Analysis Using Remote Sensing Techniques in the Chaka Sub-Basin, Purulia District, West Bengal". *Journal of Indian Society of Remote Sensing*, 26(1&2):69-76.
148. Nag, S. K. and Chakraborty, S. (2003). "Influence of rock types and structures in the development of drainage network in hard rock area". *Journal of the Indian Society of Remote Sensing*, 31(1):25-35.
149. Napolitano, P., and Fabbri, A. G. (1996). "Single-parameter sensitivity analysis for aquifer vulnerability assessment using DRASTIC and SINTACS". Proceedings of the Vienna conference on HydroGIS 96: Application of geographic information systems in hydrology and water resources management, IAHS Pub, (235):559-566.
150. Narendra, K. and Rao, K. N. (2006). "Morphometry of the Mehadrigedda watershed, Visakhapatnam district, Andhra Pradesh using GIS and Resourcesat data". *J. Indian Soc. Remote Sensing*, 34(2):101-110.
151. Nasiri, H., Bolorani, A. D., Sabokbar, H. A. F., Jafari, H. R., Hamzeh, M. and Rafii, Y. (2013). "Determining the most suitable areas for artificial groundwater recharge via an integrated PROMETHEE II-AHP method in GIS environment (case study: Garabayan Basin, Iran)". *Environ Monit Assess.*, 185:707-718.
152. Nautiyal, M. D. (1994). "Morphometric analysis of a drainage basin, district Dehradun, U. P.". *Jour. Indian Soc. Remote Sensing*, 22(4):251-261.
153. Navulur, K. C. S., and Engel, B. A. (1998). "Groundwater vulnerability assessment to non-point source nitrate pollution on a regional scale using GIS". *Transactions of the American Society of Agricultural Engineers*, 41:1671-1678.
154. Neshat, A., Pradhan, B., Pirasteh, S. and Shafri, H. Z. M. (2013). "Estimating groundwater vulnerability to pollution using a modified DRASTIC model in the Kerman agricultural area, Iran". *Environ Earth Sci*, DOI 10.1007/s12665-013-2690-7.
155. Panagopoulos, G. P., Antonakos, A. K. and Lambrakis, N. J. (2006). "Optimization of the DRASTIC method for groundwater vulnerability assessment via the use of simple statistical methods and GIS". *Hydrogeol J*, 14:894-911.
156. Pandey, A., Chowdhary, V. M. and Mal, B.C. (2004). "Morphological analysis and watershed management using GIS". *J. of hydrology*, 27(3):71-84.
157. Pandey, A., Chowdhary, V. M., Mal, B. C. and Dabral, P. P. (2010). "Remote Sensing and GIS for Identification of Suitable Sites for Soil and Water Conservation Structures". *International Journal of Land Degradation and Development*, Published online in Wiley Inter Science.

158. Pathak, D. R. and Hiratsuka, A. (2009). "An integrated GIS based fuzzy pattern recognition model to compute groundwater vulnerability index for decision making". *Journal of Hydro-environment Research*, 5:63-77.
159. Pawattana, C. & Tripathi, N. K. (2008). "Analytical Hierarchical Process (AHP)-Based Flood Water Retention Planning in Thailand". *GIScience & Remote Sensing*, 45(3):343-355.
160. Pirasteh, S., Tripathi, N. K. and Ayazi, M. H. (2006). "Localizing Ground Water Potential Zones in Parts of Karst Pabdeh Anticline, Zagros Mountain, Southwest Iran using Geospatial Techniques". *International Journal of Geoinformatics*, 2(3).
161. Pliakas, F., Petalas, C., Diamantis, I. and Kallioras, A. (2005). "Modeling of Groundwater Artificial Recharge by Reactivating an Old Stream Bed". *Water Resources Management*, 19:279-294.
162. Ponce V. M. and Hawkins, R. H. (1996). "Runoff curve number: Has it reached maturity?". *Journal of Hydrological Engineering – ASCE*, 1(1):11-19.
163. Pothiraj, P. and Rajagopalan, B. (2012). "A GIS and remote sensing based evaluation of groundwater potential zones in a hard rock terrain of Vaigai sub-basin, India". *Arab Journal of Geoscience*. DOI 10.1007/s12517-011-0512-3
164. Praharaj, T., Swain, S. P., Powell, M. A., Hart, B. R. and Tripathy, S. (2002). "Delineation of groundwater contamination around an ash pond Geochemical and GIS approach". *Environmental International*, 27:631-638.
165. Power, D. J. (2007). A Brief History of Decision Support Systems. <http://DSSResources.COM/history/dsshhistory.html>
166. Propastin, P., Muratova, N. and Kappas, M. (2006). "Reducing uncertainty in analysis of relationship between vegetation patterns and precipitation ". *7th International Symposium on Spatial Accuracy Assessment in Natural Resources and Environmental Sciences*.
167. Propastin, P. & Kappas, M. (2012). "Assessing Satellite-Observed Nighttime Lights for Monitoring Socioeconomic Parameters in the Republic of Kazakhstan". *GIScience & Remote Sensing*, 49(4):538-557.
168. Qinghai, G., Yanxin, W., Xubo, G. and Teng, M. (2007). "A new model (DRARCH) for assessing groundwater vulnerability to arsenic contamination at basin scale: a case study in Taiyuan basin, northern China". *Environ Geol* 52:923-932.
169. Raghunath, H. M. (2002). *Ground Water (Second Edition)*, New Age International Pvt. Ltd.

170. Raghunath, R., Sreedhara Murthy, T. R., and Raghavan, B. R. (2005). "Time series analysis to monitor and assess water resources: A moving average approach". *Environmental Monitoring and Assessment*, 109:65–72.
171. Rahman, A. (2008). "A GIS based DRASTIC model for assessing groundwater vulnerability in shallow aquifer in Aligarh, India". *Applied Geography*, 28(1):32-53.
172. Ramakrishnaiah, C. R., Sadashivaiah, C. and Ranganna, R. (2009). "Assessment of Water Quality Index for the Groundwater in Tumkur Taluk, Karnataka State, India". *e-journal of chemistry*, 6(2):523-530.
173. Ramakrishnan, D., Bandyopadhyay, A. and Kusuma, K. N. (2009). "SCS-CN and GIS-based approach for identifying potential water harvesting sites in the Kali Watershed, Mahi River Basin, India". *Journal of Earth System Science*, 118(4):355-368.
174. Ramasamy, Bhoop singh and Brig. R. Siva Kumar (2006). "Landslide triggered Tsunami in Norway". *Geomatics* (Ed) SM.Ramasamy et al, *Spec. Vol. on Geomatics in Tsunami*, New India Publishers, New Delhi, pp. 221–225.
175. Rao, K. H.V., Durga and Bhaumik, M. K. (2003). "Spatial Expert Support System in Selecting Suitable Sites for Water Harvesting Structures — A Case Study of Song Watershed, Uttaranchal, India". *Geocarto International*, 18(4):43-50.
176. Rao, Y. S. and Jugran, D. K. (2003). "Delineation of groundwater potential zones and zones of groundwater quality suitable for domestic purposes using remote sensing and GIS". *Hydrol Sci J*, 48(5):821-833.
177. Rashid, M., Lone, M. A. and Ahmed, S. (2011). "Integrating geospatial and ground geophysical information as guidelines for groundwater potential zones in hard rock terrains of south India". *Environ Monit Assess*, 184(8):4829-4839.
178. RaviShankar, M. N. and Mohan, G. (2005). "Assessment of the groundwater potential and quality in Bhatsa and Kalu river basins of Thane district, western Deccan Volcanic Province of India". *Journal of Environ. Geol.*, 49:990-998.
179. Ray, S. S., Dadhwal, V. K. and Navalgund, R. R. (2002). "Performance evaluation of an irrigation command area using remote sensing: a case study of Mahi command, Gujarat, India". *Agricultural water management*, 56(2):81-91.
180. Ray, S. S. and Dadhwal, V.K. (2001). "Estimation of crop evapotranspiration of irrigation command area using remote sensing and GIS". *Agric. Water Manage.*, 49(3):239–249
181. Reddy, P. R., Vinod, K. and Seshadri, K. (1996). "Use of IRS-1C data in groundwater studies". *Current Science*, 70:600–605.

182. Rejani, R., Jha, M. K., Panda, S. N. and Mull R. (2007). "Simulation Modeling for Efficient Groundwater Management in Balasore Coastal Basin, India". *Water Resour Manage*, 22:23–50.
183. Remesan, R. and Panda, R. K. (2008). "Remote Sensing and GIS Application for Groundwater Quality and Risk Mapping". *3rd International Conference on Water Resources and Arid Environments*.
184. Robins, N.S. (ed.) 1998. *Ground-water Pollution, Aquifer Recharge and Vulnerability*. Geological Society, London, Special Publications, 130:107-115.
185. Rodell, M., Velicogna, I. and Famiglietti, J. S. (2009). "Satellite-based estimates of groundwater depletion in India", *Nature*, 460(7258):933-1050.
186. Rouabhia, A., Fehdi, C., Baali, F., Djabri, L. and Rouabhi, R. (2009). "Impact of human activities on quality and geochemistry of groundwater in the Merdja area, Tebessa, Algeria". *Environ Geol*, 56:259-1268.
187. Rupert, M. G. (2001). "Calibration of the DRASTIC ground water vulnerability mapping method". *Ground Water* 39(4):625-630.
188. Rushton, K. R. (2003). "Groundwater hydrology conceptual and computational models". John Wiley and Sons, Chichester, U.K.
189. Russo, T. A., Fisher, A. T. and Lockwood, B. S. (2014). "Assessment of managed aquifer recharge site suitability using a GIS and modeling". *Groundwater*, DOI: 10.1111/gwat.12213.
190. Saaty, T. L. (1980). *The Analytical Hierarchy Process*. McGraw Hill, NY.
191. Sadat-Noori, S. M., Ebrahimi, K. and Liaghat, A. M. (2014). "Groundwater quality assessment using the Water Quality Index and GIS in Saveh-Nobaran aquifer, Iran". *Environ Earth Sci*, 71:3827-3843.
192. Saeedi, M., Abessi, O., Sharifi, F. and Meraji, H. (2010). "Development of groundwater quality index". *Environ Monit Assess*, 163:327-335.
193. Saidi, S., Bouri, S., Dhia, H. B., and Anselme, B. (2009). "A GIS-based susceptibility indexing method for irrigation and drinking water management planning: Application to Chebba-Mellouleche aquifer, Tunisia". *Agricultural Water Management*, 96:1683–1690.
194. Saleh, A., Al-Ruwaih, F. and Shehata, M. (1999). "Hydrogeochemical processes operating within the main aquifers of Kuwait". *J Arid Environ*, 42:195-209.
195. Samadder, R. K., Kumar, S. and Gupta, R. P. (2011). "Paleochannels and their potential for artificial groundwater recharge in the western Ganga plains". *Journal of Hydrology*, 400: 154-164.

196. Saraf, A.K., and Choudhury, P. R. (1998). "Integrated Remote Sensing and GIS for Groundwater Exploration and Identification of Artificial Recharge Sites". *International Journal of Remote Sensing*, 19(10):1825-1841.
197. Sargaonkar, A. P., Rathi, B. and Baile, A. (2011). "Identifying potential sites for artificial groundwater recharge in sub-watershed of River Kanhan, India". *Environmental Earth Sciences*, 62:1099-1108.
198. Sarwade, D. V., Nandakumar, M. V., Kesari, M. P., Mondal, N. C., Singh, V. S. and Singh, B. (2007). "Evaluation of sea water ingress into an Indian atoll". *Environ Geol.*, 52:1475-1483.
199. Saxena, V. K., Mondal, N. C. and Singh, V. S. (2004). "Identification of Seawater Ingress Using Strontium And Boron In Krishna Delta, India". *Current Sciences*, 86(40):586-590.
200. Schumn, S. A. (1956). "Evaluation of drainage systems and slopes in badlands at Perth Amboy, New Jersey". *Bull. Geol. Soc. Amer.*, 67:597-646.
201. Schwartz, Franklin W. (2003). *Fundamentals of ground water*, John Wiley & sons.
202. Secunda, S., Collin, M. L. and Melloul, A. J. (1998). "Groundwater vulnerability assessment using a composite model combining DRASTIC with extensive agricultural land use in Israel's Sharon region". *Journal of Environmental Management*, 54:39-57.
203. Sener, E., Davraz, A. and Ozcelik, M. (2005). "An integration of GIS and remote sensing in groundwater investigations: a case study in Burdur, Turkey". *Hydrogeol Journal*, 13(5-6):826-834.
204. Senthilkumar, M. and Elango, L. (2011). "Modelling the impact of a subsurface barrier on groundwater flow in the lower Palar River basin, southern India". *Hydrogeology Journal*, 19:917-928.
205. Shaban, M. A. and Dikshit, O. (2002). "Evaluation of the merging of SPOT multispectral and panchromatic data for classification of an urban environment". *International Journal of Remote Sensing*, 23(2):249-262.
206. Shahid, S. (2000). "A study of groundwater pollution vulnerability using DRASTIC/GIS, west Bengal, India". *Journal of Environmental Hydrology*, 8, 124 Sacramento, USA.
207. Shammas, M. I. and Jacks, G. (2007). "Seawater intrusion in the Salalah plain aquifer, Oman". *Environmental Geology*, 53:575-587.
208. Shankar, K., Aravindan, S., and Rajendran, S. (2010). "A GIS based groundwater quality mapping in paravanar river sub basin, Tamilnadu, India. *International journal of geomatics and geosciences*, 1(3).

209. Sharholly, M., Ahmad, K., Vaishya, R. C. and Gupta, R. D. (2007). "Municipal solid waste characteristics and management in Allahabad, India". *Waste management*, 27(4):490-496.
210. Sharma, S. K., Rajput, G. S., Tignath, S. K. and Pandey, R. P. (2010). "Morphometric analysis and prioritization of a watershed using GIS". *J. Indian Water Resource Society*, 30(2):33-39.
211. Shekhar, S. and Pandey, A. C. (2014). "Delineation of groundwater potential zone in hard rock terrain of India using remote sensing, geographical information system (GIS) and analytic hierarchy process (AHP) techniques, Geocarto International, DOI:10.1080/10106049.2014.894584.
212. Shen, L. and Guo, X. (2014). "Spatiotemporally characterizing urban temperatures based on remote sensing and GIS analysis: a case study in the city of Saskatoon (SK, Canada)". *Central European Journal of Geosciences*, 7:27-39.
213. Shen, L. and Guo, X. (2014). "Spatial quantification and pattern analysis of urban sustainability based on a subjectively weighted indicator model: a case study in the city of Saskatoon, SK, Canada. *Applied Geography*, 53: 117-127.
214. Shiklomanov I. A. (1999). *World Water Resources: Modern Assessment and Outlook for the 21st Century..* Federal Service of Russia for Hydrometeorology & Environment Monitoring, State Hydrological Institute, St. Petersburg.
215. Shirazi, S. M., Imran, H.M. and Akib, S. (2012). "GIS-based DRASTIC method for groundwater vulnerability assessment: a review". *Journal of Risk Research*, 15(8):991-1011.
216. Shukla, S., Mostaghimi, S., Shanholt, V. O., Collins, M. C. and Ross, B. B. (2000). "A County-Level Assessment of Ground Water Contamination by Pesticides". *Ground Water Monit. Rev.*, 20(1):104–119.
217. Sikdar, P. K., Chakraborty, S. K., Adhya, E. and Paul, P. K. (2004). "Land Use/Land Cover Changes and Groundwater Potential Zoning in and around Raniganj coal mining area, Bardhaman District, West Bengal - A GIS and Remote Sensing Approach". *Journal of Spatial Hydrology*, Vol.4.
218. Simoes, S. F., Moreira, A. B., Bisinoti, M. C., Gimenez, S. M. N. and Yabe, M. J. S. (2008). "Water quality index as a simple indicator of aquaculture effects on aquatic bodies". *Ecol Indic*, 8:476-484.

219. Singh, A. K., Mondal, G. C., Kumar, S., Singh, T. B., Tewary, B. K. and Sinha, A. (2008). "Major ion chemistry, weathering processes and water quality assessment in upper catchment of Damodar River basin, India". *Environ Geol*, 54:745-758.
220. Singh, A. K., Raviprakash, S., Mishra, D. and Singh, S. (2002). "Groundwater potential modelling in Chandraprabha subwatershed, U.P. using Remote Sensing, Geoelectrical and GIS". *Geospatial World*, Map India.
221. Singh, A., Panda, S. N., Kumar, K. S. and Sharma, C. S. (2013). "Artificial groundwater recharge zones mapping using remote sensing and GIS: a case study in Indian Punjab". *Environ Manage.*, 52(1):61-71.
222. Singh, C. K., Shashtri, S., Kumari, R. and Mukherjee, S. (2013). "Chemometric analysis to infer hydro-geochemical processes in a semi-arid region of India". *Arab J Geosci* 6:2915-2932.
223. Singh, I. B. (1987). "Sedimentological history of Quaternary deposits in Gangetic Plain". *Indian J. Earth Sci.*, 14:272-282.
224. Singh, I. B. and Rastogi, S. P. (1973). "Tectonic framework of Gangetic alluvium with special reference to Ganga river in Uttar Pradesh". *Curr. Sci.*, 42:305-307.
225. Singh, I. B. and Bajpai, V. N. (1989). "Significance of Syndepositional tectonics in facies development, Gangetic Alluvium near Kanpur, India". *J. Geol. Soc. Ind.*, 34:61-66.
226. Singh, K. P., Malik, A., Sinha, S., Mohan, D. and Singh, V. K. (2007). "Exploring groundwater hydrochemistry of alluvial aquifers using multi-way modeling". *Analytica Chimica Acta* 596:171-182.
227. Singh, S. and Singh, M. C. (1997). "Morphometric analysis of Kanhar river basin". *National Geographical Journal of India*, 43:31-43.
228. Singh et al., (2013). "Report of the committee on pollution caused by leather tanning industry to the water bodies / ground water in Unnao district of Uttar Pradesh". Ministry of Water Resources.
229. Solomon, S. and Quiel, F. (2006). "Groundwater study using remote sensing and geographic information systems (GIS) in the central highlands of Eritrea". *Hydrogeology Journal*, 14:729-741.
230. Snehamani, Singh, M. K., Gupta, R. D. and Ganju, A. (2013). "Extraction of High Resolution DEM from Cartosat-1 Stereo Imagery using Rational Math Model and Its Accuracy Assessment for a Part of Snow Covered NW-Himalaya". *Journal of Remote Sensing and GIS*, 4(2):23-34.

231. Sreedevi, P. D., Subrahmanayam, K. and Ahmed, S. (2005). "Integrating approach for delineating potential zones to explore for groundwater in the Pageru River basin, Cuddapah District, Andhra Pradesh, India". *Hydrogeology Journal*, 13(3):534-543.
232. Srivastava, A., Tripathi, N. K. and Gokhale, K. V. G. K. (1997). "Mapping groundwater salinity using IRS-1B LISS II data and GIS techniques". *International Journal of Remote Sensing*, 18(13):2853-2862.
233. Srivastava, P. and Bhattacharya, A. (2006). "Groundwater assessment through an integrated approach using remote sensing, GIS and resistivity techniques: a case study from a hard rock terrain". *International Journal of Remote Sensing*, 27(20):4599-4620.
234. Strahler, A.N. (1957). "Quantitative analysis of watershed geomorphology". *American Geophysical Union Transactions*, 38: 913-920.
235. Strahler, A.N. (1964). Quantitative geomorphology of drainage basins and channel networks: In. *Handbook of Applied Hydrology*, McGraw Hill Book Company, New York.
236. Strahler, A. N. and Strahler, A. H. (2002). *A Text Book of Physical Geography*, John Wiley & Sons, New York.
237. Subba Rao, N. (1997). "Studies on the water quality index in hard rock terrain of Guntur district, Andhra Pradesh, India". *National Seminar on Hydrology of Precambrian Terrains and hard rock areas*, pp 129-134.
238. Subramani, T., Elango, L. and Damodarasamy S. R. (2005). "Groundwater quality and its suitability for drinking and agricultural use in Chithar River basin, Tamil Nadu, India". *International Journal of Environmental Geology*, 47:1099-1110.
239. Suganthi, S., Elango, L. and Subramanian, S. K. (2013). "Groundwater potential zonation by Remote Sensing and GIS techniques and its relation to the Groundwater level in the Coastal part of the Arani and Koratalai River Basin, Southern India". *Earth Science Research Journal*, 17(2):87-95.
240. Szucs, P., Madarasz, T. and Civan, F. (2009). "Remediating overproduced and contaminated aquifers by artificial recharge from surface waters". *Environmental Modeling and Assessment*, 14(4):511-520.
241. Taheri, A. and Zare, M. (2011). "Groundwater artificial recharge assessment in Kangavar Basin, a semi-arid region in the western part of Iran". *African Journal of Agricultural Research*, 6(17):4370-4384.

242. Tariq, S. R., Shah, M. H., Shaheen, N., Khalique, K., Manzoor, S. and Jaffar, M. (2005). "Multivariate analysis of selected metals in tannery effluents and related soil". *Journal of Hazardous Materials*, 122: 17-22.
243. Terrado, M., Borrell, E., Campos, S. D., Barcelo', D. and Tauler, R. (2010). "Surface-water-quality indices for the analysis of data generated by automated sampling networks". *Trends in Analytical Chemistry*, 29(1):40-52.
244. Thakur, G. S. and Thomas, T. (2011). "Analysis of Groundwater Levels for Detection of Trend in Sagar District, Madhya Pradesh". *Journal of geological society of India*, 77:303-308.
245. Thach, N. N. and Canh, P. X. (2012). "Simulation of flash–muddy flash and inundation of western Tamdao mountain region, Vinhphuc Province, Vietnam by using integrated concept of hydrology and geomorphology". *VNU Journal of Science, Earth Sciences*, 28:44-56.
246. Thach, N. N., Hien, N. T. T. and Canh, P. X. (2011). "Sensitivity and vulnerability assessment of socio-ecosystem to oil spill and sea level rising impact at hai phong coastal zone, Vietnam". *32nd Asian Conference on Remote Sensing*, 1:1152-1162.
247. Thach, N. N., Truc, N. N. and Hau, L. P. (2007). "Studying shoreline change by using LITPACK mathematical model (case study in Cat Hai Island, HaiPhong City, Vietnam)". *VNU J. Sci., Earth Sci.*, 23:244-252.
248. Thirumalaivasan, D., Karmegam, M. and Venugopal, K. (2003). "AHP-DRASTIC: software for specific aquifer vulnerability assessment using DRASTIC model and GIS". *Environmental Modeling and Software*, 18 (7): 645-656.
249. Tiwari, R. S. and Dikshit, O. (2002). "Remote Sensing Activities in India". *ICUS/INCEDE Newsletter*, 2(3):1-5.
250. Tiwari, V. M., Wahr, J. and Swenson, S. (1999). "Dwindling groundwater resources in northern India, from satellite gravity observations". *Geophysical Research Letters*, 36:1-5.
251. Todd, D. K. (1980). "Groundwater hydrology" (2nd ed.). New York, NY: 535 pp.
252. UNEP (2008), Vital Water Graphics: An Overview of the State of the World's Fresh and Marine Waters - 2nd Edition.
253. USDA-SCS (1985). "National Engineering Handbook Section 4 Hydrology". Washington, D.C., USA: U.S. Department of Agriculture.

254. Van Stempvoort, D., Ewert, L. and Wassenaar, L. (1992). "AVI: A Method for Groundwater Protection Mapping in the Prairie Provinces of Canada". PPWD Groundwater and Contaminants Project, National Hydrology Research Institute.
255. Venugopal, T., Giridharan, L. and Jayaprakash, M. (2008). "Groundwater Quality Assessment using Chemometric Analysis in the Adyar River, South India". *Arch Environ Contam Toxicol*, 55:180-190.
256. Verma, H. N. and Tiwari, K. N. (1995). "Current status and prospectus of rain water harvesting". Indian National Committee on Hydrology, National Institute of Hydrology, India.
257. Verma, O.P. (2008). "Fluoride in water and public health with special reference to Unnao district". *A quarterly newsletter green*, 3(1).
258. Vias, J. M., Andreo, B., Perles, M. J. and Carrasco, F. (2005). "A comparative study of four schemes for groundwater vulnerability-mapping in a diffuse flow carbonate aquifer under Mediterranean climatic conditions". *Env Geol.*, 47:586-595.
259. Vittala, S. S., Govindaiah, S. and Gowda, H. (2004). "Morphometric analysis of sub-watersheds in the Pawagada area of Tumkur district, South India, using remote sensing and GIS techniques". *J. Indian Soc of Remote Sensing*, 32(4):351–362.
260. Vrba, J. and Zaporozec, A. (1994). "Guidebook on mapping groundwater vulnerability". *Int. Cont. Hydrogeol*, vol 16, Heise, Hannover
261. Wang, J. Jiangtao, H. and Chen, H. (2012). "Assessment of groundwater contamination risk using hazard quantification, a modified DRASTIC model and groundwater value, Beijing Plain, China". *Science of the Total Environment*, 432:216-226.
262. Wang, Y., Merkel, B., Li, Y., Ye, H., Fu, S. and Ihm, D. (2007). "Vulnerability of groundwater in Quaternary aquifers to organic contaminants: a case study in Wuhan City, China". *Env Geol.*, 53:479–484.
263. Wang, K., Franklin, S. E., Guo, X. and Cattet, M. (2010). "Remote Sensing of Ecology, Biodiversity and Conservation: A Review from the Perspective of Remote Sensing Specialists ". *Sensors*, 10:9647-9667.
264. Wang, L. and Cheng, Q. (2008). "Design and implementation of a web-based spatial decision support system for flood forecasting and flood risk mapping". Paper presented at the *Proceedings of the IEEE International Geoscience and Remote Sensing Symposium (IGARSS)* Barcelona, Spain.
265. Ward, C.H. (1985). "Ground water quality". John Wiley & Sons.

266. Willis, R. and Yeh, W. W. G. (1987). Groundwater system planning and management. Prentice-Hall, Englewood Cliffs, N.J.
267. Wolf, J., Barthel, R. and Braun, J. (2008). "Modeling groundwater flow in alluvial mountainous catchments on a watershed scale". *Ground Water*, 46(5):695-705.
268. Wu, Q., Zhang, H., Chen, F., and Dou, J. (2008). "A web-based spatial decision support system for spatial planning and governance in the Guangdong Province". Paper presented at the *Proceedings of the Geoinformatics 2008 and Joint Conference on GIS and Built Environment: the Built Environment and Its Dynamics*. Guangzhou, China.
269. Yang, Y. S. (2010). "Catchment-scale vulnerability assessment of groundwater pollution from diffuse sources using the DRASTIC method: a case study". *Hydrological Sciences Journal*.
270. Yin, L., Zhang, E., Wang, X., Wenninger, J., Dong, J., Guo, L. and Huang, J. (2013). "A GIS based DRASTIC model for assessing groundwater vulnerability in the Ordos Plateau, China". *Environ Earth Sci.*, 69:171-185.
271. Yu, Y. S., Zou, S. and Whittemore, D. (1993). "Non-parametric trend analysis of water quality data of rivers in Kansas". *Journal of Hydrology* 150:61-80.
272. Zume, J. and Tarhule, A. (2008). "Simulating the impacts of groundwater pumping on stream-aquifer dynamics in semiarid northwestern Oklahoma, USA". *Hydrogeology Journal*, 16:797-810.
273. Zhang, W., Yan, Y., Zheng, J., Li L., Dong, X. and Cai H. (2009). "Temporal and spatial variability of annual extreme water level in the Pearl River Delta region, China". *Global and Planetary Change*, 69:35-47.

APPENDIX - I

Exploratory Boreholes Data

No	Location	Type of well	Drilled Depth (mbgl)	Zones Tapped (mbgl)	Water Level (mbgl)	Yield (lpm)	Drawdown (m)	Transmissivity T (m ² /day)	Storativity
1	Badarka	EW	437.5	287-293 296-303 310-319 328-342 347-355 358-362 375-382 388-396 398-404 419-430	12.32	3500	7.6	2644	4.02*10E-4
2	Chamrauli	EW	454.8	296-314 324-333 336-342 360-372 381-393 396-405 429-438	10.68	2030	17.71	945	1.31*10E-4
3	Hafizabad	EW	451.42	252-261 270-282 288-297 303-324 342-348 357-375 378-384	17.2	2200	15.6	3225	
4	Kiratpur	EW	448.94	270-294 300-324 330-354 360-375	8.37	2528	4.78	2908	5.62*10E-4
5	Mauranda	EW	452	295-307 310-319 326-332 335-341 351-379 394-405	4.94	1670	7.98	2103	5.13*10E-5
6	Rajapur	EW	455.01	262-272 276-286 290-300 327-340 343-350 360-380	8.78	3500	8.88	2307	8.11*10E-3
7	Anguri	EW	427.25	224-230 252-261 279-288 294-318 324-330 349-361	8.94	1752		1357	5.99*10E-4

8	Bahadurpur-1	EW	450						
9	Bahadurpur-2	EW	450.14	127-144 325-340 351-361 380-400 415-433					
10	Baras	EW	450	248-260 270-279 296-314 320-341 352-364 368-380	9.3	2530		1892	1.47*10E-4
11	Hathnasa	EW	412.33	231-260 273-288 315-318 322-328	5.2	2528		3545	3.7*10E-6
12	Rae Bareli	EW	308.76	141-147 201-212 242-245 248-304	8.98	2182	19.33	2560	
13	Raghupur	EW	475	260-305	8.05	2350	3.87	2820	
14	Sultanpur	EW	504.25	225-238 250-258 287-300 351-374	8.55	2300	4.52	4340	
15	Sulsamau	EW	751.02	324-330 343-346 352-364 370-394 459-474	8.1	2270	23.38	306	4.8*10E-4
16	Haejendar Nagar	EW	466	120-125 141-148 160-179 202-211 246-269 284-287 300-321 343-372	10.56	2751	10.19	2905	
17	Saigaon	EW	253.2	220-221 226-232 239-245	13.47	500	5.37		

Field Photographs



Photo 1: GPS measurement of Piezometer locations

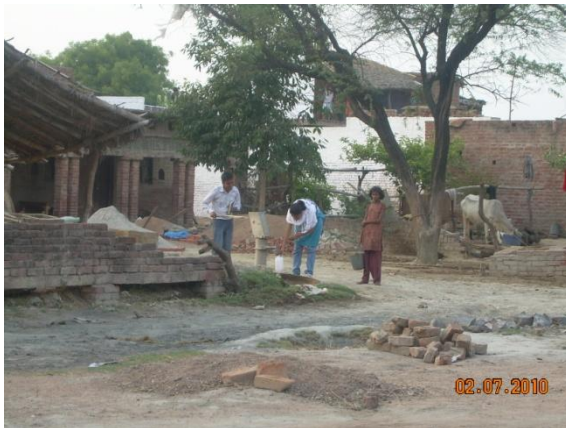


Photo 2: Collection of groundwater samples and GPS measurement



Photo 3: GPS measurement of dry wells



Photo 4: Loni River on SH-13 (Lalganj to Fatehpur Road)



Photo 5: Well on sandy area of Loni River



Photo 6: Water contamination (Loni River)



Photo 7: Check Dam 1



Photo 8: Check Dam 2

Publications from the Study**Research Papers in Peer-reviewed Journal**

1. Agarwal, E., Agarwal, R., Garg P.K. and Garg, R.D. (2010). Groundwater Status of Unnao District, Uttar Pradesh using Remote Sensing and GIS, International published Journal of Current Sciences, Vol. 15, No. 02, page 421-430.
2. Agarwal R., Garg, R.D. and Garg, P.K. (2011). Morphometric Analysis and Prioritization of Sub-watersheds in the Loni Watershed, Uttar Pradesh Using Spatial Information Technology. Journal of Indian Water Resources Society, Vol. 31, No. 3-4, page 19-27.
3. Agarwal, R., Agarwal, E., Garg P.K. and Garg, R.D. (2012). A GIS Based Study of Water Pollutants, characteristics and their affects in Hilauli Block, India, imanager's Journal on Civil Engineering, Vol. 2, No. 02, pp.
4. Agarwal, E., Agarwal, R., Garg P.K. and Garg, R.D. (2013). Delineation of Groundwater Potential Zone: An AHP/ANP approach, Journal of Earth System Sciences. Volume 122, No. 3, Page 887-898.
5. Agarwal, R., Garg P.K. and Garg, R.D. (2013). Remote Sensing and GIS Based Approach for Identification of Artificial Recharge Sites, Water Resources Management: Volume 27, Issue 7 (2013), Page 2671-2689.
6. Agarwal, R. and Garg P.K. (2014). Remote Sensing and GIS based Groundwater Potential & Recharge Zones Mapping using Multi-Criteria Decision Making Technique, Water Resources Management (Under Review).
7. Agarwal, R. and Garg P.K. (2014). Analysis of groundwater vulnerability in Loni and Morahi watersheds using geospatial approach, Environmental Monitoring and Assessment (Under Review).

Research Papers (Conference)

1. Garg, P.K., Agarwal, E., Agarwal, R., Garg, R.D. (2012). GIS based Groundwater Quality Modeling in a part of Unnao District (India) for Sustainable Development and Policy Decision of Mineral Regions and the 3rd Annual Meeting of the Regional Science Association International [C].

